Springer Series in Reliability Engineering

Kjell Hausken
Jun Zhuang *Editors*

Game Theoretic Analysis of Congestion, Safety and Security

Traffic and Transportation Theory

Springer

Springer Series in Reliability Engineering

Series editor

Hoang Pham, Piscataway, USA

More information about this series at http://www.springer.com/series/6917

Kjell Hausken · Jun Zhuang
Editors

Game Theoretic Analysis of Congestion, Safety and Security

Traffic and Transportation Theory

Springer

Editors
Kjell Hausken
Faculty of Sciences
University of Stavanger
Stavanger
Norway

Jun Zhuang
Department of Industrial and Systems Engineering
University at Buffalo, The State University of New York
Buffalo, NY
USA

ISSN 1614-7839 ISSN 2196-999X (electronic)
Springer Series in Reliability Engineering
ISBN 978-3-319-11673-0 ISBN 978-3-319-11674-7 (eBook)
DOI 10.1007/978-3-319-11674-7

Library of Congress Control Number: 2014956209

Springer Cham Heidelberg New York Dordrecht London

Printed on acid-free paper

Springer International Publishing AG Switzerland is part of Springer Science+Business Media (www.springer.com)

Preface

Game Theoretic Analysis of Congestion, Safety and Security is an interdisciplinary undertaking. Many researchers working on congestion have not extensively considered safety/security, and vice versa. However, significant interactions exist between the two research areas, which motivated this book. This book is intended to establish a new and enhanced current state of affairs within this topic, illustrate linkages between research approaches, and lay the foundation for subsequent research. Congestion (excessive crowding) is defined broadly to include all kinds of flows; e.g., road/sea/air traffic, people, data, information, water, electricity, and organisms. The book considers systems where congestion occurs, systems which may be in parallel, series, interlinked, or interdependent, with flows one way or both ways. Congestion models exist in abundance. The book makes ground by introducing game theory and safety/security. For the analysis to be game theoretic, at least two players must be present. For example, in [1] one approver and a population of normal and adversary travelers are considered. Similarly, in [2], one defender and one attacker are considered, in addition to drivers who choose the more time-efficient of two arcs of different lengths. Multiple players can be adversaries with different concerns regarding system reliability; e.g., one or several terrorists, a government, various local or regional government agencies, companies, or others with stakes for or against system reliability. Governments, companies, and authorities may have tools to handle congestion, as well as ensure safety/security against various threats. The players may have a variety of individual concerns which may or may not be consistent with system safety or security. Much of the congestion literature is not game-theoretic, and does not extensively consider safety or security. Also, most game-theoretic analyses do not account for congestion. The book consists of eight chapters.

In "Congestion Management in Motorways and Urban Networks Through a Bargaining-Game-Based Coordination Mechanism," Felipe Valencia, José D. López, Alfredo Núñez, Christian Portilla, Luis G. Cortes, Jairo Espinosa and Bart De Schutter acknowledge that road traffic networks are large-scale systems that demand distributed control strategies. Local traffic controllers for each subnetwork play a cooperative game where they communicate with each other. Their strategies

are the control sequences, their payoffs are the local performance indices such as avoiding congestion, thus balancing local against global performance.

In "Advanced Information Feedback Coupled with an Evolutionary Game in Intelligent Transportation Systems," Chuanfei Dong, Yuxi Chen, Xu Ma and Bokui Chen study a mean velocity difference feedback strategy and a congestion coefficient difference feedback strategy for intelligent transportation systems. The two strategies are based on the time-varying trend in feedback information, which could lead to higher route flux with better stability. The authors also investigate information feedback coupled with an evolutionary game in a 1-2-1-lane intelligent transportation system with dynamic periodic boundary conditions.

In "Solving a Dynamic User-Optimal Route Guidance Problem Based on Joint Strategy Fictitious Play," Tai-Yu Ma develops a multi-player repeated game to model users' compliances to route recommendations by a system administrator. Users use their experience to estimate travel time through different routes. Users can be informed or non-informed, engage in joint strategy fictitious play, and adapt their route choices progressively to reach their destinations.

In "A Psycho-Social Agent-Based Model of Driver Behavior Dynamics," Theodore Tsekeris and Ioannis Katerelos present a psycho-social agent-based model of interaction between drivers, accounting for heterogeneity and dynamic adjustment responses. Cognitive processes, risk assessment, time responsiveness of driving behavior, control dimensions of neighboring drivers, and the topology of interaction cause states such as fixed point, periodicity, and transient chaos.

In "Game-Theoretic Context and Interpretation of Kerner's Three-Phase Traffic Theory," Kjell Hausken and Hubert Rehborn interpret Kerner's three-phase traffic theory game theoretically applying the chicken game. The three phases, claimed to be incommensurable with classical two-phase theory, are free flow and two congested phases, which are synchronized flow and wide moving jam. They show how the number of chickens changes through the hysteresis loop in a density versus flow rate diagram.

In "A Heuristic Method for Identifying Near-Optimal Defending Strategies for a Road Network Subject to Traffic Congestion," Mengyao Gao, Bo Zhang, Vicki M. Bier and Tao Yao analyze how road networks are vulnerable to interdictions. An attacker interdicts links to maximize congestion. A heuristic method is developed to determine how the defender protects the road network to minimize congestion assuming that selfish drivers choose routes to minimize individual travel cost.

In "Multiple Stakeholders in Road Pricing: A Game Theoretic Approach," Anthony E. Ohazulike, Georg Still, Walter Kern and Eric C. van Berkum consider a game-theoretic approach as an alternative to the standard multi-objective optimization models for road pricing. A non-cooperative game is modeled to study road pricing strategies considering various and potentially conflicting externalities in traffic such as congestion, air pollution, and noise. The game is sequential where the leaders determine link tolls in the first stage and the road users choose routes in the second stage. A "first-best taxation" schedule is proposed to deal with the scenario that a Nash equilibrium may not exist.

In "Stackelberg and Inverse Stackelberg Road Pricing Games: State of the Art and Future Research," Kateřina Staňková and Alexander Boudewijn consider a game-theoretical toll design problem for improving the performance of road traffic systems. The road authority is modeled as the first mover to decide the toll; and the drivers are modeled as the second mover to respond to the toll by adapting driving behavior and thus impacting traffic flows. Depending on the toll structure, the authors discuss two problem formulations: a Stackelberg game where toll is uniform or time-varying; and an inverse Stackelberg game where toll is traffic-flow dependent.

References

1. Bier V, Hausken K (2013) Defending and attacking networks subject to traffic congestion. Reliab Eng Syst Safe 112:214–224
2. Wang X, Zhuang J (2011) Balancing congestion and security in the presence of strategic applicants with private information. Eur J Oper Res 212(1):100–111

Acknowledgments

The co-editor Dr. Jun Zhuang's co-editing effort for this book was partially supported by the United States Department of Homeland Security (DHS) through the National Center for Risk and Economic Analysis of Terrorism Events (CREATE) under award number 2010-ST-061-RE0001, and by the United States National Science Foundation (NSF) award numbers 1334930 and 1200899. However, any opinions, findings, and conclusions or recommendations in this document are those of the authors and do not necessarily reflect views of the DHS, CREATE, or NSF.

We thank the following scholars for reviewing chapters in this book:

Vincent Aguilera
Constantinos Antoniou
Josephina Antoniou
Ramachandran Balakrishna
Gerald Brown
Eduardo F. Camacho
Elisabetta Cherchi
Josh Clapp
Kresimir Dabcevic
Manuj Darbari
Sharon (Xuan) Di
Roberta di Pace
Chuanfei Dong
Tolou Esfandeh
Gunnar Flötteröd
Terry Friesz
Ying-En (Ethan) Ge
Jesus Gonzales-Feliu
Hai-Jun Huang
Soummya Kar
Boris Kerner
Max Klimm

Changhyun Kwon
Gregor Lämmel
Siriphong Lawphongpanich
Meng Li
Darren Lierkamp
José David López
Tai-Yu Ma
Daiheng Ni
Anthony Emeka Ohazulike
Frauke Oldewurtel
Alberto Nai Oleari
Igor Lugo Olmos
Michael Patriksson
Raffaele Pesenti
Juan Pimentel
Ashkan Rahimi-Kian
Bryan Raney
Carlo Regazzoni
Hubert Rehborn
Claudio M. Rocco S.
Claudio Roncoli
Meead Saberi
Roberto Sacile
Jan-Dirk Schmoecker
Xiaojun Shan
Rory Smead
Cole Smith
Cen Song
Joaquín Sanchez Soriano
Kateřina Staňková
Antonios Stathopoulos
Nicolas Stier
Martin Treiber
Theodore Tsekeris
Kostandina Veljanovska
Alfredo Nunez Vicencio
Dmitri Vinogradov
Qian Wang
Kevin Wood
Chi Xie
Shuang-Hua Yang
Hamed Yarmand
Wei Yuan
Jing Zhang
Xiaomei Zhao

Contents

Congestion Management in Motorways and Urban Networks Through a Bargaining-Game-Based Coordination Mechanism

Felipe Valencia, José D. López, Alfredo Núñez, Christian Portilla, Luis G. Cortes, Jairo Espinosa and Bart De Schutter

Abstract Road traffic networks are large-scale systems that demand distributed control strategies. Distributed model predictive control (DMPC) arises as a feasible alternative for traffic control. Distributed strategies decompose the whole traffic network into different subnetworks with local optimal controllers that make decisions on actions to be taken by the actuators responsible for traffic control (traffic lights, routing signals, variable speed limits, among others). However, subnetworks are interacting elements of the whole traffic network. Hence, local control decisions

F. Valencia (✉)
Solar Energy Research Center SERC-Chile, Faculty of Mathematical and Physical Sciences, Universidad de Chile, Santiago, Chile
e-mail: felipe.valencia@sercchile.cl

J.D. López
SISTEMIC, Department of Electronic Engineering, Engineering Faculty, Universidad de Antioquia UdeA, Medellin, Colombia
e-mail: josedavid@udea.edu.co

A. Núñez
Section of Road and Railway Engineering, Delft University of Technology, Delft, The Netherlands
e-mail: A.A.NunezVicencio@tudelft.nl

C. Portilla · L.G. Cortes · J. Espinosa
Departamento de Energía Eléctrica y Automática, Facultad de Minas, Universidad Nacional de Colombia, Medellin, Colombia
e-mail: crportil@unal.edu.co

L.G. Cortes
e-mail: lgcortes@unal.edu.co

J. Espinosa
e-mail: jjespino@unal.edu.co

B. De Schutter
Delft Center for Systems and Control, Delft University of Technology, Delft, The Netherlands
e-mail: b.deschutter@tudelft.nl

K. Hausken and J. Zhuang (eds.), *Game Theoretic Analysis of Congestion, Safety and Security*, Springer Series in Reliability Engineering,
DOI 10.1007/978-3-319-11674-7_1

made for one sub-network affect and are influenced by the decisions taken for the other subnetworks. Under these circumstances, the DMPC traffic problem can be treated as a game where the rules are provided by the physical system, the players are the local optimal controllers, their strategies are the control sequences, and the payoffs are the local performance indices (such as the total time spent by the users in the network). This configuration allows the achievement of a computational burden reduction, with a compromise between local and global performance. Since DMPC local controllers are able to communicate with each other, the control of the traffic network corresponds to a cooperative game. In this chapter, game-theory-based DMPC is developed and tested for control of urban and motorway networks.

Keywords Game theory · Distributed model predictive control · Large-scale systems · Motorway control · Urban traffic control · Bargaining games

1 Introduction

Sustainable mobility of people is a key issue in modern society. However, nowadays many traffic networks are operating in an inefficient way, producing several negative impacts on the environment and leading to a deterioration in quality of life for the users. Solutions such as building new roads or improving the existing infrastructure are not always feasible because of environmental and budgetary regulations. Thus the development of efficient management and control systems for traffic and transportation to satisfy the ever-increasing demand for mobility has become a crucial area of research.

Several control strategies for traffic control have been reported in the literature. Often, they are simulation based. That is, traffic models are used to determine the impact of different control strategies and the sensitivity of the performance with respect to the tuning parameters (e.g. the Adaptive Split Cycle Offset Optimisation Technique method). Among the different simulation-based strategies reported in the literature, those based on model predictive control (MPC) have been quite commonly proposed to solve traffic problems. These techniques are focused on the optimal use of the information provided by the infrastructure already installed, and on reducing the travel time while explicitly considering the physical and operational constraints of the system [3, 13, 17, 47]. However, despite the advantages of MPC over other methods, the application of this control scheme in real large-scale systems (such as traffic networks) is rendered impractical due to the computational burden of its centralized nature. In order to make the real-life implementation of MPC in large-scale systems possible, distributed model predictive control (DMPC) approaches have been proposed Camponogara et al. [4]. DMPC is a control scheme in which the system is divided into a number of subsystems. Each subsystem is able to share information with other subsystems in order to determine its local control actions [33, 42, 52]. The main goal of the DMPC approach is to achieve some

degree of coordination among subsystems that are solving local MPC problems with locally relevant variables, costs, and constraints, without solving the centralized MPC problem Jia and Krogh [14], Necoara et al. [32].

In this chapter, the application of a new bargaining-game-theory-based DMPC for the management of congestion in motorways and urban traffic networks is presented. Game theory is a branch of applied mathematics used in a wide range of disciplines (see [51] for a more detailed overview of game theory). Game theory attempts to capture behaviors in strategic situations, or games where the outcome of a player is not only a function of his own choices but also depends on the choices of others [28]. Some DMPC schemes based on game theory concepts have been reported in the literature. In Du et al. [5], Giovanini and Balderud [8], Li et al. [19], Trodden et al. [44] DMPC schemes based on Nash optimality were proposed. In such approaches, the DMPC problem was formulated as a non-cooperative game, and the convergence of the solution to a Nash equilibrium point of the resulting non-cooperative game was demonstrated. In Rantzer [39–41] the DMPC problem was related to game theory using a cooperative game framework, as proposed in Von Neumann et al. [51]. In these approaches, the Lagrange multipliers of the dual decomposition were conceived as price mechanisms in a market serving to achieve mutual agreements among subsystems, and dynamic price mechanisms were used for decomposing and distributing the optimization problem associated with the original MPC problem. More specifically, the minimization problem was converted into a min-max problem, and again the convergence of the solution to a Nash equilibrium was demonstrated. In Maestre et al. [24–26], Muñoz de la Peña et al. [27] some other DMPC approaches based on cooperative game theory were presented. In these approaches, each subsystem computes local control actions and suggests control actions to the remaining subsystems. The final control decisions are taken by each subsystem based on the local information and the suggested control actions from the other subsystems.

The congestion management described in the current chapter uses the theory of bargaining games as a mathematical framework. In previous bargaining games based approaches [48, 49, 50], the authors demonstrated that (in some cases) the convergence of the DMPC solution to a Nash equilibrium point could produce undesired results because it could give an undesirable closed-loop behavior in the controlled system. Moreover, in DMPC the controllers are able to communicate with each other. In this chapter, the communication capabilities of the controllers in a DMPC scheme will be exploited for improving the decision-making of each controller. Such improvements pertains to the knowledge each local controller has about the preferences of the remaining controllers. In this way, local control actions can be chosen in such a way that synergy among controllers arises as a consequence of their cooperative behavior. Note that this is not an additional objective of the proposed control scheme, but only an additional feature which is related to the formulation of DMPC as a bargaining game.

In order to present the proposed congestion management system, in Sect. 2 nonlinear DMPC is formulated as a bargaining game. Then, in Sects. 3 and 4 the specific application of game theory to congestion management in motorways and urban traffic networks is shown. Finally, in Sect. 5 some closing remarks are discussed.

2 Non-linear Distributed Model Predictive Control: Bargaining Game Approach

Distributed model predictive control (DMPC) is a variant of decentralized control where some information is exchanged among subsystems in order to determine the local control actions [33, 42, 52]. Compared with totally decentralized control schemes, DMPC architectures yield better closed-loop behavior due to the communication, cooperation, and perhaps negotiation between subsystems. However, these elements also increase the computational and communication burden [4, 33]. Nevertheless, DMPC is becoming important because it is effective in supporting the implementation of complex control systems with hard requirements involving fault tolerance and flexibility, it has high control capabilities and allows the implementation of optimal controllers in real-life large-scale systems through system decomposition, reducing the computational burden associated with the solution of one large centralized optimization problem [37, 53].

Figure 1 shows a DMPC control scheme. In this figure Process 1 and Process 2 have local MPC controllers. Since these processes interact with each other, sharing information between controllers is required in order to allow them to compute their own control actions. Otherwise, the system may lose performance and/or stability. So, at each time step local controllers must decide on the control actions to be locally applied, transmit them to the other controllers, and negotiate with the other

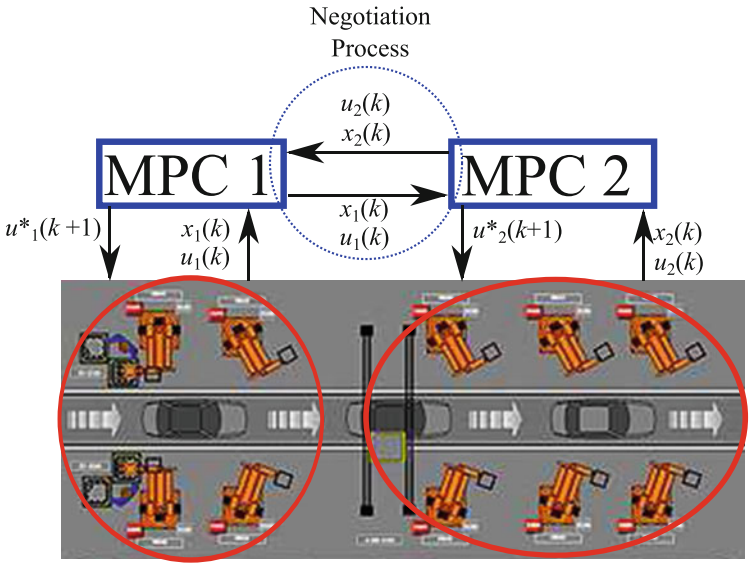

Fig. 1 Schematic diagram of a typical DMPC scheme. Here each process has a local MPC controller with the ability to share information with the other MPC controllers with the purpose of deciding on which control action to apply

controllers on which control actions will be applied. In the following sections this procedure is mathematically described and discussed using control theory and game theory as mathematical frameworks.

2.1 Problem Statement

Consider the discrete-time non-linear system given by:

$$x(k+1) = f_{\mathrm{dx}}(x(k), u(k)) \tag{1}$$

where $x(k) \in \mathbb{R}^n$ and $u(k) \in \mathbb{R}^m$ denote the state and input vectors of the dynamic system at time step k, with $f_{\mathrm{dx}}(\cdot)$ a non-linear function describing the time evolution of the dynamical system to be controlled. The general idea of non-linear model predictive control (NMPC) is to determine the sequence of control actions for the system by solving an optimization problem considering the predicted trajectories given by the non-linear discrete-time model of Eq. (1).

Commonly, a quadratic cost function (that may be interpreted as the total energy of the system) is used to measure the performance of the system:

$$L(\tilde{\mathbf{x}}(k), \tilde{\mathbf{u}}(k)) = \sum_{h=k}^{k+N_{\mathrm{p}}-1} \left[x^T(h+1|k) Q x(h+1|k)\right] + \sum_{h=k}^{k+N_{\mathrm{p}}-1} \left[u^T(h) R u(h)\right] \tag{2}$$

where the superscript T denotes the transpose operation, $x(h|k)$ denotes the predicted value of x at time step h given the conditions at time step k, $u(h)$ denotes the control input u at time step h, $\tilde{\mathbf{x}}(k) = [x^T(k+1|k), \ldots, x^T(k+N_{\mathrm{p}}|k)]^T$, $\tilde{\mathbf{u}}(k) = [u^T(k), \ldots, u^T(k+N_{\mathrm{c}}), \ldots, u^T(k+N_{\mathrm{p}}-1)]^T$, where $x(k|k) = x(k)$, and $u(h) = u(k+N_{\mathrm{c}}-1)$, for $h = k+N_{\mathrm{c}}, \ldots, k+N_{\mathrm{p}}-1$; Q and R are diagonal matrices with positive diagonal elements, and N_{c}, N_{p} are the control and prediction horizons respectively, with $N_{\mathrm{c}} \leq N_{\mathrm{p}}$. Recall that $\tilde{\mathbf{x}}(k), \tilde{\mathbf{u}}(k)$ are the projections of the state and input vectors along the prediction horizon N_{p}. Hence, $L(\cdot)$ is a function of $\tilde{\mathbf{x}}(k), \tilde{\mathbf{u}}(k)$ instead of being a function of $x(k), u(k)$.

Let $\mathbb{X} \subset \mathbb{R}^n$ and $\mathbb{U} \subset \mathbb{R}^m$ denote the feasible sets for the states and inputs of the system, i.e., $x(k) \in \mathbb{X}$, $u(k) \in \mathbb{U}$ (these sets are determined by the physical and operational constraints of the system). Then, the NMPC problem can be formulated as the non-linear optimization problem:

$$\begin{aligned} &\min_{\tilde{\mathbf{u}}(k)} \; L(\tilde{\mathbf{x}}(k), \tilde{\mathbf{u}}(k)) \\ &\mathbf{s.t.}: \\ &x(h+1) = f_{\mathrm{dx}}(x(h), u(h)) \\ &x(h+1) \in \mathbb{X}; \qquad u(h) \in \mathbb{U}; \end{aligned} \tag{3}$$

This optimization problem corresponds to the centralized formulation of the NMPC problem. Although widely studied, the solution of Eq. (3) is hard to compute in real-time for large-scale systems such as traffic networks. This fact motivates the use of distributed predictive control schemes.

For instance, following the approaches in Kotsialos et al. [16, 18], Papageorgiou et al. [34] for motorways and the approaches presented in Lin et al. [21, 22] and the references therein for urban traffic, both traffic systems can be modeled as Eq. (1). Since they are composed of several interacting elements (links in the case of the motorways and intersections in the case of the urban traffic networks), the whole network can be decomposed into those fundamental elements and local predictive control schemes can be used for an optimal local control of each element. A motivation for such a decomposition is that traffic networks are large-scale systems, therefore a centralized optimal solution is not viable due to the lack of flexibility and vulnerability of this control structure (See Table 1 for a comparison between centralized and distributed structures).

For implementing DMPC schemes the whole system must be decomposed into several subsystems. For each subsystem a local MPC is designed, and a negotiation strategy is provided to each controller in order to determine the local control actions to be applied. Assume that the whole system can be decomposed into M subsystems

$$x_r(k+1) = f_{\mathrm{dx}r}(x(k), u_r(k), u_{-r}(k)), \quad \text{for} \quad r = 1, \ldots, M \tag{4}$$

where $x_r(k) \in \mathbb{R}^{n_r}$ and $u_r(k) \in \mathbb{R}^{m_r}$ are the local states and inputs, and $u_{-r}(k) = [u_1^T(k), \ldots, u_{r-1}^T(k), u_{r+1}^T(k), \ldots, u_M^T(k)]^T$. Furthermore, assume that the sets $\mathbb{X}_r \subset \mathbb{R}^{n_r}$ and $\mathbb{U}_r \subset \mathbb{R}^{m_r}$ define the local feasible sets for $x_r(k)$ and $u_r(k)$ respectively, where $\mathbb{X} = \Pi_r^M \mathbb{X}_r$ and $\mathbb{U} = \Pi_r^M \mathbb{U}_r$, Π denoting the Cartesian product. From the system decomposition of (4) the cost function $L(\tilde{\mathbf{x}}(k), \tilde{\mathbf{u}}(k))$ can be expressed as Venkat et al. [49, 50].

Table 1 Comparison between centralized and distributed MPC

	Centralized	Distributed
Objective	Single objective	Both local and global system objectives
Prediction model	Broad system prediction model	Several prediction models (one per local controller)
Communications	All system information should be transmitted to a central unit	Local information is transmitted between local controllers
Processing	Centralized computation of the control actions to be applied to the system under control	Local controllers compute the local control actions based on the available information

$$L(\tilde{\mathbf{x}}(k), \tilde{\mathbf{u}}(k)) = \sum_{r=1}^{M} \left(\sum_{h=k}^{k+N_p-1} x_r^T(h+1|k) Q_r x_r(h+1|k) + \sum_{h=k}^{k+N_c-1} u_r^T(h) R_r u_r(h) \right) \tag{5}$$

Let $\phi_r(\tilde{\mathbf{x}}(k), \tilde{\mathbf{u}}(k))$ denote the local cost function, and for the sake of simplicity, $\phi_r(\tilde{\mathbf{x}}(k), \tilde{\mathbf{u}}(k))$ is defined as the term inside the brackets in Eq. (5). Therefore, the centralized optimization problem (3) can be equivalently solved through the solution of (6), with $r = 1, \ldots, M$.

$$\begin{aligned} &\min_{\widetilde{\mathbf{u}}(k)} \sum_{r=1}^{M} \phi_r(\widetilde{\mathbf{x}}(k), \widetilde{\mathbf{u}}(k)) \\ &\mathbf{s.t.}: \\ &x_r(h+1) = f_{\mathrm{dx}r}(x(h), u_r(h), u_{-r}(h)) \\ &x_r(h) \in \mathbb{X}_r; \quad u_r(h) \in \mathbb{U}_r; \quad y_r(h) \in \mathbb{Y}_r \end{aligned} \tag{6}$$

The optimization problem Eq. (6) defines the non-linear DMPC (NDMPC) formulation. In this formulation, each controller determines its local control actions $\widetilde{\mathbf{u}}_r(k)$ according to its local cost function $\phi_r(\widetilde{\mathbf{x}}(k), \widetilde{\mathbf{u}}(k))$. Note that from Eq. (6) a set of M local optimization problems is derived, all coupled via the cost function and the constraints. In this sense, Eq. (6) defines a situation in which the success of each controller depends upon the decisions of the remaining controllers. This situation defines a **game** referred to in this chapter as the NDMPC game.

Game-theory-based NDMPC has been previously studied by several authors. In these approaches the DMPC was analyzed as a non-cooperative game [5, 8, 19, 44], where local decisions were computed as the solution to the local optimization problem (7). In those cases, the authors demonstrated the existence of at least one Nash equilibrium point and the convergence of the distributed solution to this point.

$$\begin{aligned} &\min_{\widetilde{\mathbf{u}}_r(k)} \phi_r(\widetilde{\mathbf{x}}(k), u_r(h), u_{-r}(h)) \\ &\mathbf{s.t.}: \\ &x_r(h+1) = f_{\mathrm{dx}r}(x(h), u_r(h), u_{-r}(h)) \\ &x_r(h) \in \mathbb{X}_r; \quad u_r(h) \in \mathbb{U}_r \end{aligned} \tag{7}$$

Although there exist several strategic situations where achieving a Nash equilibrium point is desired, this is not the case in DMPC. For instance, in Venkat et al. [48–50] the authors presented some examples where DMPC approaches with assured convergence to a Nash equilibrium point exhibited an unexpected closed-loop behavior, thereby limiting the applicability of those schemes. Alternatively, [39–41] transformed the optimization problem (7) into a min-max optimization problem. Accordingly, the solution to (7) does not require information exchange and also converges to a Nash equilibrium point. However, depending on the dimensions of the system the solution to the min-max problem might not be feasible in real-time. Based on these facts, bearing in mind the work done in Venkat et al. [48–50] on feasible

cooperation MPC (where convergence of the distributed scheme to the centralized solution was demonstrated), and given that local controllers are able to communicate with each other, a cooperative game framework is used in this chapter for analyzing the situation arising from Eq. (6).

2.2 The Distributed Model Predictive Control Game

As it was stated in Sect. 2.1, in the NDMPC formulation the success of each local controller is based upon the choices of the remaining controllers. According to Myerson [28], such situations are the object of study of game theory. In the NDMPC case, the game is determined by the physical laws used to model the system to be controlled, by the models locally used to predict the system's behavior, and by the physical and operational constraints of the whole system. Since NDMPC is a discrete-time control strategy, it is played at each time step k, i.e., at each time step an optimal control action is obtained (over the decision space) based on local performance indices. Note that from Eq. (6) at each time step k each local controller has a decision space $\mathbb{U}_r$ for selecting the sequence of control actions $\widetilde{\mathbf{u}}_r(k)$, and this selection obeys the minimization of the local cost function $\phi_r(\widetilde{\mathbf{x}}(k), \widetilde{\mathbf{u}}(k))$ (moves, strategies, and choices in the NDMPC game). So, based on Nash [31], Von Neumann et al. [51] the NDMPC circumstance has all the elements required for being analyzed within the game theory framework. In order to make this concept clear, Table 2 shows a didactic comparison between Game Theory and DMPC.

Mathematically, a game G can be defined in its strategic form as a tuple $G = (\mathcal{N}, \{\Omega_r\}_{r\in\mathcal{N}}, \{\phi_r\}_{r\in\mathcal{N}})$ where $\mathcal{N} = \{1, \ldots, M\}$ is the set of players, Ω_r is the decision space (set of feasible decisions) of the r-th player; and $\phi_r : \Omega_1 \times \Omega_M \rightarrow \mathbb{R}$ is the profit function of the r-th player (i.e., we must maximize instead of minimize as in MPC). Often, ϕ_r quantifies the preferences of player r (and determines its

Table 2 Comparison between game theory and DMPC

	Game Theory	DMPC
Game	Set of rules used to describe the circumstances	Local and global system model rules, as well as physical and operational constraints
Play	Every particular instance at which the game is played	Each time step k
Move	The occasion choosing of an alternative under the conditions of the game	Each time step k (as shown at the end of Sect. 2)
Strategy	Preference and/or rule followed by each player to select an alternative	Minimization of the local system-wide-control cost function (as shown at the end of Sect. 2)
Choice	The selected alternative in a move according to the strategy	Local control action to be applied to the system, driven by the minimization of the local system-wide-control cost function

strategy), and gives to each player some degree of rationality [1]. Let $\mathcal{N}$ be the set of local controllers, $\Omega_r = \mathbb{X}_r \cap \mathbb{U}_r$ be the decision space of controller r, and $\{\phi_r(\widetilde{\mathbf{x}}(k), \widetilde{\mathbf{u}}(k))\}_{i\in\mathcal{N}}$ be the set of profit functions. Then the NDMPC game in its strategic form is a tuple $G_{\text{NDMPC}} = (\mathcal{N}, \{\Omega_r\}_{r\in\mathcal{N}}, \{\phi_r(\widetilde{\mathbf{x}}(k), \widetilde{\mathbf{u}}(k))\}_{r\in\mathcal{N}})$. In the light of (6), the game G_{NDMPC} involves a group of controllers who have the opportunity to collaborate for a mutual benefit: improving both local and whole system performance. So, G_{NDMPC} is a bargaining game according to the definition provided by Nash in Nash [29–31]. Furthermore, the game G_{NDMPC} has a group of individuals involved in the bargaining, a mutual benefit which is the objective of the bargaining, and a utopia point defined by the set of choices where all the individuals involved in the bargaining achieve at the same time their maximum benefit. Thus, the only missing element to define the game G_{NDMPC} as a bargaining game is the disagreement point.

According to Nash [29–31] the disagreement point is the benefit perceived by a player when an agreement is not possible. Such benefit is associated with an alternative plan carried out by the player in this situation, which is determined by the information locally available. Moreover, the disagreement point should give to the players a strong incentive to increase their demands as much as possible without losing compatibility. Following these statements the disagreement point $\eta_r(k) \in \mathbb{R}$ for each player (local controller) in the NDMPC game should be defined such that it reflects the expected cost associated with the non-cooperative behavior. That is, the expected value of the local cost function if the local controller "decides" not to cooperate. Associated with this cost, there is a local control action to be applied that acts as an alternative plan carried out by the controller in a non-cooperative situation. In addition, the disagreement point must be updated following a rule that provides incentives for changing the decision of the controllers that decide not to cooperate, and for enhancing the performance of the controllers that decide to cooperate.

For controller r, assume $\eta_r(k)$ as the expected maximum loss of performance. Then, at time step k : $\eta_r(k) - \phi_r(\widetilde{\mathbf{x}}(k), \widetilde{\mathbf{u}}(k))$ denotes the utility of such subsystem. Associated with the utility perceived by controller r there is a plan or sequence of local control actions $\widetilde{\mathbf{u}}_r(k)$. Thereby, as in Nash [29–31], controller r seeks a feasible local control sequence that maximizes its own utility. That is, controller r looks for a control sequence $\tilde{\mathbf{u}}_r(k)$ such that $\phi_r(\tilde{\mathbf{x}}(k), \tilde{\mathbf{u}}(k)$ is minimum and $\eta_r(k) \geq \phi_r(\tilde{\mathbf{x}}(k), \tilde{\mathbf{u}}(k))$. If that control sequence exists, the plan of action is locally to apply the first element of the control sequence $\tilde{\mathbf{u}}_r(k)$, to use a shifted control sequence as the initial condition for making the decision again in the next time step, and to reduce the disagreement according to the expression $\eta_r(k+1) = \eta_r(k) - \alpha(\eta_r(k) - \phi_r(\tilde{\mathbf{x}}(k), \tilde{\mathbf{u}}(k)))$, with $\alpha \in \mathbb{R}$, $0 < \alpha < 1$. If that control action does not exists, the plan of action is to keep applying the current local control action, to use a shifted control sequence from the initial condition as a condition for performing the next decision making stage, and to make the value of the disagreement point equal to the value of keeping the current control action, viz., $\eta_r(k) = \phi_r(\tilde{\mathbf{x}}(k), \tilde{\mathbf{u}}(k))$.

Given the updating conditions of the disagreement point, decreasing its value (which implies the controller r "decides" to cooperate) provides strong incentives for increasing their demand from the cooperative behavior; but, making its value equal to the current value of the cost function (which implies the controller r "decides" not to cooperate) provides incentives to controller r for changing its decision not to cooperate. Indeed, if the expected maximum loss of performance grows the decision space is augmented, the probability of finding a control sequence such that $\phi_r(\tilde{\mathbf{x}}(k), \tilde{\mathbf{u}}(k))$ is minimum, and $\eta_r(k) \geq \phi_r(\tilde{\mathbf{x}}(k), \tilde{\mathbf{u}}(k))$ is increased. Mathematically, the disagreement point is formulated as follows [45]:

$$\eta_r(k+1) = \begin{cases} \eta_r(k) - \alpha(\eta_r(k) - \phi_r(\tilde{\mathbf{x}}(k), \tilde{\mathbf{u}}(k))) & \text{if } \eta_r(k) \geq \phi_r(\tilde{\mathbf{x}}(k), \tilde{\mathbf{u}}(k)) \\ \eta_r(k) + (\phi_r(\tilde{\mathbf{x}}(k), \tilde{\mathbf{u}}(k)) - \eta_r(k)) & \text{if } \eta_r(k) < \phi_r(\tilde{\mathbf{x}}(k), \tilde{\mathbf{u}}(k)) \end{cases} \quad (8)$$

Despite of the similarities between the bargaining games defined by Nash in [Nash 29, 30, 31] and the game G_{NDMPC} (see Table 3), there are some differences that should be accounted for in order to define a bargaining solution to the NDMPC game (in NDMPC the solution pertains to the control actions to be locally applied by each controller). The main difference is that since it is expected that the system will operate over a long time period, the NDMPC game is a sequence of infinite bargaining games which are played at each time step, in a variable-decision environment influencing the behavior of the local controllers and their decision-making stage. Thus, the original game theory is extended in order to have a mathematical framework for analyzing NDMPC bargaining games. In this way the concept of discrete-time dynamic bargaining game for DMPC (identified as GT-NDMPC in this chapter) is introduced in Valencia [45].

A discrete-time dynamic bargaining game refers to a situation where at each time step a bargaining game is solved depending on the dynamic evolution of the decision environment. In this bargaining game the dynamic evolution of the decision

Table 3 Comparison between bargaining games and DMPC

	Bargaining game theory	DMPC
Players	A group of individuals involved in the bargaining	The set of local controllers that are able to communicate among them, and bargain
Decision Space	The set of all choices available to the individuals involved in the bargaining	The set of available control actions, determined by the physical and operational constraints
Disagreement point	Minimum level of satisfaction expected by the individuals from the bargaining	Maximum expected loss of performance by each local controller from the bargaining
Utopia point	The set of choices where all the individuals involved in the bargaining achieve at the same time their maximum benefit	The set of control actions that minimize all the local system-wide-control cost functions at the same time

environment is determined by the state $x(k) \in \mathbb{R}^n$ and input $u(k) \in \mathbb{R}^m$. Mathematically, a discrete-time dynamic bargaining game is defined as follows:

Definition 1 (*Discrete-time Dynamic Bargaining Game*) A discrete-time dynamic bargaining game for the set of players N is a sequence of games $\{(\Theta(k), \eta(k))\}_{k=0}^{\infty}$, where:

1. $\Theta(k)$ is a nonempty closed subset of $\mathbb{R}^N$ containing the feasible values for the profit function of each player, at $k = 1, 2, 3, \ldots$.
2. $\eta(k)$ is the disagreement point, $\eta(k) \in \text{int}(\Theta(k))$.
3. $\zeta_r(\Theta(k)) := \min\{\phi_r(k) : (\phi_r(k))_{r\in N} \in \Theta(k)\}$ exists for every $r \in N$ at each time step k.
4. There exist functions $f_r \in \mathbb{R}^{n_r}, g \in \mathbb{R}^z, h_r \in \mathbb{R}$, $r = 1, \ldots, N$, determining the dynamic evolution of the decision environment and the disagreement point of player r, and the dynamic evolution of the feasible set, such that:

$$\begin{aligned} x_r(k+1) &= f_r(x(k), u(k)) \\ \eta_r(k+1) &= h_r(x(k), u(k), \eta(k)) \\ \Theta(k+1) &= g(x(k), u(k), \Theta(k)) \end{aligned} \tag{9}$$

   with $x_r(k) \in \mathbb{X}_r$, $\mathbb{X}_r \subset \mathbb{X}$, z the dimensions of the feasible set of values for the profit function, and $u(k)$ the vector of actions taken by the players affecting the decision environment. Here, the function $g(x(k), u(k), \Theta(k))$ is defined by the set of time dependent constraints on $x(k)$ and $u(k)$, and the facts that can reduce the size of the decision space.
5. There exists a tuple $(\phi_1(x(k), u(k)), \ldots, \phi_M(x(k), u(k))) \in \Theta(k)$ with $\phi_r(x(k), u(k))$ the profit function of the r-th player.

Let $\Xi_r(\tilde{\mathbf{x}}(k), \tilde{\mathbf{u}}(k))$ be the set resulting from the intersection of Ω_r and the equality constraint given by the local prediction model [4]. Then, the set $\Theta(k)$ in the GT-NDMPC game is defined as $\Theta(k) := \{(\phi_1(x(k), u(k)), \ldots, \phi_M(x(k), u(k))) \in \mathbb{R}^M | (x(k), u(k)) \in \Xi_r(\tilde{\mathbf{x}}(k), \tilde{\mathbf{u}}(k))\}$. Here $g(x(k), u(k), \Theta(k))$ is equal to the whole system model [1]. Then, the game G_{NDMPC} is a discrete-time dynamic bargaining game. Although in the definition of $\{(\Theta(k), \eta(k))\}_{k=0}^{\infty}$ it is desired that $\eta(k) \in \text{int}(\Theta(k))$, from the definition of $\eta_r(k)$ such a condition cannot be guaranteed. In that case, the value of the disagreement point might lie on the boundary of the feasible set. If this happens and there exists a feasible search direction to minimize the local cost function, then a control action satisfying the constraint $\eta_r(k) \geq \phi_r(\tilde{\mathbf{x}}(k), \tilde{\mathbf{u}}(k))$ is achieved. Otherwise, there is no change in the local control actions. This allows each local controller to decide whether or not to cooperate with the remaining subsystems. Note that in these statements there exists an underlying utility concept.

For GT-NDMPC game the utility of each local controller is given by the difference between the disagreement point and the local cost function, i.e., $\eta_r(k) - \phi_r(\tilde{\mathbf{x}}(k), \tilde{\mathbf{u}}(k))$. From Nash [31], Harsanyi [11], Peters [36], Akira [1] the solution of a bargaining game is given by the maximization of the Nash products, namely, the product of the utility functions $\Pi_{r=1}^{M} \eta_r(k) - \phi_r(\tilde{\mathbf{x}}(k), \tilde{\mathbf{u}}(k))$ in the NDMPC case. Based on the axiomatic characterization proposed in Valencia [45] the outcome of the game G_{NDMPC} is given by the solution of the optimization problem (the $\log(\cdot)$ function arises from the transformation of the Nash products).

$$\begin{aligned} &\max_{\tilde{\mathbf{u}}(k)} \sum_{i=r}^{M} w_r \log(\eta_r(k) - \phi_r(\tilde{\mathbf{x}}(k), \tilde{\mathbf{u}}(k))) \\ &\mathbf{s.t.}: \\ &x_r(h+1) = f_{\text{dx}r}(x(h), u_r(h), u_{-r}(h)) \\ &\eta_r(k) \geq \phi_r(\tilde{\mathbf{x}}(k), \tilde{\mathbf{u}}(k)) \\ &x_r(h) \in \mathbb{X}_r; \quad u_r(h) \in \mathbb{U}_r \end{aligned} \tag{10}$$

Then, the maximization problem of Eq. (10) can be solved in a distributed way by locally solving the system-wide control problem of Eq. (11).

$$\begin{aligned} &\max_{\tilde{\mathbf{u}}_r(k)} \sum_{i=r}^{M} w_r \log(\eta_r(k) - \phi_r(\tilde{\mathbf{u}}_i(k), \tilde{\mathbf{u}}_{-i}(k))) \\ &\mathbf{s.t.}: \\ &x_r(h+1) = f_{\text{dx}r}(x(h), u_r(h), u_{-r}(h)) \\ &\eta_r(k) \geq \phi_r(\tilde{\mathbf{u}}_i(k), \tilde{\mathbf{u}}_{-i}(k)) \\ &x_r(h) \in \mathbb{X}_r; \quad u_r(h) \in \mathbb{U}_r \end{aligned} \tag{11}$$

considering $\tilde{\mathbf{u}}_{-r}(k)$ to be fixed and optimizing only in the direction of $\tilde{\mathbf{u}}_r(k)$. For implementing the distributed solution of the GT-NDMPC game, a negotiation model based on the model proposed in Nash [31] for two-player games is used Valencia [45]. In this negotiation model each local controller is:

- fully informed on the structure of the game;
- fully informed on the utility function of the remaining subsystems;
- assumed intelligent and rational, i.e., each controller has a set of preferences, treats, and rational expectations of its future environment.

Additionally, it is assumed that the communication architecture allows each subsystem to communicate with the remaining subsystems in order to transmit their disagreement points and their local measurements of the states and inputs. Such a model adapted for solving the GT-NDMPC game has the steps shown in algorithm 1.

The initial condition for solving Eq. (11) at time step $k+1$ is given by the shifted control input, and $\tilde{\mathbf{u}}_i(k)$ is a feasible control action used as initial condition for the optimization procedure of subsystem i at time step k (shifted control input from previous time instant). As in the case of the negotiation model proposed in Nash [31], the negotiation model for solving the GT-NDMPC game in a distributed way represents a two-moves game where the decisions are taken in steps 3 and 4.

It is worth noting that the proposed negotiation model allows for the avoidance of iterative procedures. This is the main difference of the proposed control scheme with respect to the approaches based on Lagrange multipliers, or those schemes based on game theory reported in the literature. Moreover, it provides each subsystem enough elements for deciding on whether or not to cooperate, depending of the benefit perceived to result form the cooperative behavior.

Algorithm 1 Negotiation model for GT-NDMPC games

for $k = 1, \ldots$ **do**
  Each subsystem sends the values of $\mathbf{x}_i(k),\ \eta_i(k)$ to the remaining subsystems
  for subsystem $i = 1, \ldots, N$ **do**
    Solve the local optimization problem of Eq. (11)
    if Eq. (11) is feasible **then**
      Select $u_i(k)$ as control action
      Update its disagreement point with $\eta(k+1) = \eta_i(k) - \alpha(\eta_i(k) - \phi_i(\widetilde{\mathbf{u}}(k)))$
    else
      Select the first control action of $\widetilde{\mathbf{u}}_i(k)$
      Update its disagreement point with $\eta(k+1) = \phi_i(\widetilde{\mathbf{u}}(k))$
    end if
  end for
  All subsystems send updated control actions and disagreement points to the others.
end for

The closed-loop stability of a system controlled via the proposed scheme can be derived by combining the feasibility proof in Valencia et al. [46] and the definition of a disagreement point (the disagreement point provides an upper boundary for local and whole system cost functions). From Algorithm 1, the stability of the proposed GT-NDMPC method depends on the decision of each subsystem on whether or not to cooperate. In order to demonstrate the stability of the closed-loop system, in Valencia [45] two cases were considered: All subsystems always cooperate, or some subsystems do not cooperate at first but a few time steps ahead they all start to cooperate. Following the same procedure proposed in Valencia [45] for these cases, closed-loop stability conditions can be derived.

In Sects. 3 and 4 the GT-NDMPC game formulation presented in the current section is applied to congestion management on motorways and in urban traffic.

3 Bargaining-Game-Based Coordination for Congestion Management on Motorways

3.1 Motorway Traffic Model

Let us start by introducing some concepts and notations related to the traffic model used in this section, viz. the METANET model described in Kotsialos et al. [16, 18], Papageorgiou et al. [34]. In this model, the motorway network is represented as a

directed graph in which the links represent homogeneous motorway stretches. Each stretch has uniform characteristics, e.g., no on-/off-ramps, no major changes in the geometry, and no metering lines. A node is placed at the locations where a major change in the road characteristics occurs, as well as at junctions and at the on-/off-ramps. A link is further divided into segments of equal distance. Each segment is characterized by its length (L_m), number of lanes (λ_m), vehicle density ($\rho_{(m,i)}(k)$), mean speed ($v_{(m,i)}(k)$), and output flow ($q_{(m,i)}(k)$), with m denoting the link number, (m,i) denoting the segment i of the link m, and k the time step. For each segment, the dynamic evolution of density of vehicles, mean speed, and length of the queue at the on-ramps is determined. Let $R_{(m,i)}(k)$, $C_{(m,i)}(k)$, and $A_{(m,i)}(k)$ denote the relaxation, convection, and anticipation terms, defined as in Kotsialos et al. [16, 18], Papageorgiou et al. [34]. Moreover, let the subscript o denote the origin nodes (nodes allowing the access of traffic from an external road; mainstream origin or on-ramp). For instance, d_o denotes the demand at the origin o. This traffic accessing a link by on-ramp o often is limited or controlled by a traffic light (or ramp-metering), where $r_o(k)$ denotes the ramp-metering rate, used to regulate the vehicles accessing the motorway.

The METANET model was used here because this model provides an adequate description of the traffic flow on a motorway with reduced complexity, which is desirable for control purposes. For instance, in Kotsialos et al. [16, 18], Papageorgiou et al. [34] and the references therein, there are several control strategies where the METANET model was used for representing the traffic flow dynamics. Also in Kejun et al. [15], Groot et al. [9], Baskar et al. [2], Hegyi et al. [12], Lu et al. [23] the METANET model was used for representing the dynamic behavior of the traffic flow.

Let $q_o(k)$ be the flow of vehicles incoming from the origin o to the link to which origin o is connected (1,i). The value of $q_o(k)$ is given by:

$$q_o(k) = \min\left[d_o + \frac{w_o(k)}{T_s}, C_o r_o(k), C_o\left(\frac{\rho_{\max,i} - \rho_{(1,i)}(k)}{\rho_{\max,i} - \rho_{\mathrm{cr},i}}\right)\right] \tag{12}$$

where C_o is the capacity of origin o under free flow conditions, $\rho_{\max,i}$ is the maximum density of a segment, w_o denotes the queue of vehicles on the origin node o, T_s is the sample time. Discussions on the meaning of the parameters in (12) and their selection can be found in, e.g., [16, 18, 34].

The dynamic evolution of density, speed, and queues in a traffic segment of a motorway is given by:

$$\rho_{(m,i)}(k+1) = \rho_{(m,i)}(k) + \frac{T_\mathrm{s}}{L_m \lambda_m}\left(q_{\mathrm{in},(m,i)}(k) - q_{\mathrm{out},(m,i)}(k)\right) \tag{13}$$

$$\begin{aligned} v_{(m,i)}(k+1) = {} & v_{(m,i)}(k) + R_{(m,i)}(k) + C_{(m,i)}(k) \\ & + A_{(m,i)}(k) - \frac{\delta T_\mathrm{s} q_o(k) v_{(m,i)}(k)}{L_m \lambda_m (\rho_{(m,i)}(k) - \mu)} \end{aligned} \tag{14}$$

$$w_o(k+1) = w_o(k) + T_s(d_o(k) - q_o(k)) \tag{15}$$

with

$$q_{\text{in},(m,i)}(k) = q_o(k) + q_{(m-1,i_{last})}(k) \tag{16}$$

$$q_{\text{out},(m,i)}(k) = \lambda_m \rho_{(m,i)}(k) v_{(m,1)}(k) \tag{17}$$

where $q_{(m-1,i_{last})}(k)$ is the flow from the last segment of the link $m-1$, and the term $\frac{\delta T_s q_o(k) v_{(m,i)}(k)}{L_m \lambda_m (\rho_{(m,i)}(k) - \mu)}$ defines the reduction in the speed in the link (m,i) due to the incoming flow from the origin o.

3.2 Bargaining-Game Approach to Congestion Management on Motorways

The idea of congestion management on motorways is to provide a control strategy for regulating the number of vehicles entering the traffic network. In this sense, expected travel time is used as the cost function for the NMPC. The travel time is a performance index that relates the amount of vehicles on a motorway at any one time with the changes in the timing of the traffic lights. Let $x(k) = [\rho^T(k), v^T(k), w^T(k)]^T$, and $u(k) = r(k)$, where $\rho(k)$, $v(k)$, $w(k)$, $r(k)$ are the vectors containing the densities, mean speeds, queues, and ramp-metering rates of all links, segments and origins of the motorway respectively. Thus, the performance index of the users of the motorway and the access roads over a prediction horizon N_p is given by:

$$\begin{aligned} L(\tilde{\mathbf{x}}(k), \tilde{\mathbf{u}}(k)) = T_s \sum_{h=k}^{k+N_p-1} \sum_{m \in \mathfrak{M}} \Bigg(\sum_{i \in \psi_m} \rho_{(m,i)}(h) L_m \lambda_m \\ + \alpha \sum_{o \in \mathfrak{O}} w_o(h) + \alpha_r (\Delta r_o(h))^2 \Bigg) \end{aligned} \tag{18}$$

where $\mathfrak{M}$ is the set of links, ψ_m denotes the set of segments of link m, $\mathfrak{O}$ denotes the set of origins, $\Delta r_o(k) = r_o(k) - r_o(k-1)$, and $\alpha, \alpha_r > 0$ are tuning parameters associated with the time spent by the users in the queues at the origins and with the smoothness of the changes of the control actions. Since the traffic on a motorway way is very sensitive to changes in the ramp-metering rates in Eq. (18) the norm of those changes over the prediction horizon is penalized instead of the value itself.

Since motorways are large-scale systems, implementation of centralized NMPC is not advisable [7]. Assume that the whole system can be decomposed into M subsystems r such that the local models have the form (4) for all r.

The decomposition could be made based on the inputs, or merging different segments [6]. Let $\mathfrak{M}_r$, Ψ_r, and $\mathfrak{O}_r$ denote the set of links, the set of segments, and the set of origins belonging to the subsystem r. Then, NDMPC for congestion management on a motorway is given by:

$$\begin{aligned}
&\min_{\tilde{\mathbf{u}}(k)} \sum_{r=1}^{M} \phi_r(\tilde{\mathbf{x}}(k), \tilde{\mathbf{u}}(k)) \\
&\mathbf{s.t.}: \\
&x_r(h+1) = f_{\mathrm{dx}r}(x(h), u_r(h), \tilde{\mathbf{u}}_{-r}(k)) \\
&\rho_{\min,(m,i)} \leq \rho_{(m,i)}(k) \leq \rho_{\max,(m,i)} \\
&w_{\min,o} \leq w_o(k) \leq w_{\max,o} \\
&v_{\min,(m,i)} \leq v_{(m,i)}(k) \leq v_{\max,(m,i)} \\
&r_{\min,o} \leq r_o(k) \leq r_{\max,o} \\
&m \in \mathfrak{M}_r,\ i \in \Psi_r,\ o \in \mathfrak{O}_r
\end{aligned} \tag{19}$$

with $f_{\mathrm{dx}r}(x(h), u_r(h), \tilde{\mathbf{u}}_{-r}(k))$ being the local prediction model. Furthermore, the system decomposition $\mathbb{X}_r$ and $\mathbb{U}_r$ are defined by the sets $\mathfrak{M}_r$, Ψ_r, and $\mathfrak{O}_r$ which determine the links and segments belonging to the subsystem r.

Then, the NMPC problem for travel time reduction can be equivalently formulated as in Eq. (6), with the corresponding definition for the variables and sets. Since each subsystem model requires the information from the remaining subsystems for making the prediction, the values of the local travel times $\phi_r(\tilde{\mathbf{x}}(k), \tilde{\mathbf{u}}(k))$ are coupled to each other. Thus, a situation arises belonging to the set of games G_{NDMPC}, where $\mathcal{N}$ is the set of local controllers trying to minimize their local cost function, over a feasible set $\Omega_r = \mathbb{X} \times \mathbb{U}$.

In addition, since the travel time of the users of the motorway can be expressed as $L(\tilde{\mathbf{x}}(k), \tilde{\mathbf{u}}(k)) = \sum_{r=1}^{M} \phi_r(\tilde{\mathbf{x}}(k), \tilde{\mathbf{u}}(k))$, and since the local controllers are able to communicate with each other, the game G_{NDMPC} is a discrete-time bargaining game $\{(\Theta(k), \eta(k))\}_{k=0}^{\infty}$. The outcome of the game G_{NDMPC} associated with the distributed congestion management scheme described in this section is obtained by the solution to the local optimization problems previously described in Eq. (11) considering for its implementation the algorithm 1, proposed in Sect. 1.

3.3 Simulation and Results

Consider the motorway shown in Fig. 2. It consists of a motorway with ten segments and nine on-ramps modeled as origins and it allows the entry of new vehicles to the motorway regulated by the traffic signals $r_i(k),\ i = 1, \ldots, 9$. A period of 12 h is simulated. The Matlab function *fmincon* is used for solving each local optimization problem. The solver used an interior point method. In order to test the performance of the proposed congestion management scheme a time-varying demand profile is used. Thus, the curve of demand shown in Fig. 3 is simulated at each on-ramp. The maximum number of entering cars per input is 600; and an

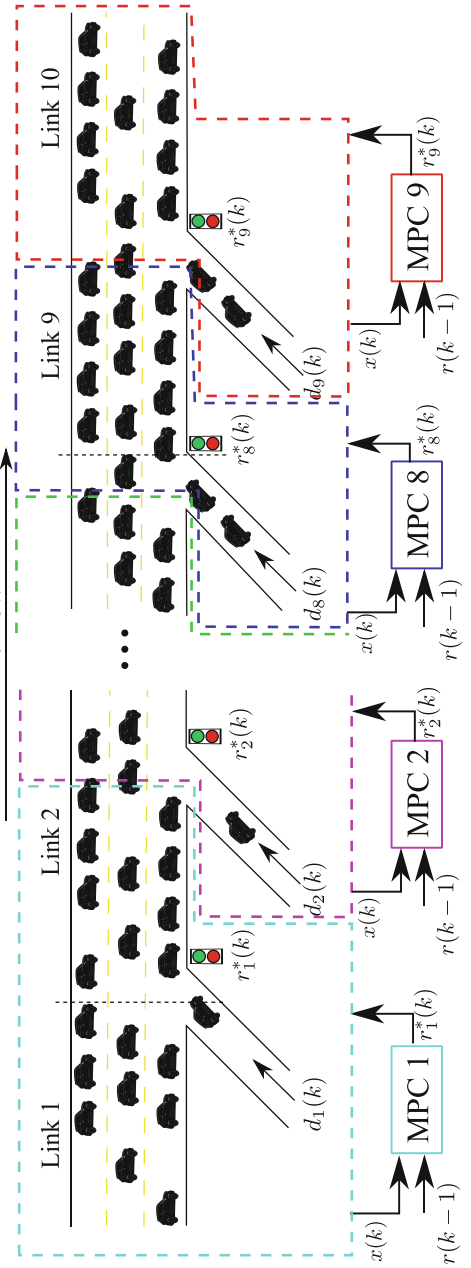

Fig. 2 Motorway used as a testbed for evaluating the performance of the proposed GT-NDMPC approach

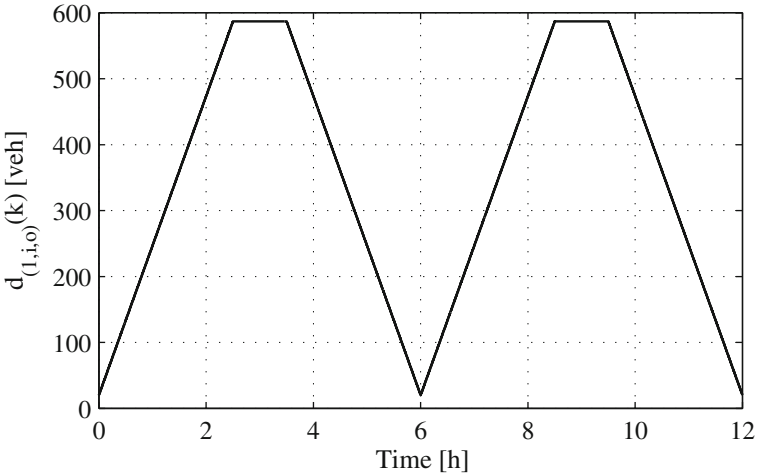

Fig. 3 Simulated demand at each on-ramp in the evaluation of the proposed GT-NDMPC approach in the case study for evaluating the performance of the proposed GT-NDMPC approach

initial queue of 10 vehicles is considered (see Fig. 3). For simulation purposes all links are assumed to have the same characteristics. The parameters for the simulations are taken from Zegeye et al. [54]. Note that in Fig. 2 the current control action is denoted by $r(k-1)$ while the control action to be locally applied is denoted by $r_i^*(k),\ i = 1, \ldots, 9$. In this case the prediction and control horizons are $N_\mathrm{p} = 10$ and $N_\mathrm{c} = 5$, respectively. For implementing the proposed scheme the whole system is divided into ten subsystems. Each subsystem has a link and an on-ramp (Fig. 2 shows the system partition). For comparison purposes a centralized NMPC is also implemented (with $N_\mathrm{p} = 10$ and $N_\mathrm{c} = 5$). The comparison between the proposed GT-NDMPC and a centralized NMPC is done because the centralized solution is the best possible. Therefore, NMPC provides the best baseline for evaluating the loss of performance of the motorway with the GT-NDMPC scheme.

From the formulation of the GT-NDMPC for congestion management purposes on the motorway of Fig. 2, the controllers at each on-ramp must share the current local control actions and the measurements of their local states. Based on this information, all controllers are able to identify the current operating conditions of the remaining controllers, and they are also able to decide which control actions should be locally applied with the purpose of minimizing their effect on the performance of the other local controllers. It is worth pointing out that the information exchange can be done using any full duplex communication channel.

Figure 4a and b show the cycle for each on-ramp light. From these figures it is evident that the centralized and the proposed congestion management schemes generate different sequences of control actions at times with higher demands. Moreover, in the off-peak time intervals, the same constant control actions are used for managing the congestion at the motorway. It is noteworthy that although at peak

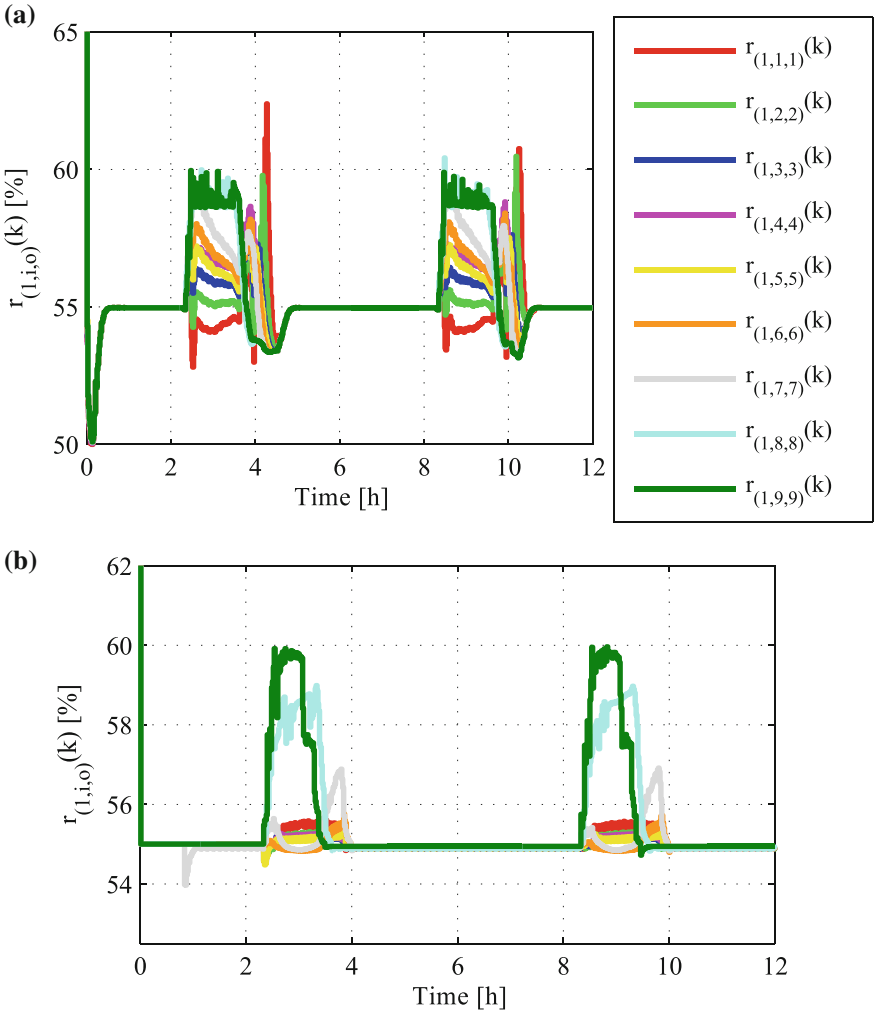

Fig. 4 Comparison of control actions at each on-ramp for the centralized and proposed schemes. **a** Control actions at each on-ramp computed using a centralized NMPC approach. **b** Control actions at each on-ramp computed by the proposed GT-NDMPC approach

demand the traffic network presents a congestion scenario (600 vehicles are expecting to get onto the motorway at each on-ramp), blocking actions are not required, i.e., flow on the motorway and on the on-ramps is reduced. This is reflected in the behavior of the speed and density of vehicles.

Figure 5a and b present the evolution along the simulation of the speed at the different links when the control actions are computed by the NMPC and the GT-NDMPC respectively. In these figures, it is clear that as the demand at the

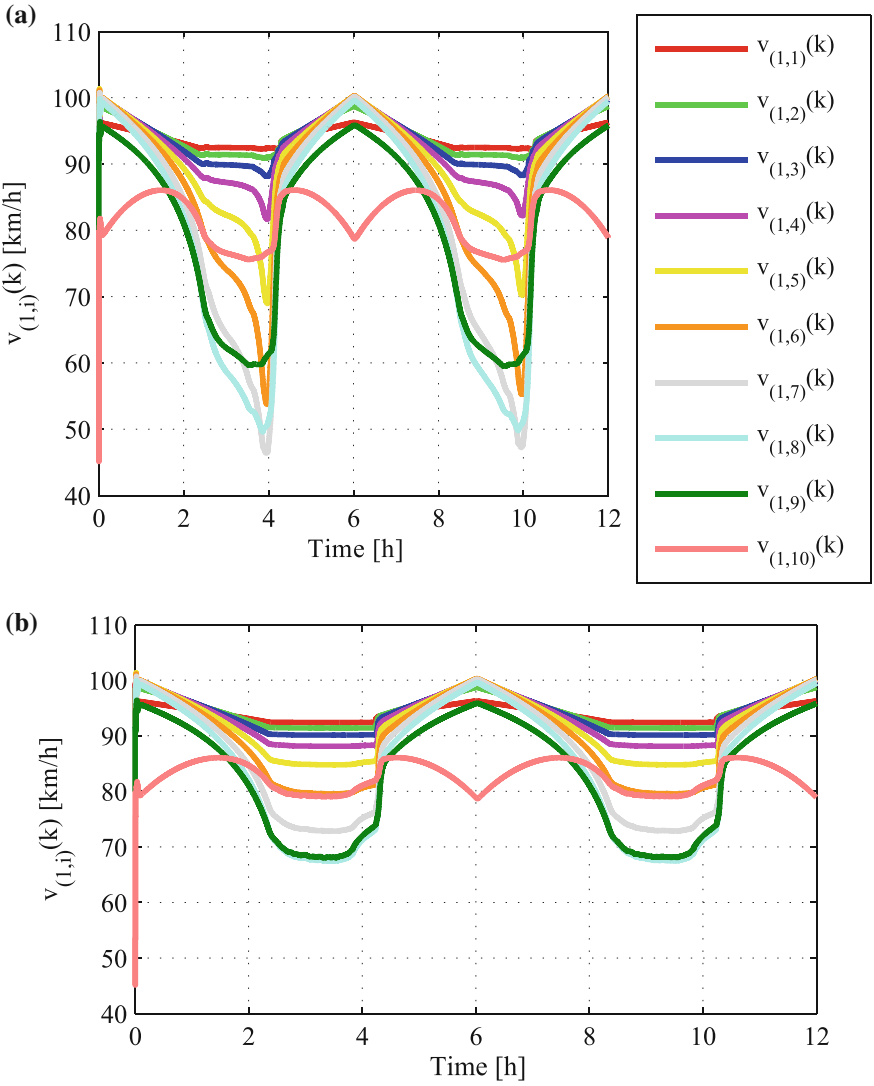

Fig. 5 Comparison of speed behavior between the proposed and centralized approaches. **a** Behavior of the speed with the NMPC approach. **b** Behavior of the speed with the proposed GT-NDMPC approach

on-ramps increases the speed at the links decreases, reaching the lowest value at the link (1,7) when the control actions are computed by the NMPC. It is noteworthy that the speed distribution over the motorway depends on the control scheme used for computing the control actions. In fact, the speed distribution with the proposed

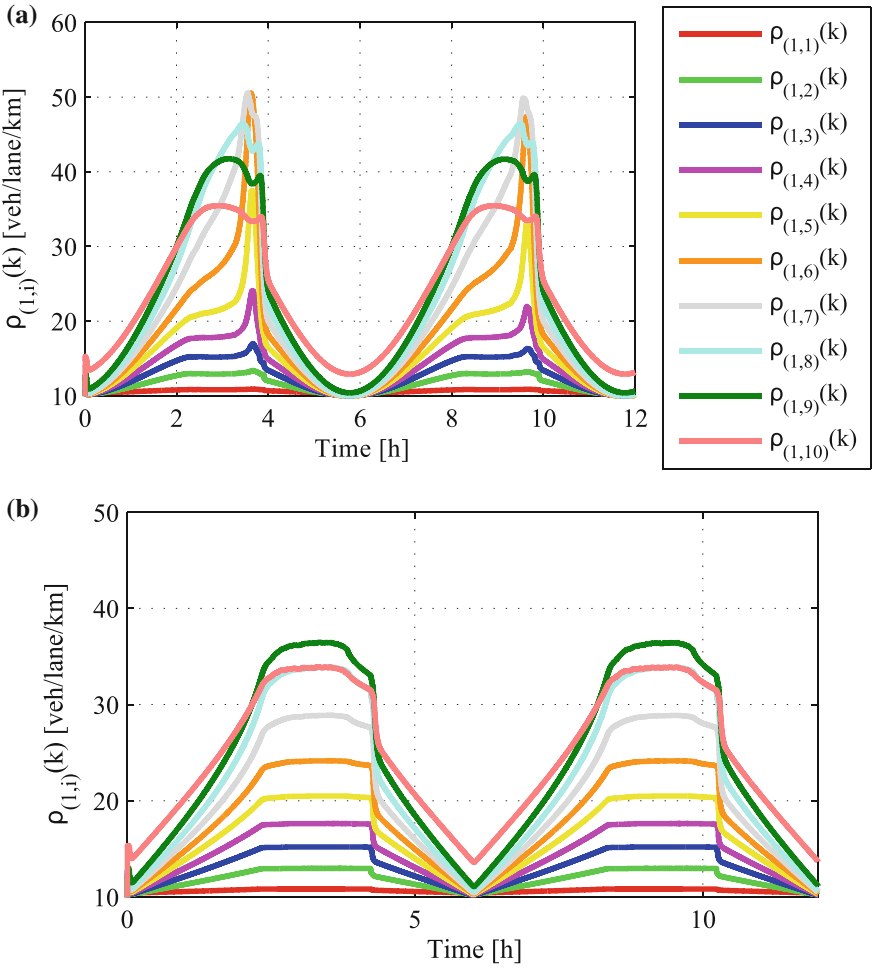

Fig. 6 Comparison of densities between centralized and proposed schemes. **a** Time evolution of the density when the control actions are computed by an NMPC approach. **b** Time evolution of the density when the control actions are computed by the proposed GT-NDMPC approach

GT-NDMPC was [60, 100]; lower than the speed distribution with the NMPC (here speed distribution is understood as the range where all the speed trajectories are moving).

Figure 6a and b show the time evolution of the density of vehicles at each link. From these figures it is possible to infer that the centralized NMPC allows a better use of the traffic infrastructure. Since NMPC performed a larger reduction of speed than the GT-NDMPC, the density of vehicles in the motorway increases. Hence, the

expected length of the queues at the on-ramps decreases. It is worth pointing out that despite the demand, the control schemes kept the density below the critical density. Thus the traffic system remained stable along the simulation.

Although GT-NDMPC presents a loss of performance with respect to the centralized NMPC, the loss of performance is not significant. Let the total time spent (TTS) by the vehicles on the motorway and the entrance ramps over the entire simulation period be defined as:

$$TTS = \sum_{l=1}^{N_{\text{sim}}} \left(\sum_{m \in \mathfrak{M}} \sum_{i \in \psi_m} \rho_{i,m}(l) L_m \lambda_m + \sum_{o \in \mathfrak{O}} w_o(l) \right) T_s \tag{20}$$

where N_{sim} is the number of simulation steps. Another performance index used for evaluating control schemes with application to motorways is the Total Waiting Time (TWT) [43], this index is computed as:

$$TWT = \sum_{i=1}^{N_{\text{sim}}} \left(\sum_{m \in \psi_0} w_m(l) \right) \tag{21}$$

Table 4 presents the TTS and the TWT for two optimization-based control techniques, namely, the centralized NMPC, the proposed GT-NDMPC, and the ALINEA method reported in Haj-Salem et al. [10], Papageorgiou et al. [35] which is a simpler approach for traffic control on motorways. In fact, the control action in the ALINEA method is a sort of integral state-feedback where $r_i(k+1) = r_i(k) + K(\rho_{\text{cr},m} - \rho_{(m,i)}(k))$, with K the gain of the controller. Note that, ALINEA is a simpler control law and the optimization-based techniques perform better (in terms of the TTS and the TWT indexes) on the motorway presented in this chapter. In fact, significant improvements are achieved even with the proposed GT-NDMPC, which (due to system partition) has a poorer performance compared to the centralized NMPC. The TTS results shown in Table 4 also confirm the loss of performance using GT-NDMPC; however, a distributed control scheme can be used as an alternative for controlling large-scale traffic networks. Note that although the TWT increases by about 77 % in the GT-NDMPC case with respect to the centralized case, the difference in the TTS is just about 4 %. This means that with GT-NDMPC there are more vehicles waiting in the queues but once they are on the motorway they are efficiently evacuated, resulting in a reduction of their TTS.

Table 4 TTS and TWT for the ALINEA, NMPC, and GT-NDMPC control schemes

Controller	TTS	Relative difference (%)	TWT	Relative difference (%)
ALINEA	3,998	0	291,683	0
NMPC	3,677	8.03	131,485	54.92
GT-NDMPC	3,833	4.127	231,830	20.51

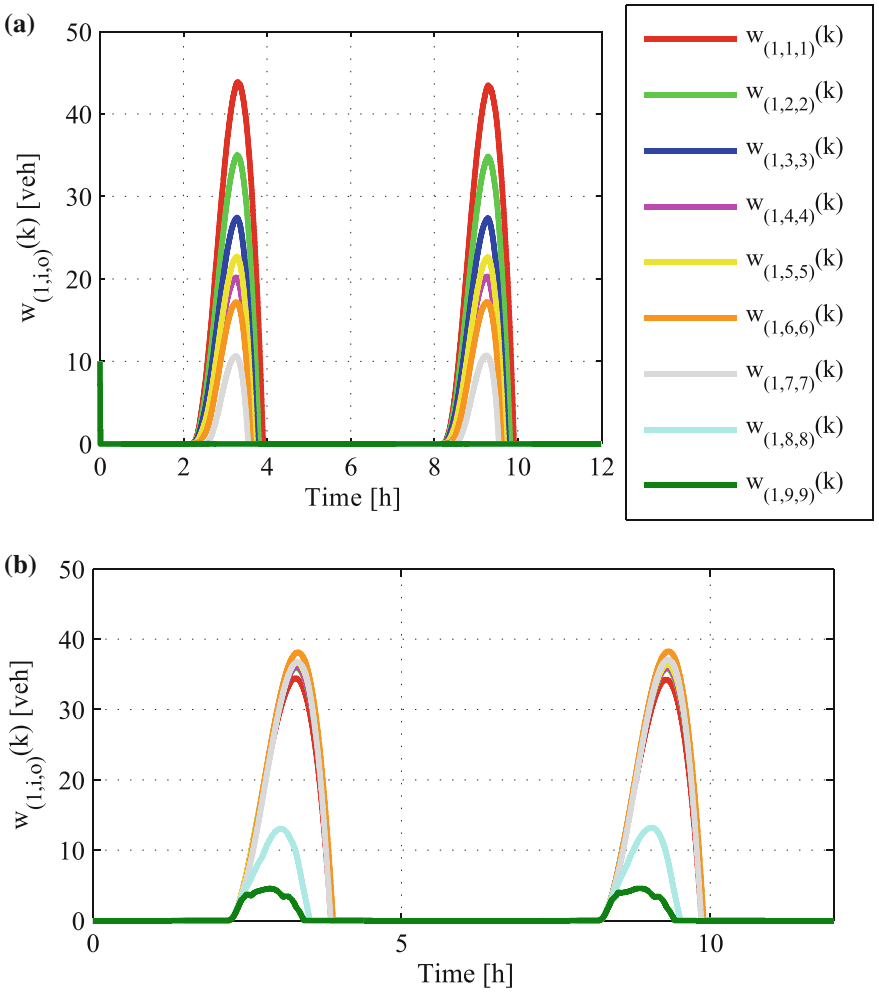

Fig. 7 Comparison of queues between the centralized and proposed schemes. **a** Time evolution of the queues when the control actions are computed by a centralized NMPC approach. **b** Time evolution of the queues when the control actions are computed by the proposed GT-NDMPC approach

Figure 7a and b show the evolution of the queues at each on-ramp. It is evident that the centralized NMPC maintains the queues at almost all on-ramps at the same length while in the case of the motorway controlled by the GT-NDMPC each on-ramp has its own queue length, resulting from the negotiation among controllers. Consequently, a better use of the infrastructure is achieved with the centralized NMPC, which is able to manage the congestion on the motorway. For instance the total waiting time index for the centralized MPC is significantly lower than in the case of the GT-NDMPC.

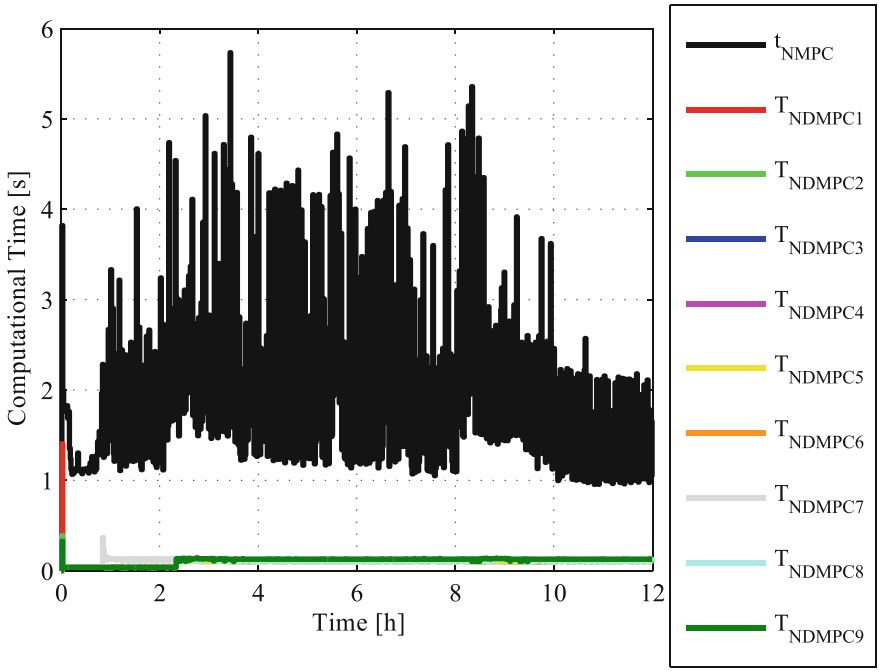

Fig. 8 Comparison of the computational time of both centralized NMPC and GT-NDMPC schemes. Here $t_{\text{NMPC}}(k)$ represents the time taken by the centralized NMPC for computing the control actions at time step k, while $t_{\text{NDMPC}r}(k)$, $r = 1, \ldots, 9$ represents the time taken by each local controller for computing the local control actions at the same time step

Figure 8 presents the computational time associated with both the solution of the centralized NMPC and that of the proposed GT-NDMPC. In Fig. 8, the time involved in the solution of each local controller was considered because it is assumed that all local controllers are working at the same time. Thus the computational time of the proposed GT-NDMPC is determined by the slowest local controller. From Fig. 8, it is evident that (as expected) the time required by the GT-NDMPC for computing the local control actions is lower than the time required by the centralized NMPC. In fact, the computational time of the centralized NMPC is higher by an order of magnitude. Accordingly, from the point of view of the computational time, the GT-NDMPC scales better than the NMPC. It is worth to point out that the sample time T_s is 60 s. Assume that there is an exponential dependence of the computational time on the number of on-ramps on the motorway. Thus with the centralized NMPC a maximum of 28 on-ramps can be controlled, while with the GT-NDMPC ideally up to 648 on-ramps can be controlled before requiring to increase the sampling time. Previous scaling results were obtained following the rules $t_{\text{NMPC}} = 0.02707\exp(0.2n)$ and $t_{\text{NDMPC}} = 0.091\exp(0.01n)$ for centralized NMPC and GT-NDMPC respectively, with n the number of on-ramps.

4 Bargaining-Game-Based Coordination for Urban Congestion Management

4.1 Urban Traffic Model

As in Sect. 3, let us begin by introducing some concepts and notations related to the traffic model used here, viz. the Macroscopic Simplified Urban Traffic Model (S model) described in Lin et al. [21, 22]. Similar to the motorway case, in urban traffic models the concepts of links and origins are also used. In this model J denotes the set of nodes or intersections, L denotes the set of links or roads, $I_{(u,d)} \subset J$ denotes the set of input nodes, and $O_{(u,d)} \subset J$ denotes the set of output nodes. Hence, each link is defined by its input and output nodes, i.e. by the pair (u, d), $u, d \in J$ marking the starting and ending intersections respectively. The S model has the particularity that each intersection takes the corresponding cycle time as its simulation time interval. Therefore, the simulation time intervals might be different for each intersection. So the input and output flow rates of each link are averaged over the cycle times (the flows leaving or entering links are described with flow rates rather than with numbers of cars Lin et al. [22]). For a link $(u, d) \in L$, let c_d be the cycle time with k_d its corresponding time step counter. Figure 9 illustrates the concepts previously introduced.

Let $\alpha^{\text{leave}}_{(u,d,o)}(k_d)$ denote the leaving flow rate of link (u, d) turning to the output link o. Let $g_{(u,d,o)}(k_d)$ be the green time signal duration allowing the vehicles to flow from link (u,d) to output link o. Then, $\alpha^{\text{leave}}_{(u,d,o)}(k_d)$ can be computed as the minimum value out of the capacity of the intersection, the number of cars waiting or arriving to the next intersection, and the available space in the downstream link:

$$\alpha^{\text{leave}}_{(u,d,o)}(k_d) = \min\left\{ \beta_{(u,d,o)}(k_d)\mu_{(u,d)} \frac{g_{(u,d,o)}(k_d)}{c_d}, \frac{g_{(u,d,o)}(k_d)}{c_d} + \alpha^{\text{arrive}}_{(u,d,o)}(k_d), \right.$$
$$\left. \frac{\beta_{(u,d,o)}(k_d)}{\sum_{u \in I_{(d,o)}} \beta_{(u,d,o)}(k_d)} \frac{C_{(d,o)} - n_{(d,o)}}{c_d} \right\} \tag{22}$$

where $\beta_{(u,d,o)}(k_d)$ is the relative fraction of the traffic at link (u,d) turning towards output link o at time step k_d, $\mu_{(u,d)}$ is the saturated flow rate leaving link (u,d), $\alpha^{\text{arrive}}_{(u,d,o)}(k_d)$ is the arriving average flow rate of the substream going towards o, $C_{(d,o)}$ is the storage capacity of the link (d,o) expressed in number of vehicles, and $n_{(d,o)}(k_d)$ is the number of vehicles at link (d,o) at time step k_d. In (22) $\alpha^{\text{arrive}}_{(u,d,o)}(k_d)$ is calculated as the fraction of the input flow rate of link (u,d) the destination of which is the output link o. Let $\alpha^{\text{arrive}}_{(u,d)}(k_d)$ be the average flow rate arriving at the end of the queue at link (u,d) at time step k_d. Thus:

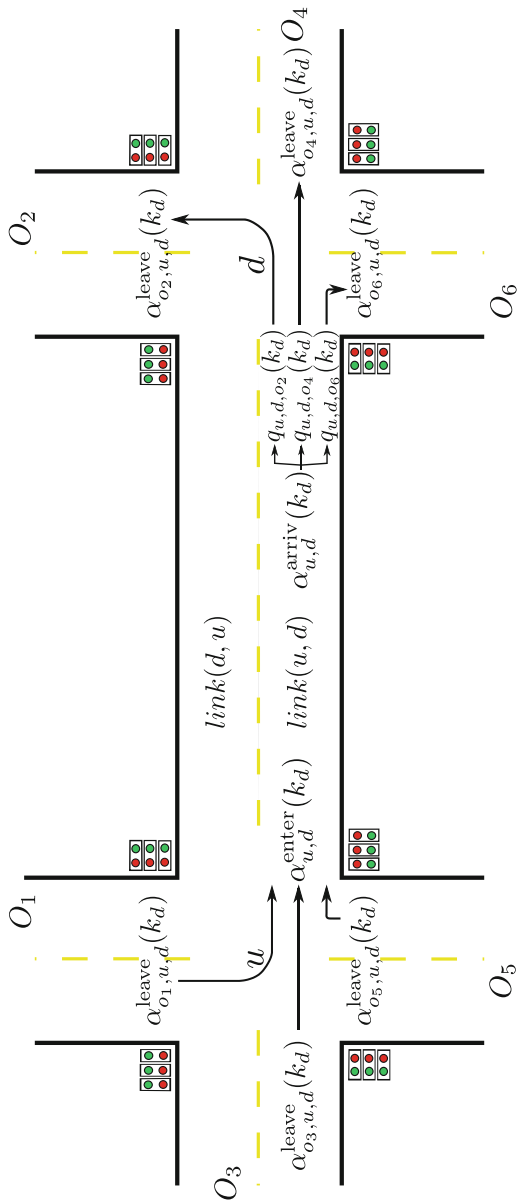

Fig. 9 Two interconnected intersections in an urban traffic network

$$\alpha^{\text{arrive}}_{(u,d,o)}(k_d) = \beta_{(u,d,o)}(k_d)\alpha^{\text{arrive}}_{(u,d)}(k_d) \tag{23}$$

with $\alpha^{\text{arrive}}_{(u,d)}(k_d)$ defined as:

$$\alpha^{\text{arrive}}_{(u,d)}(k_d) = \frac{c_d - \gamma(k_d)}{c_d}\alpha^{\text{enter}}_{(u,d)}(k_d - \delta(k_d)) + \frac{\gamma(k_d)}{c_d}\alpha^{\text{enter}}_{(u,d)}(k_d - \delta(k_d) - 1) \tag{24}$$

where $\alpha^{\text{enter}}_{(u,d)}(k_d)$ is the average flow rate entering to the link (u,d) at time step k_d $\gamma(k_d)$, and $\delta(k_d)$ being functions depending on the vehicles that arrived at the queues of the link (u,d) (see Appendix A of Lin et al. [22] for details). Note that $\alpha^{\text{enter}}_{(u,d)}(k_d) = \sum_{i \in I_{(i,u,d)}} \alpha^{\text{leave}}_{(i,u,d)}(k_d)$.

In order to derive a model for a traffic network, a balance between entering and leaving vehicles is performed. Taking the definitions for $\alpha^{\text{arrive}}_{(u,d)}(k_d)$ and $\alpha^{\text{leave}}_{(u,d)}(k_d)$ into account, and assuming that the vehicles are in the queue corresponding to their output destination o, the dynamic evolution of the number of vehicles and queues at link (u,d) is given by:

$$n_{(u,d)}(k_d + 1) = n_{(u,d)}(k_d) + \left(\alpha^{\text{enter}}_{(u,d)}(k_d) - \alpha^{\text{leave}}_{(u,d)}(k_d)\right)c_d \tag{25}$$

$$q_{(u,d,o)}(k_d + 1) = q_{(u,d,o)}(k_d) + \left(\alpha^{\text{arrive}}_{(u,d,o)}(k_d) - \alpha^{\text{leave}}_{(u,d,o)}(k_d)\right)c_d \tag{26}$$

where the number of vehicles waiting in the queue is given by the sum of the vehicles waiting in each individual queue, viz., $q_{(u,o)}(k_d) = \sum_{o \in O_{(u,d)}} q_{(u,d,o)}(k_d)$.

4.2 Bargaining-Game Approach to Congestion Management in Urban Traffic

For an urban traffic network, let $x(k) = [n^T(k), q^T(k)]^T$ be the state vector, where $n(k)$ and $q(k)$ are vectors whose components are the number of vehicles and the queues at each link of the network. Moreover, let $u(k) = g(k)$ be the input vector, with $g(k)$ a vector whose components are the green signal time durations of each traffic light in the network. Furthermore, assume that all intersections in the network have the same cycle time c_d with k its corresponding time step counter. Then, the urban traffic model of (25)–(26) can be written as Eq. (1).

Thus, this urban traffic model can be used as prediction model for implementing NDMPC. Again, the idea of this traffic network is to provide a control strategy for congestion management. Hence, the performance index (travel time) is used as the cost function. From Eqs. (25)–(26) the expected travel time inside a prediction horizon N_p is determined by Eq. (27) Lin et al. [21, 22]:

$$L(\tilde{\mathbf{x}}(k), \tilde{\mathbf{u}}(k)) = c_d \sum_{h=k}^{k+N_\mathrm{p}-1} \left(\sum_{(u,d)\in L} n_{(u,d)}(h) \right) \tag{27}$$

As in the case of motorways, urban traffic networks are large-scale systems and therefore solving the optimization problem (3) is not feasible in real-time. Assume that the whole urban traffic network can be decomposed into M subsystems r such that each local model can be expressed as Eq. (4).

Let L_r denote the set of links (u,d) belonging to subsystem r. Let $\mathfrak{P} = \{\mathfrak{p}_1, \mathfrak{p}_2, \ldots, \mathfrak{p}_T\}$ be the set of intersections in the urban traffic network, where $\mathfrak{p}_\mathrm{i},\ i = 1, \ldots, T$ are its elements. Let $\mathfrak{P}_r \subset \mathfrak{P}$ be the set of intersections belonging to subsystem r. Then, from Eq. (27) and the system decomposition, the NMPC for congestion management in an urban traffic network is given by:

$$\begin{aligned}
&\min_{\tilde{\mathbf{u}}(k)} \sum_{r=1}^{M} \phi_r(\tilde{\mathbf{x}}(k), \tilde{\mathbf{u}}(k)) \\
&\mathbf{s.t.}: \\
&x_r(h+1) = f_{\mathrm{d}xr}(x(h), u_r(h), \tilde{\mathbf{u}}_{-r}(k)) \\
&0 \le n_{(u,d)}(k) \le C_{(u,d)} \\
&q_{(u,d,o)}(k) \ge 0 \\
&0 \le g_{(u,d,o)}(k) \le c_d \\
&\sum_{(u,d)\in\mathfrak{p}_i} g_{(u,d,o)}(k) = c_d \\
&(u,d) \in L_r,\ \mathfrak{p}_i \in \mathfrak{P}_r
\end{aligned} \tag{28}$$

with $f_{\mathrm{d}xr}(x(h), u_r(h), \tilde{\mathbf{u}}_{-r}(k))$ being the local prediction model. Also, from the system decomposition, the sets $\mathbb{X}_r$ and $\mathbb{U}_r$ are determined by the sets L_r and $\mathfrak{P}_r$ defining the links and intersections belonging to each subsystem. Note that the optimization problem (28) has the same form as the optimization problem (6). Therefore, a calculated circumstance belonging to the discrete-time dynamic bargaining games $\{(\Theta(k), \eta(k))\}_{k=0}^{\infty}$ arises.

In this circumstance or game each local controller has to make a trade-off between its local control objective $\phi_r(\tilde{\mathbf{x}}(k), \tilde{\mathbf{u}}(k))$ and the common goal $L(\tilde{\mathbf{x}}(k), \tilde{\mathbf{u}}(k))$. It is worth pointing out that subsystems are able to achieve a mutual benefit because the common goal $L(\tilde{\mathbf{x}}(k), \tilde{\mathbf{u}}(k))$ provides them with the opportunity to collaborate. Moreover, in the resulting game $\{(\Theta(k), \eta(k))\}_{k=0}^{\infty}$ for the traffic network decomposition $\mathcal{N}$ is the set of local controllers, their preferences are determined by the minimization of the local cost $\phi_r(\tilde{\mathbf{x}}(k), \tilde{\mathbf{u}}(k))$, and the decision space is given by $\Omega_r = \mathbb{X}_r \times \mathbb{U}_r$. Furthermore, the decision environment evolves according to the model of the traffic network and the local model used for predicting the trajectories of the local states. Let $\Xi_r(\tilde{\mathbf{x}}(k), \tilde{\mathbf{u}}(k))$ be the set resulting from the intersection of Ω_r with the space defined by the local prediction model. Then, in the game associated with the distributed congestion management in urban networks $\Theta(k) := \{(\phi_1(\tilde{\mathbf{x}}(k), \tilde{\mathbf{u}}(k)), \ldots, \phi_M(\tilde{\mathbf{x}}(k), \tilde{\mathbf{u}}(k))) \in \mathbb{R}^M | (\tilde{\mathbf{x}}(k), \tilde{\mathbf{u}}(k))_r \in \Xi_r(\tilde{\mathbf{x}}(k), \tilde{\mathbf{u}}(k))\}$, with

$(\tilde{\mathbf{x}}(k), \tilde{\mathbf{u}}(k))_r$ the tuple defining the value of $\phi_r(\tilde{\mathbf{x}}(k), \tilde{\mathbf{u}}(k))$. Finally, a solution to the game G_{NDMPC} resulting from the urban traffic network decomposition can be obtained by solving the same local optimization problems of (11), implemented with the negotiation model proposed in Sect. 1.

4.3 Simulation and Results

For evaluating the performance of the proposed congestion management scheme an urban traffic network with three intersections is proposed. Each intersection has four links with three lanes, where each lane has a length of 452 m, and a capacity of 192 vehicles per lane. For simulation purposes, it is assumed that the vehicles have a length of 7 m and a free flow speed of 50 km/h. Moreover, a cycle time of 50 s and initial queues of 5 vehicles in each link are also considered. As in the case of the motorway, the Matlab function *fmincon* is used for solving each local optimization problem. The solver uses a interior point algorithm. Figure 10 shows the urban network used as a case study. Moreover, for implementing the proposed distributed congestion management scheme the urban traffic network is divided into three subsystems as illustrated in Fig. 10. Each subsystem is composed of the four links at interacting in the intersections.

In the network of Fig. 10 (and according to the notation used in that figure) the output flow rate for origins o_1 to o_6 is assumed constant and equal to 460 veh/h; the flow of vehicles entering through links (1,*a*) and (6,*a*) is assumed constant and equal to 705 veh/h; through links (2,*b*) and (7,*b*) 903 veh/h; through links (3,*c*) and (8,*c*) 902 veh/h; through link (5,*c*) 300 veh/h; and through link (4,*a*) it is assumed to be time-varying with the trapezoidal shape shown in Fig. 11b. Furthermore, in order to reduce the complexity of the optimization problems, two operational modes for the traffic lights are considered. As shown in Fig. 11a, in each operational mode several destinations at each link in an intersection are allowed. As a consequence, one decision variable is required for assigning the green light time to each flow rate at each intersection [20, 21, 22] (the sum of the times assigned to each operational mode must be equal to the cycle time).

As in the case of the motorways, in the distributed congestion management scheme for urban traffic the local controllers should exchange their measurements of the local states as well as their current local control actions. This allows each local controller deciding on the control action to be locally applied following the **focusing on others** criteria. That is, each local controller selects the feasible control action that minimizes the effect of the local decisions on the performance of the remaining controllers.

Figure 12a shows the evolution of the number of vehicles waiting in the queues of the urban traffic network. In this figure the centralized scheme for congestion management exhibits longer queues than the distributed scheme. However, the duration of the queues with NMPC is not longer than the duration with GT-NDMPC.

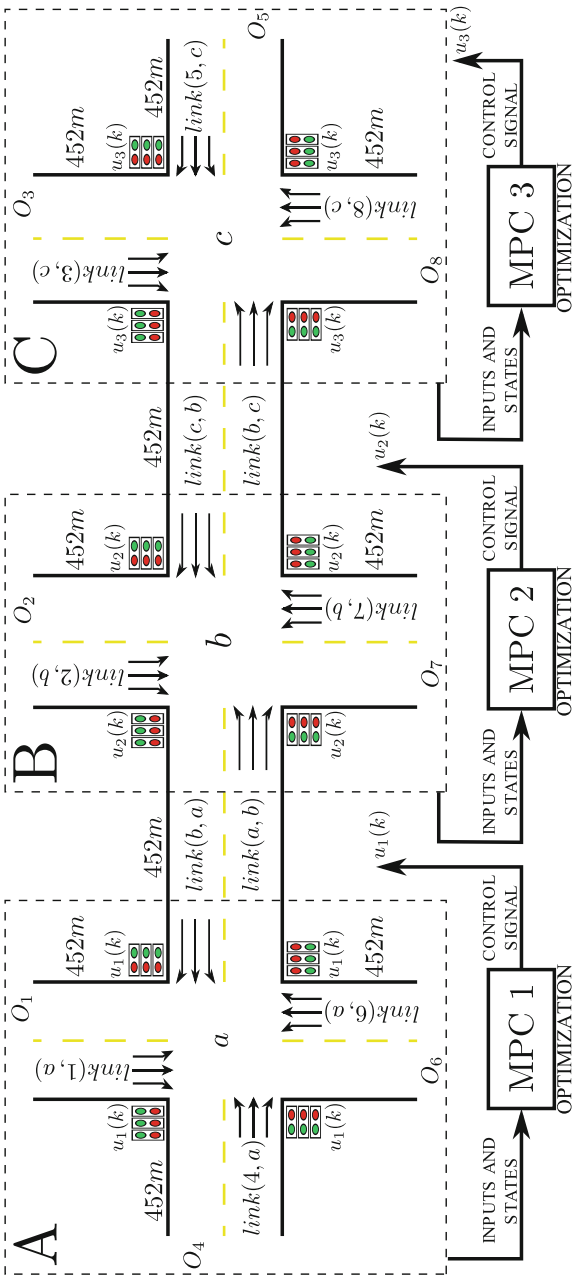

Fig. 10 Urban traffic network used as a testbed for the proposed congestion management scheme

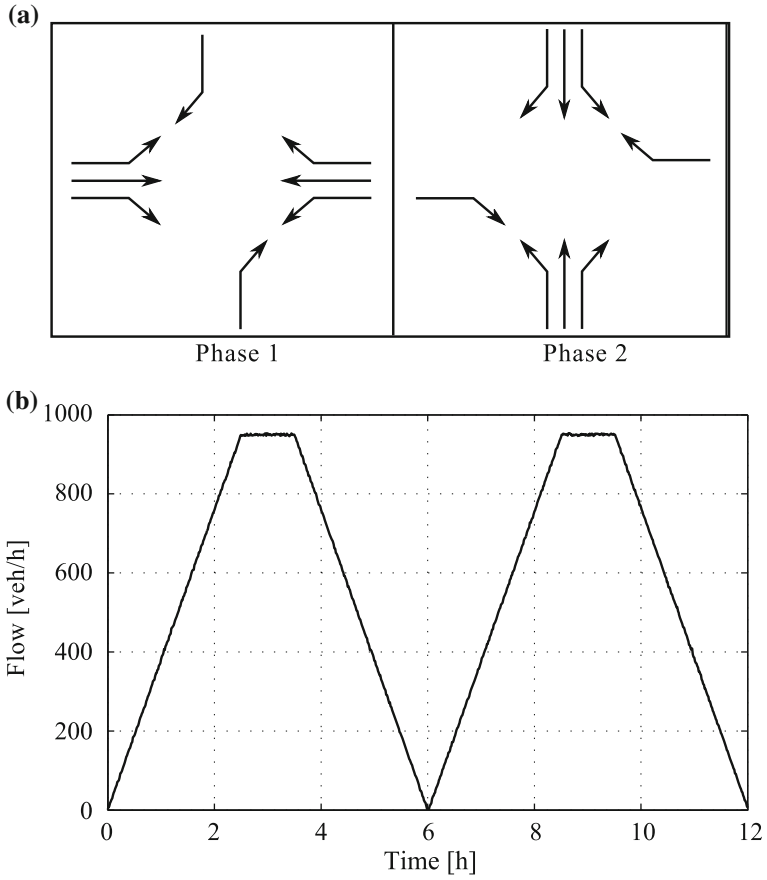

Fig. 11 Parameters of the simulation. **a** Operational modes for the traffic lights considered in the simulations. **b** Flow rate of link (4,a) used in the simulations

Recall that centralized NMPC takes all interactions into account in its predictions. Therefore, this control scheme is able to manage the increasing size of the queues more efficiently than the distributed scheme. There is a concept associated with the length of the queues that measures the time spent by the vehicles running with free flow speed from the beginning of a link until reaching the tail of the queue corresponding to its destination o. Figure 12b shows the aggregate behavior of the total time of vehicles at free flow speed (delay time) along the network. Note that when the length of the queues increases, the total time of vehicles traveling in free flow speed decreases, as expected.

For performing congestion management, the green light time must be assigned to each flow rate. Figure 13a and b show the green time for phases 1 and 2 at the intersection a (see Fig. 10). Note that the total time of the operative modes is equal to 50 s, which is the cycle time. In addition, from Fig. 13a and b it is evident that the

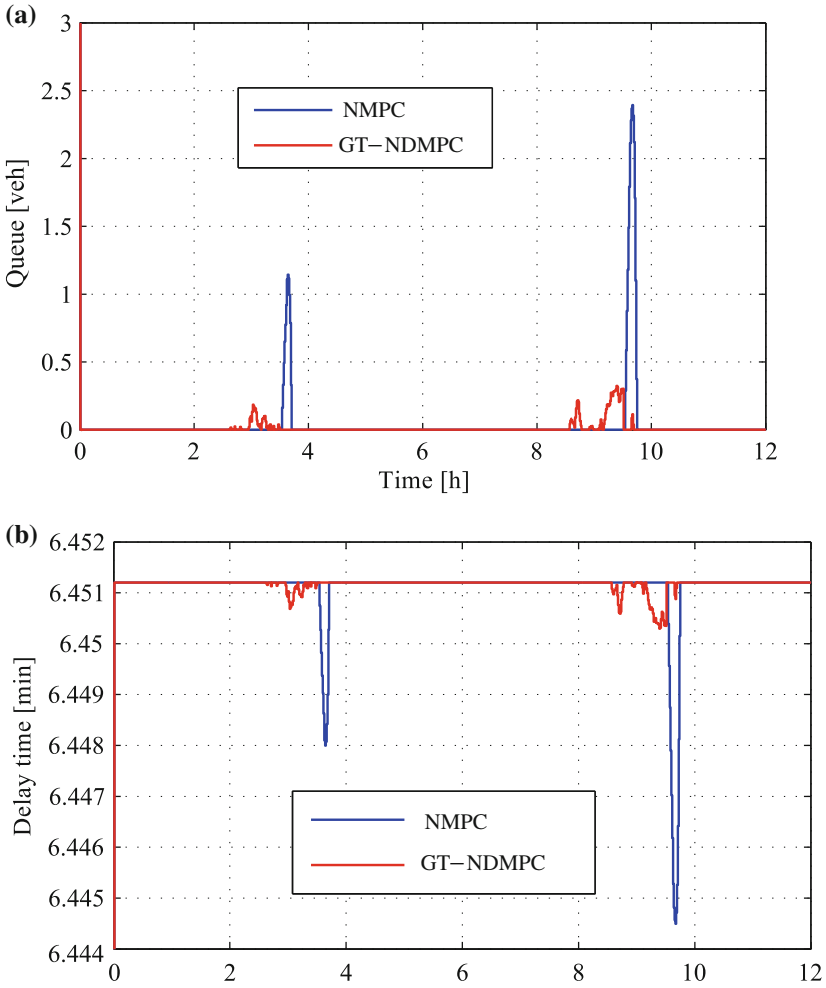

Fig. 12 Comparison of the total number of vehicles in the queue and at free flow speed for both centralized and proposed approaches. **a** The total number of vehicles waiting in the queues along the traffic network. **b** Total time of vehicles at free flow speed in the traffic network with the implemented NMPC schemes

GT-NDMPC approach uses more aggressive control actions than the centralized approach, viz. the changes of the control actions of the GT-NDMPC are bigger than the changes of the control actions in the centralized NMPC. This allows the distributed congestion management scheme to have queues that are not longer than the queues with the centralized NMPC approach.

A comparison of the total time spent by the users of the traffic network, the vehicles waiting in the queues, and the total delay time for several congestion management schemes is presented in Table 5. The adaptive SCOOT method was

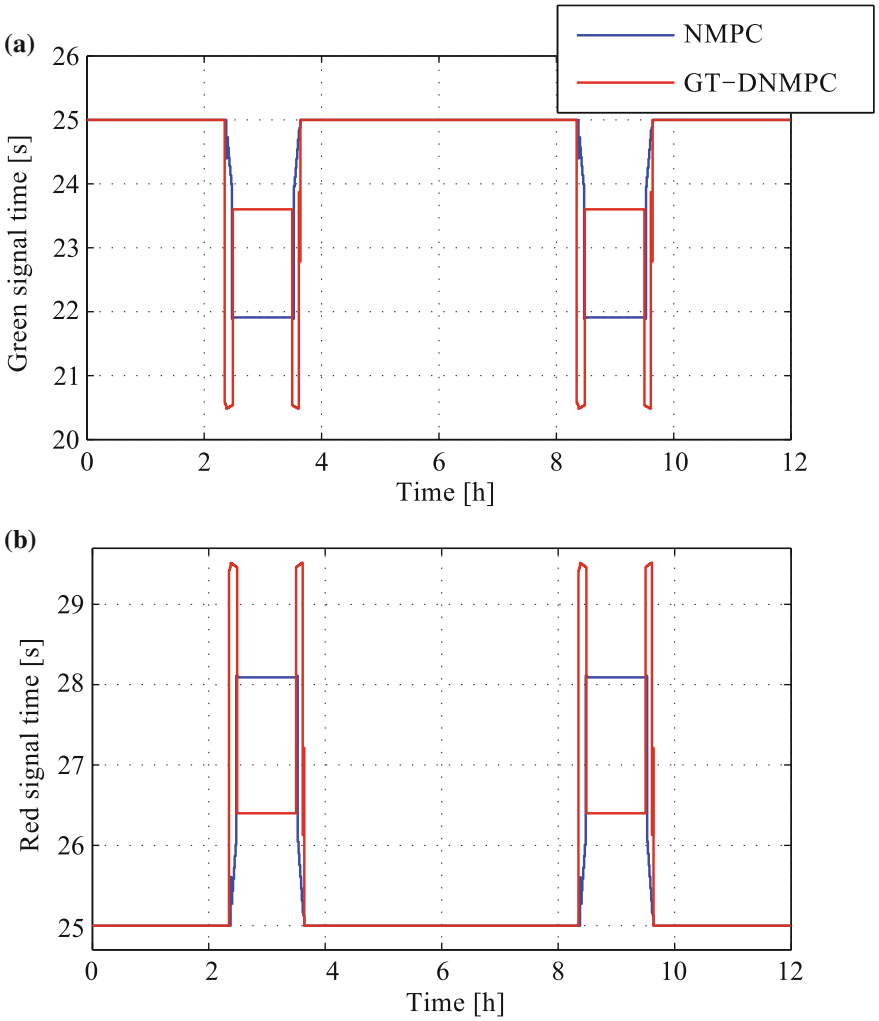

Fig. 13 Green time signal assigned by the controllers in intersection *a*. **a** Phase 1. **b** Phase 2

included because it is one of the optimization-based alternatives for traffic control in urban networks. Moreover, the SCOOT method proposed the concept of the green wave in order to reduce the complexity of the resulting optimization problem. In this table it is evident that the performance of centralized and GT-NDMPC schemes implemented for congestion management in urban networks is almost the same, while other schemes severely increased the TVQ, keeping a similar TTS. This validates the possibility of using distributed schemes based on game theory for congestion management in urban traffic networks.

Table 5 Comparison of total time spent (TTS) for a vehicle, and total vehicles in the queues (TVQ) for centralized, distributed, adaptive SCOOT, and fixed time schemes

Configuration	TTS [veh · h]	TVQ [veh]
Centralized NMPC	3,498	7,744
GT-NDMPC	3,522	9,369
State-feedback	3,769	25,612
SCOOT	3,961	38,857
Fixed time	5,142	124,125

Table 6 presents a comparison of the computational times in the urban traffic network for the centralized NMPC, the proposed GT-NDMPC, and the adaptive SCOOT method. As shown in Table 6, despite the simplifications involved in the SCOOT method, the proposed GT-NDMPC requires a lower computation time. Furthermore, with the GT-NDMPC the heuristics behind the SCOOT method (which may hinder the application of this method in large urban networks) are avoided.

4.4 Disagreement Point Analysis

From a game theory point of view, in both the motorway and urban traffic models it was observed that each local controller behaved according to its own desires and preferences. Figure 14a and b show the evolution of the disagreement point in each case (motorway and urban network respectively).

Note that in Fig. 14a and b the evolution of the disagreement point is almost the same for all controllers in the case of the motorway. This is because the similarities of the subsystems in this case (recall that all segment parameters and on-ramp demands are the same). Thus, this game is close to being a symmetric game. However, in the case of the urban traffic network the behavior of the disagreement points is different for each subsystem. This is in accordance with the flow rate specifications for the links (recall that the flow rates at the boundary of the network are different). Thus, this game is clearly non-symmetric. Note that the disagreement point trajectories present some oscillations along the simulation, which are more evident in the case of the urban traffic network. Such behavior is due to the decision making each controller performs. When they decide to cooperate the disagreement

Table 6 Comparison between computational times for centralized NMPC, for each subsystem in the proposed GT-NDMPC, and for the adaptive SCOOT method

Configuration	Computational time [s]
Centralized NMPC	390.6207
Subsystem 1	60.2311
Subsystem 2	95.2946
Subsystem 3	88.4602
SCOOT	164.6238

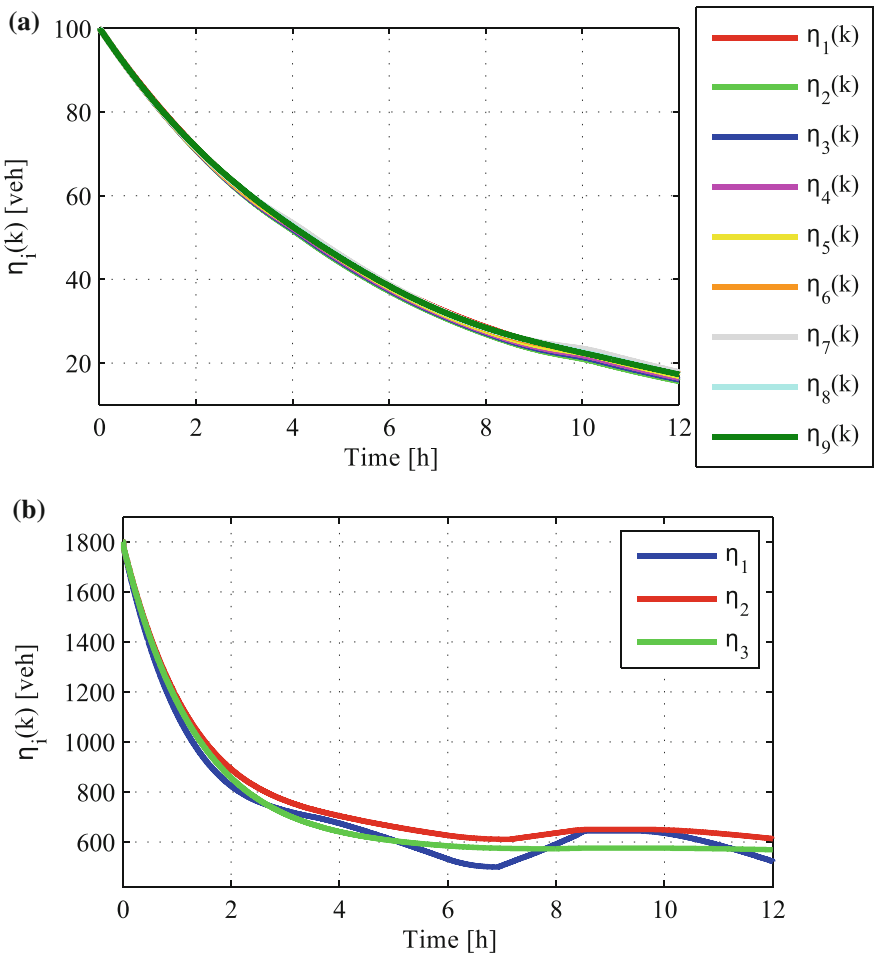

Fig. 14 Evolution of the disagreement point in the congestion management. **a** Motorways. **b** Urban traffic

point decreases, but when they decide not to cooperate the disagreement point increases. The decision regarding cooperation is defined by the perceived benefit from the cooperative behavior. So, if there are no alternatives such that the local performance index is less than the disagreement point, the controller decides not to cooperate.

5 Conclusion

In this chapter, bargaining game theory was used as a mathematical framework for analyzing the game arising from the distributed model predictive control formulation. In this way, the non-linear model predictive control –NMPC– problem was initially presented. Then the system was decomposed; motivated by the fact that implementation of NMPC in real large-scale systems is not advisable. As a consequence of the system decomposition, the NMPC problem became a set of coupled optimization problems. Since each optimization problem was locally solved, a trade-off between local and global system performance was required. Moreover, since the controllers solving the local optimization problems were able to communicate with each other, bargaining among controllers was possible. Hence, the distributed model predictive control –DMPC– formulation resulting from system decomposition can be characterized as a bargaining game (GT-NDMPC).

Once the similarities between bargaining games and GT-NDMPC were established, some extensions to the original theory were performed. Specifically, the discrete-time dynamic bargaining game concept was defined. Such a concept was required because original bargaining game theory does not consider the time evolution of the decision environment, of the decision space, and of the disagreement point. Finally, based on the concepts of a discrete-time dynamic bargaining game and a disagreement point, a solution to the GT-NDMPC game and an algorithm for computing such a solution in a distributed way were proposed.

Despite of game theory often presenting selfish procedures for strategic decision making, in this chapter the bargaining game theory afforded conditions for solving the DMPC problem inside a **focusing on others** frame, without implying that the subsystems have to solve more than one optimization problem at each time step, which would prevent the convergence of the solution on a Nash equilibrium point. This non selfish bargaining game approach is the main difference with the schemes based on game theory previously reported in the literature (see e.g., [27, 44]). Additionally, a reduction of the computational burden associated with the communications between subsystems is achieved, and avoiding the solution of more than one optimization problem. Furthermore, only local functions that depend on decisions made by the other subsystems were required. This makes the proposed bargaining approach (GT-NDMPC) to the DMPC problem more flexible than almost all the DMPC schemes presented in the literature. This statement has also been validated in Portilla et al. [38].

The bargaining-game-based formulation for distributed model predictive control –GT-NDMPC– was applied in this chapter for congestion management in motorways and urban traffic networks. To this end, macroscopic models were used to represent the dynamic behavior of the vehicles in the network. Since these models are discrete-time, they were used by the controllers as prediction models. Moreover, an expression for the travel time was derived from these models. Travel time was used as the cost function in both centralized and distributed NMPC approaches. With the models, the cost function, and the constraints defined, the centralized

NMPC was formulated. After that, the whole system was decomposed into several subsystems. Also, local models and their corresponding constraints were defined. Furthermore, the bargaining situation associated with the system decomposition was analyzed. At the end, the elements defining the corresponding discrete-time dynamic bargaining games were introduced.

Finally, the proposed scheme for congestion management was tested on a motorway with ten on-ramps, and in an urban traffic network with three intersections. The performance of the GT-NDMPC approach was compared with the performance of a centralized NMPC approach. In conclusion, the distributed congestion management scheme based on game theory presented a performance similar to the one obtained using a centralized scheme.

Acknowledgments Research supported by: COLCIENCIAS project Modelamiento y control de tráfico urbano en la ciudad de Medellín, código 1118-569-34640, CT 941-2012; the European 7th Framework Network of Excellence Highly complex and networked control systems (HYCON2) grant agreement No. 257962, by the European COST Action TU1102, and by the Solar Energy Research Center SERC-CHILE, FONDAP project 15110019.

References

1. Akira O (2005) A noncooperative approach to general n-person cooperative games. Discussion papers 2005-01, Graduate School of Economics, Hitotsubashi University
2. Baskar LD, De Schutter B, Hellendoorn J (2009) Optimal routing for intelligent vehicle highway systems using a macroscopic traffic flow model. In: 12th international IEEE conference on intelligent transportation systems, ITSC '09, pp 1–6. doi:10.1109/ITSC.2009.5309657
3. Bellemans T, De Schutter B, De Moor B (2006) Model predictive control for ramp metering of motorway traffic: a case study. Control Eng Pract 140(7):757–767. doi:10.1016/j.conengprac.2005.03.010
4. Camponogara E, Jia D, Krogh BH, Talukdar S (2002) Distributed model predictive control. IEEE Control Syst Mag 22(1):44–52
5. Du X, Xi Y, Li S (2001) Distributed model predictive control for large-scale systems. In: Proceedings of the 2001 American control conference, Arlington, USA, 25–27 June, pp 3142–3143
6. Ferrara A, Nai Oleari A, Sacone S, Siri S (2012) Freeway networks as systems of systems: an event-triggered distributed control scheme. In: Proceedings of the 7th IEEE conference on system of systems engineering, Genoa, Italy, July 2012, pp 197–202
7. Frejo JRD, Camacho EF (2012) Global versus local MPC algorithms in freeway traffic control with ramp metering and variable speed limits. IEEE Trans Intell Transp Syst 130(4):1556–1565
8. Giovanini L, Balderud J (2006) Game approach to distributed model predictive control. In: Proceedings of the international control conference, Glasgow, Scotland, 30th Aug–1st Sept 2006
9. Groot N, De Schutter B, Zegeye SK, Hellendoorn H (2011) Model-based traffic and emission control using pwa models: a mixed-logical dynamic approach. In: 14th international IEEE conference on intelligent transportation systems (ITSC), Oct 2011, pp 2142–2147. doi:10.1109/ITSC.2011.6082809

10. Haj-Salem H, Poirier P, Heylliard J-F, Peynaud J-P (2001) Alinea: a local traffic responsive strategy for ramp metering. field results on a6 motorway in paris. In: Proceedings 2001 IEEE intelligent transportation systems, pp 106–111. doi:10.1109/ITSC.2001.948638
11. Harsanyi JC (1963) A simplified bargaining model for the n-person cooperative game. Int Econ Rev 40(2):194–220
12. Hegyi A, De Schutter B, Hellendoorn H, Van den Boom T (2002) Optimal coordination of ramp metering and variable speed control-an mpc approach. In: Proceedings of the 2002 American control conference, vol 5, pp 3600–3605. doi: 10.1109/ACC.2002.1024487
13. Hegyi A, De Schutter B, Hellendoorn H (2005) Model predictive control for optimal coordination of ramp metering and variable speed limits. Transp Res Part C 130(3):185–209. doi:10.1016/j.trc.2004.08.001
14. Jia D, Krogh BH (2001) Distributed model predictive control. In: Proceedings of the 2001 American control conference, Arlington, USA, 25–27 June, pp 2767–2772
15. Long K, Yun M, Zheng J, Yang X (2008) Model predictive control for variable speed limit in freeway work zone. In: 27th Chinese control conference, CCC 2008, July 2008, pp 488–493. doi:10.1109/CHICC.2008.4605219
16. Kotsialos A, Papageorgiou M, Messmer A (1999) Optimal coordinated and integrated motorway network traffic control. In: Proceedings of the 14th international symposium on transportation and traffic theory (ISTTT), Jerusalem, Israel, pp 621–644
17. Kotsialos A, Papageorgiou M, Diakaki C, Pavlis Y, Middelham F (2002) Traffic flow modeling of large-scale motorway networks using the macroscopic modeling tool metanet. IEEE Trans Intell Transp Syst 30(4):282–292
18. Kotsialos A, Papageorgiou M, Mangeas M, Haj-Salem H (2002) Coordinated and integrated control of motorway networks via non-linear optimal control. Transp Res Part C 10:65–84
19. Li S, Zhang Y, Zhu Q (2005) Nash-optimization enhanced distributed model predictive control applied to the Shell benchmark problem. Inf Sci 1700(2–4):329–349
20. Lin S (2011) Efficient model predictive control for large-scale urban traffic networks. PhD thesis, Delft University of Technology, Delft
21. Lin S, De Schutter B, Xi Y, Hellendoorn H (2011) Fast model predictive control for urban road networks via MILP. IEEE Trans Intell Transp Syst 120(3):846–856. doi:10.1109/TITS.2011.2114652 ISSN 1524-9050
22. Lin S, De Schutter B, Xi Y, Hellendoorn H (2012) Efficient network-wide model-based predictive control for urban traffic networks. Transp Res Part C: Eemerg Technol 240:122–140. ISSN 0968-090X. doi:http://dx.doi.org/10.1016/j.trc.2012.02.003. URL http://www.sciencedirect.com/science/article/pii/S0968090X12000150
23. Lu X-Y, Qiu TZ, Varaiya P, Horowitz R, Shladover SE (2010) Combining variable speed limits with ramp metering for freeway traffic control. In: American control conference (ACC), June 2010, pp 2266–2271
24. Maestre JM, Muñoz de la Peña D, Camacho EF (2011) Distributed model predictive control based on a cooperative game. Optimal Control Appl Methods 320(2):153–176
25. Maestre JM, Muñoz de la Peña D, Jiménez Losada A, Algaba Durán E, Camacho EF (2011) An application of cooperative game theory to distributed control. In: Proceedings of the 18th IFAC world congress, Milan, pp 9121–9126
26. Maestre JM, Muñoz de la Peña D, Camacho EF, Alamo T (2011) Distributed model predictive control based on agent negotiation. J Process Control 10(5):685–697
27. Muñoz de la Peña JM, Maestre D, Camacho EF (2009) Distributed MPC based on a cooperative game. In: Proceedings of the 48th IEEE conference on decision and control and 28th Chinese control conference, Shanghai, 15–18 Dec, pp 5390–5395
28. Myerson RB (1991) Game theory: analysis of conflict. Harvard University Press, Canbridge. ISBN 978-0-674-34116-6
29. Nash J (1950) The bargaining problem. Econometrica 180(2):155–162
30. J Nash (1950) Equilibrium points in N-persons games. In: Proc Nat Acad Sci USA 360 (1):40–48

31. Nash J (1953) Two-person cooperative games. Econometrica 210(1):128–140
32. Necoara I, Doan D, Suykens JAK (2008) Application of the proximal center decomposition method to distributed model predictive control. In: Proceedings of the 2008 IEEE conference on decision and control, Cancun, 9–11 Dec, pp 2900–2905
33. Negenborn RR, De Schutter B, Hellendoorn J (2008) Multi-agent model predictive control for transportation networks: serial versus parallel schemes. Eng Appl Artif Intell 210(3):353–366
34. Papageorgiou M, Blosseville JM, Haj-Salemn H (1990) Modelling and real-time control of traffic flow on the southern part of boulevard peripherique in Paris: part ii: coordinated on-ramp metering. Transp Res Part A 240(5):361–370
35. Papageorgiou M, Kosmatopoulos E, Papamichail I, Wang Y (2008) A misapplication of the local ramp metering strategy alinea. Intell Transp Syst IEEE Trans 90(2):360–365. doi:10.1109/TITS.2008.922975 ISSN 1524-9050
36. Peters HJM (1992) Axiomatic bargaining game theory. Kluwer Academic Publishers, Dordrecht
37. Pimentel J, Salazar M (2002) Dependability of distributed control system fault tolerant units. Proc IECON 4:3164–3169
38. Portilla C, Valencia F, López JD, Espinosa J, Núñez A, De Schutter B (2012) Non-linear model predictive control based on game theory for traffic control on highways. In: Proceedings of the 4th IFAC nonlinear model predictive control conference, pp 436–441
39. Rantzer A (2006) Linear quadratic team theory revisited. In: Proceedings of the 2006 American control conference, Minneapolis, 14–16 June 2006
40. Rantzer A (2088) Using game theory for distributed control engineering. In: Proceedings of the 3rd world congress of the game theory society, Evanston, July 2008, pp 13–17
41. Rantzer A (2009) Dynamic dual decomposition for distributed control. In: Proceedings of the American control conference 2009, St Louis, 10–12 June, pp 884–888
42. Talukdar S, Jia D, Hines P, Krogh BH (2005) Distributed model predictive control for the mitigation of cascading failures. In: Proceedings of the 44th IEEE conference on decision and control, and the 2005 European control conference, Seville, 12–15 Dec, pp 4440–4445
43. Treiber M, Kesting A (2013) Traffic flow dynamics. Springer, Berlin
44. Trodden PA, Nicholson D, Richards AG (2009) Distributed model predictive control as a game with coupled contraints. In: Proceedings of the European control conference, Budapest, 23–26 Aug 2009
45. Valencia F (2012) Game theory based distributed model predictive control: an approach to large-scale systems control. PhD thesis, Facultad de Minas, Universidad Nacional de Colombia, Medellín
46. Valencia F, Espinosa JJ, De Schutter B, Staňková K (2011) Feasible-cooperation distributed model predictive control scheme based on game theory. In: Proceedings of the 18th IFAC world congress, Milan, pp 386–391
47. van den Berg M, Hegyi A, De Schutter B, Hellendoorn J (2003) A macroscopic traffic flow model for integrated control of freeway and urban traffic networks. In: Proceedings of the 42nd IEEE conference on decision and control, Maui, 09–12 Dec 2003, pp 2774–2779
48. Venkat AN, Rawlings JB, Wright SJ (2006) Implementable distributed model predictive control with guaranteed performance properties. In: Proceedings of the 2006 American control conference, Minneapolis, 14–16 June, pp 613–618
49. Venkat AN, Hiskens IA, Rawlings JB, Wright SJ (2006) Distributed MPC strategies for automatic generation control. In: Proceedings of the IFAC symposium on power plants and power systems control, Canada, pp 383–388
50. Venkat AN, Rawlings JB, Wright SJ (2006) Stability and optimality of distributed, linear model predictive control. Part I: state feedback. In: Texas-Wisconsin modeling and control consortium technical report 3
51. Von Neumann J, Morgenstern O, Kuhn HW, Rubinstein A (1947) Theory of games and economic behavior. Princeton University Press, Princeton

52. Wang FY, Cameron IT (2007) A multi-form modelling approach to the dynamics and control of drum granulation processes. Powder Technol 1790(1–2):2–11
53. Yang SH, Chen X, Alty JL (2003) Design issues and implementation of Internet-based process control systems. Control Eng Pract 110(6):709–720
54. Zegeye SK, De Schutter B, Hellendoorn J, Breunesse EA, Hegyi A (2012) A predictive traffic controller for sustainable mobility using parameterized control policies. IEEE Trans Intell Transp Syst 130(3):1420–1429. doi:10.1109/TITS.2012.2197202

Advanced Information Feedback Coupled with an Evolutionary Game in Intelligent Transportation Systems

Chuanfei Dong, Yuxi Chen, Xu Ma and Bokui Chen

Abstract It has been explored for decades how to alleviate traffic congestions and improve traffic fluxes by optimizing routing strategies in intelligent transportation systems (ITSs). It, however, has still remained as an unresolved issue and an active research topic due to the complexity of real traffic systems. In this study, we propose two concise and efficient feedback strategies, namely mean velocity difference feedback strategy and congestion coefficient difference feedback strategy. Both newly proposed strategies are based upon the time-varying trend in feedback information, which can achieve higher route flux with better stability compared to previous strategies proposed in the literature. In addition to improving feedback strategies, we also investigate information feedback coupled with an evolutionary game in a 1-2-1-lane ITS with dynamic periodic boundary conditions to better mimic the driver behavior at the 2-to-1 lane junction, where the evolutionary snowdrift game is adopted. We propose an improved self-questioning Fermi (SQF) updating mechanism by taking into account the self-play payoff, which shows several advantages compared to the classical Fermi mechanism. Interestingly, our model calculations show that the SQF mechanism can prevent the system from being enmeshed in a globally defective trap, in good agreement with the analytic solutions derived from the mean-field approximation.

C. Dong (✉) · Y. Chen
AOSS Department, College of Engineering, University of Michigan,
Ann Arbor, MI 48109, USA
e-mail: dcfy@umich.edu

X. Ma
Department of Physics, Syracuse University, Syracuse, NY 13244, USA

B. Chen
Department of Electronic and Information Engineering, Hong Kong Polytechnic University,
Hung Hom, Kowloon, Hong Kong

B. Chen
Division of Logistics and Transportation, Graduate School at Shenzhen,
Tsinghua University, Shenzhen 518055, People's Republic of China

K. Hausken and J. Zhuang (eds.), *Game Theoretic Analysis of Congestion, Safety and Security*, Springer Series in Reliability Engineering,
DOI 10.1007/978-3-319-11674-7_2

Keywords Advanced information feedback · Two-route guidance strategy · Cellular automaton model · Evolutionary game theory · Snowdrift game · Stochastic Fermi rule · Self-questioning updating rule · Self-play payoff · Intelligent transportation system · Mean-field approximation

1 Introduction

Cooperation is ubiquitous in economic and social systems [13]. These systems are filled with selfish individuals who try to maximize their own benefits. But being contrary to the view of the Darwinian selection, cooperation becomes the main behavior of these systems. The emergence of cooperation in selfish circumstances has therefore attracted much attention from physicists recently. Game theory, together with its extensions, provides a useful framework to investigate this problem [2, 31, 51]. In the recent years game theory has been introduced into traffic flow studies and related fields to solve conflicts when two or more vehicles or pedestrians compete for an empty space [7, 24, 26, 37, 40, 43, 46, 50, 55, 56, 58, 60]. For instance, Perc [43] introduced the evolutionary game between neighboring agents in the Biham-Middleton-Levine (BML) model, and he found that a traffic flow seizure is induced. The evolutionary game was also introduced into random walk to study immigration behaviors [46] and into unidirectional pedestrian flow to study its phase transition behaviors [26]. Tanimoto et al. [50] and Zheng and Cheng [60] introduced game theory to study the evacuation process. Furthermore, Wang et al. [55] proposed a memory-based Snowdrift Game (SG) [45] on networks which abandon the learning mechanism. Instead, a self-questioning mechanism and a memory-based updating rule were adopted. Gao et al. [24] extended this work and studied both the evolutionary Prisoner's Dilemma Game (PDG) [3] and Snowdrift Game (SG) [45] with a self-questioning mechanism combined with a stochastic evolutionary rule, mainly on a scale-free traffic network. In Gao et al. [24], they found the so-called "Cooperative Ping-pong Effect" occurs in both games in certain cases, and plays an important role in determining the behavior of the whole system. However, none of these studies incorporated the effect of information feedback into an evolutionary game.

For some socioeconomic systems, it is desirable to provide real-time information or a short-term forecast about dynamics. For instance, in stock markets it is advantageous to give a reliable forecast in order to maximize profits. In traffic flow, advanced traveler information systems (ATIS) provide real-time information about traffic conditions to road users by means of communication such as variable message signs, radio broadcasts, or on-board computers [1]. The aim is to help individual road users to minimize their personal travel time. Therefore traffic congestion can be alleviated, and the capacity of the existing infrastructure is used more efficiently. Figure 1 shows a schematic diagram of an information feedback system, which demonstrates that feedback information plays a significant role in the

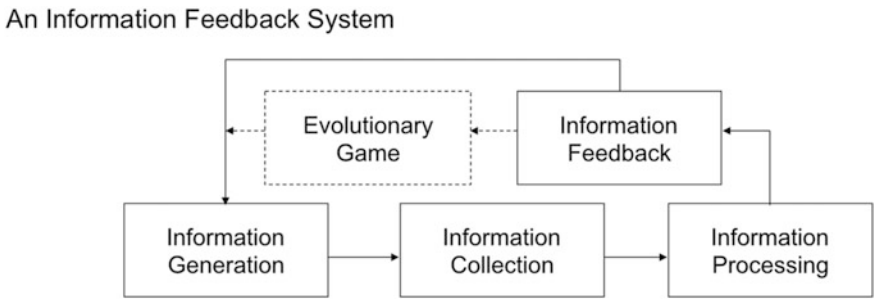

Fig. 1 The schematic diagram of information feedback coupled with an evolutionary game in an intelligent information system

loop. An intelligent transportation system (ITS) is an example of such information feedback system in our daily life. The vehicle behavior and dynamics based on the advanced information feedback in an ITS is an important research topic due to its high efficiency in controlling spatial distribution of traffic patterns.

Traffic flow and related problems have attracted considerable attention in the past decade [12, 28, 38, 42]. Understanding the characteristics of the city traffic is one of the most essential parts in the community of traffic research. This leads to the fact that traffic flow models have been studied increasingly. In order to understand significant traffic flow phenomena, traffic models such as the kinetic theory [6, 29], fluid-dynamical model [32], car-following model [25, 49] and cellular automaton (CA) model [5, 8, 36, 39, 57] have been investigated. In particular, the first CA traffic model, the Nagel-Schreckenberg model [39] is so far the most popular cellular automaton model in analyzing the traffic flow due to its simplicity and features which can well reproduce real traffic flows. Modeling traffic flow dynamics by cellular automata models has constituted the subject of intensive research by statistical physics during the past few years [12, 28]. However, it still remains an unresolved issue to propose an optimal information feedback strategy in order to essentially improve the road capacity in intelligent transportation systems (ITSs). Recently, dynamics of traffic flow based on a two-route model [52] with advanced information feedbacks have been intensively investigated [9–11, 15–17, 20–22, 27, 30, 33, 35, 44, 52–54, 59]. The route-choice strategy has also been extended to the three-route and crossing traffic systems [14, 18, 19, 23].

Each feedback strategy has its strength and weakness, e.g., Travel Time Feedback Strategy (TTFS) [52] brings a lag effect to make it impossible to provide the road users with the real situation of each route; for Mean Velocity Feedback Strategy (MVFS) [35], the random brake mechanism of the Nagel-Schreckenberg (NS) model [39] brings fragile stability of velocity [54]. In order to provide a concise and efficient feedback, two strategies named Mean Velocity Difference Feedback Strategy (MVDFS) and Congestion Coefficient Difference Feedback Strategy (CCDFS) are proposed. In contrast to Mean Velocity Feedback Strategy (MVFS) and Congestion Coefficient Feedback Strategy (CCFS), the two newly proposed feedback strategies depend on the variation of parameters from time t_1 to

t_2, and $\Delta t = t_2 - t_1$ is the time difference. Compared with Prediction Feedback Strategy (PFS) [14, 15, 19], the new feedback strategies are implemented with higher efficiency since estimates of the future road conditions in each iteration are not required. It is noteworthy that [20, 22] studied the situation where 75 % drivers exhibit aggressive behavior with the rest 25 % drivers exhibiting timid behavior near the exit, which is similar to the study of [34]. The aggressive and timid behaviors are analogous to the defection and cooperation in an evolutionary game. Dong and Ma [22] found that the aggressive behavior can cause traffic congestions near the exit especially in high-density phases and make the route saturated in a relatively low density state, which is consistent to the results shown by Perc [43].

In this study, we couple the advanced information feedback with the evolutionary SG game and the self-questioning Fermi updating mechanism (including the self-play payoff) to study the evolution of cooperation in a 1-2-1 route intelligent transportation system with dynamic periodic boundary conditions (Fig. 2). The

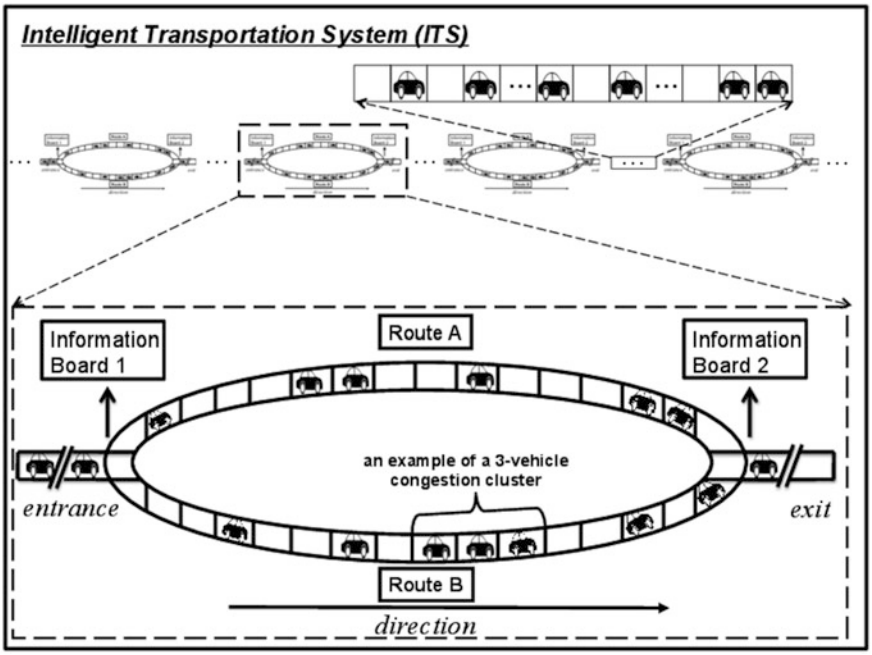

Fig. 2 The schematic diagram of an intelligent transportation system (ITS). We study one ITS pattern with dynamic periodic boundary conditions in the *dashed box* to represent the whole ITS. The lane between two ITS patterns is assumed to be long enough to hold all the waiting cars that cannot enter the system immediately. There are information boards at both entrance and exit of each ITS pattern. In each ITS pattern, two routes are assumed for simplicity, i.e., route A and route B. The dynamic drivers at the entrance follow the information feedback on board 1 while the static drivers ignore them and enter one route randomly. At the exit, when both players choose to cooperate, the cooperators will leave the ITS pattern based on the information shown on the information board 2. It is noteworthy that when we mention an ITS in the chapter, we refer to this ITS pattern with dynamic periodic boundary conditions

information feedback makes the evolutionary game unique in intelligent transportation systems. As indicated by the dashed box (Fig. 1), when cooperations take place, cooperators leave the exit in according to feedback information instead of randomly. We report the simulation results adopting four different feedback strategies MVFS, CCFS, MVDFS, and CCDFS using a revolutionary coupling approach. The remainder of this chapter is as follows: In Sect. 2, we clarify the notion and briefly introduce the evolutionary game theory, the Nagel-Schreckenberg (NS) model, the two-route model proposed by Wahle et al. [52], the exit scenario, and four feedback strategies: MVFS, CCFS, MVDFS and CCDFS. We present and discuss the simulation results and analyze the results in Sect. 3. Finally, we summarize our conclusions in the last section.

2 The Models and Feedback Strategies

2.1 Notations

Unless noted otherwise all the notations in this chapter are the same as in Table 1.

2.2 Evolutionary Game Theory

At the most elementary level, many evolutionary games can be formalized as two-person games in which each player can either cooperate (C) or defect (D). In sociology and economics, the Prisoner's Dilemma Game (PDG) [3] and Snowdrift Game (SG) [45] have been widely used to model a situation in which mutual cooperation leads to the best outcome in social terms, but defectors can benefit the most individually. In mathematical terms, this is described by a payoff matrix (Table 2, lower panel: entries correspond to the row player's payoffs), where mutual cooperation yields the reward R, mutual defection leads to punishment P, and the mixed choice gives the cooperator the sucker's payoff S and the defector the temptation T. Game theory has restricted a precondition of $2R > T + S$. For mutual cooperation, the society benefits the most, thus corresponding to the largest total payoff. In the PDG, the rank of the four payoff values is $T > R > P > S$, while in the SG it is $T > R > S > P$, so the SG is more favorable to sustain the cooperative behavior. In a real traffic system, especially a 1-2-1 route ITS, the SG is more appropriate than PDG in order to avoid collisions when both players choose to defect. Therefore, we adopt the SG in this chapter. The number in the payoff matrix shown in Table 3 describes the probability of a vehicle leaving the exit when the driver plays the game with its neighbor on an alternative route. In order to satisfy the payoff rank of the SG, we adopt small quantities ϵ and δ in the payoff matrix. As will be shown later, ϵ and δ represent the advanced characteristics that are unique to the intelligent transportation systems whereas the numbers themselves do not represent these effects. Here we set

Table 1 Major notations

F_i	The flux of route i
L_i	The length of route i
N_i	The number of vehicles on route i
ρ_i	The vehicle density on route i, $\rho_i = N_i/L_i$
N_{tot}	The total number of vehicles in the traffic system
N_c	The number of cooperators in the traffic system
N_d	The number of defectors in the traffic system
V^i_{mean}	The mean velocity of all the vehicles on route i
v_i	The velocity of the ith vehicle
v_{max}	The maximum velocity of vehicles
x_i	The position of the ith vehicle
g_i	The number of empty cells in front of vehicle i
n_j	The number of vehicles of the jth congestion cluster
q	The number of congestion clusters on one route
C	The congestion coefficient
V_D	The mean velocity difference
C_D	The congestion coefficient difference
Δt_c	The time difference in the congestion coefficient difference feedback strategy (CCDFS)
Δt_v	The time difference in the mean velocity difference feedback strategy (MVDFS)
P_e	The probability that two vehicles encounter at the exit
P_b	The random brake probability in the NS model
S_{dyn}	The fraction of dynamic drivers
β	The tunable parameter in the classical Fermi (CF) rule
f_{c0}	The initial fraction of cooperation (cooperator, C-agent) in the system
f_{d0}	The initial fraction of defection (defector, D-agent) in the system $(= 1 - f_{c0})$
f_c	The fraction of cooperation in the system (N_c/N_{tot}), $f_c(t = 0) = f_{c0}$ (a.k.a. the frequency of cooperation or cooperation ratio)
f_d	The fraction of defection in the system $(1 - f_c)$
$P_{i,j\to j}$	The probability that an agent i turns to an agent j after it plays a game with an agent j
U_i	The real payoff of agent i in the snowdrift game (SG) with the self-questioning Fermi (SQF) mechanism
$U_i^{'}$	The virtual payoff of agent i in the SG with the SQF mechanism

$\epsilon = \delta = 10^{-10}$. Since $\epsilon = \delta \ll 1$, they do not really affect the payoff matrix but satisfy the payoff rank of the SG. The advanced characteristics that two parameters (ϵ and δ) represent can be described as follows: (1) the vehicles leave the exit following the information feedback when cooperation takes place (indicated by the factor ϵ), (2) the defective penalty is imposed if both players choose to defect at the exit (implied by the factor δ, see Sect. 2.4.2 for detail). Both scenarios contribute to the payoff matrix satisfying the inequalities (both $2R > T + S$ and $T > R > S > P$), which makes the evolutionary game unique in the ITS.

Table 2 Payoff matrix of an evolutionary game

		Column	Player
		C	D
Row	C	R, R	S, T
Player	D	T, S	P, P
or equivalently			
		C	D
Row	C	R	S
Player	D	T	P

Table 3 Payoff matrix of the SG

		Column	Player
		C	D
Row	C	$0.5+\epsilon$, $0.5+\epsilon$	0, 1.0
Player	D	1.0, 0	$-\delta$, $-\delta$

The commonly used updating rules include the deterministic rule proposed by Nowak and May [41], the stochastic evolutionary rule proposed by Szabó and Töke [47] and the memory-based self-questioning updating rule proposed by Wang et al. [55]. Later, Gao et al. [24] combined the self-questioning mechanism [55] with the stochastic Fermi rule [47]. In Gao et al. [24], they considered that players get real payoffs through a game on the basis of the payoff matrix in each time step. Meanwhile, each player calculates a virtual payoff by self-questioning, i.e., to adopt its anti-strategy and play a virtual game with its neighbors who keep their strategies unchanged, and get a virtual payoff. By comparing the real payoff and the virtual payoff, players will find out whether their current strategies are advantageous. In the next round, player will change its current strategy to its anti-strategy with probability $P_{i,i'\to i'}$:

$$P_{i,i'\to i'} = \frac{1}{1+\exp[\beta(U_i - U_i')]}. \tag{1}$$

where U_i and U_i' are the real and virtual payoff of player i, respectively. The parameter $1/\beta$ denotes the noise parameter modeling the uncertainty caused by strategy adoption. It is noteworthy that a player does not play a game with itself in the study of Gao et al. [24], while in the original work of Szabó and Töke [47], the self-play, i.e., each player plays a game with itself is included. In the present work, we consider each player plays game with both itself and its neighbor. Based upon this self-play mechanism, we propose a modified SQF updating rule by redefining payoffs such that U_i and U_i' include the self-play payoffs as shown in the following table (Table 4, entries correspond to the row player's payoffs).

Table 4 The real and virtual payoffs in the SG with the SQF and the CF updating rules. The self-play is included in both cases. a and b indicate two examples of payoff calculations

	Real payoff[c] (SQF)		Virtual payoff (SQF)		Real payoff[c] (CF)	
	C	D	C	D	C	D
C	$1.0 + 2\epsilon$ [a]	$0.5 + \epsilon$	$1.0 - \delta$ [b]	-2δ	$1.0 + 2\epsilon$	$0.5 + \epsilon$
D	$1.0 - \delta$	-2δ	$1.0 + 2\epsilon$	$0.5 + \epsilon$	$1.0 - \delta$	-2δ

[a] When a C-agent plays a game with its neighboring C-agent, each C-agent gets $0.5 + \epsilon$ as the payoff. Meanwhile, the C-agent plays a game with itself and gets $0.5 + \epsilon$ as the payoff. Therefore, the real payoff that a C-agent meets another C-agent in the SG with the SQF updating rule is equal to the sum of these two payoffs, i.e., $1.0 + 2\epsilon$.

[b] When a C-agent plays a game with its neighboring C-agent, the virtual payoff is calculated as follows: the C-agent adopts its anti-strategy (D-agent) and plays a virtual game with its neighboring C-agent, the C-agent gets 1.0 as the payoff. Meanwhile, the C-agent adopts its anti-strategy (D-agent) and plays a game with itself with anti-strategy (also D-agent) and gets $-\delta$ as the payoff. Therefore, the virtual payoff that a C-agent meets a C-agent in the SG with the SQF updating rule is equal to the sum of these two payoffs, i.e., $1.0 - \delta$.

[c] The real payoff in the SG with the CF updating rule is the same as the real payoff in the SG with the SQF updating rule. Entries correspond to the row player's payoffs.

Unless noted otherwise the SQF rule hereafter refers to the modified SQF rule. For comparison, we also study the classical Fermi (CF) rule [47] case without employing the SQF mechanism, in which players update their strategies by learning from their neighbors, as the updating mechanism:

$$P_{i,j\to j} = \frac{1}{1 + \exp[\beta(U_i - U_j)]}. \tag{2}$$

where U_i and U_j are considered as real payoffs (including the self-play payoffs) of players i and j according to the payoff matrix shown above (also see Table 4). When a C-agent plays a game with another C-agent, the probability of a C-agent turns to a D-agent is $P_{c,c\to d} = 1 - P_{c,c\to c}$.

In this chapter, we study a 1-D ITS with dynamic periodic boundary conditions, which is different from the 2-D lattice case, in which each player usually has four nearest neighbors (i.e., von Neuman neighborhood). In the 2-D case, the players can randomly choose one of their immediate neighbors with equal probability and update their strategies by learning from their neighbors (i.e., with the CF updating rule). Each player will adopt the selected neighbor's strategy (C or D) with a certain probability P as shown in Eq. (2), which is usually determined by the payoffs of the two players. As the players aim at maximizing their own benefits, therefore, if the selected neighbor has a higher payoff, it is more likely that its strategy will be adopted, and vice versa [47]. Given the fact that two routes are separated in our model, the game can take place only at the 2-to-1 lane junction near the exit of each ITS pattern. Since cooperators and defectors initially are randomly distributed on each route, it is similar to the situation in which each player randomly chooses one of its immediate neighbors at the exit, as in the 2-D case.

The key quantity for characterizing the cooperative behavior is the frequency of cooperation f_c, which is defined as the fraction of cooperators in the whole population. The parameter f_c is obtained by counting the number of cooperators in the whole population (N_c/N_{tot}) after the system reaches an equilibrium state, at which the number of cooperators fluctuates slightly around an average value. In our model, we assume that the initial fraction of cooperation is f_{c0} and defectors is $f_{d0} = 1 - f_{c0}$. Since we fix the total number of vehicles N_{tot} in the ITS, the fractions of cooperation, $f_c(t)$, and defection, $f_d(t) = 1 - f_c(t)$, evolve with time t when games take place at the exit.

2.3 The NS Mechanism

The Nagel-Schreckenberg (NS) model is briefly introduced as follows, which can be divided into the following four rules [39]:

R1: Acceleration:

$$v_i(t) \rightarrow v_i(t+\frac{1}{3}) = \min[v_i(t)+1, v_{max}]; \tag{3}$$

R2: Deceleration:

$$v_i(t+\frac{1}{3}) \rightarrow v_i(t+\frac{2}{3}) = \min[v_i(t+\frac{1}{3}), g_i(t)]; \tag{4}$$

R3: Random brake:

$$v_i(t+\frac{2}{3}) \rightarrow v_i(t+1) = \max[0, v_i(t+\frac{2}{3})-1]; \tag{5}$$

with a certain brake probability P_b;

R4: Movement:

$$x_i(t+1) = x_i(t) + v_i(t+1). \tag{6}$$

In the NS model, the road is divided into cells (sites) with a length of $\Delta x = 7.5$m. The total length of the route is set to be $L = 2,000$ cells (corresponding to 15 km). $g_i(t)$ denotes the number of empty cells in front of car i, i.e., the gap or headway. A time step corresponds to $\Delta t = 1s$, the typical time a driver needs to react. In the present work, we set the maximum velocity $v_{max} = 3$ cells/time step (corresponding to 81 km/h and thus is a reasonable value) for simplicity.

2.4 Two-Route Model and Exit Scenario

2.4.1 Two-Route Scenario

We adopt the modified version of the two-route model proposed by Wahle et al. [52]. We assume that the total number of cars in a 1-2-1 route ITS is N_{tot} that includes the waiting cars. To initialize the simulation, all vehicles wait on the lane before they enter the ITS. If a driver is a so-called dynamic one, he selects the route according to the real-time information displayed on the roadside, while a percentage of drivers (referred to as static drivers) ignores the advice, thus entering a route randomly. The length of two routes A and B are equal to each other. The fractions of dynamic and static travelers are S_{dyn} and $1 - S_{dyn}$, respectively. After a vehicle enters one of two routes, the vehicle follows the dynamics of the NS model. Since we use dynamic periodic boundary conditions, after a vehicle reaches the end point, it immediately returns to the waiting lane connected to the entrance with a position next to the waiting car in front of it without a gap. In other words, the dynamic periodic boundary conditions indicate that the waiting lane length is dynamic instead of static, which can only hold the number of waiting cars at the current moment. So we do not really care about the vehicle dynamic on the waiting lane. It is important to note that if a vehicle cannot enter the preferred route, it will wait till the next time step rather than entering the un-preferred route. In simulations, vehicles could enter the preferred route only when the first three sites (given $v_{max} =$ 3 cells/time step) of the route are empty in order to avoid collisions.

2.4.2 Exit Scenario

The dashed box in Fig. 2 illustrates the "one entrance and one exit" structure of the ITS. In reality, there are different paths for drivers to choose from one place to another. Different drivers departing from the same place could choose two different paths to get to the same destination, which is analogous to a 1-2-1 route system. The rules at the exit of the two-route system are as follows:

(a) Rules at the exit when both vehicles have a chance to leave:
   (i) According to the information shown on the information board 2 (see Fig. 2), the vehicle on the route with higher vehicle density leaves first;
   (ii) If both routes have the same vehicle density, the vehicles leave randomly.

(b) For the vehicles fail to leave at the exit, their position(t) = L and velocity (t) = position(t) − position(t − 1).

In 1-D and 2-D traffic flow models (see e.g., [43, 46]), when cooperations take place, the players have equal probability to move (1-D case) or move alternately (2-D case). However, in an ITS, when both players choose to cooperate, the

cooperators have a chance to follow the information shown on the board to leave the ITS. On the other hand, when both drivers choose to defect, both of them drive to position(t) = L with velocity(t) = 0 instead of velocity(t) = position(t) − position (t − 1) for penalty. In this way, the route conditions benefit from the cooperative behavior, and the defective penalty makes the defective behavior unfavorable. As we described earlier in this chapter, the influence is implied by the parameters ϵ and δ in the payoff matrix (Table 3), respectively. It is noteworthy that when the SG is not considered in Sect. 3.1, all the drivers are forced to follow the exit scenario, which is equivalent to the situation that all the players are assumed to be cooperators when adopting the SG. In reality, in order to impose all the drivers to follow the exit scenario, there must be automatic traffic barriers at the exit. However, it is impossible to have a barrier control at the end of each 2-to-1-lane junction in real traffic systems due to the high cost, which indicates the defector is highly likely to appear and thus the game analysis shown in Sect. 3.2 is more realistic compared to the case study in Sect. 3.1.

2.5 Related Definitions

The road conditions can be characterized by the fluxes of two routes, and the flux of the ith route is defined as follows:

$$F_i = V^i_{mean}\rho_i = V^i_{mean}\frac{N_i}{L_i} \tag{7}$$

where L_i represents the length of the ith route, V^i_{mean} and N_i denote the mean velocity of all the vehicles and the vehicle number on the ith route, respectively. The physical sense of the flux F is the number of vehicles passing the exit of the traffic system at each time step. Rather remarkably, the waiting cars do not contribute to the calculation of the time-dependent flux. Therefore the larger the value of F is, the better the processing capacity of the traffic system is. We describe four different feedback strategies as follows:

MVFS: At each time step, the velocity of each vehicle is known from navigation systems (GPS). The traffic control center calculates the mean velocity of each route and displays the number on the board located at the entrance of each route. Road users at the entrance will choose one road with a larger mean velocity.

CCFS: The position of each vehicle is known by the signal transmitted from navigation systems (GPS). The traffic control center computes the congestion coefficient of each route based on this information and displays it on the board. Road users at the entrance will choose the route with a smaller congestion coefficient. The congestion coefficient is defined as

$$C(t) = \sum_{j=1}^{q(t)} n_j^2(t). \tag{8}$$

Here, $n_j(t)$ stands for vehicle number of the jth congestion cluster (see Fig. 2), in which cars are close to each other without a gap at time t. $q(t)$ is the number of clusters on one route. However, it may not be optimal for road users to make a wise choice by considering only the current road condition. Given the situation that although initially $V^A_{mean} < V^B_{mean}$, V^A_{mean} increases with time while V^B_{mean} decreases. In this circumstance, it is better for the road user to enter route A instead of route B since route A has the potential to become better. Based upon this scenario, we propose two concise and efficient feedback strategies as follows:

MVDFS: At each time step, each vehicle on the routes sends its velocity to the traffic control center. The work of the traffic control center is to calculate the velocity difference between time t_1 and t_2, and display it on the board. Road users at the entrance will choose one road with a larger mean velocity difference.

The mean velocity difference (V_D) between time t_1 and t_2 is defined as

$$\begin{aligned} V_D(t, \Delta t_v) &= V_{mean}(t_2) - |sgn(\Delta t_v)| \times V_{mean}(t_1) \\ &= V_{mean}[t - (1 - H(\Delta t_v))\Delta t_v] - |sgn(\Delta t_v)| \times V_{mean}[t - H(\Delta t_v)\Delta t_v] \\ &= \frac{\sum_{i=1}^{N(t_2)} V_i[t - (1 - H(\Delta t_v))\Delta t_v]}{N[t - (1 - H(\Delta t_v))\Delta t_v]} \\ &\quad - |sgn(\Delta t_v)| \times \frac{\sum_{i=1}^{N(t_1)} V_i[t - H(\Delta t_v)\Delta t_v]}{N[t - H(\Delta t_v)\Delta t_v]}. \end{aligned} \tag{9}$$

where $sgn(x)$ is the signum function of a real number x, which is defined as follows:

$$sgn(x) = \begin{cases} 1, & \text{if } x > 0 \\ 0, & \text{if } x = 0 \\ -1, & \text{if } x < 0 \end{cases} \tag{10}$$

and $H(x)$ is the unit step function, which defined as the integral of the Dirac delta function:

$$H(x) = \int_{-\infty}^{x} \delta(s)\,\mathrm{d}s = \begin{cases} 1, & \text{if } x \geq 0 \\ 0, & \text{if } x < 0 \end{cases} \tag{11}$$

$V_i(t)$ stands for the velocity of the ith vehicle at time t, $N(t)$ denotes the vehicle number on one route at time t, $t_2 = t - (1 - H(\Delta t_v))\Delta t_v$ and $t_1 = t - H(\Delta t_v)\Delta t_v$. It is noteworthy that for $\Delta t_v = 0$, MVDFS changes back to MVFS.

CCDFS: At each time step, the traffic control center receives data from the navigation systems (GPS) as CCFS. The work of the traffic control center is to calculate the congestion coefficient difference between time t_1 and t_2 and display it

on the board. Road users at the entrance choose one road with smaller congestion coefficient difference.

The congestion coefficient difference (C_D) between time t_1 and t_2 is defined as

$$\begin{aligned} C_D(t, \Delta t_c) &= C(t_2) - |sgn(\Delta t_c)| \times C(t_1) \\ &= C[t - (1 - H(\Delta t_c))\Delta t_c] - |sgn(\Delta t_c)| \times C[t - H(\Delta t_c)\Delta t_c] \\ &= \sum_{j=1}^{q(t_2)} n_j^2[t - (1 - H(\Delta t_c))\Delta t_c] \\ &\quad - |sgn(\Delta t_c)| \times \sum_{j=1}^{q(t_1)} n_j^2[t - H(\Delta t_c)\Delta t_c]. \end{aligned} \tag{12}$$

where the definitions of $n_j(t)$ and $q(t)$ are the same as those defined in CCFS. Similar to MVDFS, when $\Delta t_c = 0$, CCDFS returns to CCFS. Given the implementation efficiency in real traffic systems, we only focus on the situations that $\Delta t_{v,c} > 0$, but Eqs. (9 and 12) are valid for any real number of $\Delta t_{v,c}$.

Finally, we point out that initially we set the routes and information boards empty and let vehicles enter the routes randomly during the first 100 time steps in the simulation. Thus, the information feedback starts at the 101th time step. In the following section, the performance of four different feedback strategies will be shown and discussed in detail.

3 Simulation Results

3.1 Advanced Information Feedback in a 1-2-1 Route ITS

Firstly, we focus on the advanced information feedback strategy in ITSs itself, thus ignoring the evolutionary game in this section. Given the stability and convergency, the smoothed simulation results shown in Fig. 3 are obtained based on 10 times average over 90,000–100,000 time steps. Figures 3a, b show the dependence of the average flux on the time difference Δt_c and Δt_v by using CCDFS and MVDFS, respectively. As to the routes' processing capacity, there are positive peak structures, corresponding to the highest flux ~ 0.43 in both cases, at the vicinity of $\Delta t_c \approx 2$ and $\Delta t_v \approx 3$. We also test the simulation result without 10-time average, which basically shows the same curve shape and the peak location. Therefore, the average does not change the result to any significant degree. When $\Delta t_v = 0\,(\Delta t_c = 0)$, MVDFS (CCDFS) is equivalent to MVFS (CCFS), which allows direct comparison between MVDFS (CCDFS) and MVFS (CCFS). In Fig. 3, it is clear that both MVDFS and CCDFS significantly improve the road capacity compared to the previous strategies when the time difference is less than ~ 30. Supposing if we delete signum function, $sgn(x)$, in Eqs. (9–12), when $\Delta t_v = 0\,(\Delta t_c = 0)$, $V_D(t, \Delta t_v) = 0\ (C_D(t, \Delta t_c) = 0)$,

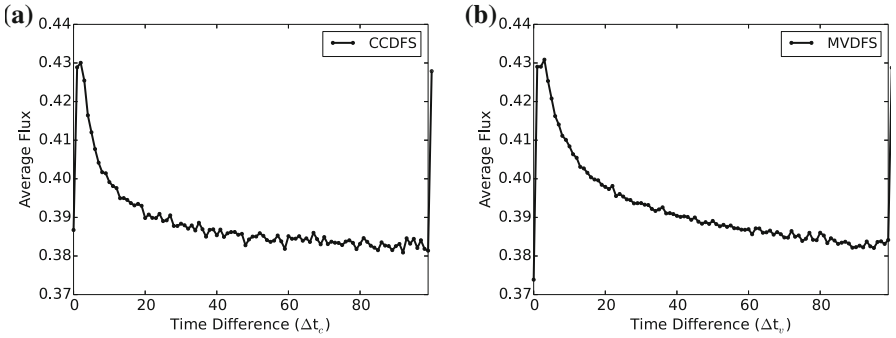

Fig. 3 **a** Average flux by performing CCDFS versus time difference Δt_c. **b** Average flux by performing MVDFS versus time difference Δt_v. The results are based on 10 times average. The parameters are, $S_{dyn} = 1.0$, and $N_{tot} = 2,000$

i.e., the random case, then we cannot intuitively see the difference between the improved strategies and previous ones in Fig. 3. Unless noted otherwise, all the parameters hereafter refer to $L_A = L_B = 2{,}000$, $P_b = 0.25$, $S_{dyn} = 1.0$, $\Delta t_c = 2$, $\Delta t_v = 3$, and $N_{tot} = 2000$.

In contrast to MVDFS and CCDFS, the fluxes of two routes adopting MVFS and CCFS show larger oscillations (see Fig. 4). These oscillations could be caused by several factors. First, as we have mentioned earlier, the NS model has a random brake scenario which causes the fragile stability of velocity, thus MVFS cannot completely reflect the real route conditions. Second, the oscillations can be partially caused by the potential information lag by using the current information [54]. When we adopt MVDFS or CCDFS, it is similar to the situation in which we implement a linear extrapolation in time and therefore it is equivalent to the prediction feedback [15, 19] for a short time scale to a certain degree. Though CCFS is better than MVFS, both MVFS and CCFS cannot reflect the tendency of road condition variation with time. For example, when adopting MVDFS, if there exist congestion clusters at the end of route A, the average velocity of the whole route will definitely decrease even though $V^A_{mean} > V^B_{mean}$. The mean velocity difference of route A, $V^A_D(t, \Delta t_v)$, is negative [see Eq. (9)] in this situation. If a road user finally chooses to enter route B, there are three possible outputs: first, $V^B_{mean}(t_2) > V^B_{mean}(t_1)$, with $t_2 > t_1$; second, V^B_{mean} remains the same; third, V^B_{mean} decreases but $V^B_D(t, \Delta t_v) > V^A_D(t, \Delta t_v)$ (both of them are negative under this circumstance). In order to prevent the congestion clusters from further expanding, the route users should enter route B whose condition tends to be better (condition I) or no worse than that of route A (condition II or III). For CCDFS, the analysis is similar. The only difference is that road users will select the route with smaller congestion coefficient difference $C_D(t, \Delta t_c)$ instead, because the large congestion coefficient indicates the unfavorable jammed states which certainly do harm to the traffic system. Compared with MVFS and CCFS, the performance by adopting MVDFS and CCDFS is remarkably improved, not only considering the value but also

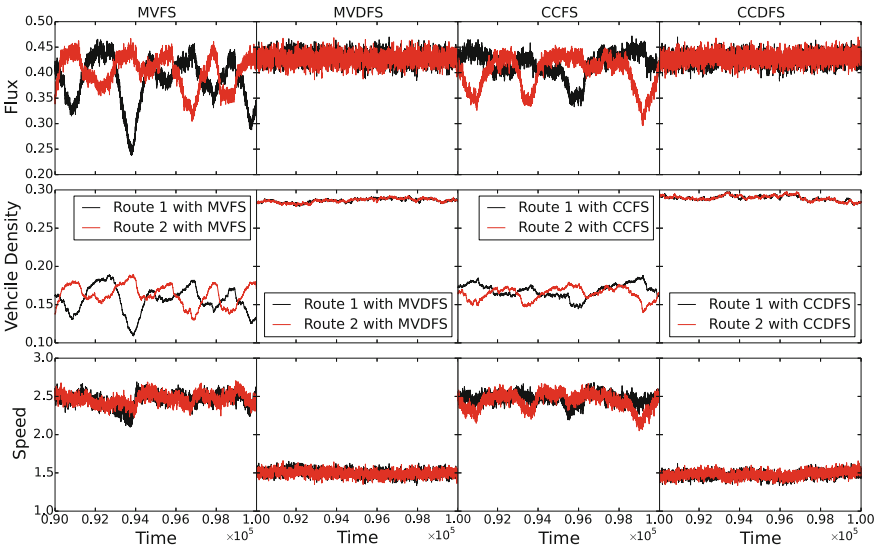

Fig. 4 Flux (the *first row*), vehicle density (the *second row*), and average speed (the *third row*) of each route with mean velocity feedback strategy (MVFS, the *first column*), mean velocity difference feedback strategy (MVDFS, the *second column*), congestion coefficient feedback strategy (CCFS, the *third column*), and congestion coefficient difference feedback strategy (CCDFS, the *fourth column*). $S_{dyn} = 0.5$

the stability of the flux. Therefore, considering the flux of the two-route system, MVDFS and CCDFS are better.

In Fig. 4, the plot of vehicle density versus time step shows a similar tendency as that of the flux. The routes' accommodating capacity is greatly enhanced with an increase in the average vehicle density from 0.16 to 0.29, thus the high fluxes of two routes with MVDFS and CCDFS are mainly due to the increase of the vehicle density. According to the stability of the vehicle density on each route, the vehicles are uniformly distributed on each route instead of staying together at the end of the route. The plot of speed versus time step shows that although the velocities are more stable by using the new strategies, they are lower than MVFS and CCFS. The reason is that the routes' accommodating capacity is more efficient by using the new strategies. As mentioned earlier, the system has only one exit, and at most one car can leave at each time step. Therefore the more cars the lane holds, the lower velocities the vehicles have. Fortunately, the traffic flux consists of two parts, the mean velocity and the vehicle density. Hence as long as the vehicle density, $\rho = N/L$, is large enough, the road flux can still be greatly improved.

Figure 5 shows the dependence of the average flux fluctuates on the fraction of dynamic travelers (S_{dyn}) by using four different feedback strategies. As to the routes' processing capacity, the new strategies are proved to be better than the

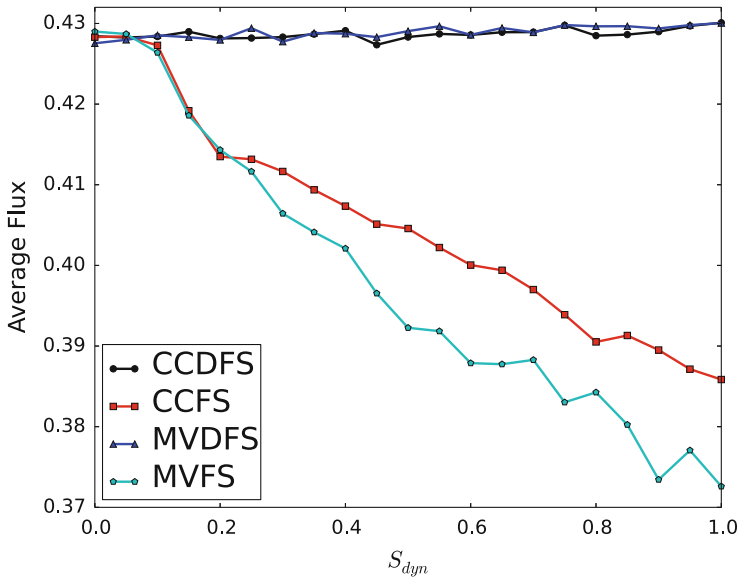

Fig. 5 Average flux by performing different strategies versus S_{dyn}

previous ones because the fluxes are always larger at each S_{dyn} value and even slightly increase with a persisting increase of dynamic drivers. The fact that the values of average fluxes in Fig. 5 by adopting MVFS and CCFS are smaller than those shown in [54] is caused by the different structures of the (1-2-1 route) traffic system and the exit scenario.

Finally, it is of particular interest to find that the newly proposed information feedback strategy seems to be independent of the selected information type and only relies on the information changing rate or tendency. Without loss of generality, we focus on the comparison of CCFS and CCDFS in the following section and set $\Delta t_c = 2$ for all cases.

3.2 Evolutionary Game Coupled with the NS Model in a 1-2-1 Route ITS

In this section, we focus on the evolutionary game coupled with the NS model in a 1-2-1 route ITS. The simulations are carried out for 200,000 time steps. The results shown in Figs. 6 and 7 are based on the average over 190,000–200,000 time steps. As will be shown later (e.g., see Fig. 8), the evolution of cooperation reaches a steady state at around 20,000 time step. Since the calculated result does not vary a lot after it reaches the steady state, the total run time steps only need to reach greater than 20,000. If a vehicle passes the exit without encountering any vehicle on the

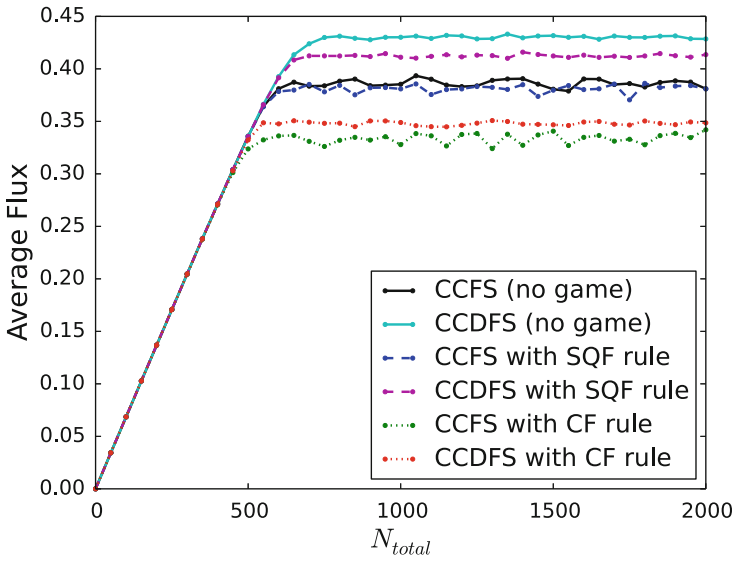

Fig. 6 Average flux versus total number of vehicles (N_{tot}) in the traffic system

alternative route, it leaves the system without changing its strategy (i.e., C-agent or D-agent). If the vehicles near the exit on both routes have a chance to leave the system, the game takes place and the players update their strategies based upon the rules described in Sect. 2.2. Once a car leaves the system, it keeps its strategy until the driver has a chance to play a game with others at the exit again, and so on and so forth.

As we described earlier, we employ the Snowdrift Game (SG) [45] in this chapter. We first investigate the dependence of the average flux on the total vehicle number, N_{tot}, in an ITS by adopting CCFS (without the SG), CCDFS (without the SG) and CCDFS coupled with the SG (with both the self-questioning Fermi (SQF) updating rule and the classical Fermi (CF) updating rule). In Fig. 6, the solid lines with different colors show the cases without adopting the SG. The dashed lines with different colors illustrate the cases with the SQF updating rule [see Eq. (1)] and the dotted lines with different colors represent the cases with the CF updating rule [see Eq. (2)]. It is clear that CCDFS without adopting the SG has the highest flux among all six cases. Given the payoff matrix (Table 3) and the fact that when the SG is not adopted, all the drivers are forced to be cooperators due to the fictitious barrier control at the exit, this result is within our expectation. However, the game analysis in this section is more realistic in a real traffic system as explained in Sect. 2.4.2. When adopting the SG, the saturated N_{tot} decreases with respect to the cases without evolutionary game, consistent with the result shown in Fig. 2 in Perc [43]; the evolutionary game has a tendency to make the road saturated (in our case) or phase state transition from free flow to fully jammed flow (in 2-D BML model [43]) occurring at a relatively low density state. Compared with the CCDFS case with the

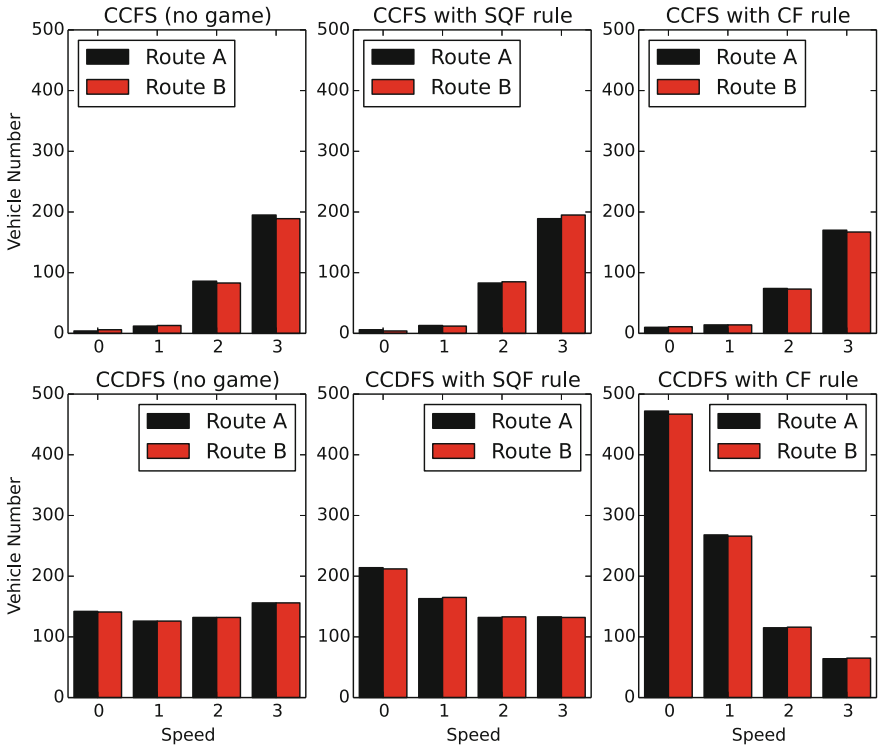

Fig. 7 The velocity distribution of each route with CCFS (the *first row*) and CCDFS (the *second row*). The *first column* shows the cases without adopting the SG. The *second* and *third columns* illustrate the velocity distribution from the information feedback coupled with the SG (the *second column*: with the SQF updating rule; the third column: with the CF updating rule)

CF rule (the red dotted line), the average flux by adopting CCDFS with the SQF rule (the magenta dashed line) is higher, indicating that the SQF rule is more favorable in terms of alleviating the traffic congestion. As expected from the earlier analysis, the worst condition occurs at the situation by adopting CCFS with the CF updating rule (the green dotted line), which corresponds to the lowest average flux and the smallest saturated vehicle density. In the following analysis of the evolutionary game, we focus on the strategy CCDFS with both the SQF and the CF updating rules. We select two values of $N_{tot} = 200$ (unsaturated state) and $N_{tot} = 2,000$ (fully saturated state) as case studies. Hereafter unless noted otherwise, we choose $f_{c0} = 0.85$ and $\beta = 10$ in this section.

Figure 7 shows the the velocity distribution of each route with and without the evolutionary game. When adopting the SG, the fraction of low speed vehicles clearly increases with respect to the cases without the SG. Compared with the cases adopting the SQF updating rule, the CF updating rule leads to a relatively large fraction of low speed vehicles (especially for the combination of CCDFS with the

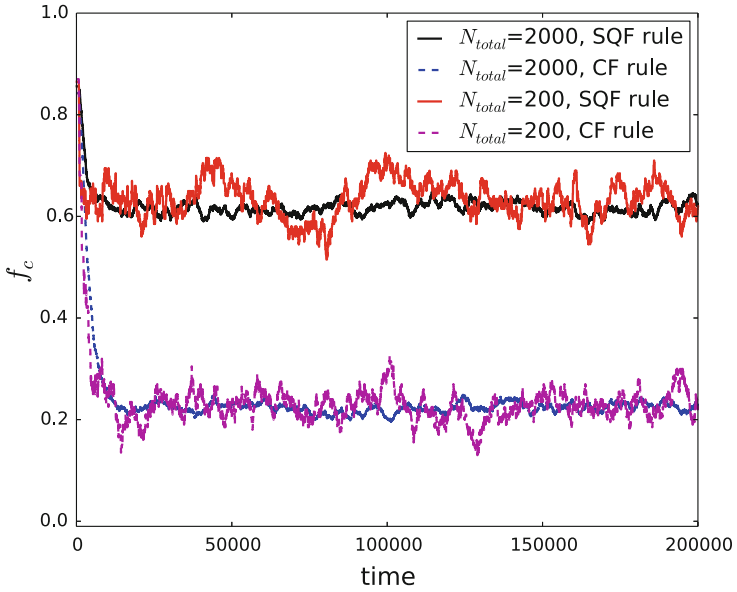

Fig. 8 Fraction of cooperation versus time by adopting CCDFS

CF rule), which indicates an unfavorable jammed state on the route. The payoff matrix (Table 3) indicates that the traffic congestion is mainly caused by the defective behavior of D-agents at the end of each route. Thus, the SQF updating rule is better than the CF updating rule in terms of alleviating the traffic congestion. The detailed analysis of the evolutionary game below will help one further understand the vehicle dynamic behavior shown above.

We first investigate the evolution of cooperation with the classical Fermi (CF) and the self-questioning Fermi (SQF) rule (see Sect. 2.2 for detail). Figure 8 shows the variation of the fraction of cooperation, f_c, with time based on different updating rules and total vehicle number, N_{tot}. It shows that the evolution of cooperation reaches a steady state at around 20,000 time steps. In both cases, the fraction of cooperation, f_c, reaches an equilibrium state with the density of cooperators fluctuating slightly around a convergent value. Although the convergent value with the SQF mechanism is higher than that with the CF mechanism, it is independent of the vehicle number or the phase state in both cases. When $N_{tot} = 200$, it converges faster than the larger $N_{tot} = 2,000$ case. Inspection of Fig. 8 reveals that the SQF mechanism can prevent the system from being enmeshed in a globally defective trap, which is a shortcoming of the existing models based on the learning mechanisms. The underlying reason lies in the fact that the players with the SQF mechanism consider both the real and virtual payoffs by playing games with themselves and their neighbors, depending on which players make their decisions on whether switching to their anti-strategy. In contrast to the case with the SQF rule, the players with the CF rule only consider the real payoffs without self-questioning, so they cannot further consider the information about their

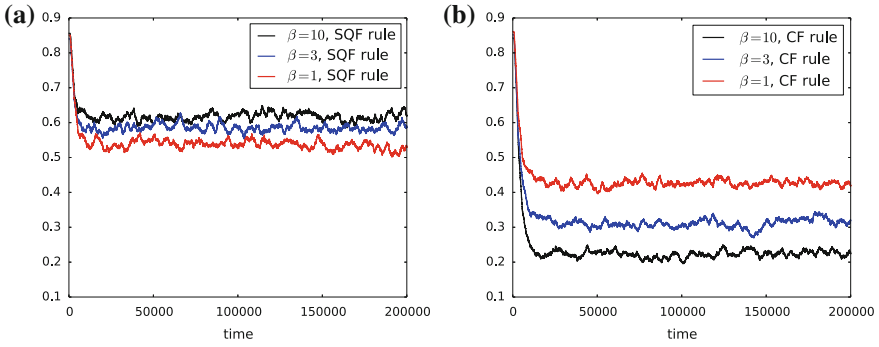

Fig. 9 Fraction of cooperation f_c versus time for different values of β by adopting CCDFS

surroundings and the mutual payoffs of the whole system. This leads to a higher possibility of selfish individuals trying to maximize their own benefit to grow in the system. The relatively low flux (Fig. 6) and large fraction of low speed vehicles (Fig. 7) with the CF rule can therefore be explained by the low fraction of C-agent in the system.

In order to show the advantages of the SQF mechanism, we also study the dependence of the updating mechanism on the value of β, which characterizes the noise introduced to permit irrational choices. Figure 9 shows the variation of the cooperation fraction, f_c, with time by adopting the SQF and the CF updating rules based on various β. We select $\beta = 1, 3, 10$ as case studies. It is of particular interest to find that the convergent value of f_c^{SQF} in the newly proposed SQF mechanism only slightly relies on the tunable parameter β; a large β corresponds to a slightly large f_c^{SQF}. With the CF mechanism, the convergent value of f_c^{CF} however, greatly relies on the noise term β; the larger the β, the smaller the convergent f_c. On average, $f_c^{SQF} > f_c^{CF}$. This comparison intuitively reveals one of the advantages of the SQF mechanism.

We also study the effect of the initial cooperation fraction, f_{c0}, on the convergent value of f_c by adopting the SQF and the CF rules. Figure 10 shows five cases with initial cooperation ratios $f_{c0} = 1.0,\ 0.85,\ 0.63,\ 0.23$ and 0.05 by adopting the SQF (Fig. 10a) and CF (Fig. 10b) rules. Despite the different initial cooperation ratios, f_{c0}, they all converge to the same steady state, $f_c \approx 0.63$ (for SQF) and 0.23 (for CF). Interestingly, the convergent value is independent of the initial fraction, f_{c0}, in both cases. We also test the case of the CF rule without self-play payoff counted, the convergent value is also independent of f_{c0}. The convergent f_c with the SQF rule is always higher than that with the CF rule at various f_{c0} in Fig. 10. Again, it demonstrates the advantages of the newly proposed SQF mechanism. The simulation results with original SQF rule [24] adopted are not shown as it is even worse than the CF rules in terms of the convergent f_c under certain circumstances. It seems to be caused by the 1-D structure of our model, where each player at most has one neighbor whereas in a 2-D lattice, each player can have 4 neighbors or 8 neighbors.

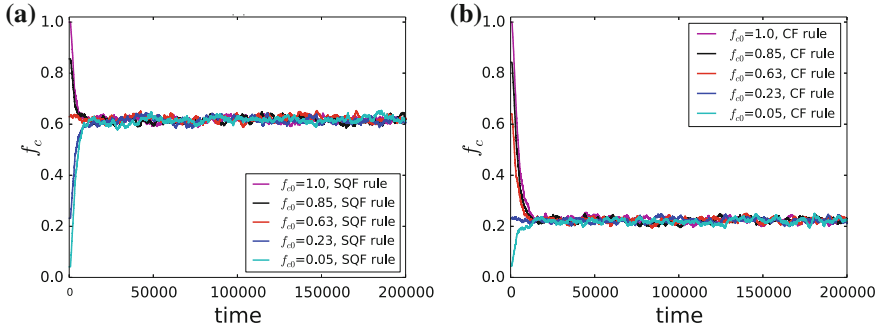

Fig. 10 Fraction of cooperation f_c versus time at various f_{c0} by adopting CCDFS

However, the self-play [47] solves the shortcoming of the original SQF rule. By all accounts, the improved SQF mechanism will be a powerful tool in the analysis of evolutionary game in both traffic networks and other social and economic systems.

Finally, we analytically calcualte the evolution of the cooperation ratio, f_c, by using a simple mean-field approximation [4, 46]. In the SG with either the SQF or CF updating rule [see Eqs. (1–2)], if one agent is cooperator and the other is defector (ignoring the parameter ϵ and δ here due to their tiny values), then

$$P^{SQF}_{c,d\to d} = \frac{1}{1+e^{0.5\beta}}; P^{CF}_{c,d\to d} = \frac{1}{1+e^{-0.5\beta}} \tag{13}$$

$$P^{SQF}_{d,c\to c} = 0.5; P^{CF}_{d,c\to c} = \frac{1}{1+e^{0.5\beta}} \tag{14}$$

If both agents are defectors, then

$$P^{SQF}_{d,d\to c} = \frac{1}{1+e^{-0.5\beta}}; P^{CF}_{d,d\to c} = 0.5 \tag{15}$$

If both agents are cooperators:

$$P^{SQF}_{c,c\to d} = 0.5; P^{CF}_{c,c\to d} = 0.5 \tag{16}$$

As $f_c + f_d = 1$, the mean-field equation can be written as an equation about f_c as follows (we choose the situation of the SG with the SQF updating rule as an example of analysis):

$$\begin{aligned}\frac{df_c}{dt} &= P_e \times \left(2f_c \cdot f_d\left(P^{SQF}_{d,c\to c} - P^{SQF}_{c,d\to d}\right) + f_d \cdot f_d\left(P^{SQF}_{d,d\to c} + P^{SQF}_{d,d\to c}\right) + f_c \cdot f_c\left(-P^{SQF}_{c,c\to d} - P^{SQF}_{c,c\to d}\right)\right) \\ &= P_e \times \left(2f_c \cdot f_d\left(0.5 - \frac{1}{1+e^{0.5\beta}}\right) + f_d \cdot f_d \frac{2}{1+e^{-0.5\beta}} - f_c \cdot f_c\right)\end{aligned} \tag{17}$$

Table 5 Comparison of the convergent value of f_c by adopting the mean-field approximation and the simulation results in the SG with the SQF and CF updating rules

	$\beta = 1$ (MFA[a])	$\beta = 1$ (SIM[b])	$\beta = 3$ (MFA)	$\beta = 3$ (SIM)	$\beta = 10$ (MFA)	$\beta = 10$ (SIM)
Convergent f_c^{SQF}	0.55	0.54	0.62	0.59	0.67	0.63
Convergent f_c^{CF}	0.44	0.43	0.35	0.32	0.29	0.23

[a] *MFA* mean-field approximation
[b] *SIM* simulation

where P_e is the probability that two cars encounter at the exit (so the SG takes place) before leaving an ITS. By either integrating Eq. (17) and assuming $t \to \infty$, or just assuming $df_c/dt = 0$, the analytic approximation of the steady state value, f_c can be obtained and compared with the corresponding simulation result (Table 5). Table 5 shows that our simulation results are in good agreement with the analytic solution from the mean-field approximation, especially when β is relatively small, e.g., $\beta = 1$.

Finally, we point out that a lot of further studies are needed, involving the study of, e.g., player cooperative behavior by using the SG/PDG in an asymmetric two-route ITS with a speed limit bottleneck on the short route (e.g., see Fig. 1 in Chen et al. [9]). This study will allow us to investigate the cases with accidents. Also, it would be interesting to study the cooperative behavior by a n-person chicken game (e.g., see [48]) when games take place at the end of a multi-route intelligent transportation system (e.g., see Fig. 1 in Dong et al. [19]). Moreover, an optimal exit scenario proposal may have a chance to increase both the fraction of cooperation and the vehicle flux.

4 Conclusion

For the first time, we studied the advanced information feedback coupled with an evolutionary game in a 1-2-1 route ITS with dynamic periodic boundary conditions. The feedback information makes the cooperative behavior unique in ITSs. When a cooperation takes place, the cooperator leaves the exit by following the information feedback shown on the board. We studied in detail the evolution of cooperation for the Snowdrift Game (SG) model with two different updating rules: an improved self-questioning Fermi (SQF) mechanism and the classical Fermi (CF) mechanism. The former one shows several advantages compared with the latter one. Note that in our model, each player not only plays game with its neighbor but also with itself, thus including the self-play payoffs. The SQF mechanism avoids the system from being enmeshed in a trap of the globally defective state, which is a shortcoming of the pre-existing models. Furthermore, we investigated the influences of total

number of vehicles in an ITS, noise term, and the initial fraction of cooperation on the SG. The results show that the steady state of the cooperation ratio, f_c, is independent with the total number of vehicles and the initial fraction of cooperation. Compared with the CF rule, the convergent values of f_c with the SQF rule are barely affected by the noise term and show relatively a higher steady cooperation ratio f_c. Our simulation results are in good agreement with the analytic solutions derived from the mean-field approximation and therefore shed new light on the study of evolutionary games in 1-D intelligent traffic networks.

In addition, the simulation results (without adopting the SG) with four different feedback strategies, i.e., MVFS, CCFS, MVDFS, and CCDFS in a 1-2-1 route ITS, were compared in terms of variations of the flux, vehicle density, speed, and average flux against the fraction of dynamic drivers. Variations of average flux with time difference (Δt) by adopting CCDFS and MVDFS indicate that MVDFS and CCDFS are better than the other two feedback strategies in an ITS with only one entrance and one exit. One highlight of this chapter is that it brings forward two new quantities, mean velocity difference and congestion coefficient difference, to radically improve road conditions. In contrast to the previous two feedback strategies, MVDFS and CCDFS can significantly improve the road conditions, in terms of increasing vehicle density and flux, reducing oscillation, and enhancing average flux with the increase of dynamic driver percentage. These advantages result from the fact that the new feedback strategies consider the tendency of road condition variations. Thus, in these situations, the system has the ability to alleviate the negative effects of congestion caused by the traffic jam. Thanks to the rapid development of modern scientific technology, MVDFS or CCDFS can be implemented in real traffic systems in the near future. If a navigation system (GPS) is installed in each vehicle, the velocity and position information of vehicles are known. Consequently, the mean velocity difference or the congestion coefficient difference in MVDFS or CCDFS can be calculated by the computers used to calculate the average velocity or congestion coefficient in previous strategies without extra cost. Taking into account the reasonable cost and more accurate description of road conditions, we conclude that these two feedback strategies are applicable.

Acknowledgments C.F. Dong appreciates many fruitful discussions with Prof. Bing-Hong Wang at the University of Science and Technology of China, and Dr. Nan Liu at the University of Chicago. The authors would like to thank the editors and the anonymous referees' helpful comments and suggestions.

References

1. Adler JL, Blue VJ (1998) Toward the design of intelligent traveler information systems. Transp Res Part C 6:157–172
2. Axelrod R (1984) The evolution of cooperation. Basic books, New York
3. Axelrod R, Hamilton WD (1981) The evolution of cooperation. Science 211:1390–1396

4. Barato AC, Hinrichsen H (2008) Boundary-induced nonequilibrium phase transition into an absorbing state. Phys Rev Lett 100:165701
5. Barlovic R, Santen L, Schadschneider A, Schreckenberg M (1998) Metastable states in cellular automata for traffic flow. Eur Phys J B 5:793–800
6. Bellouquid A, Delitala M (2011) Asymptotic limits of a discrete kinetic theory model of vehicular traffic. Appl Math Lett 24:149–155
7. Bier VM, Hausken K (2013) Defending and attacking a network of two arcs subject to traffic congestion. Reliab Eng Syst Saf 112:214–224
8. Biham O, Alan Middleton A, Levine D (1992) Self-organization and a dynamical transition in traffic-flow models. Phys Rev A 46:R6124
9. Chen BK, Sun XY, Wei H, Dong CF, Wang BH (2011) Piecewise function feedback strategy in intelligent traffic systems with a speed limit bottleneck. Int J Mod Phys C 22:849–860
10. Chen BK, Sun XY, Wei H, Dong CF, Wang BH (2012) A comprehensive study of advanced information feedbacks in real-time intelligent transportation systems. Phys A 391:2730–2739
11. Chen BK, Dong CF, Liu YK, Tong W, Zhang WY, Liu J, Wang BH (2012) Real-time information feedback based on a sharp decay weighted function. Comput Phys Commun 183:2081–2088
12. Chowdhury D, Santen L, Schadschneider A (2000) Statistical physics of vehicular traffic and some related systems. Phys Rep 329:199–329
13. Colman AM (1995) Game theory and its applications in the social and biological sciences. Butterworth-Heinemann, Oxford
14. Dong CF (2009) News story: intelligent traffic system predicts future traffic flow on multiple roads. PHYSorg.com. 12 Oct 2009
15. Dong CF, Ma X, Wang GW, Sun XY, Wang BH (2009) Prediction feedback in intelligent transportation systems. Phys A 388:4651–4657
16. Dong CF, Ma X (2010) Corresponding angle feedback in an innovative weighted transportation system. Phys Lett A 374:2417–2423
17. Dong CF, Ma X, Wang BH (2010) Weighted congestion coefficient feedback in intelligent transportation systems. Phys Lett A 374:1326–1331
18. Dong CF, Ma X, Wang BH (2010) Effects of vehicle number feedback in multi-route intelligent traffic systems. Int J Mod Phys C 21:1081–1093
19. Dong CF, Ma X, Wang BH, Sun XY (2010) Effects of prediction feedback in multi-route intelligent transportation systems. Phys A 389:3274–3281
20. Dong CF, Paty CS (2011) Application of adaptive weights to intelligent information systems: an intelligent transportation system as a case study. Inf Sci 181:5042–5052
21. Dong CF, Wang BH (2011) Applications of cellular automaton model to advanced information feedback in intelligent traffic systems. In: Salcido A (ed) Cellular automata—simplicity behind complexity, pp 237–258. ISBN 978-953-307-579-2
22. Dong CF, Ma X (2012) Dynamic weight in intelligent transportation systems: a comparison based on two exit scenarios. Phys A 391:2712–2719
23. Fukui M, Nishinari K, Yokoya Y, Ishibashi Y (2009) Effect of real-time information upon traffic flows on crossing roads. Phys A 388:1207–1212
24. Gao K, Wang WX, Wang BH (2007) Self-questioning games and ping-pong effect in the BA network. Phys A 380:528–538
25. Gazis DC, Herman R, Rothery RW (1961) Nonlinear follow-the-leader models of traffic flow. Oper Res 9:545–567
26. Hao QY, Jiang R, Hu MB, Jia B, Wu QS (2011) Pedestrian flow dynamics in a lattice gas model coupled with an evolutionary game. Phys Rev E 84:036107
27. He ZB, Chen BK, Jia N, Guan W, Lin BC, Wang BH (2014) Route guidance strategies revisited: comparison and evaluation in an asymmetric two-route traffic network. Int J Mod Phys C 25:1450005
28. Helbing D (2001) Traffic and related self-driven many-particle systems. Rev Mod Phys 73:1067–1141

29. Helbing D, Treiber M (1998) Gas-kinetic-based traffic model explaining observed hysteretic phase transition. Phys Rev Lett 81:3042–3045
30. Hino Y, Nagatani T (2014) Effect of bottleneck on route choice in two-route traffic system with real-time information. Phys A 395:425–433
31. Hofbauer J, Sigmund K (1998) Evolutionary games and population dynamics. Cambridge University Press, Cambridge
32. Kerner BS, Konhäuser P (1994) Structure and parameters of clusters in traffic flow. Phys Rev E 50:54–83
33. Kerner BS (2011) Optimum principle for a vehicular traffic network: minimum probability of congestion. J. Phys. A 44:092001
34. Laval JA, Leclercq L (2010) Mechanism to describe stop-and-go waves: a mechanism to describe the formation and propagation of stop-and-go waves in congested freeway traffic. Phil Trans R Soc A 368:4519
35. Lee K, Hui PM, Wang BH, Johnson NF (2001) Effects of announcing global information in a two-route traffic flow model. J Phys Soc Jpn 70:3507–3510
36. Li XB, Wu QS, Jiang R (2001) Cellular automaton model considering the velocity effect of a car on the successive car. Phys Rev E 64:066128
37. Li RH, Yu JX, Lin J (2013) Evolution of cooperation in spatial Traveler's Dilemma game. PLoS ONE 8:e58597
38. Nagatani T (2002) The physics of traffic jams. Rep Prog Phys 65:1331–1386
39. Nagel K, Schreckenberg M (1992) A cellular automaton model for freeway traffic. J Phys I 2:2221–2229
40. Nakata M, Yamauchi A, Tanimoto J, Hagishima A (2010) Dilemma game structure hidden in traffic flow at a bottleneck due to a 2 into 1 lane junction. Phys A 389:5353–5361
41. Nowak M, May RM (1992) Evolutionary games and spatial chaos. Nature 359:826
42. Orosz G, Wilson RE, Stépán G (2010) Traffic jams: dynamics and control. Phil Trans R Soc A 368:4455–4479
43. Perc M (2007) Premature seizure of traffic flow due to the introduction of evolutionary games. New J Phys 9:3
44. Roughgarden T (2003) The price of anarchy is independent of the network topology. J Comput Syst Sci 67:341–364
45. Sugden R (1986) The economics of rights, cooperation and welfare. Blackwell, Oxford
46. Sun XY, Jiang R, Hao QY, Wang BH (2010) Phase transition in random walks coupled with evolutionary game. Europhys Lett 92:18003
47. Szabó G, Töke C (1998) Evolutionary prisoner's dilemma game on a square lattice. Phys Rev E 58:69–73
48. Szilagyi MN (2006) Agent-based simulation of the n-person chicken game. In: Jorgensen S, Quincampoix M, Vincent TL (eds) Advances in dynamical games, vol 9. Annals of the International Society of Dynamic Games, Birkhäuser, Boston, pp 695–703
49. Tang TQ, Li CY, Huang HJ (2010) A new car-following model with the consideration of the driver's forecast effect. Phys Lett A 374:3951–3956
50. Tanimoto J, Hagishima A, Tanaka Y (2010) Study of bottleneck effect at an emergency evacuation exit using cellular automata model, mean field approximation analysis, and game theory. Phys A 389:5611
51. von Neumann J, Morgenstern O (1944) Theory of games and economic behaviour. Princeton University Press, Princeton
52. Wahle J, Bazzan ALC, Klügl F, Schreckenberg M (2000) Decision dynamics in a traffic scenario. Phys A 287:669–681
53. Wahle J, Bazzan ALC, Klügl F, Schreckenberg M (2002) The impact of real-time information in a two-route scenario using agent-based simulation. Transp Res Part C 10:399–417
54. Wang WX, Wang BH, Zheng WC, Yin CY, Zhou T (2005) Advanced information feedback in intelligent transportation systems. Phys Rev E 72:066702
55. Wang WX, Ren J, Chen GR, Wang BH (2006) Memory-based snowdrift game on networks. Phys Rev E 74:056113

56. Wang XF, Zhuang J (2011) Balancing congestion and security in the presence of strategic applicants with private information. Eur J Oper Res 212:100–111
57. Xiang Z-T, Li Y-J, Chen Y-F, Xiong L (2013) Simulating synchronized traffic flow and wide moving jam based on the brake light rule. Phys A 392:5399–5413
58. Yamauchi A, Tanimoto J, Hagishima A, Sagara H (2009) Dilemma game structure observed in traffic flow at a 2-to-1 lane junction. Phys Rev E 79:036104
59. Zhao X-M, Xie D-F, Gao Z-Y, Gao L (2013) Equilibrium of a two-route system with delayed information feedback strategies. Phys Lett A 377:3161–3169
60. Zheng XP, Cheng Y (2011) Conflict game in evacuation process: a study combining cellular automata model. Phys A 390:1042

Solving a Dynamic User-Optimal Route Guidance Problem Based on Joint Strategy Fictitious Play

Tai-Yu Ma

Abstract Dynamic route guidance systems aim to provide users with on-line information on traffic conditions and suggest relevant route guidance to facilitate route choices for users. In this study, we consider the problem as a multi-player repeated game in a dynamic multi-agent transportation system. We propose a game theory approach based on joint strategy fictitious play by explicitly modeling users' compliances to route recommendations as an inertia term. Each guided user makes his travel time estimations and local outgoing link decisions based on his historical experiences and traffic time information received en-route as provided by a system administrator. Based on the travel times estimated en-route, users adapt their route choices progressively via fast routes to their destinations. The dynamic user-optimal route guidance problem is formulated as a variational inequality problem in a queue-based traffic flow model. We show that the proposed approach can solve a dynamic user-optimal route guidance problem based on users' local outgoing link choice decisions. The numerical studies are implemented by considering two classes of users in the system: informed and non-informed users. The results demonstrate the convergence of the proposed algorithm and highlight significant travel times and delay reduction in a congested situation. Although the user-compliance mechanism for the route recommendations is currently modeled as a static term, it provides rooms for further improvement based on more realistic compliance mechanisms.

Keywords Fictitious play · Route guidance · Real-time information · Route choice behavior · Advanced traveler information systems · Adaptive learning · Correlated equilibrium · Learning in game

T.-Y. Ma (✉)
CEPS/INSTEAD, 3, Avenue de la Fonte, L-4364, Esch-sur-Alzette, Luxembourg
e-mail: tai-yu.ma@ceps.lu

K. Hausken and J. Zhuang (eds.), *Game Theoretic Analysis of Congestion, Safety and Security*, Springer Series in Reliability Engineering,
DOI 10.1007/978-3-319-11674-7_3

1 Introduction

A route guidance system is a kind of traveler information system which provides route recommendation messages to drivers equipped with in-vehicle guidance advice. Drivers input their destinations before their trips and the system computes routes with least travel times based on periodically updated predictions of the state of traffic in the network [5, 31, 47]. There are two kinds of route guidance systems: the reactive route guidance system and the anticipatory route guidance system. The first one utilizes regularly updated traffic information to compute the least travel time routes without taking into account the driver's compliance for the recommended route. The second one anticipates drivers' route choices with respect to predicted traffic conditions and provides route recommendations accordingly. The system generates route recommendations based on a current traffic situation and anticipates other drivers' route choice behavior in such a way that traffic-flow prediction is consistent with its own prediction [3, 5, 33]. According to system design objectives, if route recommendations are given in a way such that total system travel times of all drivers are minimized, it is called *system-optimal route guidance*. However, if it is based on user-optimal guidance, i.e. users are oriented to least travel time routes, the system is called *user-optimal route guidance* system. In this study, we consider the latter problem unless otherwise mentioned.

The route guidance system is expected to reduce recurring traffic congestion on a road network and enhance indirectly road safety. The empirical study indicated that traffic congestion is positively associated with accident occurrence frequency [60]. A recent comprehensive study on the relationship between road safety and congestion on motorways revealed that increasing congestion may affect significantly road safety due to unstable traffic condition and more frequently lane changing behavior [41]. The authors suggested that future research effort is needed to study the potential impact of congestion on road safety. The absence of route guidance systems may compromise safety and security on our roads. Route guidance systems can reduce travel times, remove congestion, and increase users' road safety and security. Route guidance systems have thus been increasingly used, especially in urban areas. Current route guidance systems such as Tomtom (www.tomtom.com) or Garmin (www.garmin.com) provide users with detailed real-time traffic information, which is especially helpful for users to better plan their trips, get efficiently and safely to their destinations, and avoid traffic congestion, accidents, road blocks, or other hindrances. Such systems can also reduce a user's burden to find routes, especially in unfamiliar rural areas. However, route guidance systems may also cause driver distractions and increase accident risk, e.g. because users focus more on operating the system than on being alert in traffic. Similar safety issues have been reported e.g. when crossing a road while operating a mobile phone. To reduce the risk of accident, voice guidance is generally available to reduce driver distractions while operating the system. Although the functionalities and safety issues of route guidance systems continuously improve, such systems provide advantages weighted against safety issues. The evaluation of route guidance systems from a

road safety perspective has received increased attention in recent years and has become an important issue for road safety research [1].

The problem of dynamic route guidance can be formulated as a dynamic user equilibrium problem at each user's current node (road intersection), i.e. the decision node at which users decide which outgoing link to choose or are split (guided) to routes from that node to their respective destinations [5]. It states that at user equilibrium, *all guided users use the least travel time routes towards their destinations*. Hence the route guidance problem is a generation of dynamic traffic assignment problem, but it differently incorporates pre-trip/en-route traffic information and driver compliance to route recommendations to generate consistent route guidance [6]. The problem is difficult to solve due to the fact that there is no closed form of travel time function in a simulation-based traffic flow model. Several dynamic traffic assignment solution methods have been proposed for solving route guidance problem [29, 31, 69]. The reader is referred to [51, 57, 67] for a comprehensive review of dynamic traffic assignment model and solution methods.

The state-of-the-art solution methods are generally based on an iterative route adjustment procedure based on the *method of successive averages* (MSA) to obtain an approximate solution [68]. This method consists of shifting users to cheaper routes on a day-to-day basis until a stable state (user equilibrium) is achieved. The system first predicts network conditions for next time slices and then recommends the time-dependent shortest routes to guided users accordingly. However, this approach does not consider the resistance in drivers' route choice behavior and may generate later congestion if too many guided users are assigned to these routes [5, 14, 33]. Bottom [5] proposed an analytical framework for consistent route guidance problem in which three system components, i.e. route splits, network conditions and guidance messages, are identified and the causal relationships between pairs of these components are analyzed. The author formulated the consistent route guidance problem as a fixed point problem and proposed solution methods based on the MSA and Polyak iterate averaging methods. As mentioned by Paz and Peeta [48], the solution method of Bottom [5, 6] is computational intensive for real time implementation. Moreover driver's compliance behavior modeling is still missing in the solution method. For this issue, the authors focused particularly on modeling driver's route choice behavior with information provision [49, 50] and proposed a behavior consistent route guidance framework based on the control theory [48].

Other approaches based on control theory for optimizing the route guidance system were also studied [15, 21, 43]. The drawback of these methods is that drivers' reactions to received information are not taken into account which results in an inaccurate traffic flow prediction. For this issue, Peeta and Yu [49, 50] proposed a hybrid, rule-based approach to model day-to-day and within-day adaptive route choice behavior under information provision. The perception of the cost of route is updated based on an individual's current experience for that day. The within-day route choice considered an individual's compliance and inertia for received information which are modeled by some probabilistic decision rules. Jha et al. [32] applied the discrete choice model to capture a driver's day-to-day departure time and route choice behavior under information provision. The driver's perception was

updated based on a weighted combination of historical perceptions of travel cost and traffic information. In an experimental study, Selten et al. [54] reported laboratory experiments on the driver's day-to-day route choice game in a simple two-route network. They found that drivers adjust their daily route choices based on their received payoff history. Wahle et al. [59] proposed a multi-agent micro-simulation model to study the impact of online information provisions on a two-route scenario. Drivers are modeled as agents shifting their route choices with minimum travel times under dynamic information provision. However, the driver's adaptive learning behavior was not incorporated into this study.

The effectiveness of route guidance system depends on consistent forecast of future network states under driver compliance assumption. Modeling driver's compliance and response to traffic information have become active research issues. Related work on these issues concerns modeling the feedback effect of the advanced traveler information system (ATIS) on traffic state prediction [8, 16, 17], driver's response to information [11, 22, 55] and modeling compliance rate of route guidance related to the quality of information [10, 62, 64].

Game theory has been widely studied for the Nash equilibrium problem in N-player repeated games [20, 65]. It was applied for system-optimal routing [23], distributed controls [52] and optimization [36]. One of the promising learning processes in games is *fictitious play* (FP) which is an N-player repeated game in which each player selects a best action based on the assumption that other players' choices follow their historical frequencies of past decisions [7]. It has been proven that the FP process converges to Nash equilibrium for N-player repeated games with identical payoff functions and other classes of games [4, 45]. The FP process is promising for modeling route choice behavior because it is similar to a driver's day-to-day route choice adaptation behavior based on his past experiences [49]. Existing applications of the FP process mostly focused on the congestion game problem, i.e. how to compute the pure Nash equilibrium of a route choice based on an adaptive learning process [12, 44]. The reader is referred to Hurkens [30], Young [65] and Hart [26] for related learning processes of N-player games.

This paper aims to propose a game-theory based approach for solving the user-optimal route guidance problem. We consider the user-optimal route guidance problem as a distributed and individual routing problem. The term "distributed" is related to local link choice decisions based on each individual user's expected time-dependent shortest route computation and best reply strategy. Our motivation is that in a multiplayer dynamic congestion game, each player (user or driver) makes his route decision at his current node based on an estimated travel time to his destination. Like in the joint strategy fictitious play process [42], each player makes his individual decision based on information gained from both his historical experience and the updated traffic condition information obtained. The added value of the proposed method is that it is convenient to model driver's compliance to route recommendations. We demonstrate that the proposed approach can achieve an effective reduction in travel time through such a self-learning process.

The rest of this paper is organized as follows. In Sect. 2, we present a mathematical formulation of the route guidance problem based on the variational

inequality formulation of dynamic user equilibrium [19]. An iterative adjustment process is described as its general solution method. For the implied traffic flow model the point queue model is applied. Section 3 recalls the FP process for an N-player repeated game. It follows the distributed *joint strategy fictitious play with inertia* (JSFP) process for the dynamic route guidance problem. As far as the numerical study is concerned, we test the performance of the proposed method and compare it with classical iterative solution method in an illustrative test network. Finally, we draw the conclusions and future extensions.

2 User-Optimal Route Guidance Problem

We first state briefly the notation used in this study. The physical road network is modeled by a directed graph $G(N, E)$ where N is a set of nodes $\{n\}$ and E is a set of directed links $\{e\}$. Note that a node is defined as a road intersection, and a link is defined as a road section connected by its head node and tail node. Both origins(o)/destinations(d) are nodes where travelers depart from/arrive at on the road network.

Notation

o	Origin, $\forall o \in O$. O is the set of origins
d	Destination, $\forall d \in D$. D is the set of destinations
k	Origin-destination pair (o, d), $\forall k \in K$. K is the set of origin-destination pairs
s	Node not belonging to destination set, $\forall s \in S$. $S = N \setminus D$
u	Tail node of a directed link where its head node is s
r_{sd}	Route from node s to destination d. A route is defined as a concatenation of links or nodes without cycles connecting from node s to destination d. R_{sd} is the set of r_{sd}
$c_r(t)$	Travel time on route r for guided and non-guided users when entering initial node of the route at time t
g	Superscript label for guided users
$c_r^g(t)$	Travel time on route r for guided users when entering initial node of the route at time t
$f_r^g(t)$	Flow of guided users (number of guided users per time unit) on route r at time t
$\Phi_{sd}^g(t)$	Travel demand rate of guided users (number of guided users per time unit) from node s to destination d when entering the node at time t
t	Time, continuous floating variable. t_0 denotes the time when the first user enters the network
Δ	Discretized time slice on which traffic information is regularly updated
T	The predefined and fixed time that exceeds the simulation times for all users moving on the network to their destinations
h	Discretized time interval index $h \in H$, where $h = \lfloor t/\Delta \rfloor$ with $\lfloor x \rfloor$ being the operator denoting the largest integer smaller than or equal to x

H	Set of discretized time interval indexes over T
z	Departure time interval index $z \in Z$, where $z = \lfloor t/\Delta_z \rfloor$ with Δ_z being the discretized departure time slice
Z	Set of departure time interval indexes over a predefined departure time period T_z
w	Iteration index

The user-optimal route guidance problem (URG) can be formulated as a user-optimal dynamic equilibrium problem based on the variational inequality formulation. The problem consists of finding user-optimal route recommendations at each node of the network stating that all guided users use least travel time routes from their current node to their respective destination. The problem is a generalization of dynamic user equilibrium problem and has been widely studied in the past [5, 47, 68]. In what follows, we present the mathematical formulation of the problem and apply a point queue model and classical iterative solution method.

2.1 Problem Formulation

Consider a dynamic user-optimal routing problem on a road network with given fixed time-dependent origin-destination demand. Users (drivers) on the road network are distinguished as two classes: guided users and non-guided users. Each user determines himself whether to be guided (by purchasing a route guidance system) or non-guided (by not purchasing a route guidance system). The former are equipped with an in-vehicle device capable of receiving regularly updated traffic condition information and making en-route route changes to the destination. The latter are assumed to be non-informed users who utilize time-dependent shortest routes, fixed at the time of departing from his node of origin. This simplification reflects that non-guided users select their minimum cost routes based on their prior knowledge of network conditions. The two classes of users are loaded in the road network with respective routing rules and determine jointly the traffic conditions and the travel times on each route. Although the user-optimal route guidance problem is relevant to the guided users, the system simulates the traffic flow propagation in the simulator of the two types of users based on the same traffic flow model (described later). The system can then obtain experienced travel times of each guided and non-guided user and updates route recommendations for guided users accordingly. Route recommendations are not provided to non-guided users, and are thus also not updated for non-guided users. The URG problem is related to the class of guided users[1] and can be formulated as a fixed-point problem for each generic node-destination pair of (s, d) [5, 68], i.e. a user-optimal route choice

[1] Note that one can also incorporate the learning behavior of non-guided users in the URG problem and solve the corresponding fixed point problem for both classes of users [6].

problem from a guided user's current node to his destination. The fixed-point problem can be formulated mathematically as an infinite dimensional variational inequality problem with respect to each pair (s, d) as follows [19, 28]:

Given a pair (s, d), find a user-optimal route flow vector for the class of guided users $\mathbf{f}^{g*} = \left\{f_r^{g*}(t) | r \in R_{sd}, t \in [t_0, T]\right\}$ where R_{sd} is the set of routes connecting (s, d) such that

$$\int_{t_0}^{T} \left\{ \sum_{r \in R_{sd}} c_r^g(t) [f_r^g(t) - f_r^{g*}(t)] \right\} dt \geq 0, \tag{1}$$

for all $\mathbf{f}^{g*} \in \Xi_{sd}^g$, where superscript * expresses user-optimal route flow for guided users. Ξ_{sd}^g is the set of feasible route flows for guided users which satisfies the following conditions:

$$\sum_{r \in R_{sd}} f_r^g(t) = \Phi_{sd}^g(t), \forall s \in S, \forall d \in D \, (\textit{flow conservation}) \tag{2}$$

$$f_r^g(t) \geq 0, \ \forall t \in [t_0, T] \, (\textit{non-negativity of route flow}) \tag{3}$$

The above variational inequality problem aims to find a set of user-equilibrium route assignments for guided users. Equations (2) and (3) show flow conservation for each node-destination pair and non-negativity constraints of route flow respectively. The solution of the problem states that only routes with least travel times are used [18, 19]:

$$\begin{cases} c_r^g(t) > \min\limits_{r \in R_{sd}} (c_r(t)) \Rightarrow f_r^{g*}(t) = 0 \\ f_r^{g*}(t) > 0 \ \Rightarrow \ c_r^g(t) = \min\limits_{r \in R_{sd}} (c_r(t)) \end{cases} \text{for all } t \in [t_0, T] \tag{4}$$

This user-optimal equilibrium in (4) states that travel time on the routes used by guided users are the minimum of the travel times by guided and non-guided users on all possible routes connecting the same origin and destination on a road network. There is no analytical form to obtain such a user-optimal equilibrium for a simulation-based traffic flow model. The solution approaches are based on iterative procedures (described in Sects. 2.3 and 3) to iteratively update route recommendations for guided users toward user-optimal equilibrium states. Hence, there is no circular issue to achieve Eq. (4), i.e. for any user, route choices are always determined before loading on their chosen route. The last equation sign in Eq. (4) is interpreted as in computer programming of the simulator, where all $c_r(t)$ such that $r \in R_{sd}$ are inserted into the Min function on right hand side to determine $c_r^g(t)$ on the left hand side. Equation (4) states Wardrop's user-optimal equilibrium in traffic theory [61]. In the context of the route guidance problem, it can be stated as "*the journey times on all the routes actually used by guided users are equal, and less than those which would be experienced by a guided user on any other routes*",

i.e. at a Wardrop user-optimal equilibrium, no guided user can reduce his travel time by unilaterally changing his own route choice. This concept is equivalent to a Nash equilibrium concept [13]. It is also a correlated equilibrium of an N-player game in our dynamic routing problem context [27]. Note that we can observe that the dynamic-user equilibrium assignment problem in transportation science is a special case of the dynamic URG problem at a user's origin node [5, 68].

2.2 Traffic Flow Model and Link Travel Time Prediction

The traffic dynamic is modeled using the point queue model without taking into account physical dimension at intersections [24, 34]. Although the point queue model is very simple, it represents approximately realistic traffic flow propagation similar to Nagel-Schreckenberg microscopic traffic flow model [46]. The basic concept of the point queue model is based on traffic flow supply and demand dynamics at intersections. If flow demand (inflow rate) is superior to its supply (time-dependent flow capacity) queues are formed at the end of the link. Let link flow capacity be defined as the maximum rate of flow at time t [58]. We distinguish link inflow (outflow) capacity $\sigma_e(t)$ ($\delta_e(t)$) stating maximum flow rate at the head (tail) node of a link. Each link is characterized by its maximum flow capacity $\delta_e^{\max} = \sigma_e^{\max}$ and its maximum speed constraint. The number of vehicles can be stocked on a link is determined by $\rho_e^{\max} l_e$ where $\rho_e^{\max}$ is maximum traffic density, and l_e is link length. When a vehicle arrives at link, a least travel time based on free flow speed is calculated for passing through that link. The outflow at the end node u of that link depends on total demand (outflows from all upstream links of node u) and supply (flow capacities on that link and its downstream links). If the demand at node u is superior to its supply, a priority queue is generated at node u. Later arriving vehicles joint this queue and wait for already queued vehicles to be cleaned. We formulate the basic concept of the point queue model as follows.

Let $Y_e(t)$ and $X_e(t)$ denote the cumulative number of users (vehicles) arriving and leaving link e at time t, respectively. For any user (guided or non-guided user), the link travel time $c_e(t)$ when entering link e at time t is calculated as

$$c_e(t) = X_e^{-1}(Y_e(t)) - t \tag{5}$$

The above function computes user's experienced link travel times, which depend on the entering time and traffic state of that link. We assume that the First-In-First-Out principle is respected for each link, which guarantees that link travel time is a non-decreasing function of traffic flow. The partial flow capacity from upstream links to downstream links depends on the number of lanes and the priorities associated with the links [24]. The point queue model assures that traffic flow propagation in the network respects basic physical rules of traffic. Consider a node s with a set of upstream links $J^-(s)$ and a set of downstream links $J^+(s)$. Let e_- and

e_+ be an upstream and downstream link of node s, respectively. In the merge case, flow from the upstream links e_- to a specific downstream link e_+ cannot exceed the link flow capacity of e_+ at time t, i.e.

$$\sum_{e_- \in J^-(s)} q_{e_- e_+}(t) \leq \sigma_{e_+}(t), \ \forall e_+ \in J^+(s), \tag{6}$$

where $q_{e_- e_+}(t)$ is link outflow from e_- to e_+ at time t. In the diverge case, the outflow from e_- to e_+ is constrained by the following equation (supply-demand approach, Lebacque [37]; Lebacque and Khoshyaran [38]):

$$q_{e_- e_+}(t) \leq \min(\alpha_{e_- e_+} \delta_{e_-}^{\max}, \sigma_{e_+}(t)), \tag{7}$$

where $\alpha_{e_- e_+}$ is a split coefficient between 0 and 1, corresponding partial outflow capacity allocation from e_- to e_+, depending on physical configuration and number of lanes on link. The link inflow capacity at time t is determined by

$$\sigma_{e^+}(t) = \begin{cases} \sigma_{e^+}^{\max} & \text{if } \vartheta_{e^+}(t) < \rho_{e^+}^{\max} l_{e^+} \\ 0 & \text{otherwise} \end{cases}, \tag{8}$$

where $\vartheta_{e^+}(t)$ is the number of vehicles on link e_+ at time t. Note that the point queue model can be replaced by other more realistic traffic flow models to capture queue spillovers at intersections [25, 35, 39, 40]. The route guidance system provides route recommendations for the guided users based on predictions of future traffic conditions. It is important to estimate travel times of routes for the route recommendations that are computed. Consider a guided user currently located at node s. We aim to estimate a travel time from the guided user's current node s by taking a link e_{su} to his destination d. This estimation can be calculated by summing up the link travel time of e_{su} plus the estimated minimum travel time from u to d, i.e.:

$$\tilde{c}_{r_{sd}}(t) = \tilde{c}_{e_{su}}(t) + c^*_{r_{ud}}(t), \tag{9}$$

where the first term represents the estimated travel time on link e_{su} at time t. The second term is estimated as the shortest travel time at time t based on time-dependent shortest route computation by a variant of the Dijkstra algorithm [66]. We assume that the system administrator has current traffic state information based on road traffic monitoring sensors. The link travel times can then be estimated as their free-flow travel times plus their waiting times in queues. The queuing time is estimated as $\lambda_e(t)/\delta_e(t)$, where $\lambda_e(t)$ is the number of vehicles queuing on link e and $\delta_e(t)$ is the outflow capacity of link e at time t. In case $\delta_e(t) = 0$, the queuing time of last leaving vehicle is used. The computation of Eq. (9) is based on the most recent traffic information update. Note that more realistic travel time prediction methods based on traffic physics and data-mining techniques can also be applied if needed [53].

2.3 Iterative Solution Algorithm Based on the MSA

The iterative solution algorithm is a widely used solution method for the URG problem [3, 68]. It consists of finding a dynamic user equilibrium (Nash equilibrium) for routes from the guided users' current node to their destinations by iteratively shifting flow towards cheaper routes based on current network state and travel time prediction. The route guidance is assumed to be unchanged during each discretized time slice Δ. The guided users are progressively propagated toward their destinations. The process is repeated until the maximum number of iteration is achieved or the gap in relation to the idealized user equilibrium state is stabilized. The objective of the iterative solution algorithm is to obtain a stabilized user-optimal splitting rate at each node of the network for the guided users. The iterative solution algorithm is described as follows.

Main algorithm

Step 1: Initialization. Initialize link travel time by free flow travel time. Set the flow splitting rates (choice probabilities of next outgoing links for given destinations) $\phi^0_{sud}(h) = 0$ for all discretized time indexes $h \in H$, destinations $d \in D$, non-destination nodes$s \in S$ and outgoing nodes of s. Set iteration index $w = 0$.

Step 2: Dynamic network loading and route guidance advice update.

a. Update link travel time prediction $\tilde{c}_{eh}$ for all $e \in E$. Compute time-dependent shortest routes $r^{*w}_{sd}(h)$ for all nodes $s \in S$ and $d \in D$.

b. Compute *temporal route guidance advice* $\widetilde{\phi}^w_{sud}(h)$ as (Zuurbier [68]):

$$\widetilde{\phi}^w_{sud}(h) = \begin{cases} 1 \text{ if } r = r^{*w}_{sd}(h) \text{ and } e_{su} \in r \\ 0 \text{ otherwise} \end{cases}, \tag{10}$$

for all $h \in H, s \in S, d \in D$

c. The updated route guidance advice is weighted by the MSA as

$$\phi^w_{sud}(h) = (1-\alpha)\phi^{w-1}_{sud}(h) + \alpha\widetilde{\phi}^w_{sud}(h), \text{for all } u \in \Gamma(s), \tag{11}$$

for all $h \in H, s \in S, d \in D$, where $\alpha = 1/w$, and $\Gamma(s)$ is the set of outgoing nodes of s. The above route advice update is the weighted average of previous route guidance advice and *temporal* route guidance advice. We have the property that $\sum_{u\in\Gamma(s)} \phi^w_{sud}(h) = 1$. This property can be verified without difficulty by updating $\phi^w_{sud}(h)$ for each $u \in \Gamma(s)$ on the time-dependent shortest route from any node s to destination d.

Step 3: Stop criteria. We define a gap function for the dynamic user (Nash) equilibrium which measures how far users' experienced travel times are from ideal shortest route travel times. The gap function is defined as

$$\text{Gap} = \frac{\sum_{z\in Z,k\in K,r\in R_{zk},m\in\Omega_{zkr}} [c_m(t) - c^*_{zk}]}{\sum_{z\in Z,k\in K} \hat{\Phi}_{zk} c^*_{zk}}, \tag{12}$$

where m is a user. Ω_{zkr} is the set of users (guided and non-guided) on route r with origin-destination pair k and departure time interval z. $c_m(t)$ is user m's experienced travel time with departure time t. $\hat{\Phi}_{zk}$ is the number of guided and non-guided users for origin-destination pair k and departure time interval z. c^*_{zk} represents minimum travel time with respect to z and k. If the gap value is stabilized or the maximum number of iterations is achieved then stop; otherwise, set w: = w + 1 and go to Step 2.

3 Joint Strategy Fictitious Play for Dynamic User-Optimal Route Guidance Problem

This Sect. 3 applies only for guided users to solve the URG problem. The iterative solution algorithm in Sect. 2.3 is based on a centralized time-dependent shortest route computation to assign guided users to those shortest routes. Differently, the following proposed route guidance approach is based on individual users' learning strategy in response to day-to-day traffic congestion and en-route traffic state information. Guided user's learning strategy is based on the FP process to decide a sequence of outgoing links toward his destination. In this way, guided user's compliance to route recommendations or behavioral inertia can be incorporated, and en-route traffic information can be useful to estimate expected travel time to destination. We show that such distributed route guidance decisions undertaken at each individual level can achieve similar travel time reduction result as the iterative solution algorithm. In this section, we first recall the concept of the FP process for an N-player repeated game. Then we propose a distributed joint strategy fictitious play with inertia process for the URG problem.

3.1 Fictitious Play

Let us recall the FP process for the congestion game problem. Consider a finite set of players (guided users) $I = \{1, \ldots, v\}$ where each player has to select a finite set A_i of actions (routes) to his destination. A payoff function of player i is determined

by the profile of actions of all players, written as $U_i : A \rightarrow \Re$, where $A = \times_{i=1,\ldots,v} A_i$ is the Cartesian product of each player's action choices. Let $a_i \in A_i$ be the action choice of player i. The actions of all other players are denoted as $a_{-i} = \{a_1, \ldots, a_{i-1}, a_{i+1}, \ldots, a_v\} \in A_{-i}$. Let $a = (a_i, a_{-i}) \in A$ be an action profile of all the players. The user-optimal strategy can be defined as

$$a_i^* = \text{Arg} \max_{a_i \in A_i} [U_i(a_i, a_{-i})] \tag{13}$$

The pure Nash equilibrium is achieved for the action profile $a^* = (a_i^*, a_{-i}^*)$ if for any player i the following condition holds [42]:

$$U_i(a_i^*, a_{-i}^*) = \max_{a_i \in A_i} [U_i(a_i, a_{-i}^*)] \tag{14}$$

The well-known FP process states that each player selects his optimal action following a strategy (probability distribution over his action set) which best responds to the empirical frequencies of actions taken by all other players. The empirical frequency of a player is evaluated as the percentage of the number of iterations (or days in user's day-to-day route choice learning context) that an action has been taken until previous iteration (day). The FP process requires that each player knows the empirical frequencies of all other players and selects a best response based on the assumption that other players select their action independently based on their empirical frequencies. The payoff function is computed by the joint probability distribution of all other players. It has been proven that the FP process converges to Nash equilibrium in potential games [45]. However, the FP process is not computationally feasible for a large-scale N-player repeated game due to the high computational times of the payoff function for very large action choice sets [56]. An alternative way is that each player considers the actions of all other players jointly and selects a best action based on the joint empirical frequencies of all other players. This process is called JSFP process, which reduces the computational burden of the FP process [42]. On each iteration, each player only needs to compute the expected payoffs of his actions and selects a best action randomly from among his best action choice set. To model a player's unwillingness to change, a stochastic mechanism called *inertia* needs to be taken into account. The inertia takes into account a player's probabilistic resistance to change his behavior in his action choice [42]. Note that the inertia can be considered as a human risk aversion behavior to reduce his cognitive effort. The inertia strength is in general related to a player's learning process under uncertainty [9, 63]. In this study, we propose a *distributed JSFP process with inertia,* which consists of learning optimal route guidance policy at local level with updated online traffic information. Each time when a player (guided user) arrives at a node of the network, he computes the expected payoffs (travel times) for each outgoing link (action) based on the empirical, average payoffs made by the other players as well as on updated travel time estimation. Each player does not need to track the actions made by all other players but instead he needs to estimate the average payoff of actions based on the joint actions of all other players. The distributed JSFP process is described as follows.

3.2 Distributed Joint Strategy Fictitious Play Algorithm Under Information Provision

Consider a finite set of guided users $i \in I = \{1, \ldots, v\}$. Each guided user has a finite number of routes to select to his destination. To avoid the difficulty of enumerating all possible routes for each origin-destination pair, we consider the route choice problem locally, i.e. each guided user constructs his route progressively by selecting an outgoing link from his current node until he arrives at his destination. Consider guided user i arriving at a node s. A finite set of routes from s to user's destination $d \in D$ is denoted by R_i^{sd}. The action profile of all guided users' route choices can then be defined as $R^{sd} = \times_{i=1,\ldots,v} R_i^{sd} = R_1^{sd} \times R_2^{sd} \times \cdots \times R_v^{sd}$. The payoff function $U_{i,sd} : R^{sd} \rightarrow \Re$ states user i's experienced travel times on his route from s to d. As it is practically impossible to observe and enumerate all possible actions of all routes in R^{sd}, direct computation of the best route based on mixed strategies of all other users is not feasible. To reduce the computational difficulty of the FP process, the JSFP process only needs to compute the predicted payoffs of actions. We assume that a road network administrator observes current network states and sends travel time predictions based on Eq. (9) to guided users. Based on regularly updated travel time estimations of routes, guided users select their best routes progressively until they arrive at their destinations.

The distributed JSFP with inertia

Step 0 (Initialization): initialize free flow link travel time. Set initial iteration (day) index $w = 0$.

Step 1: Each time a guided user $i \in I$ arrives at a node s, compute the expected (average) payoffs up to iteration w for each action candidate e (outgoing link of s) as:

$$\bar{U}_{i,sd}^{w}(e) = \frac{1}{w} \sum_{\tau=0}^{w-1} U_{i,sd}^{\tau}(e), \forall e \in J^{+}(s), \tag{15}$$

where $J^{+}(s)$ is the set of outgoing links of node s. $U_{i,sd}^{\tau}(e)$ is the empirical (experienced) payoffs for taking the outgoing link e to guided user i's destination d at iteration τ, i.e.

$$U_{i,sd}^{\tau}(e) = -\sum_{e \in r_{sd}} c_i^{\tau}(e), \tag{16}$$

where $c_i^{\tau}(e)$ is the experienced travel times of link e of guided user i at iteration τ. It is important to note that the experienced payoffs can be obtained a posteriori once guided users arrive at their destination. Therefore each guided user needs to

estimate these expected travel times based on future travel time prediction. The expected payoff of Eq. (15) is then approximated by

$$\bar{U}_{i,sd}^{w}(e) \approx \frac{w-1}{w}\bar{U}_{i,sd}^{w-1}(e) + \frac{1}{w}\tilde{U}_{i,sd}^{w}(e), \forall e \in J^{+}(s), \tag{17}$$

where $\tilde{U}_{i,sd}^{w}(e)$ is the estimated travel time for guided user i for taking link e to his destination, estimated by Eq. (9). Each guided user computes his best response action set as:

$$B_{i,sd}^{w} = \left\{ e \in J^{+}(s) : \arg\max_{e \in J^{+}(s)} [\bar{U}_{i,sd}^{w}(e)] \right\}, \tag{18}$$

The best response action set represents the outgoing links with the best expected payoffs at iteration w.

The action $a_{i,sd}^{w}$ chosen by guided user i at iteration w when arriving at node s is defined by the following rules:

$$\text{If } a_{i,sd}^{w-1} \in B_{i,sd}^{w} \quad \Rightarrow \quad a_{i,sd}^{w} = a_{i,sd}^{w-1} \tag{19}$$

$$\text{If } a_{i,sd}^{w-1} \notin B_{i,sd}^{w} \text{ then } \begin{cases} a_{i,sd}^{w} \in \text{Rand}(B_{i,sd}^{w}) & \text{with probability } 1-\varepsilon \\ a_{i,sd}^{w} = a_{i,sd}^{w-1} & \text{with probability } \varepsilon \text{ (inertia)} \end{cases} \tag{20}$$

where $\text{Rand}(B_{i,sd}^{w})$ is a random element in $B_{i,sd}^{w}$. Rule (19) states that if the action on a previous day is still optimal, guided users retain the same choices. Otherwise, guided users will either randomly choose an action among their best action set with probability $(1-\varepsilon)$ or retain their previous actions through inertia ε. Note that the MSA approach updates route guidance advices by a weighting of current advice and historical advices whereas the JSFP approach re-uses previous successful advice (on the previous day) if current advice is identical. In case when current advice is different from the previous day, the probabilistic rule of Eq. (20) applies. Based on the distributed JSFP process with inertia described above, each guided user constructs the best route towards their destination progressively. When each guided user arrives at their destination, experienced average payoffs $\bar{U}_{sd}^{w}(e)$ are updated by Eqs. (15) and (16) for all $s \in S, d \in D$. Note that the expected payoff for actions is computed based on average experienced payoffs for users of the same class with the same destination when arriving at node s at the same time interval.

Step 2: If the gap function value stabilizes, i.e. $\left|\text{Gap}^{w} - \text{Gap}^{w-1}\right| / \text{Gap}^{w-1} \leq \zeta$ with ζ being a small constant (e.g. 0.001) for three consecutive iterations or when a predefined number of maximum iterations is achieved then stop; otherwise set $w := w + 1$ and go to Step 1.

The FP process with identical interest, i.e. all players share a common interest, has been proved to converge to Nash equilibrium [21, 45]. The JSFP with inertia process with self interest was proved to converge to a pure Nash equilibrium in all generalized ordinal potential games [42]. The convergence property of the distributed JSFP with inertia to a near Nash equilibrium for the route guidance problem is based on the established proof by Marden et al. [42]. The numerical result in Sect. 4 supports this argument. Indeed the convergence to a pure Nash equilibrium depends on consistent traffic prediction. How the traffic prediction influences obtained near Nash equilibrium needs to be further studied in the future. The distributed JSFP process for the route guidance problem can be considered as an iterative user-optimal route learning process. Each guided user computes expected travel times to destination on each alternative links and makes his best response under the assumption that other users would follow their historical routing decisions. This procedure [Eqs. (18)–(20)] is similar to the route adjustment of the MSA [Eqs. (10) and (11)] but differently it is based on a microscopic approach (individual user's route choice decision and learning) compared to the macroscopic shortest route flow split of the MSA.

4 Numerical Study

The numerical study is implemented using a road network with 32 nodes and 94 links (Fig. 1). The travel demand profile is set in such a way to generate congestion during a two-hour traffic generation period. There are four origins and one destination. For network attribute setting, link length is set randomly between 3 and 3.5 km. The number of lanes is set as two for orthogonal links and as one for negatively sloped links. The departure time is randomly selected from each user's departure time interval on the first day and then kept unchanged for subsequent days in order to analyze the impact of route guidance recommendation. Moreover, to test the performance of the proposed approach, two classes of users are implemented: guided users and non-guided users. Only guided users can receive regularly updated traffic information. Different scenarios with respect to the variation in travel demand and the percentages of guided users are implemented to test the

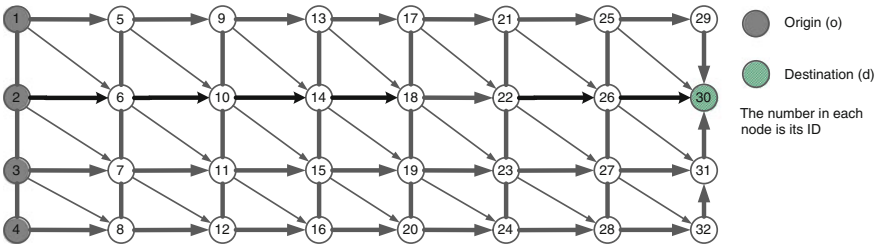

Fig. 1 A simple network

performance of the proposed algorithm. The implementation of microscopic traffic flow simulation is based on discrete event simulation technique programmed using C++ language.

4.1 Computational Results

The demand profile is shown on the right side of Fig. 2. The number of users increases gradually until it reaches the peak hour traffic flow of 8,640 users/h and then decreases gradually to 960 users/h. Travel time delay for the scenario of not using a route guidance system is shown on the right side of Fig. 2. Traffic information update frequency is adapted to the size of the network as 1 min. Note that if the information update frequency is too low it may reduce the effect of the route guidance system on travel time reduction.

The convergence result of the proposed distributed JSFP with inertia is shown on the left side of Fig. 2. The gap function decreases rapidly and then stabilizes. When comparing the effect of market penetration of route guidance systems on the convergence, it is reasonable to find higher gap function value for higher market penetration. This is because increasing the number of guided users on recommended routes may generate congestion on these routes and reduce its benefits. To verify the performance of the proposed route guidance algorithm, we compare the average travel times of each class for various market penetrations. The left subplot

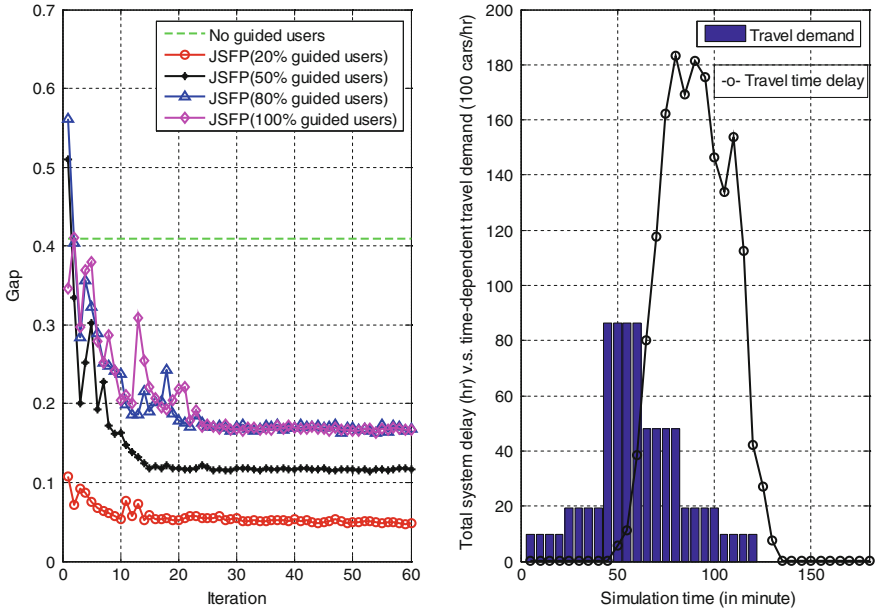

Fig. 2 The convergence result of the gap function (*left*) and travel demand profile and total system travel time delay which illustrates the congestion pattern over time (*right*)

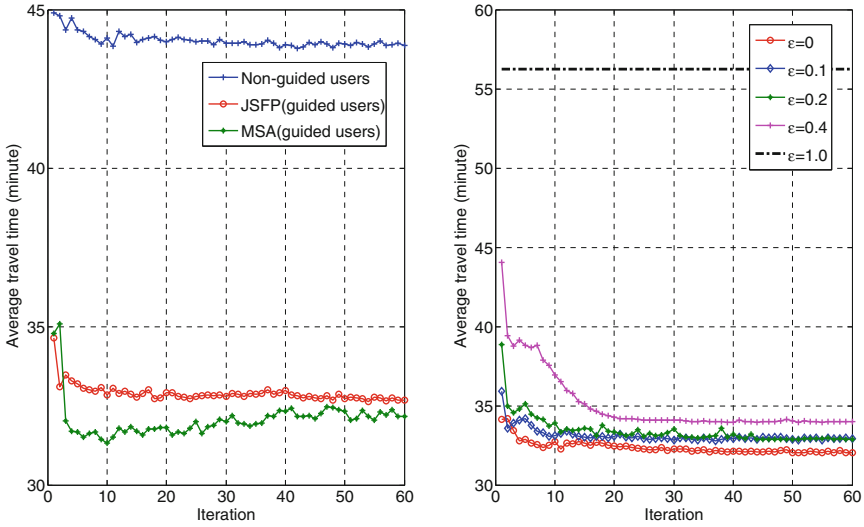

Fig. 3 Average travel time comparison (scenario of 20 % of guided users, *left*) and sensitivity analysis with respect to the parameter ε (inertia) (*right*)

of Fig. 3 illustrates a significant average travel time reduction for guided users in the scenario of 20 % market penetration of route guidance. The average travel times of guided users converge rapidly after three iterations. The subplot on the right of Fig. 3 illustrates the impact of inertia parameter ε on average travel times of guided users. Inertia is an important parameter which reflects a guided user's sensitivity to and/or confidence in route guidance. Small inertia values mean that guided users have a lot of confidence in the route guidance recommendations and follow recommended routes. Higher inertia values indicate that guided users have less confidence and thus a higher probability of re-using their past routes. It is observed that when the inertia value increases significantly the average travel times of guided users increase accordingly.

Table 1 compares the performance of the JSFP and MSA algorithms with respect to different demands (number of users) and to the market penetration of route guidance. The reference case is a less-congested situation. We define the loading factor as the ratio of number of users with respect to the reference case. We consider a highly-congested scenario with a loading factor of 2 and test the performance of the two algorithms. As illustrated in Table 1, the advantage of the route guidance system is relatively limited with about 2–3 % average travel time reduction for the reference case. However, in a congested case, the average travel times for guided users are significantly reduced compared with non-guided users. The average travel time reduction is 25.5 and 7.8 % for market penetrations of 20 and 50 % respectively. The advantage of the route guidance system for guided users decreases as the percentage of guided users increases. This is due to the over-reaction effects resulting from inconsistent travel time prediction [2] and from the simplification of

Table 1 Total and average travel times of guided and non-guided users

Loading factor	% of guided users	JSFP			MSA		
		Total TT (h)	Avg. TT (min)		Total TT (h)	Avg. TT (min)	
			Non-guided users	Guided users		Non-guided users	Guided users
1.0	0	1,663	31.2	–	–	–	–
	20	1,630	30.7	30.1	1,630	30.7	30.0
	50	1,621	30.4	30.4	1,618	30.3	30.4
	80	1,630	30.3	30.6	1,622	30.4	30.4
	100	1,646	–	30.9	1,634	–	30.6
2.0	0	5,237	49.1	–	–	–	–
	20	4,444	43.9	32.7	4,522	44.9	32.2
	50	3,962	38.6	35.6	4,011	40.5	34.7
	80	3,838	33.7	36.6	4,067	39.8	37.7
	100	3,889	–	36.5	4,698	–	44.0

Remark: 1. TT is total travel times; 2. Reported values are the average value for the last 5 of 60 iterations

user's compliance elasticity by a constant inertia term. We argue that when consistent travel time prediction is provided, the over-reaction effect can be reduced and a consistent travel time reduction for guided users can be achieved. When comparing the JSFP and MSA algorithms, the result illustrates similar average travel times for these two algorithms for low market penetrations but higher average travel times of guided users with the MSA method in the high market penetrations of route guidance scenarios (left subplot of Fig. 4). A similar result is found for the comparison of

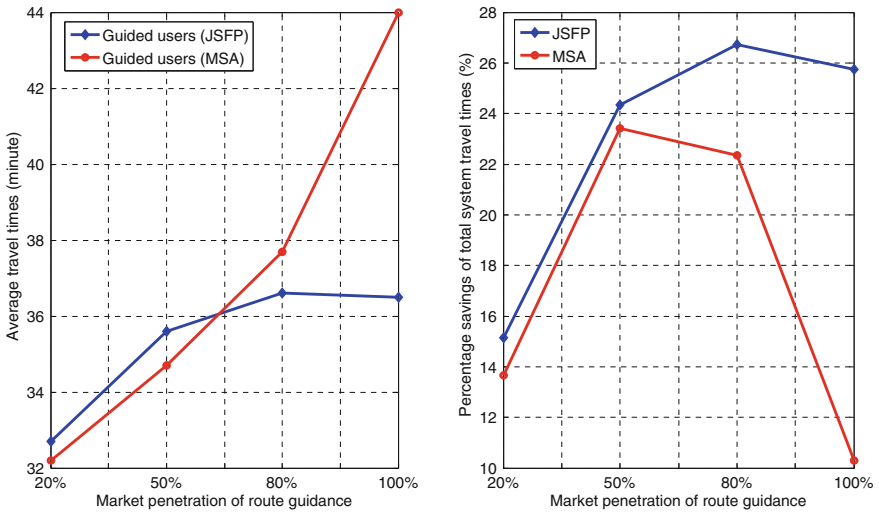

Fig. 4 Average travel time profile (*left*) and percentage savings of system travel times (*right*) with respect to different market penetration of the route guidance system

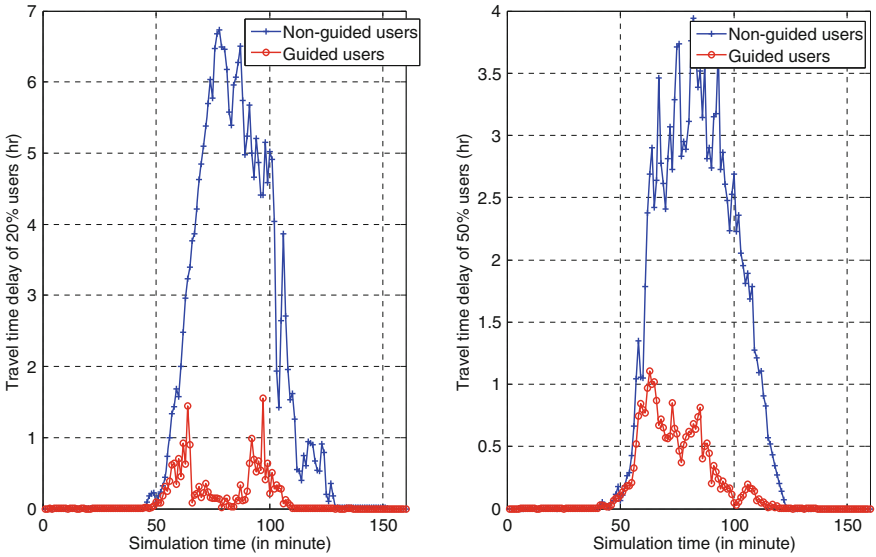

Fig. 5 Comparison of travel time delay profile (*left*: scenario of 20 % guided users; *right*: scenario of 50 % guided users)

percentage savings of total travel times for all users (right side of Fig. 4). Figure 5 illustrates actual travel time delay for the same number of users in each class over the simulation period. It illustrates a significant travel time delay reduction for guided users during the peak hour period. Moreover when the percentage of guided users increases from 20 to 50 %, their experienced delay increases accordingly due to the aforementioned inconsistent travel time predictions.

5 Conclusions

In this study, we propose a distributed algorithm based on joint strategy fictitious play with inertia to solve the dynamic user-optimal route guidance problem. The proposed algorithm incorporates users' inertia and en-route traffic information when computing route guidance recommendations. The en-route traffic information consists of periodically updated link travel times and time-dependent shortest travel times provided by a system administrator for guided users. The proposed approach is based on individual selfish adaptive online route choice behavior with real-time traffic information provision. The numerical results demonstrate the convergence of the proposed algorithm to Nash equilibrium in a dynamic congested network. The advantages of the proposed algorithm reside in its distributed and self-guidance aspects. We compare the performance of the proposed method with the method of successive averages. The result shows the effectiveness of the proposed algorithm

for not only reducing the average travel times of guided users but also improving the total fluidity of the congested network.

Currently, the guided user's compliance mechanism is modeled as a constant inertia term to reflect the guided user's habits/resistance to the recommended route guidance information. However, experiments on the route choice behavior of users revealed that their adaptive route choice behavior may depend on many other factors such as travel distance/times, descriptive information, familiarity and route complexity [50]. More realistic decision rules for the compliance mechanism can be elaborated to replace the static inertia term in the proposed JSFP process. Moreover, in this study our traffic condition prediction method doesn't consider the route choice decisions of guided users in the future and accordingly cannot provide consistent travel time prediction. This issue may induce too much traffic on the recommended routes if the market penetration (the percentage of guided users) were to become too high and would thus reduce the benefits of the system. Furthermore, modeling compliance elasticity related to the information accuracy needs to be studied in the future extensions.

Examples of future extensions are the dynamic compliance mechanism with online information provision and with the aforementioned route choice decision factors. How to provide the consistent traffic prediction to increase the effectiveness of the route guidance system needs to be studied. Some case studies on large-scale road networks with consistent travel time predictions are also necessary to assess the performance and effectiveness of the proposed approach to reducing travel times and delays for users. Moreover, different information acquisition schemes such as vehicle-to-vehicle communication, radio broadcasting and variable message signs (VMS) could also be incorporated into the model. It would be also interesting to compare the performance of the proposed algorithm with existing route guidance systems. From a theoretical point of view, the convergence property and the stability of the algorithm still need to be analyzed in the future. Currently, the effect of adoption of a route guidance system on road safety is still less studied, this issue can be further studied in the future to evaluate the benefits of such a system on road safety.

Acknowledgments The author acknowledges helpful comments of anonymous referees and the editor to improve the quality of this paper.

References

1. Aichinger C, Aigner-breuss E, Aleksa M, Kaiser S, Müller A, Russwurm K (2014) Evaluation of navigation systems from a road safety perspective. Paper presented in european conference on human centered design for intelligent transport systems, Vienna, Austria
2. Balakrishna R, Koutsopoulos HN, Ben-Akiva M, Fernandez-Ruiz BM, Mehta M (2005) Simulation-based evaluation of advanced traveler information systems. Transp Res Rec 1910:90–98
3. Ben-Akiva M, Bierlaire M, Bottom J, Koutsopoulos HN, Mishalani R (1997) Development of a route guidance generation system for real-time application. In: Proceedings of the 8th IFAC symposium on transportation systems, Chania, Greece

4. Berger U (2007) Two more classes of games with the continuous-time fictitious play property. Games Econ Behav 60(2):247–261
5. Bottom JA (2000) Consistent anticipatory route guidance. Ph.D. thesis, Massachusetts institute of technology
6. Bottom J, Kachani S, Perakis G (2006) The anticipatory route guidance problem: Formulations, analysis and computational results. Working paper
7. Brown GW (1951) Iterative solution of games by fictitious play. In: Activity analysis of production and allocation. Wiley, New York
8. Chen B, Xie Y, Tong W, Dong C, Shi D, Wang B (2012) A comprehensive study of advanced information feedbacks in real-time intelligent traffic systems. Phys A 391:2730–2739
9. Chorus CG, Dellaert BGC (2012) Travel choice inertia: The joint role of risk aversion and learning. J Transp Econ Policy 46(1):139–155
10. Chorus CG, Arentze TA, Timmermans HJP (2009) Traveler compliance with advice: A Bayesian utilitarian perspective. Transp Res Part E 45:486–500
11. Chorus CG, Walker JL, Ben-Akiva M (2013) A joint model of travel information acquisition and response to received messages. Transp Res Part C 26:61–77
12. Cominetti R, Melo E, Sorin S (2010) A payoff-based learning procedure and its application to traffic games. Games Econ Behav 70(1):71–83
13. Correa JR, Stier-Moses NE (2011) Wardrop equilibria. Wiley encyclopedia of operations research and management science. Wiley, New York
14. Crittin F, Bierlaire M (2003) Solving the anticipatory route guidance generation problem using a generalization of secant methods. In: Proceedings of the 3rd swiss transport research conference, Monte Verità
15. Deflorio FP (2003) Evaluation of a reactive dynamic route guidance strategy. Transp Res Part C 11(5):375–388
16. Dong CF, Ma X, Wang GW, Sun XY, Wang BH (2009) Prediction feedback in intelligent traffic systems. Phys A 388:4651–4657
17. Dong CF, Ma X, Wang BH, Sun XY (2010) Effects of prediction feedback in multi-route intelligent traffic systems. Phys A 389:3274–3281
18. Friesz T, Mookherjee R (2006) Solving the dynamic network user equilibrium problem with state-dependent time shifts. Transp Res Part B 40:207–229
19. Friesz TL, Bernstein D, Smith T, Tobin R, Wie B (1993) A variational inequality formulation of the dynamic network user equilibrium problem. Oper Res 41:80–91
20. Fudenberg D, Levine DK (1998) The theory of learning in games. MIT Press, Cambridge, MA
21. Gaetani F, Minciardi R (2002) Dynamic models and optimal control methods for route guidance in urban traffic networks. The 5th IEEE international conference on intelligent transportation systems, Singapore, pp 454 – 459
22. Gao S, Huang H (2012) Real-time traveler information for optimal adaptive routing in stochastic time-dependent networks. Transp Res Part C 21:196–213
23. Garcia A, Reaume D, Smith RL (2000) Fictitious play for finding system optimal routings in dynamic traffic networks. Transp Res Part B 34:147–156
24. Gawron C (1998) An iterative algorithm to determine the dynamic user equilibrium in a traffic simulation model. Int J Mod Phys C 9(3):393–408
25. Gentile G, Meschini L, Papola N (2007) Spillback congestion in dynamic traffic assignment: A macroscopic flow model with time-varying bottlenecks. Transp Res Part B Methodol 41 (10):1114–1138
26. Hart S (2005) Adaptive heuristics. Econometrica 73(5):1401–1430
27. Hart S, Mas-Colell A (2000) A simple adaptive procedure leading to correlated equilibrium. Econometrica 68:1127–1150
28. Huang H-J, Lam WHK (2002) Modeling and solving the dynamic user equilibrium route and departure time choice problem in network with queues. Transp Res Part B 36(3):253–273
29. Huang H-J, Lam WHK (2003) A multi-class dynamic user equilibrium route and departure time choice problem in queuing networks with advanced traveler information systems. J Math Model Algorithms 2:349–377

30. Hurkens S (1995) Learning by forgetful players. Games Econ Behav 11(2):304–329
31. Jahn O, Möhring R, Schulz A, Moses NS (2005) System-optimal routing of traffic flows with user constraints in networks with congestion. Oper Res 53(4):600–616
32. Jha M, Madanat S, Peeta S (1998) Perception updating and day-to-day travel choice dynamics in traffic networks with information provision. Transp Res Part C 6:189–212
33. Kaufman DE, Smith RL, Wunderlich KE (1991) An iterative routing/assignment method for anticipatory real-time route guidance. In: Proceedings of IEEE vehicle navigation and information systems conference, pp 693–700
34. Kuwahara M, Akamatsu T (1997) Decomposition of the reactive assignments with queues for many-to-many origin-destination pattern. Transp Res Part B 31(1):1–10
35. Kuwahara M, Akamatsu T (2001) Dynamic user optimal assignment with physical queues for a many-to-many OD pattern. Transp Res Part B Methodol 35(5):461–479
36. Lambert TJ III, Epelman MA, Smith RL (2005) A fictitious play approach to large-scale optimization. Oper Res 53(3):477–489
37. Lebacque JP (1996) The Godunov scheme and what it means for first order traffic flow models. In: Lesort JB (eds) Proceedings of the 13th international symposium on transportation and traffic theory, Pergamon, Amsterdam, pp 647–678
38. Lebacque J-P, Khoshyaran MM (2005) First order macroscopic traffic flow models: intersection modeling, network modeling. In: Mahmasani, H.S. (eds) Proceedings of the 16th international symposium on transportation and traffic theory, Elsevier, pp 365–386
39. Lebacque J-P, Mammar S, Haj-Salem H (2007) Generic second order traffic flow modeling. In: Proceedings of the 17th international symposium on transportation and traffic flow theory, London, pp 755–776
40. Ma T-Y, Lebacque J-P (2013) A cross-entropy based multiagent approach for multiclass activity chain modeling and simulation. Transp Res Part C 28:116–129
41. Marchesini P, Weijermars W (2010) The relationship between road safety and congestion on motorways. Report No. R-2010-12, SWOV institute for road safety research–Leidschendam, The Netherlands
42. Marden JR, Arslan G, Shamma JS (2009) Joint strategy fictitious play with inertia for potential games. IEEE Trans Autom Control 54(2):208–220
43. Minciardi R, Gaetani F (2001) A decentralized optimal control scheme for route guidance in urban road networks. In: Proceedings of IEEE intelligent transportation systems conference, pp 1195–1199
44. Miyagi T, Peque G Jr, Fukumoto J (2013) Adaptive learning algorithms for traffic games with naive users. Procedia–Soc Behav Sci 80:806–817
45. Monderer D, Shapley L (1996) Fictitious play property for games with identical interests. J Econ Theor 68:258–265
46. Nagel K, Schreckenberg M (1992) A cellular automaton model for traffic flow. J Phys I 2 (12):2221–2229
47. Papageorgiou M (1990) Dynamic modeling, assignment, and route guidance in traffic networks. Transp Res Part B 24:471–496
48. Paz A, Peeta S (2009) Behavior-consistent real-time traffic routing under information. Transp Res Part C 17:642–661
49. Peeta S, Yu JW (2004) Adaptability of a hybrid route choice model to incorporating driver behavior dynamics under information provision. IEEE Trans Syst Man Cybern Part A 34 (2):243–256
50. Peeta S, Yu JW (2005) A hybrid model for driver route choice incorporating en-route attributes and real-time information effects. Netw Spat Econ 5(1):21–40
51. Peeta S, Ziliaskopoulos AK (2001) Foundations of dynamic traffic assignment: the past, the present and the future. Netw Spat Econ 1:233–265
52. Rantzer A (2008) Using game theory for distributed control engineering. Technical report ISRN LUTFD2/TFRT–7620–SE, Department of automatic control, Lund University, Sweden. Paper presented at Games 2008, 3rd world congress of the game theory society

53. Rehborn H, Klenov SL (2009) Traffic prediction of congested patterns. Encyclopedia of complexity and systems science. Springer, Berlin, pp 9500–9536
54. Selten R, Schreckenberg M, Chmura T, Pitz T, Kube S, Hafstein SF, Chrobok R, Pottmeier A, Wahle J (2004) Experimental investigation of day-to-day route-choice behaviour and network simulations of autobahn traffic in North Rhine-Westphalia. In: Schreckenberg A, Selten R (eds) Human behaviour and traffic networks. Springer, Berlin, pp 1–21
55. Sinuany-Stem Z, Stern E, Sfaradi Z, Holm E (1997) The effect of information on commuters' behavior: A comparative micro-simulation approach. Eur J Oper Res 96:455–470
56. Swenson B, Kar S, Xavier J (2012) Distributed learning in large-scale multi-agent games: A modified fictitious play approach. In: 46th Asilomar conference on signals, systems, and computers, pp 1490–1495
57. Szeto WY, Wong SC (2012) Dynamic traffic assignment: model classifications and recent advances in travel choice principles. Cent Eur J Eng 2(1):1–18
58. Transportation Research Board (U.S.) Highway Capacity Manual HCM 2010. Washington, DC
59. Wahle J, Bazzan A, Klügl F, Schreckenberg M (2002) The impact of real-time information in a two-route scenario using agent-based simulation. Transp Res Part C 10:399–417
60. Wang C (2010) The relationship between traffic congestion and road accidents: An econometric approach using GIS. PhD Thesis. Loughborough university, UK
61. Wardrop JG (1952) Some theoretical aspects of road traffic research. Proc Inst Civ Eng Part II 1:325–378
62. Weymann J, Farges J-L, Henry J-J (1995) Optimization of traffic dynamic route guidance with drivers reactions in a queue-based model. IEEE Trans Syst Man Cybern 25(7):1161–1165
63. Xie C, Liu Z (2014) On the stochastic network equilibrium with heterogeneous routing inertia. Trans Res Part B. doi: http://dx.doi.org.proxy.bnl.lu/10.1016/j.trb.2014.01.005
64. Yang H, Huang H-J (2004) Modeling user adoption of advanced traveler information systems: A control theoretic approach for optimal endogenous growth. Transp Res Part C 12:193–207
65. Young PH (2005) Strategic learning and its limit. Oxford University Press, Oxford
66. Ziliaskopoulos AK, Mahmassani HS (1993) A time-dependent shortest path algorithm for real-time intelligent vehicle/highway systems. Transp Res Rec 1408:94–104
67. Ziliaskopoulos AK, Waller S, Li Y, Byram M (2004) Large-scale dynamic traffic assignment: implementation issues and computational analysis. J Transp Eng 130(5):585–593
68. Zuurbier FS (2010) Intelligent Route Guidance. PhD thesis, Technische Universiteit Delft
69. Zuurbier FS, van Zuylen HJ, Hoogendoorn SP, Chen Y (2006) Generating optimal controlled prescriptive route guidance in realistic traffic networks: A generic approach. Transp Res Rec 1944:58–66

A Psycho-Social Agent-Based Model of Driver Behavior Dynamics

Theodore Tsekeris and Ioannis Katerelos

Abstract This paper suggests a psycho-social agent-based model, referred to as Holistic-Emergent Social Interaction-Oriented Dynamics (HESIOD) model, to simulate the drivers' behavior dynamics under various types of interaction among vehicles. The HESIOD model allows representing the heterogeneity and dynamical processes involved in such control dimensions as risk assessment and time responsiveness of driving behavior (controlled dimension). It is shown that highly differentiated states may arise, such as fixed point, periodicity and transient chaos. The dynamical state is found to be mostly affected by the degree to which the control dimensions of neighboring vehicle drivers depart from each other, and the topology of interaction among drivers. In contrast with the aggregate statistical-probabilistic models, this agent-based model can offer valuable insights into the role of both cognitive processes and interactions of drivers on their actual driving behavior. The findings may have useful implications for improving the level of service, safety and security in roads.

Keywords Road traffic behavior · Agent-based model · Risk assessment · Time response · Road safety

1 Introduction

Modern pervasive wireless technologies and high-performance monitoring systems enable one to identify with reasonable accuracy the spatio-temporal vehicle trajectories and possible interactions between them in road networks. In conjunction

T. Tsekeris (✉)
Centre of Planning and Economic Research (KEPE), 11 Amerikis, 10672 Athens, Greece
e-mail: tsek@kepe.gr

I. Katerelos
Department of Psychology, Panteion University, Athens, Greece
e-mail: ioannis.katerelos@hesiodproject.net

K. Hausken and J. Zhuang (eds.), *Game Theoretic Analysis of Congestion, Safety and Security*, Springer Series in Reliability Engineering,
DOI 10.1007/978-3-319-11674-7_4

with the road infrastructure and operational characteristics and traffic composition, heterogeneity of drivers is also an important factor influencing the vehicular interaction (congestion) patterns, level-of-service, safety and security conditions. The modeling and interpretation of users' heterogeneity can enhance the design and evaluation of mechanisms for the efficient monitoring, prediction and control of traffic congestion, as well as the design of appropriate measures to improve safety and security in road networks.

Several methodological approaches have been developed and implemented to investigate the heterogeneity of driver behavior. Some of them have focused on the risk assessment and time responses according to different traffic flow and vehicle interaction scenarios. Observatory analysis, by use of driver simulator, has stressed the importance of such psychological attributes as aggressiveness, attentiveness or risk on their passing behavior [1]. These attributes can be categorized among the drivers' population with respect to the age and/or experience and possibly other individual (cognitive/behavioral) characteristics [21, 29].

Particularly, it has been found that the younger the driver is, the more risky and frequent the passing becomes. In addition to the *interpersonal* (driver-to-driver) interactions, there are also *intrapersonal* factors that influence risk-taking and responsiveness of drivers. Farah et al. [4] examined the cognitive style of thinking of drivers, their goal-directed behavior, the focus of attention and emotional control to predict their risk proneness. Statistical-probabilistic models have further been developed to interpret and predict the risk associated with the passing behavior. In such a study, Farah et al. [5] accounted for variables related to personal driver characteristics (age, gender), in addition to those capturing the impact of road geometry and traffic conditions. Moreover, Farah and Toledo [6] suggested a probabilistic model to additionally capture drivers' desire to pass and their gap acceptance decisions to complete a desired passing maneuver. Very few artificial intelligence approaches, such as rule-based neural networks [2] and pattern recognition techniques [30], have also been considered to analyze the heterogeneities of road driving behavior.

Agent-based traffic micro-simulations offer a flexible and accurate framework that allows one to represent naturally the heterogeneity and learning capabilities of driver-vehicle agents [3, 11, 23]. The specification of such models can express in detail several intricate parameters of the behavior of drivers under different network topologies and traffic conditions. Hence, they can be employed to tackle a variety of traffic state representation and control problems. These problems can involve the design of adaptive self-organized traffic signal control in urban road networks and of in-vehicle driver assistance systems, through application of decentralized information propagation and inter-vehicle communication protocols [14, 27].

The present article suggests an agent-based simulation model, referred to as Holistic-Emergent Social Interaction-Oriented Dynamics (HESIOD) model [13], to represent the dynamics of driver behavior in terms of their risk assessment and time responsiveness. In contrast with other agent-based traffic micro-simulation models, it consistently accounts for both intrapersonal and interpersonal (driver-to-driver) factors that influence these characteristics and emergent road traffic phenomena.

Section 2 describes the main components of the HESIOD model. Section 3 presents the simulation setup (model parameters and topologies) and Sect. 4 the results of the simulations. Section 5 offers insights into validation and implementation issues and concludes.

2 Holistic-Emergent Social Interaction-Oriented Dynamics (HESIOD) Model

The HESIOD model relies on a minimum set of micro-prerequisites concerning the characteristics of cognitive agents in order to represent the emergence of (non) stationary macro-outcomes. The HESIOD model follows a bottom-up approach where each agent has to obey in two simple rules: (a) strives to attain social consensus and (b) simultaneously, attempts to maintain internal consistency, in the sense of a stabilized internal cognitive state.

An indicative example can be given by assuming that other drivers influence my behavior. Hence, if all drivers I see around me are speeding, I want to cope with them and *I will speed up*, since I am not considering myself as a "worse" driver than them.[1] This response strives to keep my internal cognitive equilibrium in order. If every driver follows the same rationale, then the overall speed will escalade quickly to an unreasonable scale. On the other hand, if I see that all drivers around me are decelerating, I may suppose that there is some trouble ahead (or even a police control); therefore, I would also decelerate but only as much as needed for demonstrating that I am not a "worse" driver than they are. In this way, the model could enable a deeper understanding and interpretation of the dynamical features, stability and self-organization properties of inter-drivers' network interactions.

The two basic principles of the HESIOD model refer to a psychological and a sociological one. Both of them correspond to specific individual characteristics of the agents. The psychological principle focus on the maximum change of an internal balance factor Ψ (Psi), in each iteration of the HESIOD algorithm, to restore the internal equilibrium of every agent (e.g. I am a skilled driver vs. I am an incompetent driver). The sociological principle involves the consideration of a social regulation parameter, K (Kappa), in analogy with the internal consistency regulation through factor Ψ. The K factor denotes the impact of social influence on the individual. This may also encompass the influence of social norms, customs or historical conventions in driving [28]. As it is described later, these two model parameters affect the way in which the control dimensions of the behavior of each driver agent change over time, in the social context of the connected neighboring drivers.

[1] Particularly, headlight flashing can be very irritating, at this point! A very antagonistic view of my fellow co-driver. This kind of behavior is strongly associated with cultural parameters, mainly in reference to the driving style usually met in southern European countries.

Specifically, in each iteration (corresponding to one time interval) t, each agent i considers the control dimension $A_{t,j}$ of other agents $j = 1, \ldots, n$ within his/her Bound of Confidence (BC),[2] and "calculates" the point of social convergence; here, this is defined as the mean $\bar{A}_{t,j} = \sum_j^n A_{t,j} \Big/ n$. Then, the agent updates his/her previous value (new position) $A_{t,i}$ as a function of his/her own factor κ_i, as follows:

$$A_{t+1,i} = A_{t,i} + \left(\frac{\sum_j^n A_{t,j}}{n} - A_{t,i} \right) \times \kappa_i \tag{1}$$

By defining the realistic range of values $0 < \mathrm{K} \leq 2$, a value $\kappa_i = 0.5$ means that the agent i will move half-way to the point of convergence, with $\kappa_i = 1$ will move exactly at the point of convergence, with $\kappa_i = 1.5$, will move one and a half times towards the point of convergence, etc. Through factor K, an agent decides to move towards a point of social convergence only to an adjustable degree.[3] The same procedure is respected regarding the second control dimension $B_{t,j}$.

Following the changes in control dimensions due to the social negotiation (inter-drivers' interaction) process described above, the control dimension sustained the maximum (largest) change is identified and left intact for each agent.[4] The factor Ψ will determine the exact change concerning the other control dimension. By defining the realistic range of values $0 < \Psi \leq 2$, with $\Psi = 0.5$, the half of change sustained by the dimension with maximum change is subtracted, with $\Psi = 1$, exactly the change sustained by the dimension with maximum change is subtracted, and, with $\Psi = 1.5$, one and a half of change sustained by the dimension with maximum change is subtracted. Namely, agents with $\Psi < 1$ or $\Psi > 1$ tend to underestimate or overestimate, respectively, the cognitive change occurred, in terms of re-establishing internal consistency. The above operations are outlined in the following steps:

---

[2] The Bound of Confidence (BC) expresses the bound within which each agent takes other agents' opinions (driving behaviors) into account [10]. For instance, if I get surpassed by a car having the triple of my speed and I am already driving to the speed limit (into the city), then this behavior (driving at such a high speed) can be outside my bound of confidence; so, I am not at all influenced (this behavior is far too riskier than I can bear) and therefore, it does not influence me: I will pass the challenge.. As one can easily understand, if a driver has a very wide bound of confidence, then s/he is susceptible to be influenced by almost any driving behavior no matter how risky it is.

[3] K can also be of zero value. This means that a driver with K = 0, insists in retaining his/hers speed no matter what the other drivers in proximity are doing.

[4] A cognitive procedure named Focus On Max Change (FOMC, [12]). Although this procedure may seem arbitrary, since it is not backed up by concrete data, the mechanism tends to imitate satisfyingly real behaviors when one is oriented more to assess dynamically a given situation than to apprehend it statically. In the real world, the FOMC can be easily depicted: if someone is receiving two stimuli, the one which differs maximally from his/her own position (state) will attract his/her attention in priority. Nevertheless, the above mentioned mechanism is subjected to ongoing research and testing; so, a better refinement can be expected in future projects.

Step I: Find the differences (social shifts):

$$\partial A_{t,i} = \left|A_{t-1,i} - A_{t,i}\right|, \partial B_{t,i} = \left|B_{t-1,i} - B_{t,i}\right| \quad (2)$$

Step II: Focus on maximum change and correct (psychological shifts):

$$\left(\partial A_{t,i} > \partial B_{t,i}\right) \rightarrow A_{t,i} = A_{t,i} \quad \& \quad B_{t,i} = B_{t-1,i} - \partial A_{t,i} \cdot \psi_i \quad (3)$$

$$\left(\partial B_{t,i} > dA_{t,i}\right) \rightarrow B_{t,i} = B_{t,i} \quad \& \quad A_{t,i} = A_{t-1,i} - \partial B_{t,i} \cdot \psi_i \quad (4)$$

Due to successive subtractions, values out-of-range [1, 5] may arise: a rescale algorithm is needed for the reposition of the values. In this study, values below or above this range are truncated to the corresponding lower or upper limit, respectively. The above constraints denote that the influence of other drivers is bounded and, hence, large changes in behavior are properly avoided to account for safety considerations, but small ones are (and must be) taken into account.

Therefore, in the HESIOD model, every decision of each driver is bi-dimensional: it is simultaneously socially (with the other drivers) negotiated and this negotiation potentially provokes cognitive inconsistencies internal to each driver. Social influence destabilizes the internal cognitive consistency and, in turn, each attempt of restoring it destabilizes the previously attained social consensus (equilibrium). These interactions are performed within a network whose topology plays a crucial role on the dynamic outcome of the system. In other words, changes in the structure of the network of interactions among drivers can yield overwhelming changes in the dynamical state of the whole system. Keeping the parameters K and Ψ intact, but changing the topology, highly differentiated dynamic states may arise, such as fixed point, periodicity, transient chaos, and pure chaos [13].

Given that the social and individual factors are *opposite and complementary* with each other, it is then sufficient to maintain the same sum (Ψ + K = 2). Katerelos [13] showed that, when Ψ + K = 2, the HESIOD model ends up to a periodic equilibrium if the topology is a complete graph. In the described phase space of the system (p. 73), with Ψ + K > 2, one observes transient or pure chaos when [Ψ + K > 2 & Ψ ≤ 1] and [Ψ + K > 2 & Ψ > 1] respectively. When Ψ + K < 2, the system equilibrates in a fixed point (a flat-line): no change is expected to the future.[5]

3 Control Dimensions and Communication Topologies

The simulation setup is basically defined in terms of the model control dimensions, which concern the cognitive processes of driver agents, and the communication topology between them. This setup and appropriate definition and interrelationship

[5] These simulations use homogenous agents: they all share a common K and Ψ.

of the control dimensions of the driver agents render the present model different from any other that adopts the HESIOD modeling framework. The heterogeneity of drivers reflect two control dimensions (i) the risk assessment, R_a, and (ii) the time responsiveness, R_t, to avoid risk and/or increase speed and comfort. These two control dimensions may be related to either an aggressive or a defensive driving behavior, according to their initial values and their change over time, as they are adjusted in real time in response to the interactions among driver agents.

It is noted that the present model specification cannot fully capture the whole range of aspects (e.g. driving style, cultural factors, social beliefs, safety attitudes, security concerns etc.) explaining/influencing the actual driving behavior. The interrelations among driver agents' behavior are multi-determined. Nonetheless, it provides a general framework within which a whole range of special cases may be considered (for instance, setting K = 0 would denote that there is no influence from other drivers). The model adopts the plausible assumption -and a normal practice in cognitive social psychology- of the emotional contagion effect from one agent on the others. Specifically, each driver agent is able to encounter the beliefs/responses of the neighboring agents, in terms of their risk assessment and time responsiveness. In other words, one by observing actual behaviors can make successful assumptions about how other people think.

Information about these two control dimensions can provide crucial insight into the cognitive processes underlying the decisions of driver agents. In addition, they can be experimentally measured, with the aid of historical data about the driver and vehicle operation, as ordinal variables, e.g., by assigning scores relative to the ability of each driver to assess risk (including health, safety and security issues) and timely respond to changing road conditions [8].

A generalized relationship between the rate of change of traffic speed v (acceleration/deceleration) and the two control dimensions can be expressed as:

$$\frac{\partial v}{\partial t} = f(\gamma + \alpha R_a + \beta R_t), \tag{5}$$

where γ, α, β are parameters whose magnitude and sign may vary with the driver characteristics under different traffic conditions. For instance, according to Kerner's three-phase traffic flow theory [15–17, 19], the speed of drivers along a freeway may change in a different way, according to whether the density increases at a constant flow rate (from free flow to synchronized flow), which gives rise to a spontaneous or induced traffic breakdown, the flow rate decreases at constant density (from synchronized flow to wide moving jam) and the density decreases (from wide moving jam to free flow). Each of the above three phases are associated with a different causal relationship among the two control dimensions and the speed variability, as drivers in a congested environment (as density increases) tend to become more anxious, fearful, and cautious about accidents. The present model can potentially enrich such traffic flow theories, by taking into account the socio-psychological micro-foundations of driver behavior. Especially, it can possibly offer interpretation to road traffic phenomena (e.g., sudden rise of congestion, and unexpected occurrence of accident and

volatile conditions), which are largely regarded as unexplained from existing traffic flow theories.

These control dimensions may vary among drivers due to a variety of (neuro-) psychological functions, such as attention, perception and executive functions [7]. These functions may perform a tradeoff between age and driving experience: a decline is typically associated with age, but, at some extent, this is compensated by experience. The values of R_a dimension range from 1 (worst value) to 5 (best value), i.e., risk assessment is maximized when $R_a = 5$. The values of R_t range from 1 (signifying under-responsiveness) to 5 (signifying over-responsiveness), and its value is considered to be optimized when $R_t = 3$.

The K factor moderates the changes of R_a and R_t, while the Ψ factor moderates the relationship between R_a and R_t. The current simulation setup includes three driver agents moving with their vehicles along a road segment, where overtaking is allowed, from left (upstream) to right (downstream) direction and interacting with each other (Fig. 1). At the initial time interval $t = 0$, the initial values for driver agent 1, whose age is 65 years old, are $R_a = 3$ and $R_t = 2$, for driver agent 2, whose age is 25 years old, are $R_a = 2$ and $R_t = 5$, and for driver agent 3, whose age is 35 years old, are $R_a = 3$ and $R_t = 3$. The bound of confidence (BC) for all agents is set equal to 5, meaning that, in the current set of simulations, it has no effect on the interaction between agents. In other words, the network of interactions among driver agents is dependent on their communication topology (or graph topology) and an equal weight is assigned to each link between them (Fig. 2).

Several topologies, such as those of all-to-all (complete graph topology), one-to-all, peer-to-peer and in-tandem interaction patterns, can be employed to define the human environment affecting the responses of one driver agent with respect to the actions of all the others. Each specific topology can correspond to a set of road environment and design (capacity) characteristics influencing the interaction among drivers. Such characteristics may be related to the road geometry and typology (highway or arterial street), deployment of vehicle-to-vehicle communication systems, speed limit, and weather and visibility conditions.

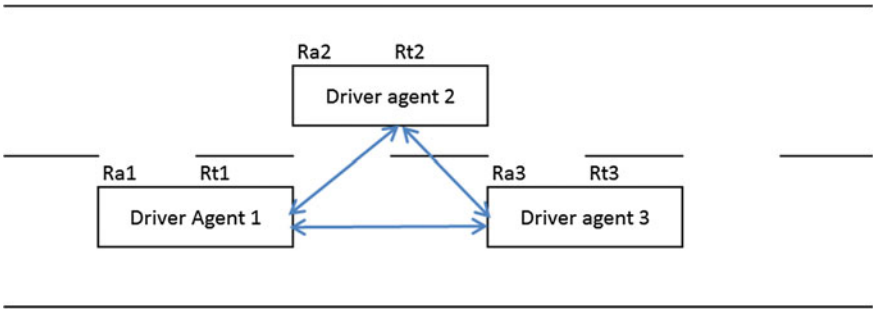

Fig. 1 Basic configuration of a complete graph topology (undirected graph) of driver agents in a road segment

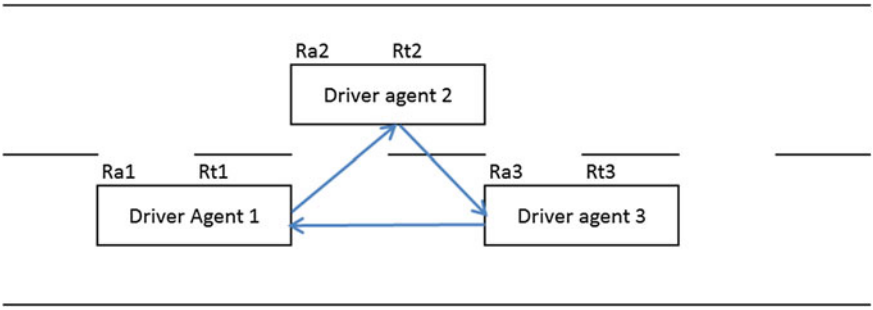

Fig. 2 Basic configuration of an incomplete graph topology (directed graph) of driver agents in a road segment

A Cellular Automata (CA) topology can be well suited to the given problem to designate the set of possible interactions within a group of drivers moving along a road segment (e.g., [18, 22]). The CA topology is based on the concept of "locality": every driver agent i can negotiate R_{ai} and R_{ti}, only with his/her "neighbor" driver agents. Nevertheless, other topologies where information scarcity exists (e.g., in low-density rural roads) or communication channels between drivers are ubiquitous (e.g., in fully automated highway systems) may be adopted according to the specific conditions of the road operation environment.[6] Figure 1 illustrates the basic configuration of a complete graph topology (CGT), wherein every driver agent bilaterally interacts with the others in the locality of a road segment, as reflect the bidirectional arrows between them.

4 Results

The simulation period encompasses 30 time intervals t. By considering an adequately short interval $t = 2$ s for driver agents to adjust/correct their risk assessment and driving responses (remaining steady, breaking, decelerating or accelerating), the total period refers to $30 \times 2 = 60$ s (1 min). Figures 3, 4, 5 and 6 show the behavior of the model for the CGT and various sets of K, Ψ values, i.e., $K + \Psi < 2$ (Fig. 3), $K + \Psi = 2$ (Fig. 4), $K + \Psi > 2$ (Fig. 5), for all driver agents, as well as a combination of these sets among the driver agents (Fig. 6). Figures 7, 8, 9 and 10 illustrate the corresponding behavior of the model for the IGT. For the case of the CGT, the results generally indicate a periodic behavior and, finally, the achievement of a flat equilibrium at the end of the period. In other words, the final equilibrium

[6] Since an indicative example of three vehicles (very small number of active agents) is employed here, the notion of cellular automata topology can be translated ad hoc to a directed graph (3 node-incomplete graph) compared to an undirected graph (3 node–complete graph).

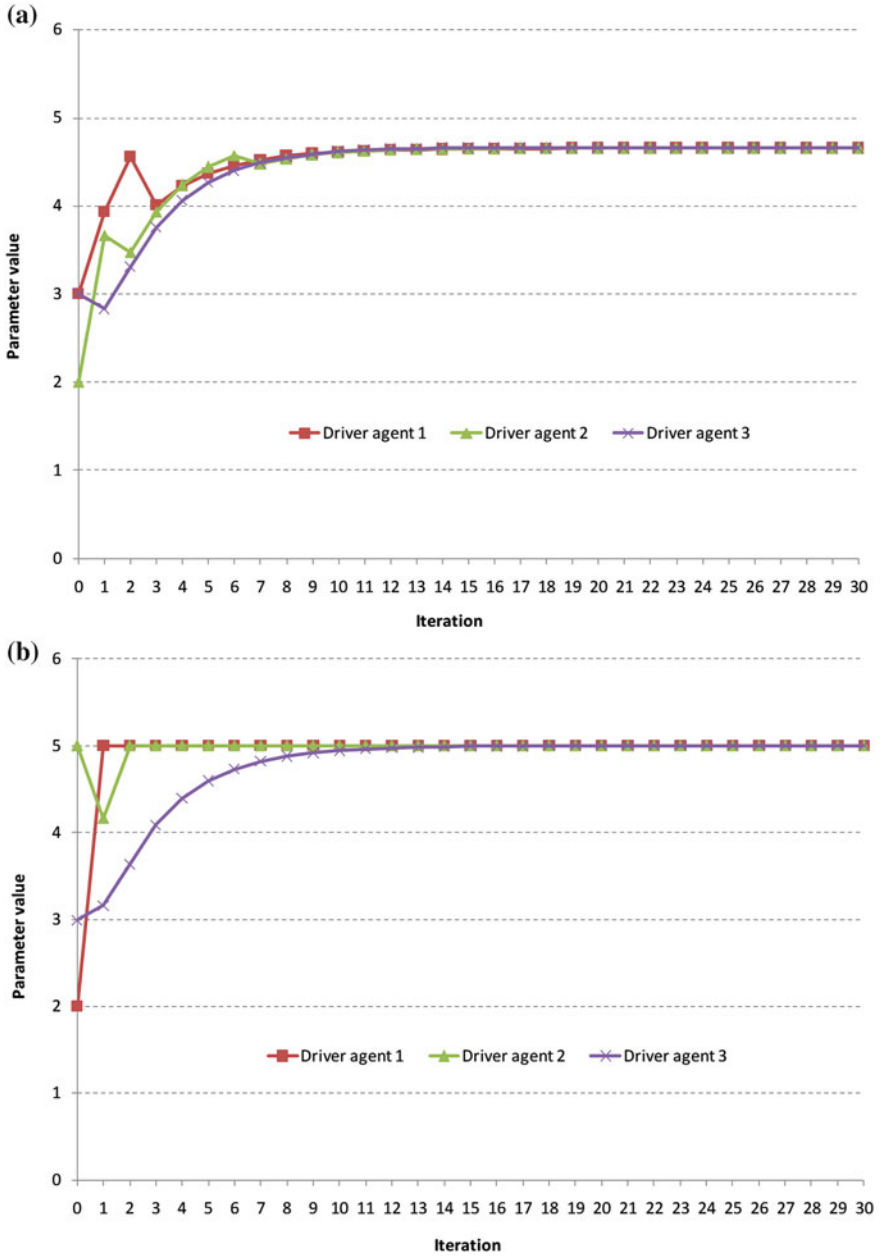

Fig. 3 Simulation results of **a** R_a and **b** R_t for CGT and K, Ψ pairs of agents (0.7, 0.5), (1, 0.8) and (0.5, 1) respectively

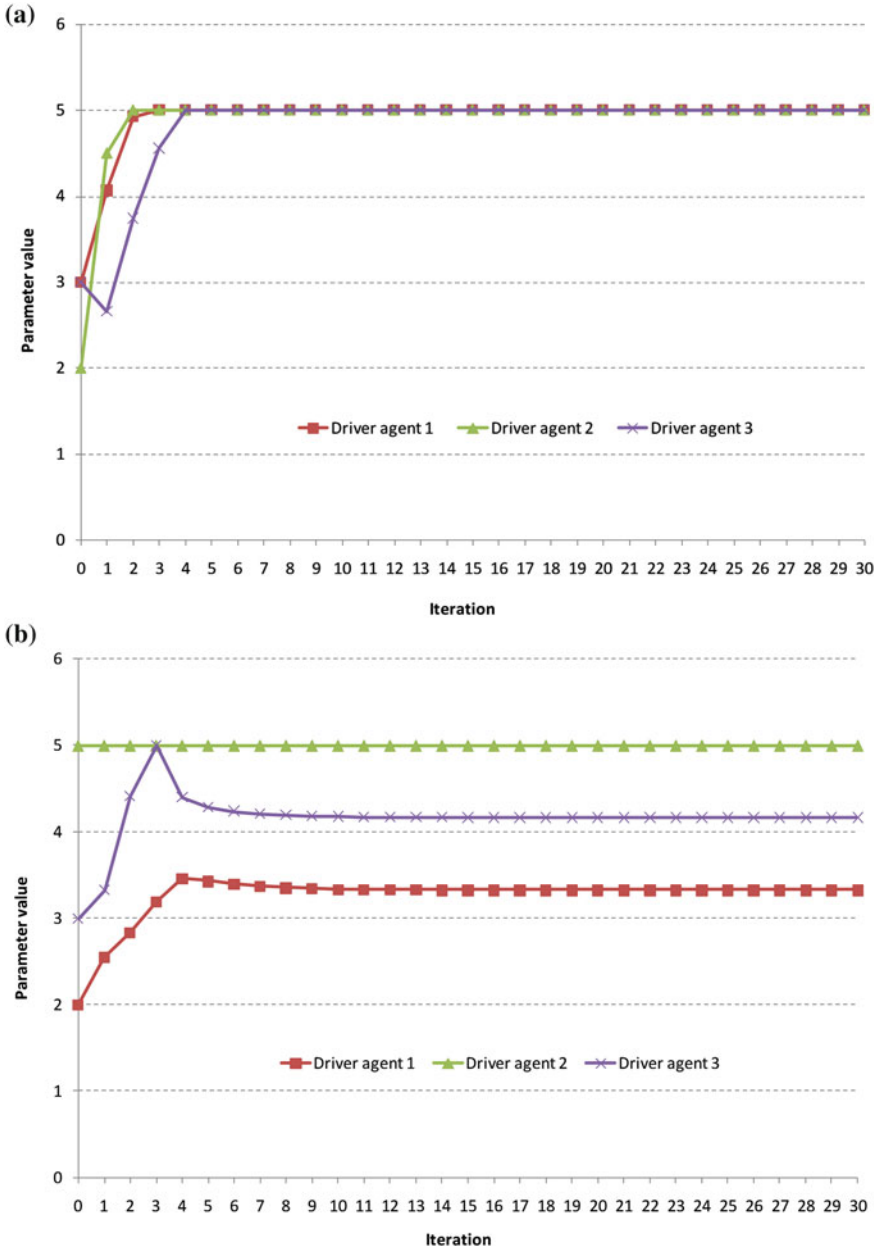

Fig. 4 Simulation results of **a** R_a and **b** R_t for CGT and K, Ψ pairs of agents (0.8, 1.2), (1.5, 0.5) and (1, 1) respectively

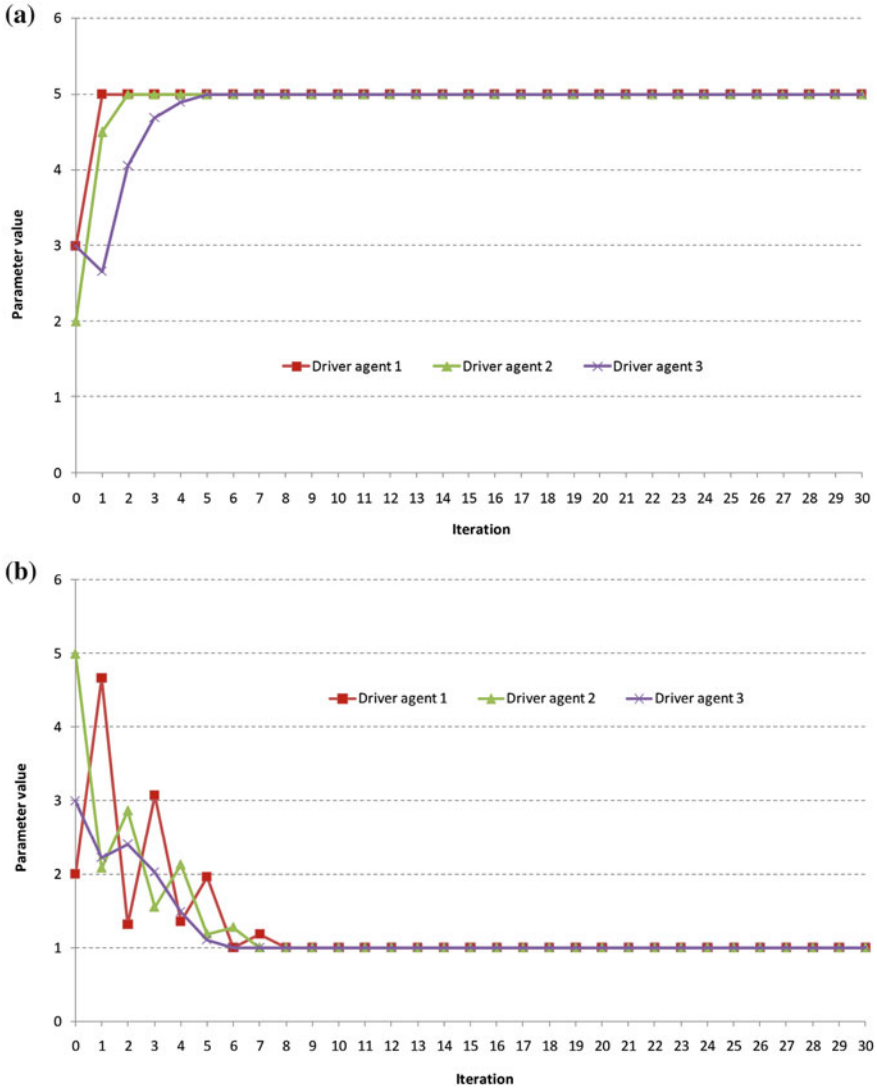

Fig. 5 Simulation results of **a** R_a and **b** R_t for CGT and K, Ψ pairs of agents (1, 2), (1.5, 1.2) and (1, 1.5) respectively

state denotes the achievement of a 'social consensus' among driver agents. This type of consensus suggests an increased efficiency of road operation through smoother flow conditions as well as increased road security and safety, by reducing the risks of misperception and collision.

Nevertheless, this dynamical outcome stands as a *desirable result* provided that, after social negotiation between them, drivers will "agree" not to exceed the speed limit or, more generally, to engage in actions compromising severely rules of road

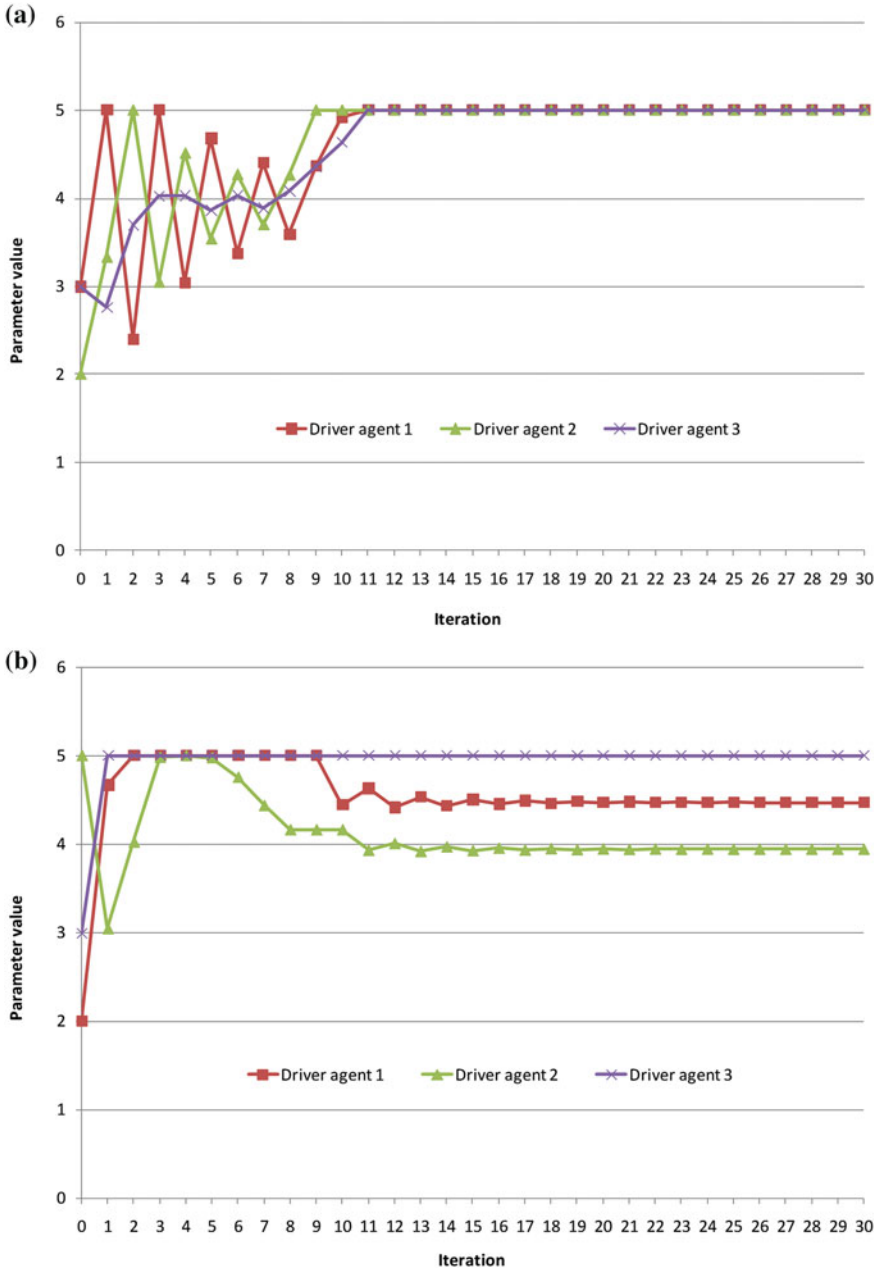

Fig. 6 Simulation results of **a** R_a and **b** R_t for CGT and K, Ψ pairs of agents (1, 2), (0.8, 1.2) and (0.7, 0.5) respectively

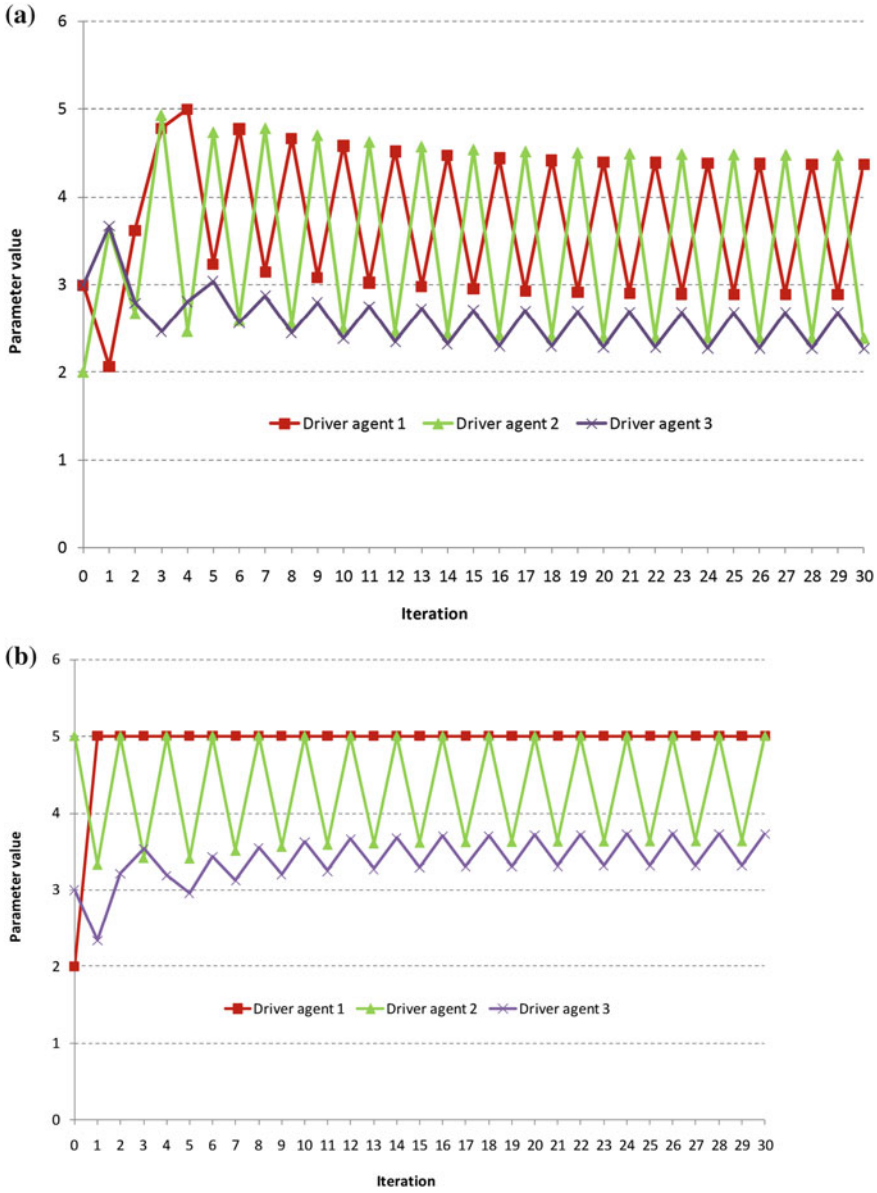

Fig. 7 Simulation results of **a** R_a and **b** R_t for IGT and K, Ψ pairs of agents (0.7, 0.5), (1, 0.8) and (0.5, 1) respectively

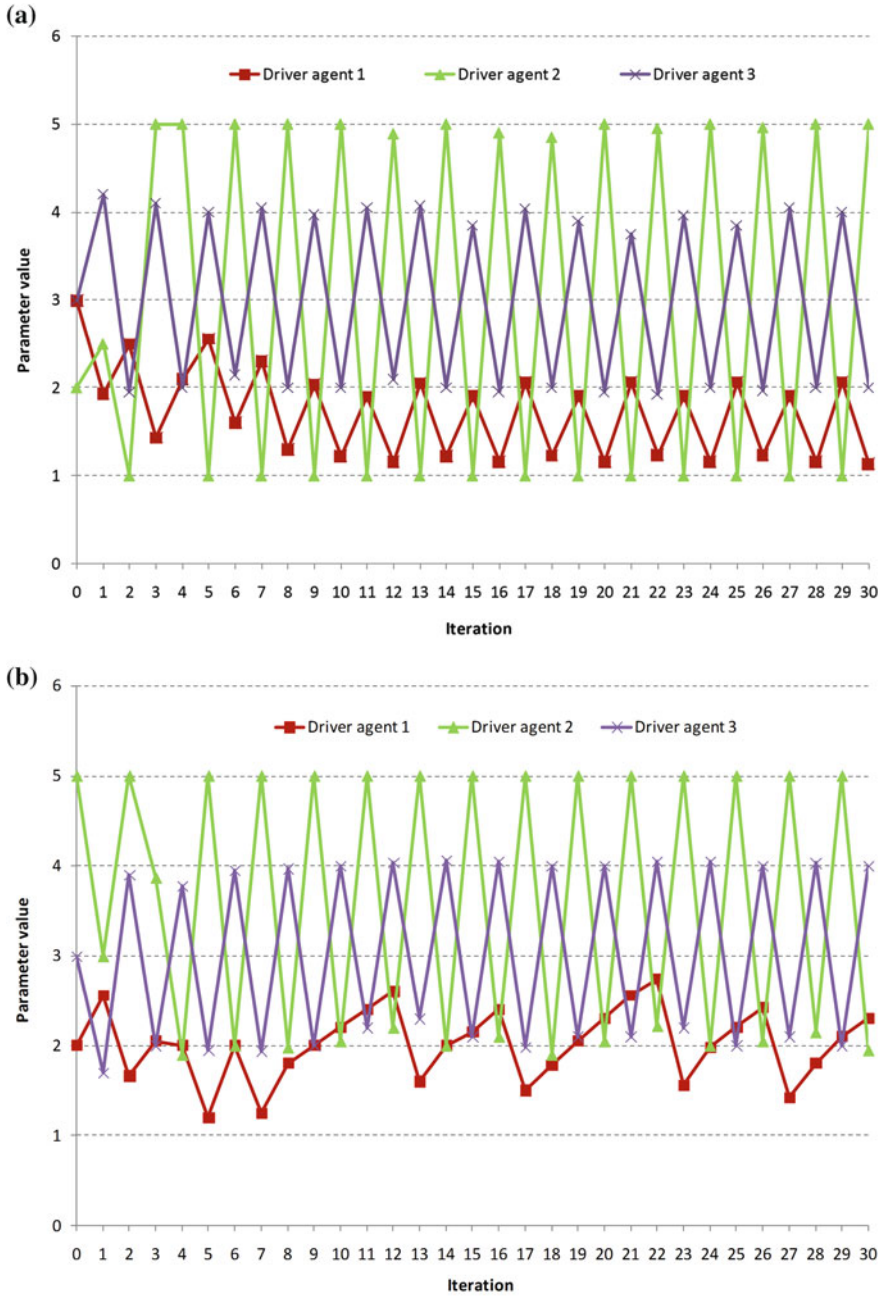

Fig. 8 Simulation results of **a** R_a and **b** R_t for IGT and K, Ψ pairs of agents (0.8, 1.2), (1.5, 0.5) and (1, 1) respectively

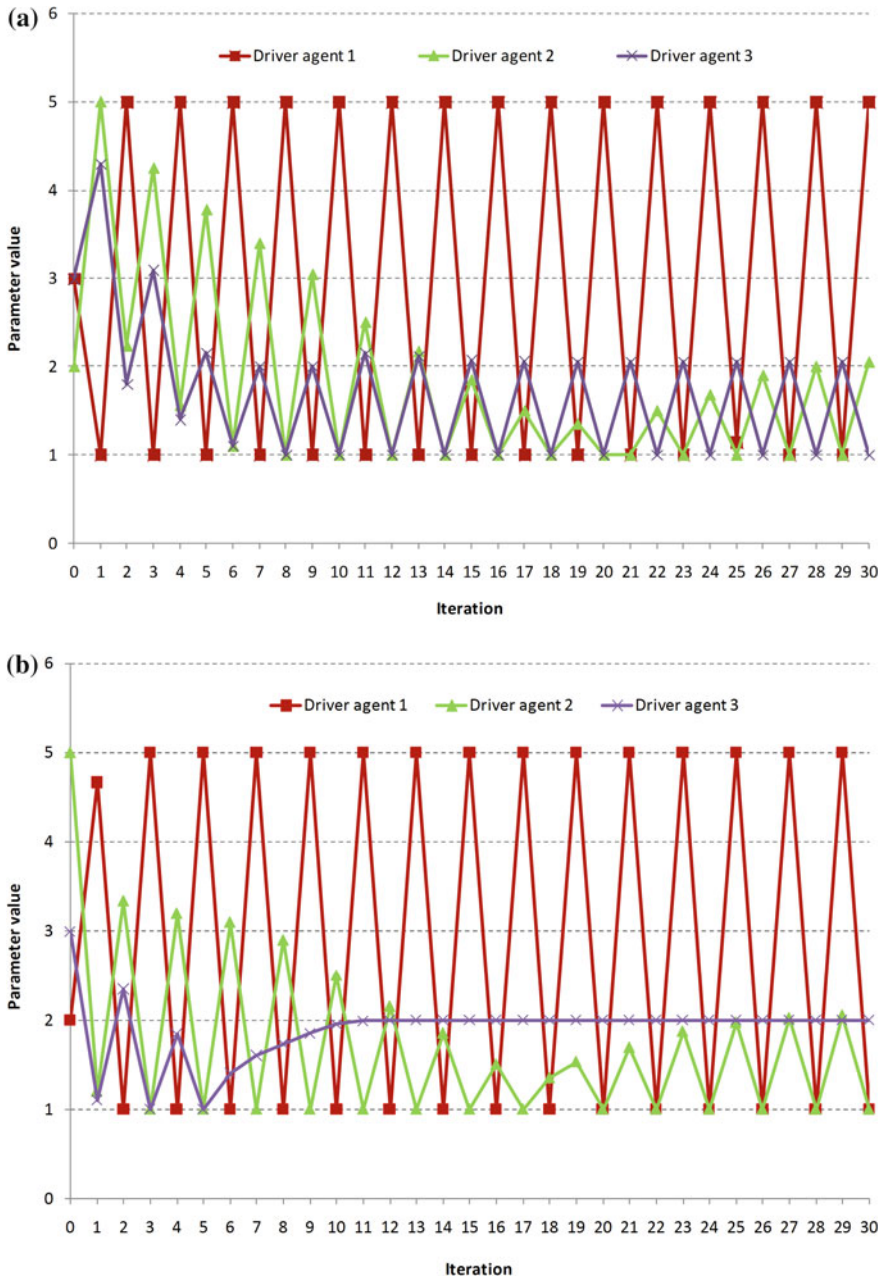

Fig. 9 Simulation results of **a** R_a and **b** R_t for IGT and K, Ψ pairs of agents (1, 2), (1.5, 1.2) and (1, 1.5) respectively

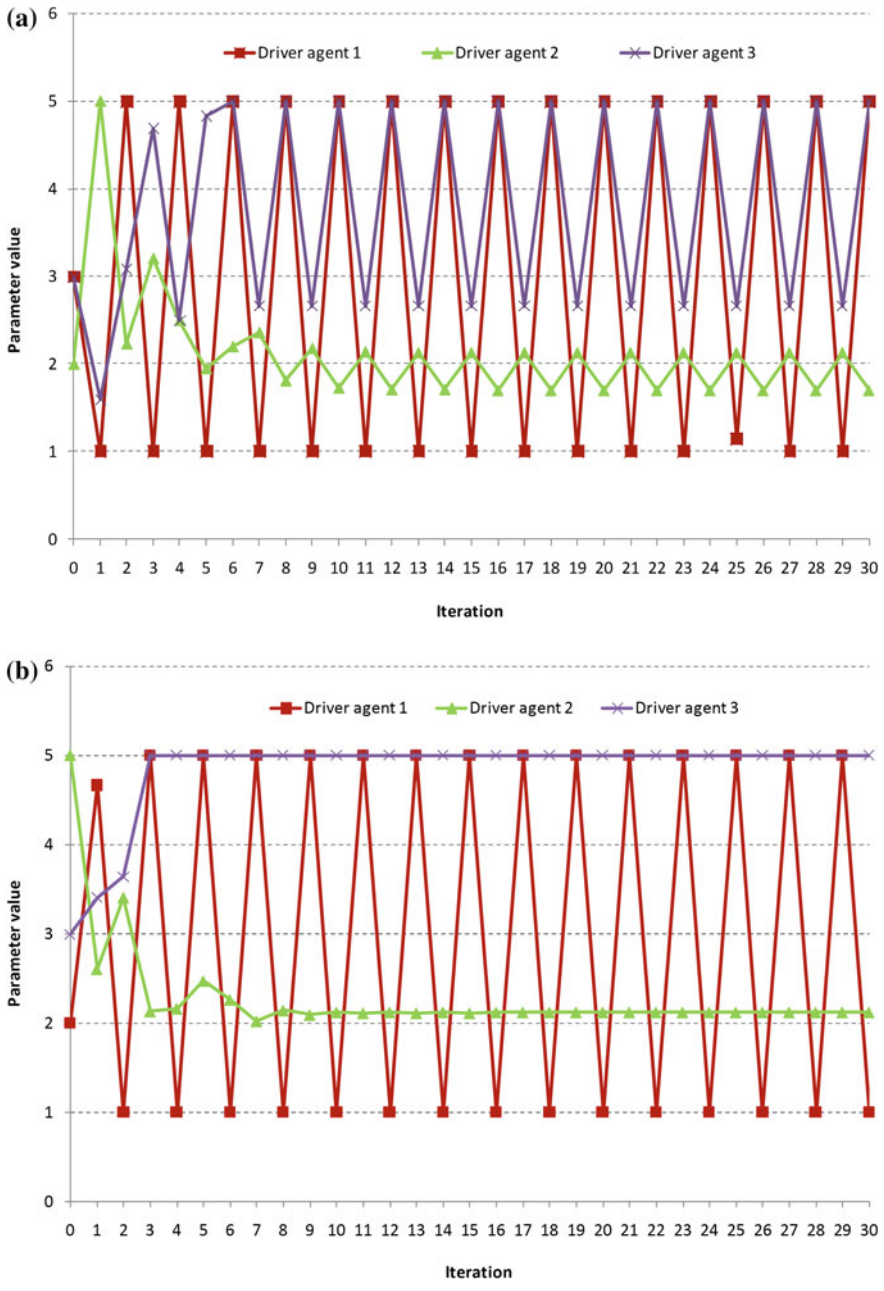

Fig. 10 Simulation results of **a** R_a and **b** R_t for IGT and K, Ψ pairs of agents (1, 2), (0.8, 1.2) and (0.7, 0.5) respectively

security and safety.[7] Otherwise, psychosocial negotiation could end up in *collectively* adopting risky behaviors[8] and maintain them as long as there is no external intervening (restraining) factor.[9]

From a closed system point of view, these drivers will attain equilibrium between them; thus, no further changes of behavior are expected and the predictability horizon of the whole system becomes infinite. In other words, the system behavior is fully predictable. On the other hand, considerable differences are observed in the dynamics of driver agent behavior when the communication topology between them is incomplete. Specifically, the results generally show a highly periodic behavior and/or transient chaotic processes which emerge after a few iterations. These processes can be considered as a type of social 'fragmentation' or 'polarization' (particularly in Figs. 9 and 10) among the behavior of driver agents, which move far away from a flat equilibrium or consensus regime. The increase of the volatility of the underlying dynamics can be associated with less controllable road traffic operations and, hence, reduced levels of security and safety, due to the higher risk of misperception and collision [25].

As one can clearly observe in Figs. 7, 8, 9 and 10, the system dynamics do not achieve an equilibrated/stable collective behavior. Although drivers never agree with each other in a steady state, they are in a dynamic process of constantly changing agreement. In this case, the system is much more flexible and adaptive. This is to say that, in certain circumstances, driving behaviors can change instantly from one extreme to another (especially for drivers with $K + \Psi > 2$), with regard to the risk assessment and perceived responsiveness.

In most common driving conditions (even in official racing conditions), predictability of the fellow drivers' behavior is of paramount importance: every decision (conscious or not) is made by making predictions of each other's behavior. Namely, predictability is attained by either the absence of changes of behavior or the successful assumption and adjustment of each driver to the immediate expected responses of the other drivers. Unpredictable driving can (and most of times, does) end up in a series of unfortunate events. This kind of driving behavior is associated, for instance, with abrupt deceleration (causing more severe impacts when it is less expected) or with zig-zag turning (causing unwilling and uncontrollable drifting), combined with the "panic" provoked to other drivers. It seems like this kind of

[7] In a rather theoretical view, in real life, this case can look like a race between supercars in Daytona or, even more vividly, the race of "24 h of Isle of Man": the drivers maintain extreme speeds while very close to one another.

[8] Such as "spontaneous races", "drifting", "spinning", "chicken-game" etc.

[9] Police controls/blocks, "car chasing", etc. During the recent years, the common procedure adopted by police officers confronting suspects of unlawful actions when they try to get away via driving through the road network, is to stay behind and wait either for the suspect to run out of fuel or for the suspect to enter a controlled environment minimizing possible collateral damage. Evidently, a certain tactic of "pushing" the suspect to a kind of "road race/car chase" (and, therefore "negotiating" with him/her either his/her driving skills or his/her vehicle's potential regarding acceleration and handling), could challenge the suspect and augment dramatically the probability of harming him/herself or others.

driver is *relying heavily* on other fellow drivers' *readiness* in reacting to his/her own unpredictable behavior.[10] At the network level, characteristic examples refer to abrupt exogenous disturbances to capacity/supply conditions or sudden changes in demand due to unexpected or planned events, which in turn can impact security and safety.

5 Concluding Remarks and Further Issues

The present results, as obtained from a series of diverse computational simulations, on the basis of the HESIOD agent-based model, suggest how many and much different states may emerge in the interaction among road drivers. Specifically, the interaction dynamics of driver agents is affected by their own behavior, in terms of such control dimensions as risk assessment and time responsiveness, the behavior of neighboring agents, and the topology (or communication pattern) between them. The consideration of cognitive processes involved in these road traffic interaction patterns can enrich and improve the robustness of future micro-simulation models of drivers' behavior.

The findings can also help to address challenging questions concerning the ability of advanced driver assistance and vehicle control systems, based on real-time vehicle-to-vehicle information and communication protocols, to improve road safety, enhance security and facilitate evacuation procedures in response to attack situations, and support new-generation traffic control strategies. In particular, the results show that symmetric driver interaction may lead to a more stable equilibrium state and smoothed traffic flow conditions, while asymmetric interaction may lead to a periodic state with some potential for chaos. In addition, interconnected drivers who reach a social agreement in their cognitive parameters create more predictable and less risky driving situations, compared to drivers who do not reach such an agreement. The above cognitive issues can enhance the design of advanced driver support systems, as the enhancement of connectivity and cooperation among drivers and the improvement of the predictability of traffic conditions can help to smooth out dynamic behavioral adjustment patterns and, thus, improve the efficiency, reliability, safety and security of road network operations in both urban/suburban and rural environments.

Furthermore, traffic law enforcement by police/patrol stations and knowledge about the efficacy of law enforcement measures (e.g., red-light cameras and speed radar detectors) may substantially mitigate the feeling of anger and make driving experience less stressful, or happier, for motorists [24]. The current results may provide theoretically supportive evidence about the impact of such measures on increasing the predictability of fellow drivers' responses and avoiding enervation

[10] This holds without taking into account possible enervation of other drivers and, consecutively, the adoption of an aggressive (and dangerous if escalades) stance against the trespasser (him/her)!

and aggressiveness, thus, preventing overreaction and decreasing the risk of accident.

At the next stages of the model development, changes in behavioral parameters and traffic flow conditions may be considered to provide a feedback to local network topology, in terms of the interconnectivity among driver agents. Several validation and implementation issues arise for further research, including:

(a) The transformation of risk assessment and response time to speed and acceleration changes over time (e.g., [9, 20]).
(b) Theoretical validation of the present model estimates on the basis of readily available traffic flow measurements and comparison with traditional car-following/lane-changing models and the observed average flow versus speed relationship (i.e., the fundamental diagram of traffic flow) for selected road segments and types/conditions of road operation.
(c) As far as the calibration of model and empirical validation of results are concerned, different types of vehicular interactions and passing maneuvers may occur anywhere on a section of road. Therefore, field studies to collect the appropriate data are expensive and inefficient, since they cannot adequately control over all the explanatory variables, especially those concerning the personal driver characteristics. In the current context, driving simulators can provide a reliable alternative to observe individual driving behavior.

Real-world interviews and field surveys could also be used to measure different control variables of drivers' behavior in various road environment and traffic conditions. Moreover, experimental results from neuro-psychological tests of on-road driving behavior could provide valuable information on measures concerning the driving performance, speed, attention, visual-spatial abilities and executive functioning of specific groups of drivers, such as the older ones [7]. For calibration purposes, this information may be coupled with processed data concerning the trajectories and flow variables of individual vehicles equipped with global positioning system (GPS).

Finally, the present model setup could be extended in a network setting, e.g., that of a downtown area or an inter-city network [26], to include a set of links with interdependent flows and explain macroscopic congestion phenomena. In that case, the dynamics of interaction among drivers moving in a specific road link, or a terrorist attack of one or several agents, would possibly affect the behavior of drivers moving at upstream links, for instance, through the delay propagation and cascading effects resulting from the formation of a downstream bottleneck. The behavior adjustment of upstream driver agents, or even agents before starting their trips, located at the sources of demand (home or employment location), may additionally encompass a range of travel choices, such as route, departure time and mode choices. Relevant implications and extensions can include capacity decisions, which should be properly made to reduce uncertainty and ensure an appropriate level of network reserve capacity. Such decisions may significantly impact the overall cost of measures to address concerns about reliability, safety and security.

References

1. Bar-Gera H, Shinar D (2005) The tendency of drivers to pass other vehicles. Transp Res Part F: Traffic Psychol Behav 8(6):429–439
2. Chong L, Abbas MM, Medina Flintsch A, Higgs B (2013) A rule-based neural network approach to model driver naturalistic behavior in traffic. Transp Res Part C: Emerg Technol 32:207–223
3. Esser J, Schreckenberg M (1997) Microscopic simulation of urban traffic based on cellular automata. Int J Mod Phys C 8(5):1025–1036
4. Farah H, Yechiam E, Bekhor S, Toledo T, Polus A (2008) Association of risk proneness in overtaking maneuvers with impaired decision making. Transp Res Part F: Traffic Psychol Behav 11(5):313–323
5. Farah H, Bekhor F, Polus A (2009) Risk evaluation by modeling of passing behavior on two-lane rural highways. Accid Anal Prev 41(4):887–894
6. Farah H, Toledo T (2010) Passing behavior on two-lane highways. Transp Res Part F: Traffic Psychol Behav 13(6):355–364
7. Ferreira I, Simoes M, Marques S, Figueiredo M, Marmeleira J (2010) Neuropsychological assessment of older drivers: review and synthesis. In: Proceedings of the 12th world conference on transport research, Lisbon, Portugal
8. Gupte A (2008) System and method for monitoring driving behavior with feedback. U.S. Patent Application No. 12/079,837
9. Hamdar SH, Treiber M, Mahmassani HS, Kesting A (2008) Modeling driver behavior as sequential risk-taking task. Transp Res Rec J Transp Res Board 2088(1):208–217
10. Hegselmann R, Krause U (2002) Opinion dynamics and bounded confidence: models, analysis and simulation. J Artif Soc Soc Simul 5(3)
11. Helbing D (2001) Traffic and related self-driven many-particle systems. Rev Mod Phys 73 (4):1067–1141
12. Katerelos I, Koulouris A (2004) Is prediction possible? Chaotic behaviour of multiple equilibria regulation model in cellular automata topology. Complexity 10(1):23–36
13. Katerelos I (2013) Chaos and order in social systems. The HESIOD model: social dynamics simulations. Papazisis, Athens
14. Kesting A, Treiber M, Schonhof M, Helbing D (2008) Adaptive cruise control design for active congestion avoidance. Transp Res Part C: Emerg Technol 16(6):668–683
15. Kerner BS, Klenov SL, Wolf DE (2002) Cellular automata approach to three-phase traffic theory. J Phys A: Math Gen 35(47):9971
16. Kerner BS (2004) The physics of traffic: empirical freeway pattern features, engineering applications, and theory. Springer, Berlin
17. Kerner BS (2009) Introduction to modern traffic flow theory and control. Springer, Heidelberg
18. Kerner BS, Klenov SL, Schreckenberg M (2011) Simple cellular automaton model for traffic breakdown, highway capacity, and synchronized flow. Phys Rev E 84(4):046110
19. Kerner BS, Klenov SL, Hermanns G, Schreckenberg M (2013) Effect of driver over-acceleration on traffic breakdown in three-phase cellular automaton traffic flow models. Physica A 392(18):4083–4105
20. Kesting A, Treiber M, Helbing D (2009) Agents for traffic simulation. In: Uhrmacher AM, Weyns D (eds) Multi-agent systems: simulation and applications, Part III, CRC Press, Boca Raton, pp 325–356
21. Matthews G, Dorn L, Hoyes TW, Davies DR, Glendon AI, Taylor RG (1998) Driver stress and performance on a driving simulator. Hum Factors 40(1):136–149
22. Muchuruza V, Moses R, Thuo G (2010) Estimating the probability of rear-end crashes from a behavioral cellular-based traffic model. Adv Transp Stud 21:63–72
23. Raney B, Cetin N, Vollmy A, Vrtic M, Axhausen K, Nagel K (2003) An agent-based microsimulation model of swiss travel: first results. Netw Spat Econ 3(1):23–41

24. Roseborough JEW, Wiesenthal DL (2014) Roadway justice—making angry drivers, happy drivers. Transp Res Part F: Traffic Psychol Behav 24:1–7
25. Tsekeris T, Stathopoulos A (2006) Real-time traffic volatility forecasting in urban arterial networks. Transp Res Rec: J Transp Res Board 1964:146–156
26. Tsekeris T, Vogiatzoglou K (2011) Spatial agent-based modeling of household and firm location with endogenous transport costs. Netnomics 12(2):77–98
27. Wischhof L, Ebner A, Rohling H (2005) Information dissemination in self-organizing intervehicle networks. IEEE Trans Intell Transp Syst 6(1):90–101
28. Young HP (1996) The economics of convention. J Econ Perspect 10(2):105–122
29. Zhang J, Fraser S, Lindsay J, Clarke K, Mao Y (1998) Age-specific patterns of factors related to fatal motor vehicle traffic crashes: focus on young and elderly drivers. Publ Health 112 (5):289–295
30. Zhang Y, Lin WC, Chin YKS (2010) A pattern-recognition approach for driving skill characterization. IEEE Trans Intell Transp Syst 11(4):905–916

Game-Theoretic Context and Interpretation of Kerner's Three-Phase Traffic Theory

Kjell Hausken and Hubert Rehborn

Abstract We present four classical developments in traffic theory and Kerner's (Phys A 392:5261–5282, 2013, [36]) critique that these are not consistent with fundamental empirical features of traffic breakdown at a highway bottleneck (transition from free flow (F) to congested traffic at the bottleneck) that is the basic empiric of traffic theory. Kerner argued that traffic breakdown is probabilistic, can be spontaneous (emerging internally at the bottleneck) or induced (emerging from a downstream bottleneck), and is a transition from free flow to synchronized flow (S) (synchronized flow is one of the two traffic phases of congested traffic) called as a $F \rightarrow S$ transition, after which wide moving jam (J) (J is another from two phases of congested traffic) may arise. Return to free flow occurs through hysteresis and usually at smaller flow rates. Common games in traffic theory are presented and exemplified, i.e. the chicken game, battle of the sexes, prisoner's dilemma, and coordination game. The four developments and Kerner's theory are linked to game theory, and especially to the chicken game. For the first $F \rightarrow S$ transition the density increases at a constant flow rate. Increasing density increases the prevalence of the chicken strategy due to drivers in a congested environment becoming apprehensive, fearful, and wary of accidents. For the second $S \rightarrow J$ the chicken strategy is equally likely while the flow rate decreases at constant density. For the third $J \rightarrow F$ transition the density decreases which decreases the prevalence of the chicken strategy. Finally, within free flow F where the flow rate and density again increase, the chicken strategy is played with higher probability.

Keywords Features of traffic breakdown · Induced and spontaneous transitions · Kerner's three-phase traffic theory · Empirical flow measurements · Kerner's BM

K. Hausken (✉)
Faculty of Social Sciences, University of Stavanger, 4036 Stavanger, Norway
e-mail: kjell.hausken@uis.no

H. Rehborn
Group Research and Advanced Engineering, Daimler AG, HPC: 059-X832,
71063 Sindelfingen, Germany
e-mail: hubert.rehborn@daimler.com

K. Hausken and J. Zhuang (eds.), *Game Theoretic Analysis of Congestion, Safety and Security*, Springer Series in Reliability Engineering,
DOI 10.1007/978-3-319-11674-7_5

principle · Game theory · Chicken game · Battle of the sexes · Prisoner's dilemma · Coordination game

1 Introduction

Since the classical empirical work of Greenshields [23] about the fundamental diagram and highway capacity, traffic and transportation theory has developed substantially, empirically and theoretically, based on the achievements in the understanding of real traffic, as reviewed for example in [11, 19, 20, 26, 28, 47, 52, 53, 71].

Traffic theory experienced substantial developments in the 1950s, in particular due to classical works of Lighthill and Whitham [45], Richards [60], Herman et al. [27], and Gazis et al. [21, 22]. Relationships between flow rate and density were developed, and congestion, breakdown, and driver behavior upstream and downstream of bottlenecks were studied. Minimizing travel costs from the individual driver's perspective, and from a system optimal perspective, were also analyzed based on the classical Wardrop's [75] User Equilibrium (UE) and System Optimum (SO) principles. More recently, developments such as the kinetic traffic theory and the probabilistic traffic flow theory have been developed. See [44] regarding rear-end collisions related to kinematic waves near bottlenecks. See [63] for references to recent developments, and [18, 57, 67, 72, 74] for dynamic traffic theory.

Among the many available traffic theories, this chapter focuses strongly on Kerner's [36] theory. Whereas classical theories distinguish between free flow F and congested traffic, Kerner [36] compiled empirical data on freeways and argues that empirical data including findings in the form of real traffic data are inconsistent with the earlier classical developments. He divides congested traffic into synchronized flow S and wide moving jam J. Synchronized flow expresses continuous traffic flow with no significant stoppage, and speed synchronization within and across lanes, with bunching of vehicles, and low probability of passing. A wide moving jam, as a whole localized structure on a road system, moves upstream through any highway bottlenecks, maintaining the mean speed of the downstream front. A wide moving jam differs from other, e.g. narrower moving jams which usually do not maintain the mean speed of the downstream jam front. These three phases give room for probabilistic $F \rightarrow S$ transition between free flow and synchronized flow through hysteresis, probabilistic $S \rightarrow J$ transition from synchronized flow to wide moving jam, and probabilistic spontaneous or induced $F \rightarrow S$ breakdown. Spontaneous $F \rightarrow S$ breakdown means breakdown given earlier free flow at the bottleneck, and up- and downstream of the bottleneck, caused by internal disturbance in free flow around a bottleneck. Induced $F \rightarrow S$ breakdown occurs through congested traffic emerging downstream of the bottleneck, usually caused by upstream propagation.

Some research has tested Kerner's [36] theory. Mendez and Velasco [49] apply kinetic traffic flow theory for aggressive drivers and determine $F \rightarrow S$ transitions

under specific conditions, qualitatively in accordance with Kerner's three-phase theory. Knorr and Schreckenberg [42] reproduce the three phases F, S, J. Jin et al. [31] confirm that the $S \rightarrow J$ transition is more difficult in single-lane traffic. Jin et al. [32] confirms the $F \rightarrow S$ transition. Rehborn et al. [59] find that three phases are common on freeways in the UK, the USA and Germany. Schönhof and Helbing [64] apply data from the freeway A5 near Frankfurt and identify findings inconsistent with the three-phase traffic theory, and question the concept of a "general pattern" of congested traffic flow. Kerner [36, p. 5269, Footnote 5] and Kerner [34, Sects. 10.3.7, 10.3.10 and 10.5] have countered this criticism as invalid. Kerner et al. [40] argue that three-phase and two-phase traffic-flow theories are incommensurable in the sense of Kuhn's [43] scientific revolution. Kuhn [43] compares the transition between two scientific paradigms with a gestalt switch in psychology, where an irrational element plays a role rather than deliberate rational discussion. See [8, 30, 76] for further studies related to Kerner's [36] theory.

This chapter intends to make a first step towards extending the classical developments, and in particular Kerner's [36] theory, into the game theoretic domain. Game theory assumes multiple players choosing multiple strategies, and the payoffs to each depend on the combination of strategies chosen by all players [17]. Traffic theory is largely not game theoretic. A few exceptions exist. First, some attempts have been made to account for drivers choosing different strategies. For example, Daganzo [12, 13] proposes a behavioral theory of multi-lane traffic flow which in the idealized form assumes two types of drivers, aggressive (referred to as rabbits) and timid (referred to as slugs). Second, Rosenthal [61] propose congestion games where each player's payoff depends on the resources it chooses and the number of players choosing the same resource. Rosenthal proved that any congestion game is a potential game and Monderer and Shapley [51] prove the converse. It is well known that Beckmann et al.'s [2] classical optimization problem leading to a Wardrop equilibrium is the potential function of a congestion game. For further work on congestion games see [46, 62, 73]. Third, fictitious play was first introduced by Brown [7], and has been applied e.g. to system-optimal routing, see [18]. Peeta and Yu [55] show that route choice is similar to a driver's adaptation behavior based on his past experiences. Fourth, Stackelberg [66] games have been applied in bi-level-programming [50, 72]. Researchers are encouraged to extend research on traffic and transportation theory more thoroughly into game theory.

One difference between the classical models and Kerner's theory is that the former is typically based on theoretical hypotheses that have been developed and compared against measurements, whereas Kerner's theory is more directly based on empirics. Philosophy of science distinguishes between a theoretical domain of justification and an empirical domain of discovery. Our view is that one may in principle start in any domain, but should move back and forth to ensure that the concerns of both domains are satisfied. The classical developments typically started in the theoretical domain, and may potentially be criticized for not adequately testing the proper hypotheses. Kerner's theory started in the empirical domain, and may potentially be criticized for being driven too exclusively by empirical concerns.

The objective of this chapter is first to present these developments. Thereafter we present and exemplify common games in traffic theory, which we assess to be the chicken game, battle of the sexes, prisoner's dilemma, and coordination game. This means both modeling specific traffic theory examples using game theory, and using game theory to model specific traffic theory examples. Finally we link the developments in traffic theory to game theory. We focus mainly on highway traffic, but some of the game theory examples allude also to urban and rural traffic. Section 2 outlines four classical developments in traffic theory. Section 3 presents and discusses Kerner's empirically based theory. Section 4 describes and exemplifies common games in traffic theory. Sections 5 and 6 link Sects. 2 and 3 to game theory. Section 7 concludes.

2 Four Classical Developments in Traffic Theory

Let us outline four developments within traffic theory. These are somewhat separated in the description but are chosen since they in our view are historically representative and have laid and lay the foundation for subsequent and future developments. First, Lighthill and Whitham [45] and Richards [60] proposed in 1955–1956 that the maximum flow rate determines the free flow capacity at a bottleneck. If that capacity is exceeded, traffic breakdown will follow with congestion upstream of the bottleneck. The relationship between flow rate and density satisfies the law of conservation of the number of vehicles. The solutions are discontinuous with shock waves. The main problem with the model is that it cannot explain induced traffic breakdown, see [36].

Second, Herman et al. [27] and Gazis et al. [21, 22] proposed in 1959–1961 that traffic breakdown follows from the over-deceleration effect. One vehicle decelerates, the subsequent driver overreacts after a time delay by decelerating more, and the subsequent driver decelerates even more after a time delay, etc. This causes decreasing speed for subsequent vehicles propagating upstream causing $F \rightarrow J$ transition from free flow F to wide moving jam J. This model has influenced a plethora of traffic models. One problem with the model shown in [36] is that real traffic data shows no $F \rightarrow J$ transition, but instead $F \rightarrow S$ transition from free flow F to synchronized flow S.

Third, the free flow capacity at a bottleneck has classically been assumed to have a specific value (see [48, 70] and references therein) or a probabilistic or stochastic value (see, e.g., [5, 6]). One problem with this assumption is that it predicts that free flow persists when below this value, which contradicts the empirics that traffic breakdown can be induced by a wide moving jam or a moving synchronized flow pattern occurring elsewhere but reaching the bottleneck, see [36].

Fourth, Wardrop [14, 75] proposed in 1952 two classical principles for minimum travel costs. His user equilibrium principle states that traffic distributes so that travel times on all routes used from any origin to any destination are equal, while all unused routes have equal or greater travel times. His system optimal principle states

that the network-wide travel time should be minimum from a system optimal point of view. One problem with these two principles is that when the flow rate is between minimum and maximum capacity, the vehicle speed can either be large as in free flow or lower as in synchronized flow, see Fig. 5d and [36]. Kerner [36] thus proposed the breakdown minimization (BM) principle which minimizes the congestion probability. Beyond Wardrop's [14, 75] two principles, a third possible principle is macroscopic models in which costs of a large group of drivers are taken into account.

3 Kerner's Empirically Based Theory

Kerner [33, 34, 36] applies empirical traffic breakdown data (see [5, 6, 16, 24, 33, 34, 36, 48, 56, 70] and references therein) to present a theory based on the following four empirical features:

1. Traffic breakdown is a phase transition from free flow F to synchronized flow S. Downstream of synchronized flow, vehicles accelerate into free flow (Figs. 1, 2 and 3).
2. Traffic breakdown can be spontaneous (Figs. 1 and 2) or induced (Fig. 3).
3. The traffic breakdown probability increases logistically in flow rate, see [56].
4. Traffic breakdown exhibits hysteresis. With probabilistic breakdown at a certain flow rate causing synchronized flow, return to free flow usually occurs at smaller flow rates (Fig. 4).

Figures 1 and 2 show free flow upstream and downstream of a bottleneck before breakdown, and thereafter spontaneous breakdown with synchronized flow. Figure 3 shows induced traffic breakdown caused by, e.g., breakdown at a downstream bottleneck causing a wide moving jam eventually reaching the upstream bottleneck inducing breakdown.

In Kerner's three phase theory, with flow rate below the minimum capacity in Fig. 5d, $F \rightarrow S$ transition from free flow F to synchronized flow S is impossible. Free flow F is maintained, guaranteed, and stable. With flow rates between minimum and maximum capacity, all three phases F, S, and J are possible. This means that free flow is metastable with respect to an $F \rightarrow S$ transition. Metastability within a phase means that transition to another phase is possible, but may not occur.[1] With flow rate above the maximum capacity in Fig. 5d, the free flow transforms with probability one to synchronized flow S. Above the minimum capacity the probability of $F \rightarrow S$ transition is an increasing function with increasing flow rates up to the maximum capacity. In contrast to the classical developments in Sect. 2, Kerner [36] argues that $F \rightarrow J$ transitions, from free flow to wide moving jam, are impossible, and have never been observed in empirical data. Instead a cascade of

[1] See [29] for a new mechanism for metastability.

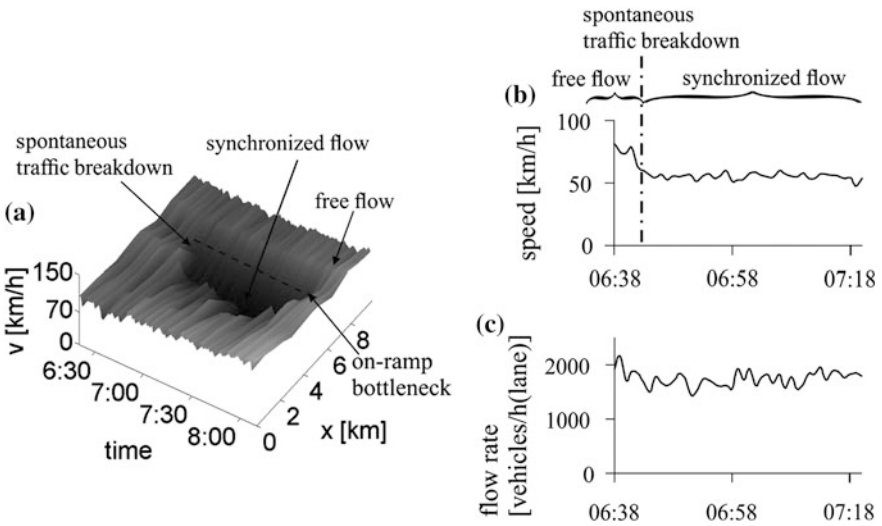

Fig. 1 Empirical example of spontaneous traffic breakdowns at on-ramp bottleneck (real measured traffic data of road detectors installed along three-lane freeway): **a** averaged speed in space and time. **b**, **c** Time-functions of average speed (**b**) and flow rate (averaged between freeway lanes) (**c**) at bottleneck location. 1-min average data. Taken from [33, 36]

$F \rightarrow S$ transitions occurs, and subsequently a $S \rightarrow J$ transition[2] may occur from synchronized flow to wide moving jam. That is, to get from F to J an $F \rightarrow S \rightarrow J$ transition is needed, where the $S \rightarrow J$ transition occurs and at a different location than the initial $F \rightarrow S$ transition.

In Kerner's three-phase theory, the probability of spontaneous $F \rightarrow S$ breakdown in Fig. 5c is the logistic function found by Kerner et al. [41] in numerical simulations of the cellular automata (CA) model in 2002, i.e.

$$P_{FS}^{B} = P_{FS}^{B}(q_{\text{sum}}) = \frac{1}{1 + \text{Exp}[\alpha(q_P - q_{\text{sum}})]}, \tag{1}$$

which increases from a negligible strictly positive value when the flow rate q_{sum} is small towards $P_{FS}^{B} = 1$ as q_{sum} approaches infinity, where superscript B means breakdown and subscript FS means $F \rightarrow S$ transition. We define $q_{\text{sum}} = q_{\text{in}} + q_{\text{on}}$, where q_{in} is the flow rate on the main road and q_{on} is the on-ramp inflow rate. The parameters α and q_P are determined by curve fitting, see [41]. See Brilon et al. [5, 6] for a qualitatively similar function found from empirical studies of traffic breakdown.

[2] The difference between S and J is that while the downstream front of a wide moving jam propagates through a highway bottleneck upstream with a mean velocity (often about −15 km/h), the downstream front of synchronized flow is usually fixed at the bottleneck (Figs. 1, 2 and 3).

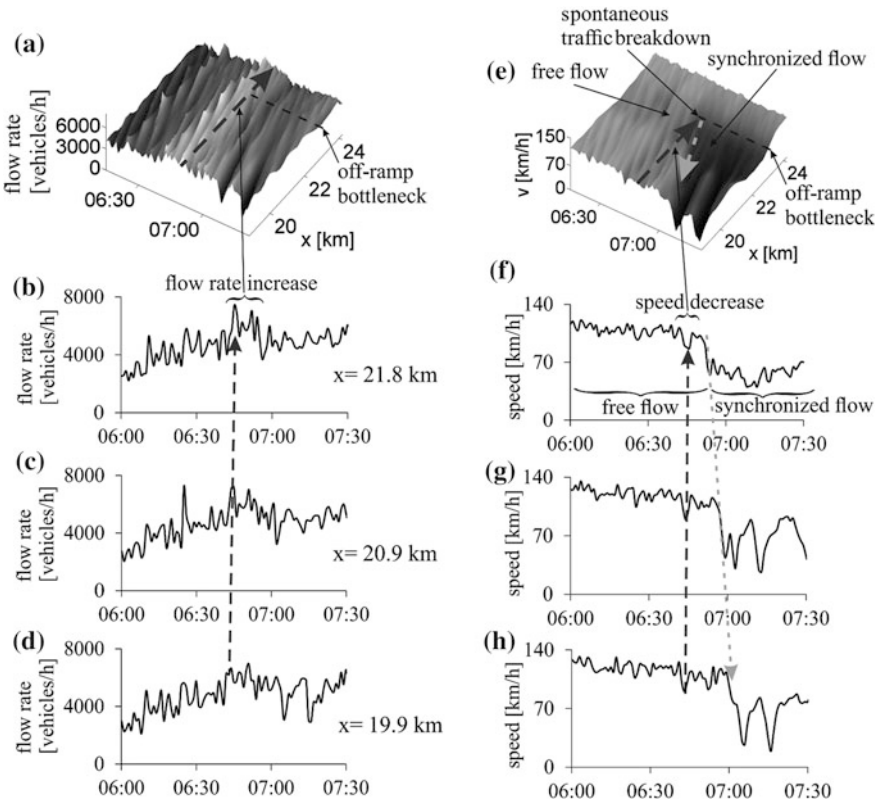

Fig. 2 Empirical example of spontaneous traffic breakdown at off-ramp bottleneck. Real measured traffic data of the flow rate (**a–d**) and average speed (**e–h**) through road detectors installed along three-lane freeway: **a**, **e** Total flow rate (**a**) and average speed (**e**) on the main road in space and time. **b–d**, **f–h** Time-functions of total flow rate across freeway (**b–d**) and average speed (**f–h**) measured at three locations of road detectors ($x = 21.8$ (b, f), 20.9 (c, g), and 19.9 km (d, h); road location 21.8 km is about 1.1 km upstream of the beginning of the off-ramp merging region). 1-min average data. Dashed arrows in the flow direction shown in **a, e** mark the spatiotemporal propagation of a flow rate impulse and the related decrease in the free flow speed; this impulse of the flow rate increase and speed decrease in free flow is marked by *dashed up-arrows* at the locations of road detectors in **b–d**, **f–h** as well as labeled by "flow rate increase" and "speed decrease" in (**b, f**). *Dashed arrow* in the upstream direction shown in **e** marks the propagation of the upstream front of synchronized flow after the breakdown has occurred; *dashed down-arrow* in **f–h** marks this upstream front of synchronized flow at the locations of road detectors. *Dashed lines* in **a**, **e** mark the bottleneck location at which the downstream front of synchronized flow resulting from the breakdown is localized. For a more detailed explanation of this spontaneous traffic breakdown at the off-ramp bottleneck see Sect. 3.3.1.2 of [34]. Taken from [36]

When traffic at N different bottlenecks breaks down independently of each other (usually requires more than 300 m between each bottleneck, see [36]), the probability of spontaneous $F \rightarrow S$ traffic breakdown in at least one bottleneck is

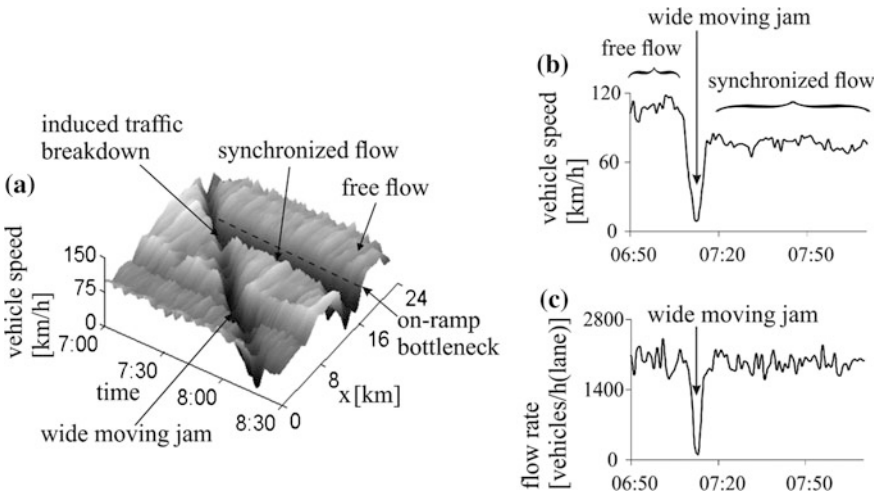

Fig. 3 Empirical example of traffic breakdown at on-ramp bottleneck induced by wide moving jam propagation (real measured traffic data of road detectors installed along three-lane freeway): **a** Averaged speed in space and time. **b**, **c** Time-functions of average speed (**b**) and flow rate (averaged between freeway lanes) (**c**) at bottleneck location (x = 17.1 km). 1-min average data. Taken from [33, 36]

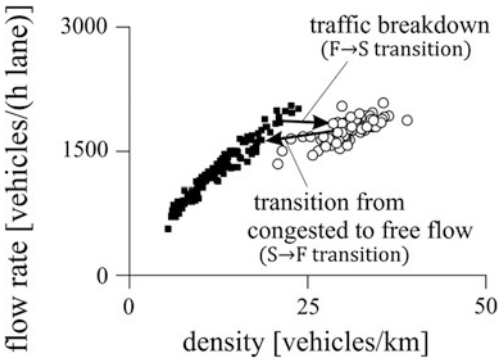

Fig. 4 Example of well-known empirical hysteresis phenomenon caused by traffic breakdown ($F \rightarrow S$ transition) and return transition from congested traffic to free flow ($S \rightarrow F$ transition) (real measured traffic data of road detectors). Taken from [33]

$$P_{FS,\text{net}} = 1 - \prod_{k=1}^{N} (1 - P_{FS}^{B,k}), \tag{2}$$

where P_{FS}^{B}, using Eq. (1), is the probability of $F \rightarrow S$ breakdown at bottleneck k, $k = 1,...,N$, $N > 1$. Kerner [35] proposes that the network optimum is reached at

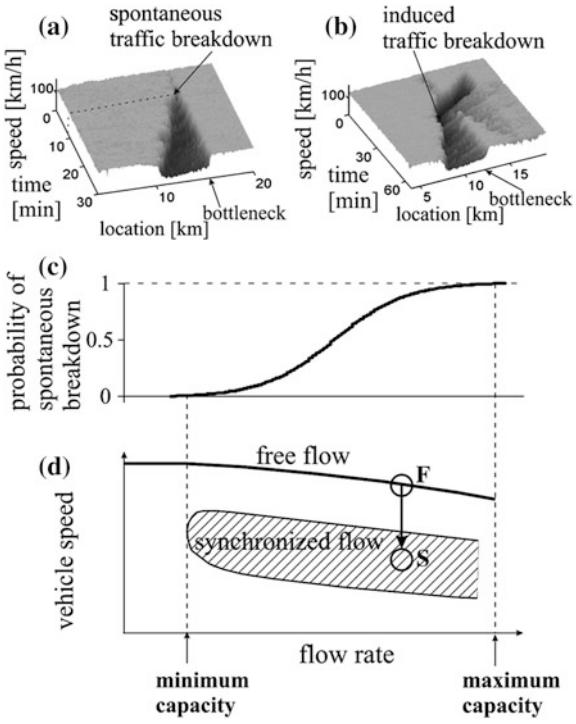

Fig. 5 Explanations of the fundamental empirical features of traffic breakdown at a highway bottleneck with Kerner's three-phase theory [33, 34]: **a**, **b** Simulations of spontaneous (**a**) and induced (**b**) breakdown at on-ramp bottleneck taken from [39]. **c** Simulations of the probability of spontaneous traffic breakdown at on-ramp bottleneck on a single-lane road taken from [41]. **d** Qualitative Z-speed-flow-rate characteristic for traffic breakdown; *F* free flow, *S* synchronized flow (results of simulations of the Z-speed-flow-rate characteristic for traffic breakdown can be found in [33, 34, 37–39]; see, for example, Fig. 3.17b of [34]. Taken from [36]

$$\underset{q_1,\ldots,q_M,q_m\geq 0}{\text{Min}} P_{FS,\text{net}}(q_1,\ldots,q_M), \quad m=1,\ldots,M, \quad M>1, \tag{3}$$

where M is the number of network links for which flow rates can be adjusted, and q_m is the link inflow rate for link m. The optimization in Eq. (3) is constrained by $q_m \geq 0$ since a link inflow rate cannot be negative. An infinite inflow rate $q_{\text{sum}} = \infty$ in Eq. (1) causes $P_{FS}^{B} = 1$ and thus $P_{FS,\text{net}} = 1$ in Eq. (2), which it is the objective of Eq. (3) to prevent, and hence an upper constraint on q_{sum} is not needed. Principle (3) for optimization of traffic and transportation networks introduced by Kerner et al. [41] in 2011 is called Kerner's breakdown minimization (BM) principle.

Verbally, the BM principle means that the optimum of traffic network is reached when the breakdown probability in at least one bottleneck is minimum. This is equivalent to maximizing the probability of breakdown at none of the bottlenecks, i.e. [35]

$$\underset{q_1,\ldots,q_M,q_m\geq 0}{\text{Max}} P_{C,\text{net}}(q_1,\ldots,q_M), \quad P_{C,\text{net}}=\prod_{k=1}^{N} P_C^{B,k}, \quad P_C^{B,k}=1-P_{FS}^{B,k}. \tag{4}$$

The product sign to determine $P_{C,\text{net}}$ in Eq. (4) expresses the probability $P_C^{B,1}$ of no breakdown at bottleneck 1, multiplied with the probability $P_C^{B,2}$ of no breakdown at bottleneck 2, etc., and eventually multiplied with the probability $P_C^{B,N}$ of no breakdown at bottleneck N. Wardrop's [14, 75] two principles minimize travel costs for each driver and maximize traffic throughput. In contrast, the BM principle depends neither on travel time nor travel costs. However, Kerner [36, p. 5274] argues that applying "the BM principle should result in relatively small travel costs associated with free flow in a network." More specifically, as evidence of this claim, Kerner [35] compares Wardrop's [14, 75] two principles with the BM principle for two alternative routes, each of which have exogenous on-ramp inflows, and applies traffic data and microscopic traffic simulations to show that the maximum network inflow rate allowing free flow is "considerably greater" (and equivalent to the empirical measurements) when using the BM principle rather than Wardrop's [14, 75] two principles.

To illustrate how the probability P_{FS}^{B} of spontaneous $F \rightarrow S$ breakdown at the on-ramp in Eq. (1), and shown in Fig. 5c, can be derived practically, we use the KKW-1 model (see [41] for detail) with many runs of the same duration T_{Ob} for given flow rates q_{sum} and q_{on}. Each of the runs begins with free flow and it was checked whether the $F \rightarrow S$ transition at the on-ramp occurred within the given time interval T_{Ob} or not. Then the number of realizations with the KKW-1 model, n_P, where the $F \rightarrow S$ transition at the on-ramp had occurred, was divided by the total number of realization, N_P, and approximated with the probability P_{FS}^{B} of spontaneous $F \rightarrow S$ breakdown in Eq. (1), i.e.

$$P_{FS}^{B} \approx n_P/N_P, \tag{5}$$

Equation (5) expresses that the approximate probability that the $F \rightarrow S$ transition at the on-ramp in an initial free flow occurs during the time interval T_{Ob} at given flow rates q_{sum} and q_{on}. Equation (5) converges towards the probability for $N_P \rightarrow \infty$ (taken from [41]). Figure 6 shows with two curves labelled 1 and 2, for different values of α and q_P, exponential increase of P_{FS}^{B} as functions of the flow rate q_{sum} at a chosen flow rate to the on-ramp q_{on}.

4 Common Games in Traffic Theory

Game theory requires two players at least or multiple players, that at least one player has a strategy set of at least two strategies, and that the payoff to each player depends on the combinations of strategies chosen by all players. This chapter

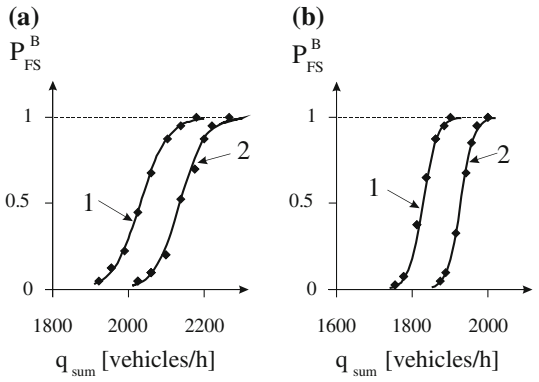

Fig. 6 Probability of breakdown phenomenon at the on-ramp for the KKW-1 model [41]: **a**, **b** The probability P_{FS}^{B} that the $F \rightarrow S$ transition occurs within $T_{Ob} = 30$ min (*curve 1*) or already within $T_{Ob} = 15$ min (*curve 2*), after the on-ramp inflow was switched on (at $t_0 = 8$ min), versus the traffic demand upstream of the on-ramp, $q_{\text{sum}} = q_{\text{min}} + q_{\text{on}}$. Results are shown for two different flow rates to the on-ramp, $q_{\text{on}} = 60$ vehicles/h in **a** and $q_{\text{on}} = 200$ vehicles/h in **b**. The following criterion that a $F \rightarrow S$ transition has occurred is used: The vehicle speed just upstream of the on-ramp drops below the level 80 km/h and then remains at nearly the same low level for more than 4 min. The probabilities were obtained from $N_P = 40$ independent runs. The curves in **a**, **b** are fitted with Eq. (1). The values (α, q_P) are: **a** *curve* 1 (0.014, 2031) and *curve* 2 (0.015, 2135), **b** *curve* 1 (0.027, 1828) and *curve* 2 (0.029, 1927). Taken from [41]

confines attention to two strategies for each player. Future research can generalize to arbitrarily many strategies for each player. The authors are unaware that the games in this section have been considered in the traffic theory literature, and thus this section is presented without references, aside from [58]. This section is based on theoretical reasoning and applies analogies. Empirical support is left for future research.

4.1 Two-Player Traffic Games

Many traffic encounters involve two players, e.g. two drivers meeting in an intersection. Rapoport and Guyer [58] classified the 78 ordinally ranked 2 × 2 games, i.e. games between two players where each player can choose between two strategies. We confine attention to two strategies for each player to retain simplicity and illustrate key basic features. For example, although intermediate strategies in practice exist between the two extreme strategies "driving safely" and "driving recklessly", e.g. "driving reasonably safely" or "driving slightly recklessly," the two extremes illustrate what we seek to convey. For our purpose, with individual drivers encountering each other, we start with the game in Table 1, where the payoffs can be ordinally ranked in 24 different manners. The payoff before the comma is earned by the row player. The payoff after the comma is earned by the column player.

Table 1 Symmetric 2 × 2 game

		Column player	
		C	D
Row player	C	*R*, *R*	*S*, *T*
	D	*T*, *S*	*P*, *P*

For the two games chicken game and prisoner's dilemma, explained below, *C* means cooperation and *D* means defection, and *R*, *T*, *S*, *P* are defined as follows: Cooperation *C* means driving safely according to the law and to ensure overall efficient traffic development, assuming that these objectives coincide. Defection *D* means driving recklessly with various objectives such as minimizing one's travel time from point *A* to point *B*, maximizing adventure, making other drivers nervous, enjoying the thrill of driving fast, and behavior which often means breaking the law. If both players (drivers) cooperate, they will both receive the reward payoff *R* in the upper left cell in Table 1. If the row player defects while the column player cooperates, the row player will receive the temptation payoff *T* shown before the comma in the lower left cell in Table 1, and the column player receives the sucker payoff *S* shown after the comma in the lower left cell. Conversely, if the row player cooperates while the column player defects, their payoffs will be reversed shown in the upper right cell in Table 1. Finally, if both players defect, they will both receive the punishment payoff *P*. For the two games battle of the sexes and coordination game, also explained below, *C* and *D* simply mean two different strategies, and *R*, *T*, *S*, *P* are four different payoffs with ordinal rankings discussed below.

Table 2 shows four common symmetric 2 × 2 games, assuming that the four payoffs *R*, *T*, *S*, *P* can take the four values 1, 2, 3, 4, and each payoff differs from the other three payoffs. The Nash [54] equilibria are marked in bold. Strategies by multiple players will constitute a Nash [54] equilibrium if no player has an incentive to deviate unilaterally, i.e. unilaterally changing his strategy. Having looked at typical traffic situations, we judge these four to be especially common in traffic. This research has revealed that the chicken game is especially common, and we present the other three games to illustrate that these are also possible.

Table 2 Four common symmetric 2 × 2 games

Chicken game				Battle of the sexes			
		Column player				Column player	
		C	*D*			*C*	*D*
Row player	*C*	3, 3	**2, 4**	Row player	*C*	2, 2	**3, 4**
	D	**4, 2**	1, 1		*D*	**4, 3**	1, 1
Prisoner's dilemma				Coordination game			
		Column player				Column player	
		C	*D*			*C*	*D*
Row player	*C*	3, 3	1, 4	Row player	*C*	**4, 4**	1, 2
	D	4, 1	**2, 2**		*D*	2, 1	**3, 3**

4.1.1 Two-Player Chicken Game

In the chicken game each player prefers the daredevil strategy (not to yield to the other), but the lowest payoff is earned when both players choose the daredevil strategy (do not yield). The second highest payoff is earned when both players choose the chicken strategy (which means yielding to the other). The chicken game ($T \geq R \geq S \geq P$) is exemplified by the 1955 Warner Brothers drama film "Rebel Without a Cause" where Jim Stark (James Dean) and Buzz Gunderson (Corey Allen) race stolen cars towards an abyss. The first one who jumps out of the car loses and is deemed the "chicken". They might alternatively have driven the cars towards each other, exemplified by the 1984 Paramount Pictures musical drama film "Footloose" where Ren McCormack (Kevin Bacon) and Jim Youngs (Chuck Cranston) drive two tractors towards each other. The preferred temptation payoff $T = 4$ is obtained by being the last to jump or the one driving straight ahead (daredevil, i.e. defection) while the other is the first to jump or swerve to one side (chickens out, i.e. cooperates). If both defect they will be punished by mutual death or injury expressed with the lowest ranked payoff $P = 1$. Ordinally ranked payoffs means that the cardinally ranked mutual punishment payoff can be arbitrarily negative. If both cooperate they will both get the reward payoff $R = 3$ which is second best since they avoid injury or death, and avoid being the single chicken which gives the second lowest ordinally ranked sucker payoff $S = 2$.

The chicken game describes many traffic situations, and is probably the most common game in traffic theory. One example is two drivers heading towards the same intersection where the First-In-First-Out (FIFO) law applies. The FIFO law applies e.g. in roundabouts and in regular intersections in some countries, specifying that the first reaching the intersection or roundabout has the right to proceed through the intersection. Despite traffic law, doubts may arise about who chooses to proceed through the intersection and who chooses to yield. First, the drivers may arrive simultaneously, leaving other factors to determine who proceeds first, such as the size, color, and type of vehicle (bus, car, taxi, motorbike), the car's speed, the curvature of the terrain, whether one incoming road is broader than the other, the characteristics of the driver (age, sex, cultural background, clothing, personality, and biological factors, etc.). Second, the drivers may have different subjective conceptions about who arrives first, due to high speed, various disturbances (passengers, music, etc.), and limited capacity for processing information and preferences. Third, one driver may arrive after the other driver, but the late incoming driver may drive a more dangerous looking car, drive downhill on a broader road at higher speed, and display more aggressive driving behavior. In intersections where the FIFO law does not apply, e.g. because the law is right-of-way based (e.g. the one coming from the right or riding on the larger road has priority), the same dilemma will exist if the drivers don't arrive simultaneously. For example, the driver dictated by traffic law to yield may choose not yield because he arrives at the intersection slightly before or slightly after, but dangerously close in time, the other driver. Ample opportunities for both drivers exist in such situations, with or without the FIFO rule, to choose the chicken strategy or the daredevil strategy. The two

equilibria are that they choose opposite strategies, which prevents accidents caused by the driver choosing the chicken strategy. Choosing the chicken strategy ensures that no risky situations arise. Choosing the chicken strategy presupposes that the drivers are in a chicken game. Given that the traffic situation is a chicken game, choosing the chicken strategy is consistent with choosing safe and less aggressive driving behavior which conceptualizes different degrees of a driver's reactions to other drivers.

Designing traffic law where drivers choose opposite strategies is not particularly feasible. Hence traffic law is designed to remove uncertainty, risk, and unclarity, for example specifying that the first driver reaching an intersection or roundabout has the right to proceed. This means recommending the chicken strategy. Breaking the law by choosing the daredevil strategy has consequences such as risk of fine, incarceration, losing one's driver's license, injury, death, etc. One challenge for traffic theory is that recommending the chicken strategy for all drivers means dictating that all drivers play the non-equilibrium of mutual cooperation to obtain the second best reward payoff. This places a tall order on drivers, since the incentives for the daredevil strategy is usually or often lurking underneath many traffic situations.

4.1.2 Two-Player Battle of the Sexes

The battle of the sexes ($T \geq S \geq R \geq P$) closely resembles the chicken game, but the S and R payoffs are reversed. This preserves the two equilibria, but the mutual cooperation reward payoff is now third best and the discrepancy between temptation and sucker is smaller. Both players are thus more pleased with either equilibrium than with both choosing C or both choosing D, in contrast to the chicken game where one player in either equilibrium gets lower payoff than when both choose C. One example of the battle of the sexes is two routes [3, 9, 57, 74] from point A to point B. Assume that both routes are narrow roads where passing and overtaking another driver is impossible. Assume that two drivers need to drive back and forth between points A and B. They thus prefer to choose opposite routes to avoid meeting and having to overtake each other. The battle of the sexes assumes different preferences for the two players for the two equilibria, (4, 3), (3, 4), which is usually realistic since two routes usually differ regarding length, quality, surface, curvature, steepness, scenery, lighting, etc., vehicles differ regarding size, weight, power, acceleration, gas consumption, etc., and drivers differ regarding abilities, competence, preferences, beliefs, etc. Beneficial for the battle of the sexes is that both players have the same or similar facts and information (realistic, e.g. when both know the road geography, or common congestion phenomena through time), and that they can communicate to agree on their opposite choices (realistic, e.g. if they know each other, meet for various purposes, or communicate electronically). However, choosing either of the two equilibria can also be accomplished by tacit understanding, trial and error, and adjustment over time if the game is repeated. Inferior in all regards, for the battle of the sexes, since both T and S are smaller than

both R and P, are that they choose the same route. This stands in contrast to the chicken game where the non-equilibrium chicken strategy chosen by both players, giving payoff R to both players, is preferred over the chicken strategy when the other player chooses the daredevil strategy, giving the lower payoff S to the player choosing the chicken strategy.

Another example is two drivers driving along a narrow road at night over a mountain in freezing temperatures, or along a scorching hot desert road. Assume that they drive back and forth between points A and B repeatedly around the clock, e.g. transporting sand. They prefer to drive together in order to benefit from jointly lighting up the surroundings, to benefit from safety for the event that one vehicle brakes down, and to benefit from companionship. Inferior for both drivers is to drive apart from each other, regardless who drives first, since both T and S are smaller than both R and P. Two drivers driving together may have different preferences for who shall drive first. For example, one driver may prefer to drive second which simply means following the lights of the front car, passively enjoying an easy ride with limited need for attention. However, it is also possible for a driver to prefer driving first, for example if that driver feels more experienced and capable of staying on the road, or to experience a sense of adventure when driving into the dark.

4.1.3 Two-Player Prisoner's Dilemma

Starting from the chicken game, if the S and P payoffs are reversed we will get the prisoner's dilemma ($T \geq R \geq P \geq S$). This minor alteration means that mutual defection does not give the lowest payoff. In contrast, the lowest payoff follows from cooperating when the opponent defects, which causes the detrimental sucker payoff. More detrimentally, mutual defection is the one unique equilibrium. Defection is the dominant strategy regardless what the other player chooses. The prisoner's dilemma is especially descriptive of public goods provision where free riding on others' provision is beneficial. The prisoner's dilemma is descriptive of traffic situations where one's strategy is costly for oneself and beneficial for others in the sense of providing a public good. For example, consider a driver in the front of a queue headed towards an intersection with no approaching drivers in the opposite direction. Using the blink light to indicate a left or right turn is costly for a driver (the manoeuver requires attention, takes time, and the cost is embedded in the car's cost), causes no or negligible benefit for the driver, but is beneficial for the drivers further back in the queue who can adjust their driving behavior accordingly, knowing whether the front driver plans to turn left or right. Second, consider a large lorry ahead of a motorcycle. Installing braking lights in the lorry is costly and has no or negligible benefit for the lorry driver to the extent that being rear ended does not substantially damage the lorry, but is beneficial for the motorcycle driver who gets a forewarning that the lorry is braking which may prevent the motorcycle driver from rear ending the lorry with potential injury or death.

4.1.4 Two-Player Coordination Game

Starting from the prisoner's dilemma, if the temptation payoff T is moved from most preferred to third preferred, thus virtually eliminating incentives to be tempted, we will get the coordination game ($R \geq P \geq T \geq S$) with two equilibria. As an example, consider two persons stranded with one car and one bicycle each in an uninhabited area, or assigned the task of developing traffic law for an uninhabited area. They have to agree on whether to drive on the right or left side of the road. This is a coordination game such as in the lower right corner of Table 2. Both prefer to agree on the law for which side to drive on, but the law has no or minor importance. For the bicycle the law has no importance and the payoff is the same for left and right, and low payoff if they choose opposite laws. For cars with driving wheel on the left, and persons from countries where the law is to drive on the right side, some preference exists for driving on the right side expressed with $4 > 3$ in the lower right corner of Table 2. For cars with driving wheel on the right preferences may be opposite, and preferences may depend on whether the persons are Englishmen, Americans, etc. Other conventions are the law in some countries of yielding for traffic coming from the right (Norway), or that the first driver to reach an intersection has the right to proceed first (United States), and the various colors of the various lights on vehicles. Conventions such as these, where agreement is more important than what one agrees on, is widespread in traffic situations, illustrating the applicability of the coordination game.

4.2 n-Player Traffic Games

Although many traffic situations consist of or can be simplified to encounters between two drivers, many traffic situations inevitably have to be analyzed as encounters between more than two drivers. For example, four drivers may simultaneously reach an intersection. Two or three drivers may simultaneously assess whether to overtake a slow driver. These play games with each other and with meeting drivers. Drivers in a platoon interact complexly with each other. Changing lanes, or merging when lanes merge, usually means relating to more than one other driver. Braking abruptly may cause being rear-ended, which may cause a chain collision with many drivers in a queue. More generally, congested traffic means interacting with many drivers. Over the next subsections we consider situations with more than two drivers.

4.2.1 n-Player Chicken Game

Figure 7 shows the n-player chicken game. If $n = 2$, the horizontal axis shows the second player choosing defection (daredevil) at $X = 0$ (causing the first player to get the sucker payoff S with the chicken strategy, and the detrimental punishment payoff

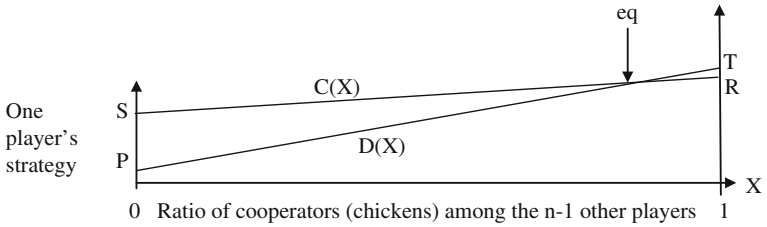

Fig. 7 *n*-player chicken game with many chickens, $T > R > S > P$, where X, $0 \le X \le 1$, is the fraction of chickens, $C(X)$ is the cooperation payoff, $D(X)$ is the defection payoff, eq means equilibrium, T, R, S, P are defined in Tables 1 and 2, and the vertical axis is an ordinal scale

P with the daredevil strategy) and cooperation (chicken) at $X = 1$ (causing the first player to get the reward payoff R with the chicken strategy, and the beneficial temptation payoff T with the daredevil strategy). With more than $n = 2$ players, the curve from S to R expresses the cooperation payoff $C(X)$ to the one player given that a fraction X of the other $n - 1$ players chooses cooperation. The curve, which does not have to be linear, is upward sloping since $R \ge S$, which expresses that more players choosing the chicken strategy is beneficial for the one player choosing the chicken strategy. The curve from P to T expresses the defection payoff $D(X)$ to the one player given that a fraction X of the other $n - 1$ players chooses cooperation. This curve, which also does not have to be linear, is upward sloping with a steeper slope since $T \ge R \ge S \ge P$, which expresses more players choosing the chicken strategy is beneficial for the one player choosing the daredevil strategy. Consequently, the two curves cross each other at an equilibrium number of cooperators, assuming that the number n of players is sufficiently large so that the integer problem can be ignored. That is, when $n = 2$, the one player chooses S when $X = 0$ and chooses T when $X = 1$. When n is large, an intermediate number of cooperators is optimal. To verify that the crossing point is an equilibrium, assume that X is low. This means that defectors have an incentive to switch to cooperation which increases X towards the equilibrium. Conversely, assume that X is high. This means that cooperators have an incentive to switch to defection which decreases X towards the equilibrium.

Figure 7 illustrates an equilibrium with many cooperators (chickens). It is descriptive of stable traffic situations where incentives for the temptation payoff are low or harshly punished e.g. by surveillance, police presence, or cultural norms. This equilibrium is beneficial from a collective and public safety point of view since the incentives to go for the temptation payoff T are low. Eliminating the incentives for the temptation payoff is hard, illustrated by the prevalence of the chicken game, and thus the equilibrium occurs for an X strictly below $X = 1$. In less stable traffic situations, e.g. with no surveillance, police, or different cultural norms, incentives for the temptation payoff may be much larger. This is accomplished by moving the curve from P to T in Fig. 7 vertically upwards causing Fig. 8 where the curves cross at a much lower X. That is, in Fig. 8 the payoff for being a daredevil is strictly higher than in Fig. 7, whereas the cooperation curve $C(X)$ from S to R is equivalent for Figs. 7 and 8. Figure 8 thus illustrates an equilibrium with few cooperators (chickens).

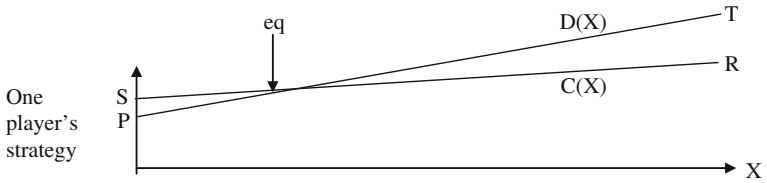

Fig. 8 n-player chicken game with few chickens, $T > R > S > P$, where X, $0 \le X \le 1$, is the fraction of chickens, $C(X)$ is the cooperation payoff, $D(X)$ is the defection payoff, eq means equilibrium, T, R, S, P are defined in Tables 1 and 2, and the vertical axis is an ordinal scale

Many of the examples of two-player chicken games in Sect. 4.1.1 are readily generalized to more than two players. For an example, an intersection or roundabout may have five or more incoming roads. If five drivers headed simultaneously towards the intersection are likely to choose the chicken strategy, accident may be prevented, but not if the five drivers are more likely to choose the daredevil strategy.

A second example is lane changing behavior. Changing lanes is risky. The safest strategy from a system optimal viewpoint is that all drivers remain in their chosen lanes. However, drivers may change lane or not depending on other drivers' decisions to accelerate or decelerate or other actions. A daredevil may change lanes repeatedly, as a slalom strategy, to get ahead in traffic. If he is the sole daredevil, and all the others are chickens, the daredevil will gain substantially, while the nervous chickens hold back to prevent accidents. However, if all drivers choose the daredevil strategy, that is $X = 0$ in Figs. 7 and 8, traffic will become chaotic, and they will all receive the lowest punishment payoff P, which as an ordinal payoff can be arbitrarily negative.

Also illustrative of the chicken game are merge methods for roads narrowing from n to n-1 lanes in one given direction, e.g. the late merge or zipper method, early merge, and dynamic late merge. Traffic law specifies merging which means the chicken strategy. But, incentives exist to choose the daredevil strategy to get ahead. Irritation, frustration, and uncertainty usually arise among the other drivers, but the driver choosing the daredevil strategy benefits as long as accidents are prevented.

Another example of the chicken strategy is drivers in a queue or platoon.[3] The daredevils overtake the driver ahead eventually reaching their destinations earlier but at enhanced risk. The chickens are left behind using more time to reach their destination, but enjoying more safety and security. For analysis of the n-player chicken game see [67–69].

[3] A platoon is a group of vehicles following each other with low distance between each vehicle, accomplished by electronic, and sometimes mechanical, coupling. Traffic throughput increases because of the synchronization where e.g. reaction times are decreased or eliminated.

4.2.2 n-Player Battle of the Sexes

Figure 9 shows the *n*-player battle of the sexes. The logic of the equilibrium for intermediate *X* is the same as for the chicken game in Figs. 7 and 8. The only difference is that the *C*(*X*) curve from *S* to *R* in Fig. 9 is downward sloping, as opposed to upward sloping in Figs. 7 and 8. This reflects that in the battle of the sexes being the sole player choosing *C* (which means chicken in the chicken game) is not as bad as in the chicken game. Quite the contrary, the sole player choosing *C* gets the second best payoff. Whereas in the chicken game more cooperators (chickens) benefit each cooperator, so that many chickens together is preferred given that one is a chicken, and being the sole chicken is worst, for the battle of the sexes more players choosing *C* hurt each player choosing *C*, so that many players choosing *C* is worst, and being the sole player choosing *C* is best, given that one chooses *C*. The same logic applies for choosing *D*, with the asymmetry that the maximum payoff *T* is reached if one is the only player choosing *D*, and the minimum payoff *P* is reached if all players choose *D*.

The two-player battle of the sexes examples in Sect. 4.1.2 are generalizable to *n* players. A further example is lanes in most cities for designated purposes, most commonly public transportation e.g. in the form of buses, taxis, drivers with certain privileges, or vehicles with certain characteristics such as e.g. electric cars. These lanes for specific purposes account for the battle of the sexes equilibrium in Fig. 9 for intermediate *X*. Given that most drivers use the other lanes, the first driver using the designated lane benefits tremendously, gaining the payoff *T* in Fig. 9. Also, as more and more designated drivers switch to the designated lane, the load of the non-designated lanes decreases which benefit the non-designated drivers. The two lowest payoffs are earned when the designated lane is empty, and the non-designated lanes are empty. One purpose of designated lanes is to make public transportation more attractive, by shifting the incentives of some drivers of cars to switch to taking the bus, which alleviates the overall traffic load. Other purposes, when such lanes allow electric cars, are to decrease air pollution, and shift incentives from driving conventional cars to driving electric cars. Allowing increased use of designated lanes will be beneficial only if the load of the designated lane is low. If electric cars become too numerous, so that the flow rate in the designated lane

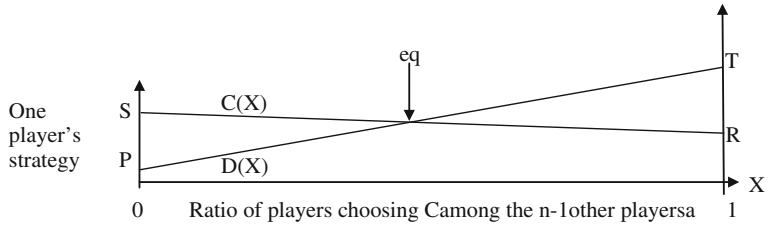

Fig. 9 *n*-player battle of the sexes, $T > S > R > P$, where X, $0 \le X \le 1$, is the fraction of chickens, $C(X)$ is the cooperation payoff, $D(X)$ is the defection payoff, eq means equilibrium, T, R, S, P are defined in Tables 1 and 2, and the vertical axis is an ordinal scale

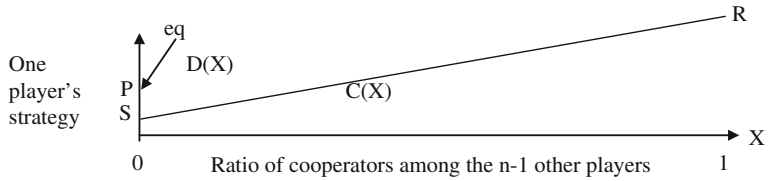

Fig. 10 *n*-player prisoner's dilemma, $T > R > P > S$, where X, $0 \le X \le 1$, is the fraction of chickens, $C(X)$ is the cooperation payoff, $D(X)$ is the defection payoff, eq means equilibrium, T, R, S, P are defined in Tables 1 and 2, and the vertical axis is an ordinal scale

becomes lower than in the non-designated lanes, the electric cars, and also the other designated drivers, will start driving in the non-designated lanes. At that point, traffic law usually changes, e.g. forbidding electric cars from using designated lanes.

4.2.3 n-Player Prisoner's Dilemma

Figure 10 shows the *n*-player prisoner's dilemma. That defection is the dominant strategy regardless what the other players choose means that the $D(X)$ curve gives strictly higher payoff than the $C(X)$ curve for all X, so that these two curves don't cross. The one unique equilibrium is thus where the $D(X)$ curve crosses the left vertical axis giving the mutual defection payoff P to all players. The public goods provision examples in Sect. 4.1.3 for the two-player prisoner's dilemma are directly generalizable to n players.

4.2.4 n-Player Coordination Game

Figure 11 shows the *n*-player coordination game. The $C(X)$ curve is upward sloping, but in contrast to Figs. 7, 8, 9 and 10, the $D(X)$ curve is downward sloping, and exceeds $C(X)$ for low X. That means that with a lower fraction than X of players choosing C, a player choosing C switches to D which decreases the fraction X of

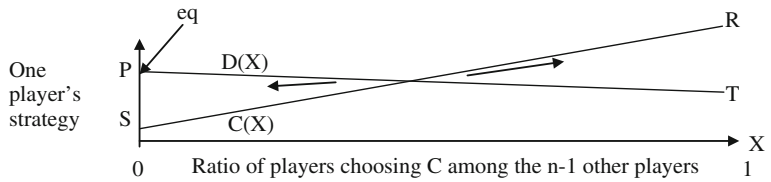

Fig. 11 *n*-player coordination game, $R > P > T > S$, where X, $0 \le X \le 1$, is the fraction of chickens, $C(X)$ is the cooperation payoff, $D(X)$ is the defection payoff, eq means equilibrium, T, R, S, P are defined in Tables 1 and 2, and the vertical axis is an ordinal scale

players choosing C eventually causing the equilibrium with no players choosing C, i.e. $X = 0$ and payoff P to all players choosing D. Conversely, with a higher fraction than X of players choosing C, a player choosing D switches to C increasing the fraction X of players choosing C eventually causing the equilibrium with only players choosing C, i.e. $X = 1$, and payoff R to all players choosing C. The crossing of the two curves $D(X)$ and $C(X)$ is thus a tipping point from which movement to either of the two corner equilibria can occur. The coordination examples in Sect. 4.1.4 for the two-player coordination game are directly generalizable to n players. Consider an early society which has not yet established a convention or law of driving on the right or left side of the road. If roughly half the drivers drive on the right side and the other half on the left side, some time may elapse before one or the other convention gets established, especially if some drivers recalcitrantly insist on their preference. However, as one convention gets a slight advantage, the process towards one of the corner equilibria can be expected to speed up as the payoff difference between the two curves $D(X)$ and $C(X)$ increases with movement away from the tipping point in Fig. 11.

5 Linking the Four Classical Developments with Game Theory

First, congestion as described, e.g. by Lighthill and Whitham [45] and Richards [60], see also [15] means that each driver has to react to more drivers in the surroundings. The opposite of congestion is one single driver where the choice of daredevil versus chicken is irrelevant. As congestion increases, we know from Figs. 7 and 8 that all drivers prefer a large fraction of chickens, which causes predictability and stability. This gives room for daredevils to take advantage which disrupts the stability.

Second, the over-deceleration effect, see e.g. Herman et al. [27] and Gazis et al. [21, 22], can be expected to be more pronounced with many chickens. Chickens are risk averse. When a preceding driver brakes, the subsequent chicken may brake excessively, and the subsequent chicken even more excessively. This may bring the queue of drivers to a standstill. The probability of accident may be low, but the flow rate will also be low. As an opposite consideration, with only daredevils, where all drivers know that all drivers are alert daredevils, the queue may not come to a standstill, but the traffic situation will be more volatile with probability of accident. Overall, the over-deceleration effect is risky with the joint presence of chickens and daredevils with different conceptions of how much deceleration is needed.

Third, using the classical conception, e.g. [4, 70], where the free flow capacity has a fixed value, the game theoretic analyses are simpler since it is clear-cut whether traffic is in free flow or not. Conversely, with Kerner's [36] theory, no such fixed value exists, impact of congested patterns from other bottlenecks, hysteresis, etc. impact, which the game theoretic analysis has to account for.

Fourth, Wardrop's [14, 75] user equilibrium principle is of the same nature as Nash's [54] equilibrium. The two concepts were developed separately. Haurie and Marcotte [25] proved that a Nash equilibrium in a network game with a finite number of players converges to a Wardrop equilibrium when the number of players increases. In such an equilibrium no driver can beneficially deviate unilaterally. Wardrop's [14, 75] system optimal principle is of the same nature as collective optimization principles in economics, and can be obtained by marginal cost road pricing. To obtain system optimality, culture, incentives, or laws may be needed for all drivers to choose the chicken strategy.

6 Linking Kerner's Three-Phase Traffic Theory with Game Theory

This section uses Kerner's three phase theory from Sect. 3, uses the gametheoretic insights from Sects. 4 and 5, and describes Kerner's three phases game theoretically by applying the chicken game. In the first phase with free flow the fractions of chickens and daredevils can vary greatly up and down within certain ranges of the density and flow rate. For the first transition $F \rightarrow S$ from free flow F to synchronized flow S more drivers become chickens. For the second transition from synchronized flow S to wide moving jam J the fraction of chickens remains constant. In the third transition from wide moving jam J to free flow F, the fraction of chickens decreases.

Let us describe this more thoroughly, showing with reference to Figs. 7 and 8 the mathematical relations that specify that the three phases can in fact be parallelized to the chicken game. See for example Antoniou and Pitsillides [1, Chap. 2] for parallelism between real life situations and games. Figures 4 and 5d illustrate three transitions between the three exhaustive and mutually exclusive phases F, S, and J. The first phase is free flow F. In free flow F an intermediate (which can be large or small) number of drivers cooperate as chickens, where the $C(X)$ and $D(X)$ curves cross each other for an equilibrium value of X between that of Figs. 7 and 8. That is, in free flow F intermediately many drivers choose the chicken strategy at a given speed, density, and flow rate, or the probability that a given driver chooses the chicken strategy in a given situation, is intermediate. The linear relationship between density and flow rate in Fig. 4, from zero and up to the maximum point shown in Fig. 4, illustrates greatly varying density and flow rate within this range. Close to the lower extreme, with only two drivers in a given direction, the density and flow rate are low, the drivers hardly interact, and whether they choose the chicken strategy or daredevil strategy has little importance. As the flow rate and density increase, more chickens ensure stability, and daredevils cause instability and uncertainty. Nevertheless, within free flow F the fraction of chickens and daredevils can vary up and down within certain ranges.

When the flow rate exceeds the minimum capacity shown in Fig. 5d, the probability of $F \rightarrow S$ transitions increases with increasing flow rates. $F \rightarrow S$ transitions can occur at many flow rates above the minimum capacity flow rate shown in Fig. 5d. When this $F \rightarrow S$ transition occurs, this marks the transition from free flow F to synchronized flow S which is the second phase. For this first transition, as the driver density (vehicles/km) exceeds a minimum level, the flow rate (vehicles/(hour × lane)) might no longer increase but might remain almost constant. This almost constant flow rate despite increased density follows either from drivers decreasing their speed, or follows from more drivers entering the network at an on-ramp, or follows from vehicles reducing their headways (i.e. distance or time between vehicles). Decreasing speed follows from drivers becoming increasingly apprehensive, fearful, and wary of accidents, due to the larger number of drivers surrounding them in a congested environment. If drivers become increasingly apprehensive in this manner, the chicken strategy will become more likely. Increasing density at constant flow rate is correlated with higher prevalence of the chicken strategy. Hence the first $F \rightarrow S$ transition means that some drivers switch from the daredevil strategy to the chicken strategy, or that a given driver chooses the chicken strategy with higher probability. Graphically in Fig. 8, this means that the curve from P to T gets shifted downwards, causing Fig. 7, as the benefit of defection (daredevil) decreases. This shifts the intersection between the P-T curve and the S-R curve towards the right, as in Fig. 7, which increases the number of cooperators, i.e. chickens. That is, in synchronized flow S, with more congestion, the benefit of the daredevil strategy decreases, as drivers become more risk averse and seek to avoid risky and costly accidents in a congested environment with many possibilities of accident. In other words, any given daredevil gets a lower payoff $D(X)$ as the P-T curve shifts downwards, which increases the equilibrium value of X, which increases the payoff $C(X)$ of any given chicken. Assume that the fraction of daredevils is unusually high at a certain place and time, e.g. due to hooligans driving home from a soccer match or drivers for various reasons becoming aggressive in dense traffic. The $F \rightarrow S$ transition then occurs for lower than usual values of flow rate and density. The smaller than usual number of chickens becomes even more apprehensive, and the subsequent transitions through the hysteresis loop back to free flow become more problematic and proceed more slowly.

A direct reversal from synchronized flow S to free flow F is impossible without the flow rate decreasing first, which means fewer vehicles/(hour × lane). A decrease in the flow rate can be linked to a second transition $S \rightarrow J$, from synchronized flow to wide moving jam. For this $S \rightarrow J$ transition, we assume that the flow rate decreases while the fraction of chickens remains constant, and the speed and density are constant. That is, unchanged speed and density does not change the curves and equilibrium value of X in Fig. 7 (or Fig. 8).

When the flow rate has decreased sufficiently at constant density, a new transition can occur. That is, for the third $J \rightarrow F$ transition, the density can again decrease at constant flow rate and constant low speed. Decreasing density gives more space around each driver which increases the prevalence of the daredevil strategy, causing fewer chickens. More space around each driver (lower density)

raises the *P-T* curve in Fig. 7 to that of Fig. 8, causing intersection with the *S-R* curve for a lower equilibrium value of X. Any given daredevil thus gets a higher payoff $D(X)$ as the *P-T* curve shifts upwards, which decreases the equilibrium value of X, which decreases the payoff $C(X)$ of any given chicken. With lower congestion in the sense of lower flow rate, the density eventually decreases towards the initial density, but with lower flow rate and lower speed than before the first transition, due to the hysteresis phenomenon, and we are back at the free flow phase F.

As the density has decreased sufficiently, within the free flow phase, due to bottleneck disappearances and the removal of drivers from the network, causing low congestion, the flow rate and speed again increase and the density increases, while within the free flow phase. The increasing density again means that the *P-T* curve in Fig. 8 gets shifted downwards causing Fig. 7, with higher equilibrium value of X, higher payoff $C(X)$ to any given chicken, and drivers switch from the daredevil strategy to the chicken strategy, within the free flow phase. The drivers remain in free flow until the flow rate and density again exceed certain levels, and the new transitions $F \rightarrow S \rightarrow J \rightarrow F$ emerge.

Summing up, for the first $F \rightarrow S$ transition the chicken strategy becomes more likely. For the second $S \rightarrow J$ transition the chicken strategy is equally likely while the flow rate decreases at constant density. For the third $J \rightarrow F$ transition strategy the chicken strategy becomes less likely while the density decreases. Finally, within free flow F where the flow rate and density again increase, the chicken strategy becomes more likely. Figure 12 summarizes the changes in the number of chickens during these three transitions.

The arguments in this section of how driver behavior leads to spatio-temporal congestion patterns are in our view intuitive. We have conceptualized joint changes in flow rate and density game theoretically. The presentation is currently phrased more in terms of driving-behavioral conjectures than in terms of results. Future research should validate the conjectures, applying real data and for example microsimulation. Data should be compiled from different locations, and at different times during the day and week, to elicit different driving behavior. One approach is to incorporate the chicken strategy in a car-following model to show numerically how the relationship in Fig. 11 happens. Real data can be used to estimate the probabilities of Eqs. (1) and (2) in numerical examples to enhance the understanding

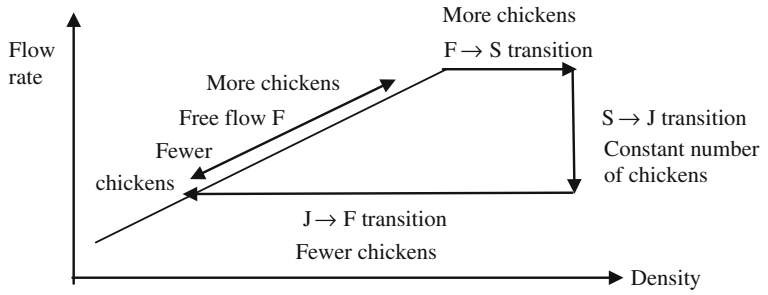

Fig. 12 Changes in the number of chickens during the three transitions, $F \rightarrow S$, $S \rightarrow J$, $J \rightarrow F$

of the chicken traffic game and the relevant probabilities to follow the chicken or the daredevil strategy, which signify the transitions $F \rightarrow S$, $S \rightarrow J$, and $J \rightarrow F$. Chen et al. [10] shows that hysteresis arises due to variable driver characteristics, which should be scrutinized further to determine how hysteresis prevalence and the shape of the hysteresis loop depend on fractions of chickens and daredevils. Future research should also scrutinize whether aspects of Kerner's three phase theory can be linked to other games than the chicken game. Future research should furthermore consider other observed forms of flow-density relationships, e.g. hypercongestion where, as the flow rate decreases, the density slowly increases until reaching a jam density. For hypercongestion see e.g. [4, 65].

7 Conclusion

This chapter presents four classical developments in traffic theory, and Kerner's [36] theory, and links these to game theory. First, Lighthill and Whitham [45] and Richards [60] suggested that flow rate and traffic density satisfies the conservation law for the number of vehicles, and that traffic breaks down when exceeding the free flow capacity. Second, Herman et al. [27] and Gazis et al. [21, 22] suggested that over-deceleration impacts breakdown, where subsequent drivers decelerate excessively. Third, May [4] and others suggested that the free flow capacity is a fixed deterministic or stochastic value. Fourth, Wardrop [14, 75] suggested one principle which minimizes individual travel costs for each driver, of the same spirit as Nash [54] equilibrium, and one principle which minimizes traffic throughput, analogous to collective welfare maximization in economic theory. Fifth, Kerner [36] argued that the first four classical developments, which constitute generally accepted fundamentals of traffic theory, are not consistent with the empirics of traffic breakdown.

Kerner [36] suggested the three phases free flow F, synchronized flow S with congestion, and wide moving jam J. He argued that traffic data shows no $F \rightarrow J$ transition, as commonly believed, but instead breakdown as $F \rightarrow S$ transition, and subsequent $S \rightarrow J$ transition. Furthermore, traffic breakdown is not only spontaneous, but can be induced e.g. by a wide moving jam propagating upstream. Observing that the traffic breakdown probability increases logistically in flow rate, Kerner [36] demonstrated hysteresis where, after an $F \rightarrow S$ transition, return to free flow usually occurs at smaller flow rates. Kerner argued for minimizing breakdown as the key principle.

We present and exemplify common games applicable for traffic theory, i.e. the chicken game, battle of the sexes, prisoner's dilemma, and the coordination game. The chicken game is especially prevalent in traffic. The chicken game is a quite risky game with ample issues related to safety and security. Traffic theory dictates that all drivers choose the chicken strategy which is not an equilibrium. The first driver switching from the chicken strategy to the daredevil strategy benefits, and benefits more with the presence of many chickens. With more daredevils in traffic, and especially when these encounter each other, the probability of accident

increases. From a traffic safety point of view it is of interest to design laws, culture, incentives, sanctions, and punishments to foster the proliferation of the chicken strategy and prohibit or limit the attractiveness of the daredevil strategy. For these two player and n-player games future research should develop simulation environments and test situations to determine and verify empirically which traffic situations correspond to which games.

We proceed to link the four classical developments with game theory, and formulate Kerner's three-phase theory game theoretically, applying the chicken game. In the first $F \rightarrow S$ transition from free flow to synchronized flow, where the density increases at a constant flow rate, more drivers choose the chicken strategy, or the probability that any given driver in a given situation chooses the chicken strategy increases. This $F \rightarrow S$ transition, which can be spontaneous or induced, occurs through increasing density at constant flow rate where drivers become increasingly apprehensive, fearful, and wary of accidents, caused by the larger number of drivers surrounding them in a congested environment. In the second $S \rightarrow J$ transition from synchronized flow to wide moving jam the chicken strategy is equally likely while the flow rate decreases at constant density. The propagation of the wide moving jam phase is very stable and independent of the driver behavior (e.g., aggressive, calm). For the third $J \rightarrow F$ transition strategy the chicken strategy becomes less likely while the traffic density decreases giving increased incentives for the daredevil strategy. Finally, within free flow F where the flow rate and density again increase, the chicken strategy becomes more likely and the daredevil strategy less likely. This closes the hysteresis circle. A new hysteresis circle will start if the density again increases at a constant flow rate.

A few practical implications of this chapter are to raise awareness of which games play a role in traffic, which strategies in these games are likely in certain circumstances, and the implications. Future research should consider practical implications of the proposed game-theoretic analysis of traffic flow dynamics, e.g., for modeling and controlling traffic flow under various congestion conditions.

Future research should generalize, empirically and theoretically, Kerner's [35] comparison of his BM principle with Wardrop's [14, 75] two principles for two alternative routes to general networks, e.g. determining necessary and sufficient conditions for optimum. The probabilistic occurrence of hysteresis certainly complicates such analyses. Kerner's [35] analyses of the three principles should also be merged with Bier and Hausken's [4] analysis of two alternative routes, where safety and security are accounted for in the sense of defense and attack, modeling congestion in accordance with Small and Verhoef [65]. More generally, future research should conduct simulations and more thorough numerical analysis, compare the discussed game theory approaches with real data, provide a more thorough quantitative analysis, and test empirically on freeways and city traffic.

Acknowledgments Hubert Rehborn thanks for the funding in the project "UR:BAN—Urbaner Raum: Benutzergerechte Assistenzsysteme und Netzmanagement," funded by the German Federal Ministry of Economic Affairs and Energy. We thank Boris S. Kerner, Micha Koller, Peter Hemmerle, and anonymous referees for their helpful suggestions.

References

1. Antoniou J, Pitsillides A (2012) Game theory in communication networks: cooperative resolution of interactive networking scenarios. CRC Press, Inc, Boca Raton
2. Beckmann MJ, McGuire CB, Winsten CB (1956) Studies in the economics of transportation. Yale University Press, New Haven
3. Bell MGH, Iida Y (1997) Transportation network analysis. Wiley, Hoboken, pp 07030–6000 (Incorporated)
4. Bier V, Hausken K (2013) Defending and attacking networks subject to traffic congestion. Reliabil Eng Syst Safety 112:214–224
5. Brilon W, Regler M, Geistefeld J (2005) Zufallscharakter der Kapazität von Autobahnen und praktische Konsequenzen—Teil 2. Straßenverkehrstechnik Heft 4:195–201
6. Brilon W, Zurlinden H (2004) Kapazität von Straßen als Zufallsgröße. Straßenverkehrstechnik Heft 4:164–172
7. Brown GW (1951) Iterative solutions of games by fictitious play. In: Koopmans TC (ed) Activity analysis of production and allocation. Wiley, New York
8. Carrillo FA, Delgado J, Saavedra P, Velasco RM, Verduzco F (2013) Traveling waves, catastrophes and bifurcations in a generic second order traffic flow model. Int J Bifurcat Chaos 23(12):1350191
9. Cascetta E (2001) Transport systems engineering: theory and methods. Kluwer Academic Publishers, Dordrecht
10. Chen DJ, Ahn S, Laval J, Zheng ZD (2014) On the periodicity of traffic oscillations and capacity drop: the role of driver characteristics. Transp Res Part B: Methodol 59:117–136
11. Chowdhury D, Santen L, Schadschneider A (2000) Statistical physics of vehicular traffic and some related systems. Phys Rep 329(4–6):199–329
12. Daganzo CF (2002) A behavioral theory of multi-lane traffic flow. Part I: long homogeneous freeway sections. Transp Res Part B: Methodol 36(2):131–158
13. Daganzo CF (2002) A behavioral theory of multi-lane traffic flow. Part II: merges and the onset of congestion. Transp Res Part B: Methodol 36(2):159–169
14. Davis LC (2009) Realizing Wardrop equilibria with real-time traffic information. Phys A 388:4459–4474
15. Davis LC (2010) Predicting travel time to limit congestion at a highway bottleneck. Phys A 389:3588–3599
16. Eleftheriadou L, Roess RP, McShane WR (1995) Probabilistic nature of breakdown at freeway merge junctions. Transp Res Rec 1484:80–89
17. Fudenberg DM, Tirole J (1991) Game theory. MIT Press, Cambridge
18. Garcia A, Reaume D, Smith RL (2000) Fictitious play for finding system optimal routings in dynamic traffic networks. Transp Res Part B 34:147–156
19. Gartner NH, Messer J, Rathi A (eds) (2002) Traffic flow theory. Transport Research Board, Washington
20. Gazis DC (2002) Traffic theory. Springer, Berlin
21. Gazis DC, Herman R, Potts RB (1959) Car-following theory of steady-state traffic flow. Oper Res 7(4):499–505
22. Gazis DC, Herman R, Rothery RW (1961) Nonlinear follow-the-leader models of traffic flow. Oper Res 9(4):545–567
23. Greenshields BD (1935) A study of highway capacity. In: Highway research board proceedings, vol 14, pp 448–477
24. Hall FL, Gunter MA (1986) Further analysis of the flow-concentration relationship. Transp Res Rec 1091:1–9
25. Haurie A, Marcotte P (1985) On the relationship between Nash-Cournot and Wardrop equilibria. Networks 15(3):295–308
26. Helbing D (2001) Traffic and related self-driven many-particle systems. Rev Mod Phys 73:1067–1141

27. Herman R, Montroll EW, Potts RB, Rothery RW (1959) Traffic dynamics: analysis of stability in car following. Oper Res 7(1):86–106
28. Highway Capacity Manual (2000) National research council. Transportation Research Board, Washington
29. Jiang R, Hu MB, Jia B, Gao ZY (2014) A new mechanism for metastability of under-saturated traffic responsible for time-delayed traffic breakdown at the signal. Comput Phys Commun 185 (5):1439–1442
30. Jin CJ, Wang W, Jiang R (2014) On the modeling of synchronized flow in cellular automaton models. Chin Phys B 23(2):024501
31. Jin CJ, Wang W, Jiang R, Wang H (2014) An empirical study of phase transitions from synchronized flow to jams on a single-lane highway. J Phys A: Math Theor 47(12):125104
32. Jin CJ, Wang W, Jiang R, Zhang HM, Wang H (2013) Spontaneous phase transition from free flow to synchronized flow in traffic on a single-lane highway. Phys Rev E 87(1):012815
33. Kerner BS (2004) The physics of traffic. Springer, Berlin
34. Kerner BS (2009) Introduction to modern traffic flow theory and control. Springer, Heidelberg
35. Kerner BS (2011) Optimum principle for a vehicular traffic network: minimum probability of congestion. J Phys A: Math Theor 44:092001
36. Kerner BS (2013) Criticism of generally accepted fundamentals and methodologies of traffic and transportation theory: a brief review. Phys A 392:5261–5282
37. Kerner BS, Klenov SL (2003) Microscopic theory of spatial-temporal congested traffic patterns at highway bottlenecks. Phys Rev E 68:036130
38. Kerner BS, Klenov SL, Hermanns G, Schreckenberg M (2013) Effect of driver over-acceleration on traffic breakdown in three-phase cellular automaton traffic flow models. Phys A 392:4083–4105
39. Kerner BS, Klenov SL, Schreckenberg M (2011) Simple cellular automaton model for traffic breakdown, highway capacity, and synchronized flow. Phys Rev E 84:046110
40. Kerner BS, Klenov SL, Schreckenberg M (2014) Probabilistic physical characteristics of phase transitions at highway bottlenecks: incommensurability of three-phase and two-phase traffic-flow theories. Phys Rev E 89(5):052807
41. Kerner BS, Klenov SL, Wolf DE (2002) Cellular automata approach to three-phase traffic theory. J Phys A: Math Gen 35:9971–10013
42. Knorr F, Schreckenberg M (2013) The comfortable driving model revisited: traffic phases and phase transitions. J Stat Mechan-Theory Exp P07002. doi:10.1088/1742-5468/2013/07/P07002
43. Kuhn TS (1962) The structure of scientific revolutions. University of Chicago Press, Chicago
44. Li ZB, Ahn S, Chung K, Ragland DR, Wang W, Yu JW (2014) Surrogate safety measure for evaluating rear-end collision risk related to kinematic waves near freeway recurrent bottlenecks. Accid Anal Prev 64:52–61
45. Lighthill MJ, Whitham GB (1955) On kinematic waves. I & II. Proc R Soc A 229:281–345
46. Lin H, Roughgarden T, Tardos E, Walkover A (2011) Stronger bounds on Braess's paradox and the maximum latency of selfish routing. SIAM J Discrete Math 25(4):1667–1686
47. Mahnke R, Kaupuzs J, Lubashevsky I (2005) Probabilistic description of traffic flow. Phys Rep 408(1–2):1–130
48. May AD (1990) Traffic flow fundamentals. Prentice-Hall Inc, New Jersey
49. Mendez AR, Velasco RM (2013) Kerner's free-synchronized phase transition in a macroscopic traffic flow model with two classes of drivers. J Phys A: Math Theor 46 (46):462001
50. Migdalas A (1995) Bilevel programming in traffic planning: models, methods and challenge. J Global Optim 7:381–405
51. Monderer D, Shapley L (1996) Fictitious play property for games with identical interests. J Econ Theory 68:258–265
52. Nagatani T (2002) The physics of traffic jams. Rep Prog Phys 65:1331–1386
53. Nagel K, Wagner P, Woesler R (2003) Still flowing: approaches to traffic flow and traffic jam modeling. Oper Res 51:681–716

54. Nash J (1951) Non-cooperative games. Ann Math 54(2):286–295
55. Peeta S, Yu JW (2005) A hybrid model for driver route choice incorporating en-route attributes and real-time information effects. Netw Spat Econ 5(1):21–40
56. Persaud BN, Yagar S, Brownlee R (1998) Exploration of the breakdown phenomenon in freeway traffic. Transp Res Rec 1634:64–69
57. Rakha H, Tawk A (2009) Traffic networks: dynamic traffic routing, assignment, and assessment. In: Meyers RA (ed) Encyclopedia of complexity and system science. Springer, Berlin, pp 9429–9470
58. Rapoport A, Guyer M (1966) A taxonomy of 2 × 2 Games. Gen Syst 11:203–214
59. Rehborn H, Klenov SL, Palmer J (2011) An empirical study of common traffic congestion features based on traffic data measured in the USA, the UK, and Germany. Phys A: Stat Mechan Appl 390(23–24):4466–4485
60. Richards Paul I (1956) Shock waves on the highway. Oper Res 4(1):42–51
61. Rosenthal RW (1973) A class of games possessing pure-strategy Nash equilibria. Int J Game Theory 2:65–67
62. Roughgarden T, Tardos E (2004) Bounding the inefficiency of equilibria in nonatomic congestion games. Games Econ Behav 47(2):389–403
63. Schadschneider A, Chowdhury D, Nishinari K (2010) Stochastic transport in complex systems: from molecules to vehicles. Elsevier, New York
64. Schönhof M, Helbing D (2009) Criticism of three-phase traffic theory. Transp Res Part B: Methodol 43(7):784–797
65. Small KA, Verhoef ET (2007) Economics of Urban transportation. Routledge, New York
66. Stackelberg H (1952) The theory of market economy. Oxford University Press, Oxford
67. Szilagyi M N (2006) Agent-based simulation of the N-person chicken game. In: Jorgensen S, Quincampoix M, Vincent TL (eds) Advances in dynamical games: annals of the international society of dynamic games, vol 9. Birkhäuser, Boston, pp 695–703. doi:10.1007/978-0-8176-4553-3_34
68. Szilagyi MN (2009) Cars or buses: computer simulation of a social and economic dilemma. Int J Internet Enterp Manag 6(1):23–30. doi:10.1504/IJIEM.2009.022932
69. Szilagyi MN, Somogyi I (2010) A systematic analysis of the n-person chicken game. Complexity 15(5):56–62
70. Transportation Research Board (2010) Highway capacity manual 2010. National Research Council, Washington, DC
71. Treiber M, Kesting A (2013) Traffic flow dynamics. Springer, Berlin
72. Ukkusuri S, Doan K, Abdul Aziz HM (2013) A bi-level formulation for the combined dynamic equilibrium based traffic signal control. Procedia Soc Behav Sci 80:729–752
73. Vazirani VV, Nisan N, Roughgarden T, Tardos É (2007) Algorithmic game theory. Cambridge University Press, Cambridge
74. Wahle J, Bazzan ALC, Klügl F, Schreckenberg M (2000) Decision dynamics in a traffic scenario. Phys A 287:669–681
75. Wardrop JG (1952) In: Proceedings of Institute of Civil Engineering. II, vol 1, pp 325–378
76. Xiang ZT, Li YJ, Chen YF, Xiong L (2013) Simulating synchronized traffic flow and wide moving jam based on the brake light rule. Phys A: Stat Mechan Appl 392(21):5399–5413

A Heuristic Method for Identifying Near-Optimal Defending Strategies for a Road Network Subject to Traffic Congestion

Mengyao Gao, Bo Zhang, Vicki M. Bier and Tao Yao

Abstract In this study we investigate the vulnerability of road networks to interdictions. We consider that an intentional attacker wants to maximize the congestion level on the network by interdicting some links of the network. The drivers are assumed to be selfish and always choose the route that minimizes the individual travel cost. In this case, network traffic flow follows user equilibrium (UE) traffic assignment, which however is affected by the interdiction initiated by the attacker. In this problem, the role of the defender is to minimize the damage that can be caused by an attack. A heuristic method is developed to solve for near-optimal attack (interdiction) and defense strategies, the effectiveness of which is demonstrated by simulation results. Numerical experiments are conducted to examine factors that influence the application of this method. Specifically, we compare the efficiency of this method when applied to different Cartesian grid-like networks. Managerial insights into the vulnerability and defense of road networks are drawn from the analysis.

1 Introduction

In recent decades, there have been more and more cases of terrorist attacks on transportation systems, not only endangering human beings' lives, but also destroying infrastructure systems such as food supply, telecommunication, finance and electric power. The most well-known are bombings of railway transit in Madrid, London, and Singapore, as well as "9.11." Reports give an impression that railway and flight are at higher risk than other modes of transport. However, a

M. Gao · T. Yao
Pennsylvania State University, State College, PA, USA

B. Zhang
Department of Industry Solutions, IBM Research-china, Beijing, China

V.M. Bier (✉)
University of Wisconsin, Madison, WI, USA
e-mail: bier@engr.wisc.edu

K. Hausken and J. Zhuang (eds.), *Game Theoretic Analysis of Congestion, Safety and Security*, Springer Series in Reliability Engineering,
DOI 10.1007/978-3-319-11674-7_6

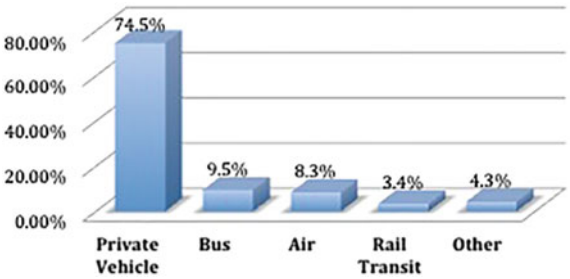

Fig. 1 Terrorist incidents involving transportation (1967–2007)

project named "Light Rail Now" [10] reveals that most terrorist incidents actually occurred on road networks, based on data from the US State Department and Wikipedia for the 41-year period from 1967 to 2007. Figure 1 shows the terrorist incident counts in different transport modes [10]. Over 80 % of terrorist incidents occurred on road networks, including 74.9 % involving private vehicles and 9.5 % involving buses, causing about 30,000 deaths and injuries. Thus, defending the road network against terrorist attacks is clearly important.

How can we defend a road network? Let us imagine a terrorist attack on a road network. At the beginning of the attack, no government agency would be able to respond immediately. Each driver or pedestrian on the road would try to rush to a safe place, which would make traffic highly congested. After a while (maybe several minutes, if the attack occurred in a large modern city), ambulances and police would rush to the site to save lives. However, they may not be able to get to their destination quickly, because of congestion and damage to the transportation infrastructure. Therefore, actions of defending should ideally be taken before an attack in order to increase the robustness and defensibility of the road network. In this chapter, we develop a heuristic method to determine a near-optimal group of links to be protected to minimize the cost associated with a potential terrorist attack.

Optimizing networks against interdiction is often a multi-objective problem. Royset and Wood [14] define an attacker's network interdiction process as a bi-objective maximum-flow network-interdiction problem, i.e., minimizing post-interdiction maximum flow (capacity of the network) and minimizing "total interdiction cost" (interdiction resource cost). The problem is modeled from the attackers' perspective, aiming at destroying as much of the network as possible at the lowest cost. They propose a new structure of algorithms to find the efficient frontier in the cost-to-effectiveness tradeoff. Murray and Mahmassani [11] create a bi-level mathematical program to identify vulnerable links in various scenarios. Feng and Wen [5] optimize a traffic control system for earthquake disasters which cause interdictions in the transportation. To maximize the traffic volume and minimize travel time, they build a bi-level programing model. A study by Ng et al. [12] about shelter allocation in emergency evacuations is also a bi-objective problem in static user equilibrium, using bi-level programming. Objectives in that study are to maximize the volume of people sheltered and to minimize the routes. However, these researchers base their models on shortest path theory without considering congestion. In their models, each route is

given a fixed weight representing either distance or travel time, and each driver is assumed to choose the route with the minimum weight. If some link on that route is interdicted, the driver will then select the route with the second minimum weight, etc. These models cannot accurately characterize road network flow when the travel demand on the network is large enough to cause congestion on some links. However, congestion is widespread in urban traffic, and as we mentioned earlier will become more serious when the urban transportation network is attacked.

To our knowledge, only Bier and Hausken [2] take congestion into account when choosing network defense strategies. Two cases on a two-arc network are studied—one when both arcs work, and one when one of the arcs is interdicted. The authors also assume that a driver may refuse to travel if the travel time exceeds some reservation time, which creates a penalty. By comparing the total travel time and penalty time in these two cases, they suggest that more defense effort should be assigned to less congested arcs, and to routes with larger capacity.

Although there are not many studies on interdiction and defense of traffic networks, there is a rich literature about interdiction and defense of other networks, like power and security systems. These studies provide us an effective strategy for reducing loss from attacks, which is to identify the critical links in the network and then defend them or allocate fortification resources nearby. For example, Church and Scaparra [4] apply the p-median model to identify the assets whose failures would result in the maximum loss to a system. In power systems, Bier et al. [3] identify the transmission lines with the maximum current flow as critical and defend them against interdictions. The authors propose a nested algorithm to iteratively choose the critical links to secure. In this chapter, we borrow the idea of a nested algorithm, and develop a heuristic method to identify near-optimal defense strategies for a road network subject to congestion.

In particular, we address network defense problems subject to traffic congestion on networks of more reasonable size than in [2], but without the concept of reservation times. Specifically, we define three types of players (drivers, a defender, and an attacker), and two types of strategic actions (attacking and defending). The attacker, such as a terrorist, plans an intentional attack on one or more links of a road network to maximize social loss. The defender knows of the threat from the attacker, but does not know which links will be attacked. In order to minimize the loss, the defender wishes to secure some links so that they cannot be interdicted by the attacker. The drivers in the network are assumed to be selfish, and the traffic flow can be characterized by UE. We view the problem from the perspective of the defender and develop a heuristic method to solve for near-optimal defense strategies. Numerical experiments are conducted to demonstrate that the proposed method can apply to realistic Cartesian-grid networks.

The remainder of this chapter is organized as follows. In Sect. 2, we show our UE model and present a convex combination method to solve the model. We propose a heuristic method to find near-optimal defense strategies for a congested traffic network in Sect. 3, and give a simple example of its application in Sect. 4. Section 5 presents two sets of numerical experiments to explore the effectiveness of our method. We conclude our study in Sect. 6.

2 Problem Formulation

2.1 Notation

The network can be represented as a graph $G = (V, E)$, where V is a set of nodes and E is a set of links. Let q_{rs} be the travel rate between origin r and destination s, comprising the origin-destination (O-D) demand matrix. In this chapter, the O-D demand matrixes are given beforehand. Let x_m denote the flow on link m, and t_m denote the travel time on link m. For the case of congestion, $t_m = t(x_m)$, indicating that the travel time on link m is a function of the flow. Let ψ_i^{rs} be the flow on route i between origin r and destination s. Thus, we have the relationship $x_m = \sum_r \sum_s \sum_i \psi_i^{rs} \delta_{m,i}^{rs}$, $\forall m$, meaning that the flow on each link is the sum of the flows on all routes using that link, where $\delta_{m,i}^{rs} = 1$ if route i goes through link m and $\delta_{m,i}^{rs} = 0$ if not. Table 1 summarizes the notation.

The assumptions of this chapter are that:

1. The attacker knows what has been defended and won't waste his/her attack on defended infrastructure;
2. All flows are simultaneous.

2.2 UE Model

Wardrop's two principles [18] are commonly used to characterize traffic assignment on a network. The first principle assumes that the driver chooses the route from origin to destination with the shortest travel time among all available routes, neglecting how his or her decision affects other drivers. The second principle [18] assumes that every driver's route choice is controlled by a central planner who aims to efficiently utilize the system to obtain the minimum average travel time. UE and system optimum (SO) models (stemming from the first and second principles,

Table 1 Notation

Symbol	Description
G	Network
V	A set of nodes in the network
E	A set of links in the network
x_m	Flow on link m
t_m	Travel time on link m
ψ_i^{rs}	Flow on route i from origin r to destination s
$\delta_{m,i}^{rs}$	$\delta_{m,i}^{rs} = 1$ if route i goes through link m and $\delta_{m,i}^{rs} = 0$ if not
q_{rs}	Travel rate between origin r and destination s

respectively) can be applied to calculate traffic flows and travel times for each route. In this chapter, we assume that the attack on the network is sudden, so that a central planner would not be able to react immediately. Therefore, in this case, UE fits the problem better than SO.

To obtain the link-flow pattern, the UE model can be constructed as a program with a nonlinear objective function and linear constraints. Beckmann et al. [1] give the following formulation:

$$\min z\left(\overrightarrow{x}\right) = \sum_{m} \int_{0}^{x_m} t(\tau) d\tau \tag{1a}$$

subject to

$$\sum_{i} \psi_i^{rs} = q_{rs} \quad \forall r, s \tag{1b}$$

$$x_m = \sum_{r} \sum_{s} \sum_{i} \psi_i^{rs} \delta_{m,i}^{rs} \quad \forall m \tag{1c}$$

$$\psi_i^{rs} \geq 0 \quad \forall i, r, s. \tag{1d}$$

In this formula, optimizing the objective function guarantees equilibrium. The objective function (1a) is to minimize the sum of the integrals of the travel time function for links. It is a strictly mathematical construct to solve equilibrium problems, without any economic or behavioral indication. Constraint (1b) illustrates that the flow on all routes from an origin to a destination is equal to the corresponding O-D travel demand. Equation (1c) defines the flow on link m. Constraint (1d) is the non-negativity constraint.

Beckmann et al. [1] prove the equivalence of formulation (1a, 1b, 1c, 1d) and the UE problem, as well as the uniqueness of the solution. For details, see [1].

2.3 Convex Combination Algorithm

Researchers have proposed various methods to determine vehicle flows using a UE model. Scarf [15], Todd [17], and Garcia and Zangwill [12] develop a fixed point method and explore its application. Pang and Chan [13] create a generalized linear method, as well as successive linearization with Lemke's method. Frank and Wolfe [7] first proposed the convex combination method, which was later improved by Florian and Nguyen [6]. For comparison of these methods, please refer to Friesz [8] and Sheffi [16]. Here, for reasons of both computational efficiency and accuracy, we select Frank and Wolfe's convex combination method to solve our UE model.

The convex combination method transforms the original nonlinear objective function to a linear approximation function. With subsequent iterations, the optimum of the linear program gets closer and closer to the optimum of the original program. Once it satisfies the convergence condition, the optimal solution for the UE model is obtained from the transformed program.

In detail, in the nth iteration, the direction that minimizes $z\left(\overrightarrow{x^n}\right)$ is $\overrightarrow{y} - \overrightarrow{x^n}$. The slope of $z\left(\overrightarrow{x^n}\right)$ in this direction is

$$-\nabla z\left(\overrightarrow{x^n}\right) \cdot \frac{\left(\overrightarrow{y} - \overrightarrow{x^n}\right)^T}{\left\|\overrightarrow{y} - \overrightarrow{x^n}\right\|} \tag{2}$$

Here $\overrightarrow{y}$ is an auxiliary feasible solution in the feasible region. For any given $\overrightarrow{y}$, the dropped objective function can be changed to a linear approximation:

$$\begin{aligned} z^n\left(\overrightarrow{y}\right) &= z\left(\overrightarrow{x^n}\right) - \left[-\nabla z\left(\overrightarrow{x^n}\right) \cdot \frac{\left(\overrightarrow{y} - \overrightarrow{x^n}\right)^T}{\left\|\overrightarrow{y} - \overrightarrow{x^n}\right\|}\right] \cdot \left\|\overrightarrow{y} - \overrightarrow{x^n}\right\| \\ &= z\left(\overrightarrow{x^n}\right) + \nabla z\left(\overrightarrow{x^n}\right) \cdot \left(\overrightarrow{y} - \overrightarrow{x^n}\right) \end{aligned} \tag{3}$$

Then, in the nth iteration, the descent direction that minimizes the objective function can be found through the approximate linear program,

$$\min z^n(\overrightarrow{y}) = z(\overrightarrow{x^n}) + \nabla z(\overrightarrow{x^n}) \cdot (\overrightarrow{y} - \overrightarrow{x^n}) \tag{4a}$$

subject to

$$\sum_i \psi_i^{rs} = q_{rs} \quad \forall r, s \tag{4b}$$

$$y_m = \sum_r \sum_s \sum_i \psi_i^{rs} \delta_{m,i}^{rs} \quad \forall m \tag{4c}$$

$$\psi_i^{rs} \geq 0 \quad \forall i, r, s \tag{4d}$$

After the direction $\overrightarrow{y} - \overrightarrow{x^n}$ is known, it is easy to show that the flow assignment for the next iteration is

$$\overrightarrow{x^{n+1}} = \overrightarrow{x^n} + \alpha\left(\overrightarrow{y} - \overrightarrow{x^n}\right) \tag{5}$$

where α is the step size. Since z is a convex function, when it reaches its maximum value, the differential of this function is equal to zero. In this way, α can be calculated from the following formula:

$$\frac{\partial}{\partial \alpha} z\left[\overrightarrow{x^n} + \alpha\left(\overrightarrow{y} - \overrightarrow{x^n}\right)\right] = 0 \tag{6}$$

To conclude, the convex combination algorithm can be stated as follows:

Step 0: Initialization. Load flow $\overrightarrow{x^1}$ onto the empty network according to $t_m^1 = t(0), \forall m$. Set $n = 1$.

Step 1: Direction search. Solve the approximate linear program (4a, 4b, 4c, 4d) to get descent direction $\overrightarrow{y} - \overrightarrow{x^n}$.

Step 2: Step size. Find α by solving

$$\frac{\partial}{\partial \alpha} z\left[\overrightarrow{x^n} + \alpha\left(\overrightarrow{y} - \overrightarrow{x^n}\right)\right] = 0 \tag{7}$$

Step 3: New flow. Set the flow $\overrightarrow{x^{n+1}} = \overrightarrow{x^n} + \alpha\left(\overrightarrow{y} - \overrightarrow{x^n}\right)$

Step 4: Convergence. If the stopping criteria $\left(\left|z\left(\overrightarrow{x^n}\right) - z\left(\overrightarrow{x^{n-1}}\right)\right| < 0.01\right)$ is satisfied, output $\overrightarrow{x^{n+1}}$; otherwise, set $n = n + 1$ and go back to step 1.

3 Algorithm

3.1 A Heuristic Method

In order to improve the road network in terms of congestion after attacks, our task is to deal with two critical issues. The first issue is to find the equilibrium vehicle flow in the traffic network under the assumption of UE. The convex combination method introduced in Sect. 2.3 works here to optimize the UE model. The second issue is to protect the network against supposed attacks, which will be discussed in this section.

To solve the second issue, we here propose the heuristic of identifying the arcs transporting the largest vehicle flow as the most critical links, and protecting them from attack. Specifically, the heuristic interdicts the unprotected link with maximum flow by deleting it from the original network; after multiple "vulnerable" links are identified in sequentially updated versions of the network, these deleted links are added back into the network but are considered to be invulnerable to attack.

The complete algorithm combines this heuristic method with the convex combination method. At each iteration, the heuristic assumes that terrorists will attack the link with maximum flow, as computed by the convex combination method, and removes this link from the original network. We define a set K which stores these vulnerable links temporarily. When a predetermined number of links have been interdicted, these deleted links are selected for protection, removed from K and put into a protection set Ω. The specific steps are listed below.

Step 0–1: Initialization. Set $j = 0$ and $\Omega = \emptyset$.
Step 0–2: Initialization. Set $l = 0$ and K = Ø.
Step 1: Attacks. Run the convex combination method to assign the equilibrium flow. Select the arc with maximum flow and remove it from the network. If there is more than one such arc, select randomly. If the selected arc is already an element of Ω, select the arc with the next highest flow to attack, etc. This selected arc is added into K.
Step 2: Set $l = l+1$ and go back to step 1, until l equals to u (where u is the predetermined number of arcs to be added to the set Ω per iteration).
Step 3: Set $\Omega = \Omega + K$. This is to add the links in K into the protection set Ω.
Step 4: Set $j = j + 1$ and return to step 0–2, until j equals to v (where v is a predetermined number of iterations).

4 An Illustrative Example

4.1 Data Description

We now apply our method to the Manhattan road network. From Fig. 2, we can tell that the Manhattan transportation network is a Cartesian grid. The Cartesian grid traffic network is common in U.S. cities. As a result, our research focuses on this kind of network. Since actual traffic flows are complicated, we simplify the network by focusing on a smaller region of ten avenues and ten streets (9 blocks by 9 blocks) around Times Square, as displayed in Fig. 3, and labeled as shown in Fig. 4. For simplicity, we further assume that the distance between any pair of adjacent nodes is 0.1 mile, and that all the streets are one-direction. The speed limit is taken to be 20 miles/h when there is no congestion. We assume that the relationship between the travel time and flow is quadratic in the form $t = b + cx^2$. When $x = 0$, the travel time is 0.1 miles divided by 20 miles/h, or 18 s per block. The congestion coefficient is assumed to be 0.05, so the congestion function is $t_m = 18 + 0.05x_m^2$.

Since Times Square is at the center of this network, we set a small square (three blocks by three blocks) as the center area, and assume 100 vehicles enter or exit from this area every minute. The corresponding origins or destinations for these O-D pairs are averagely located in our study area, i.e. Manhattan. Note that in this chapter we measure flow by volume per unit time and allow the flow on a specific arc to be fractional.

4.2 Measurement

This new approach is expected to protect some important streets so as to reduce the impact of attacks. Based on this goal, the performance of this method can be measured as the improvement in overall cost (i.e., travel time) compared to the overall cost of the unprotected network:

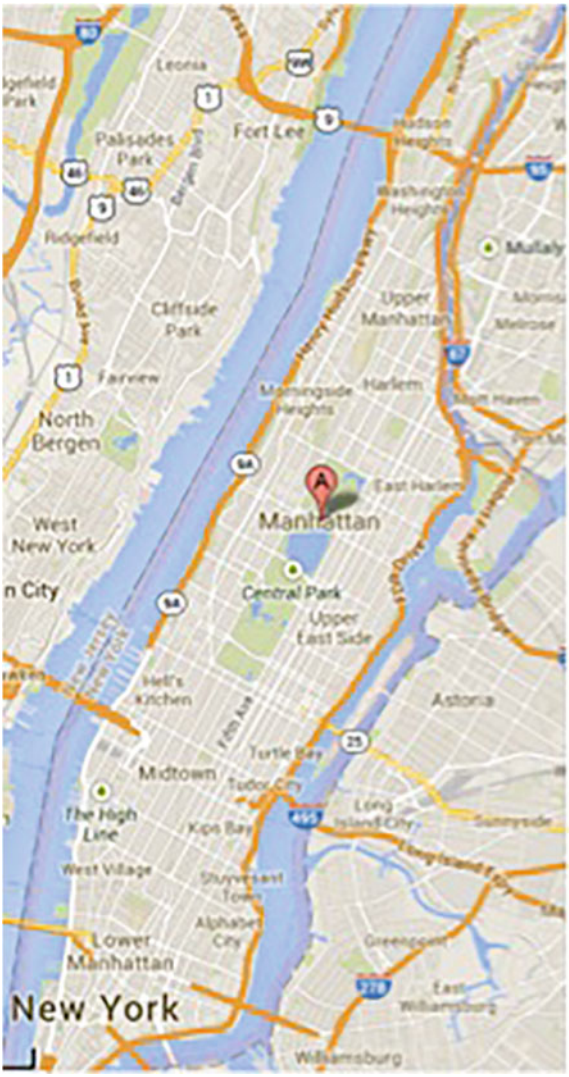

Fig. 2 Overview of Manhattan

$$improvement = -\frac{(c_2 - c_0) - (c_1 - c_0)}{c_1 - c_0} \tag{8}$$

Here, c_2 is the expected system cost of the protected network after a random attack. c_1 is the expected cost of the corresponding unprotected network after a random attack, and c_0 is the cost of the original network without attacks.

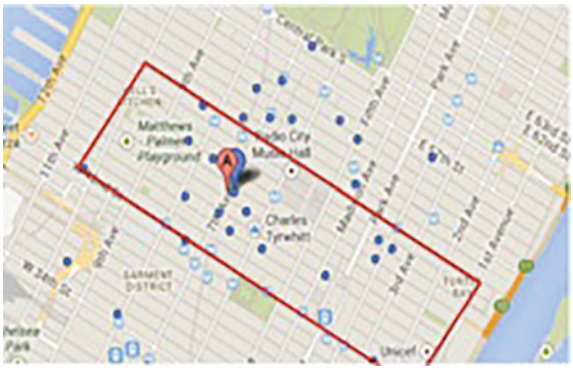

Fig. 3 Studied area

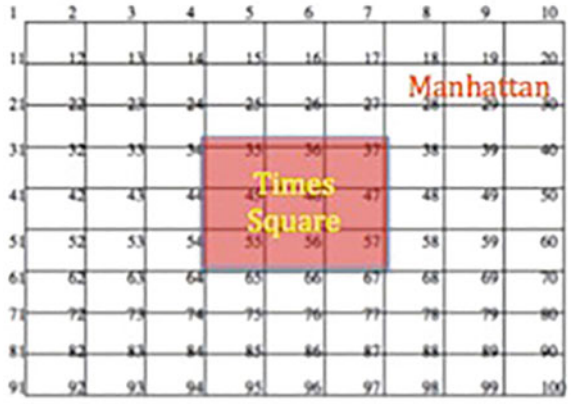

Fig. 4 Simplified network model

4.3 Result

MATLAB 2012b was used for our numerical experiments because of its advantages for matrix calculations. Input data consist of the network description and the O-D pairs. According to features of Manhattan, the network is a 10×10 grid, with one business center, one-way streets, and 100 vehicles entering and exiting from the network every minute. The network is represented by a connectivity matrix, where a value of 1 in the *i, j* element means that a link connects nodes *i* and *j*. O-D pairs are stored in an $n \times 2$ matrix whose first column is origins and second column is destinations. The experiment is implemented on a platform with Intel Xeon at 3.06 GHz.

We set four iterations for our method, and in each iteration identify the four links with maximum flow to be interdicted. The Lion-XC system takes about 10 h to calculate the 16 links that need to be protected. They are listed in Table 2, and highlighted in red in Fig. 5. Since our algorithm is built on the assumption of attackers' greedy strategy, the links with more flow are more likely to be selected as the critical links. From Fig. 5, we find these identified links are mainly distributed in

Table 2 Critical links

Link number	Link (node, node)
1	(34, 35)
2	(54, 55)
3	(14, 15)
4	(56, 66)
5	(56, 57)
6	(36, 37)
7	(16, 17)
8	(68, 78)
9	(45, 46)
10	(35, 45)
11	(65, 66)
12	(26, 36)
13	(45, 55)
14	(43, 53)
15	(47, 57)
16	(41, 51)

Fig. 5 Protected network

Times Square, which conforms to our anticipation and to our traditional view that a center area is more vulnerable than other areas.

We randomly attack five links of this network after the 16 links identified above are assumed to be protected, to test the effectiveness of our defense. After 100 replicates, we get an average improvement of 14.1 % in this network. (The standard deviation is 1.625 with 99 degrees of freedom, showing that we had enough replications.) Verified by t-test, the average is a good estimate, with statistical significant of 0.05 and t statistic of 0.875. This indicates that if we protect the critical links listed in Table 2, we can get roughly 14 % better performance than that of the unprotected network.

5 Numeric Experiments

In this section, we conduct two sets of numerical experiments, in order to get insights into the performance of our heuristic method. The first set of experiments explores the range of applicability of the method. The second set of experiments determines the relationship between vulnerability and defense of road networks.

5.1 Experiment 1

Our method may of course perform differently in different networks, even if we protect the same number of links. To explore the range of applicability, we therefore vary the networks along four dimensions:

1. Size (numbers of nodes and arcs).
2. Traffic flow (amount of travel between given O-D pairs).
3. Number of business centers in the network (assuming that most O-D pairs will have either an origin or a destination within a business center).
4. Directionality of streets (one-way or two-way).

In order to figure out which factors affect the performance of our method most significantly, we design a 2^{4-1} fractional factorial experiment and study a set of eight hypothetical urban traffic networks based on the example in Sect. 4. (As before, we consider only Cartesian grids, and every node except for boundary nodes is assumed to be linked with the four other closest nodes.)

The input parameters are listed in Table 3.

For convenience, the high value of each factor is coded as +, and the low value is coded as −. The resulting two-level fractional factorial design is shown in Table 4. This experiment provides sufficient information to estimate both main effects and two-factor interactions between the four factors.

Table 5 summarizes the analysis of variance for this experiment. Of the four factors we considered, size appears to be the most significant factor influencing the

Table 3 Data of factors

Codes	Factor	Level	Data	Indication
A	Size	Low	10 × 10 nodes	Small
		High	20 × 20 nodes	Large
B	Flow	Low	100	Non-peak hour
		High	200	Peak hour
C	Center	Low	1	Single business center
		High	2	Multiple business centers
D	Directionality	Low	1-direction	One-way streets
		High	2-direction	Two-way streets

Table 4 Experimental design

Run	Size	Flow	Center	Directionality	Improvement (%)
1	−	−	−	−	14.1
2	+	−	−	+	2.3
3	−	+	−	+	22.3
4	+	+	−	−	6.8
5	−	−	+	+	11.8
6	+	−	+	−	4.3
7	−	+	+	−	22.9
8	+	+	+	+	4.7

Table 5 Analysis of variance for improvement (%)

Source	DF	Seq SS[a]	MS	F	p
Main effects	4	430.86	107.715	12.23	0.034
Size	1	351.13	351.13	39.87	**0.008**
Traffic flow	1	73.20	73.20	8.31	0.063
Business center	1	0.40	0.40	0.05	0.844
Directionality of streets	1	6.13	6.13	0.70	0.465
Residual error	3	26.42	8.81		
Total	7	457.28			

[a] Seq SS represents sequential sum of squares

performance of our algorithm. The p-values of all factors except size (highlighted in bold in the table) are larger than 5 %, suggesting that these factors don't affect the performance of our algorithm significantly.

These results indicate that our method is widely applicable to Cartesian grid networks with differing numbers of business centers, amounts of traffic, and street directionality. In terms of size, since we protect 16 links in both cases, the percentage of protected links in a large network (2.1 %) will obviously be lower than in a small network (8.9 %), so it makes sense that measured performance would be worse in large networks.

5.2 Experiment 2

Differing numbers of streets to be protected may of course also result in different levels of improvement. Therefore, in this experiment, we will vary the number of protected links, keeping the rest of the network constant.

We arbitrarily pick the third network in Table 4 as our study subject. This is a 10 × 10 road network, with one business center, 200 vehicles entering and exiting from the network every minute, and two-way streets. Protecting different numbers

Table 6 Improvement as a function of protection effort

Number of links protected	Percentage of protected links[a]	Improvement (%)	Improvement/percentage of protected links
8	4.44	12.7	2.86
16	8.89	22.3	2.51
24	13.33	34.1	2.56
32	17.78	45.7	2.57
40	22.22	56.4	2.54
60	33.33	68.1	2.04
80	44.44	74.5	1.68
100	55.56	86.4	1.56
120	66.67	89.7	1.35
140	77.78	94.1	1.21
162	100.00	100.0	1.00

[a] Percentage of protected links is calculated as the number of protected links divided the total number of links in the network (i.e., 180), times 100

of links, we get different effectiveness, as shown in Table 6. In this table, we also calculate the proportion of protected links and the benefit/cost ratio (improvement divided by proportion of protected links).

By plotting percent improvement as a function of percent defended in Fig. 6, the relationship is apparent. Below 25 % of links defended, the relationship is approximately linear. As the percentage of defended links increases, the improvement approaches 100 %, so the marginal benefit of additional protection effort must decrease.

Analyzing the data for less than 25 % of links protected in Minitab, Table 7 shows that the percentage of protection links is significantly related to the improvement achieved, with p-value = 0.000. The R-squared value of 99.9 % also shows the near-perfect linear relationship between protection and improvement, as illustrated in Fig. 7.

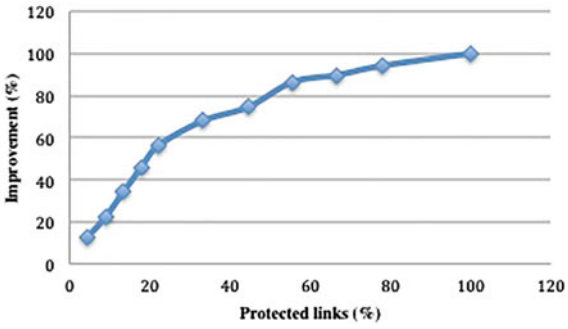

Fig. 6 Improvement effectiveness (%) versus protected links (%)

Table 7 Regression analysis of improvement as a function of protection effort

The regression equation is improvement (%) = 1.05 + 2.29 protected links (%)				
Predictor	Coefficient	SE Coefficient	t	p
Constant	1.0076	0.6903	1.46	0.240
Protected links (%)	2.49268	0.04683	53.22	0.000
S = 0.658319	R-Sq = 99.9 %	R-Sq (adj) = 99.9 %		

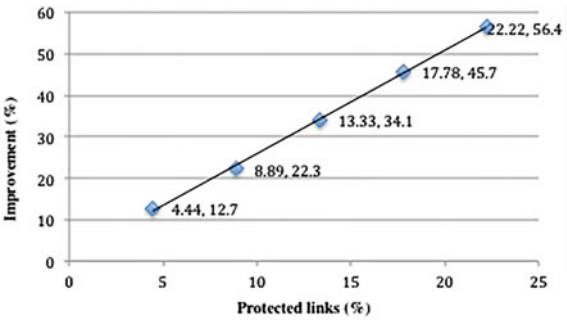

Fig. 7 Scatterplot of improvement (%) versus protection effort (%)

With this linear relationship, the government has to decide on the acceptable risk level and/or the available budget for protection, and can then get a near-optimal decision for this multiple-criteria decision making problem.

6 Conclusion

In this chapter, we developed a heuristic method to identify near-optimal defense strategies for a road network subject to congestion. In particular, when applied to a realistic-sized Cartesian grid-like network, we can significantly reduce the cost caused by attacks. For instance, in Manhattan, protecting 5 % of the total of 180 links in our network, the expected cost associated with an attack can be successfully reduced by 14 %.

Moreover, we designed a 2^{4-1} fractional factorial experiment to analyze the factors influencing the improvement achieved by the proposed method. The results show that factors such as traffic demand, the number of business centers, and street directionality (one-way or two-way) have much less impact on the performance of the method than the percentage of protected links. Therefore, keeping the other factors constant, we change the percentage of protected links, and find that the degree of improvement is almost perfectly linearly related to the percentage of secured links when that percentage is less than a threshold. Once the percentage exceeds that threshold, defending additional links becomes less effective.

In future research, we will extend our study by evaluating the effectiveness of protection against attacks that target the most heavily traveled arcs, rather than

random attacks. Moreover, more numerical tests can be conducted to examine how close to optimal our heuristic is and what can be done to improve the effectiveness and efficiency of heuristic. In addition, we may explore the problem along another direction by using an SO model to characterize the network traffic under attack, assuming that government agencies are able to respond to an attack rapidly enough and act as a central planner to control the traffic. It would be interesting to study the differences between that case and the UE model.

References

1. Beckmann M, McGuire CB, Winsten CB (1956) Studies in the economics of transportation. Yale University Press, New Haven
2. Bier VM, Hausken K (2013) Defending and attacking a network of two arcs subject to traffic congestion. Reliab Eng Syst Saf 112:214–224
3. Bier VM, Gratz ER, Haphuriwat NJ, Magua W, Wierzbicki KR (2007) Methodology for identifying near-optimal interdiction strategies for a power transmission system. Reliab Eng Syst Saf 92(9):1155–1161
4. Church RL, Scaparra MP (2007) Protecting critical assets: The r-interdiction median problem with fortification. Geog Anal 39(2):129–146
5. Feng C, Wen C (2003) Traffic control management for earthquake-raided area. J East Asia Soc Transp Stud 5:3261–3275
6. Florian M, Nguyen S (1976) An application and validation of equilibrium trip assignment methods. Transp Sci 10(4):374–390
7. Frank M, Wolfe P (1956) An algorithm for quadratic programming. Naval Res Logistics Q 3 (1–2):95–110
8. Friesz TL (2010) Dynamic optimization and differential games. International series in operations research and management science, vol 135. Springer, New York
9. Garcia CB, Zangwill WI (1981) Pathways to solutions, fixed points, and equilibria. Prentice-Hall, Michigan
10. Light Rail Now Project Team (2008) Nearly 3/4 of surface transport terror attacks involve personal motor vehicles—so US security officials focus on … trains? Retrieved 23 July 2014, from http://www.lightrailnow.org/
11. Murray-Tuite PM, Mahmassani HS (2004) Methodology for determining vulnerable links in a transportation network. Transp Res Rec J Transp Res Board 1882(1):88–96
12. Ng M, Park J, Waller T (2010) A hybrid bilevel model for the optimal shelter assignment in emergency evacuations. Comput Aided Civ Infrastruct Eng 25:547–556
13. Pang JS, Chan D (1982) Iterative methods for variational and complementarity problems. Math Program 24(1):284–313
14. Royset JO, Wood RK (2007) Solving the bi-objective maximum-flow network-interdiction problem. INFORMS J Comput 19(2):175–184
15. Scarf H (1967) The approximation of fixed points of a continuous mapping. SIAM J Appl Math 15(5):1328–1343
16. Sheffi Y (1985) Urban transportation networks: equilibrium analysis with mathematical programming methods. Prentice-Hall, Michigan
17. Todd MJ (1976) The computation of fixed points and applications. In: Lecture notes in economics and mathematical systems, vol 124. Springer, Berlin
18. Wardrop JG (1952) Some theoretical aspects of road traffic research. ICE Proc Eng Divisions 1 (3):325–362

Multiple Stakeholders in Road Pricing: A Game Theoretic Approach

Anthony E. Ohazulike, Georg Still, Walter Kern and Eric C. van Berkum

Abstract We investigate a game theoretic approach as an alternative to the standard multi-objective optimization models for road pricing. Assuming that various, partly conflicting traffic externalities (congestion, air pollution, noise, safety, etcetera) are represented by corresponding players acting on a common network, we obtain a non-cooperative game where each player pursues a different road pricing strategy to control a specific externality. The game is actually a Stackelberg game, but now with multiple leaders/actors in the upper level determining link tolls, and road users as followers in the lower level, adapting their route choice to the tolls imposed. This chapter reviews our earlier results on the game theoretic models, and the existence of Nash Equilibrium (NE). In order to cope with the fact that NE may not exist in the game, we propose a "*first-best taxation"* scheme, allowing the government to enforce pre-described NE (analogous first-best pricing schemes). We further discuss the stability of this taxing mechanism.

Keywords Road pricing game · Nash equilibrium · Multi-level optimization · Multi-objective optimization · Equilibrium problem with equilibrium conditions · Mechanism design

A.E. Ohazulike (✉) · G. Still · W. Kern
Faculty of Electrical Engineering, Mathematics and Computer Science,
Department of Applied Mathematics, University of Twente, Enschede,
The Netherlands
e-mail: a.e.ohazulike@alumnus.utwente.nl

G. Still
e-mail: g.still@utwente.nl

W. Kern
e-mail: w.kern@utwente.nl

A.E. Ohazulike · E.C. van Berkum
Faculty of Engineering Technology, Centre for Transport Studies,
University of Twente, Enschede, The Netherlands
e-mail: e.c.vanBerkum@utwente.nl

K. Hausken and J. Zhuang (eds.), *Game Theoretic Analysis of Congestion, Safety and Security*, Springer Series in Reliability Engineering,
DOI 10.1007/978-3-319-11674-7_7

1 Introduction

Over the past years, vehicle ownership has increased tremendously. It has been realized that the social cost of owning and driving a vehicle does not only include the purchase, fuel, and maintenance fees, but also the cost of man hour loss to congestion and road maintenance, costs of health issues resulting from accidents, exposure to poisonous compounds from exhaust pipes, and high noise level from vehicles. Therefore, routing traffic flow requires a model that optimizes several different objectives which may be in conflict with each other. Such model should also consider the user benefit. Optimization of more than one traffic externality has been considered by many authors. Road pricing that simultaneously treats time losses, increased fuel consumption, and emission is discussed in [7, 33]. Traffic congestion, air pollution and accident externalities are considered in [6]. Single- and bi-criteria Pareto optimization that deal with users with two objectives (time and money) and different values of time are studied in [4, 10, 34]. Road damage externality is incorporated in the road pricing models in [14]. Authors in [24] discuss a road charge design that includes multiple objectives and constraints. In particular, objective functions or constraints considered in [24] include social welfare improvement, revenue generation, and distributional equity impact.

All the models mentioned above are based on the idea of multi-objective optimization where one leader decides which point on the Pareto-front is chosen. They do not address issues arising when different stakeholders/autonomous cities with possibly conflicting objectives toll the road. There is need for such models since autonomy of states/cities or regions is increasingly becoming popular in the area of infrastructure or road management. In the literature, there are few works dealing with this subject: competition among stakeholders[1] with privately owned network aiming at maximizing their toll revenue is studied in [31, 35]. They formulate their problem as equilibrium problem with equilibrium constraints (EPEC). Both toll and capacity competition among private asymmetric roads with congestion in a network with parallel links are studied in [29]. In their paper, [3] analyse the allocative efficiency of private toll roads vis a vis free access and public toll road pricing on a network with two parallel routes connecting a common origin and destination. In one of their study regimes, they considered a mixed duopoly with a private road competing with a public toll road. On the other hand, tax competition on a parallel road network when different governments have tolling authority on the different links of the network is studied in [2]. The existence and efficiency of oligopoly equilibrium in a congested network with parallel roads, in which operators compete for traffic by simultaneous toll and capacity choices was studied in [9]. They establish sufficient conditions for the existence of a pure-strategy oligopoly equilibrium. In contrast to parallel network, road pricing in a serial network was studied in [12]. They use two links in series where private operators own one link each. The paper investigates the traffic patterns and pricing rules under various regimes of road operation in serial

[1] We use stakeholders, leaders and actors interchangeably.

networks. Further discussions on toll competition among operators of serial links can be found in [23, 26]. Authors in [28] also discuss toll and capacity competition among owners of private toll roads on general networks. In their work, they provide a theoretical proof of the existence of the constant *volume*/*capacity* (v/c) ratio property over general traffic networks. The effects of alternative pricing and investment policies on service level of cross-border transport infrastructure and economic welfare of two neighboring countries are studied in [13]. They show that the investment rule becomes efficient if infrastructure charge is levied. They established that this result holds for all regimes with charging, regardless of their differences in objective functions, financial constraints, and organization of decision units. Study of a bilateral monopoly situation on a private highway, involving strategic interactions between a private highway operator and a private transit operator who uses the same highway for its services can be found in [27].

The studies mentioned above assume that network or road segments are privately owned or managed by private stakeholders. Authors in [36] propose practical pricing schemes that can take into account competition and/or collaboration between different administrative regions of the network. Using numerical examples, they demonstrate that local/regional pricing may be beneficial or detrimental to the whole network, depending on the structure and O–D pattern of the network. They showed that cooperation among regions in congestion pricing can improve overall system performance in terms of total social welfare. However, they only consider competition among separate regions in a network. Furthermore, their results and findings are based on numerical examples. This motivated us to study the existence of Nash Equilibrium among competing stakeholders on the same network infrastructure [18]. To this end, we assume that private stakeholders (with possibly contradicting objectives) may influence the implementation of road pricing during policy making on one and the same network. With regards to their individual objectives, they propose tolls that may contradict the interests of others. In practice, it happens quite often that stakeholders with different interests jointly own the same network infrastructure. Our model thus generalizes the one of [36]. Again, how to incorporate road users' acceptability of road pricing has not yet been fully discussed in earlier literature; road users were modelled to have no say on the imposed tolls. Campaigns for the implementation of road pricing have failed in many cities like Edinburgh (in 2002), Trondheim (in 2005), New York (in 2008), Hong Kong (in 1986), as well as several cities in the Netherlands, due to lack of users support. This lack of support is a consequence of the fact that the debate on the implementation involves stakeholders with conflicting interests. Moreover, users are often not taken into consideration at the same level as stakeholders. In this chapter, we address these issues and formulate a general model that allows each stakeholder (including users) to partake in toll setting. We allow users' interest to be represented at the same level as the stakeholders (by making one stakeholder represent users' interest). In conformity with literature, our model shows that competition among stakeholders may deteriorate social welfare. To counter this effect, we design a

mechanism that induces a system optimal toll pattern among competing actors. In our model, tolls are used to maximize stakeholder's or system's social welfare and not to generate revenue. We assume that the tolls are reinvested into the transportation system so as to not increase the societal cost. Nevertheless, when a stakeholder's objective is to maximize his toll revenue, the model is still valid.

This chapter is an excerpt from our publications [16, 18]. The rest of the chapter is organized as follows: Sect. 2 gives the basic traffic model for our road pricing problem and extends the usual single leader single-objective road pricing to single leader multi-objective road pricing. Section 3 then extends the single leader to multi-leader multi-objective road pricing using a game theoretical approach, and further introduces the concept of Nash Equilibrium for the road pricing game as discussed in [18] and investigates the elastic demand case. In Sect. 4, we introduce the optimal Nash inducing mechanism which ensures that Nash Equilibrium exists, and that it coincides with system optimum. Finally, Sect. 5 concludes the chapter and opens up further research directions.

2 Basic Traffic Model for Road Pricing

2.1 Notations

Let $G = (N, A)$ be a network, with N the set of all nodes and A the set of (directed) arcs or links in G. We use the notations given in Table 1:

2.2 Single Leader Problem Formulation

2.2.1 Stakeholder's Problem

The stakeholder problem describes what the objective of a stakeholder is, and what the constraints and possible strategies are in achieving his objectives. We summarize the "tolling problem" for fixed demand, which each stakeholder k would like to solve as if he was the unique leader. We assume that each stakeholder controls a unique objective, and he wishes to minimize his own costs $C_k(v)$ under user flow and environmental feasibility conditions. We have also assumed a uni-modal model. Extending the result to a multimodal model is straightforward by adding a superscript on each flow related entity, parameter and/or variable to indicate the user class.

We will focus on fixed demand. The problem of stakeholder k can thus be stated as follows:

Table 1 Notations

A	Set of all arcs (links) in G
R	Set of all paths
W	Set of all OD pairs
f	Path flow vector
v	Vector of link flows
d	Travel demand vector
Γ	OD-path incident matrix
Λ	Arc-path incident matrix
$D(\lambda)$	Vector of demand functions
$B(d)$	Inverse demand (or benefit) function
λ_w	Least cost to transverse the wth OD pair
K	Set of all actors in the pricing game
C	Vector of actors' network cost functions
$Z(v)$	Total network cost i.e. $Z(v) = \sum_{k \in K} C_k(v)$
a	Index for links in G
r	Index for paths (routes)
w	Index for OD pairs
f_r,	Flow on path r
v_a	Flow on link a
d_w	Demand for the wth OD pair
R_w	Set of all paths connecting OD pair w
V	Set of feasible flow
D_w (λ_w)	Demand function for the wth OD pair
B_w (d_w)	Inverse demand function for the wth OD pair
$t(v)$	Vector of link travel time functions
k	Index for actors
$C_k(v)$	Objective with $C_k(v) = \sum_{a \in A} C_k^a(v_a)$

$$SP_k: \quad \min_{v} \; Z_k := C_k(v) \text{ s.t. } \left.\begin{array}{ll} v = \Lambda f & \psi \\ \Gamma f = \bar{d} & \lambda \\ f \geq 0 & \rho \end{array}\right\} \quad (FeC\_FD)$$
$$\left.\begin{array}{ll} g(v) \leq 0 & \xi \end{array}\right\} \quad Side\ Constraints(SC) \tag{1}$$

The first set of constraints is the flow feasibility conditions for fixed demand (*FeC_FD*); the first constraint states that the flow on a link is equal to the sum of all path flows that pass through this link, while the second equation states that the sum of flows on all paths originating from origin node p and ending at destination node q for an OD pair pq equals the demand $\bar{d}$ for this OD pair. The bar sign "–" indicates a fixed parameter. The third inequality simply states that the path flows

(and thus the link flows) are non-negative. We have also indicated the corresponding multipliers $(\psi,\ \lambda,\ \rho,\ \xi)$ in the Karush-Kuhn-Tucker (KKT) conditions (see Eq. 1). The last constraint $g(v) \leq 0$ (where $g(v)\ \epsilon \mathbb{R}^{|A|\times|K|}$) contains possible side constraints on the link flow vector v. These side constraints (which we assume to be convex or linear in v) may be standardization constraints such as:

The total emission on certain links should not exceed the stipulated emission standard.
The total noise level on certain links should not exceed the standard allowed dB (A) level.
The number of cars on certain roads should not exceed certain upper bounds, so as to preserve the pavements and check accidents, etcetera.

Assumption 1

- Throughout the chapter we assume that the link cost (or travel time) function vector $t(v)$ is continuous and satisfies $(t(v) - t(\bar{v}))^T(v - \bar{v}) > 0 \quad \forall v \neq \bar{v},\ v,\ \bar{v} \in V$ and all functions $C_k(v)$ are continuous, strictly convex, and strictly monotone (in the sense that $\partial C_k(v)/\partial v_a \geq 0 \quad \forall k, a$), and the side constraints $g(v) \leq 0$ [see Eq. (1)], if used, are linear.

Elastic demand can be modelled by subtracting the term $\gamma_k \sum_{w\epsilon W} \int_0^{d_w^k} B_w(\varsigma)d\varsigma$ in the objective of stakeholder k, where γ_k is a constant parameter that indicates how much user benefit actor k considers in his objective (see [18]).

2.3 Multi-objective Model (MO)

2.3.1 System Problem (SP)

In a standard MO model that considers all stakeholders, the system optimizer has to solve a program of type:

$$MO: \quad \min_v\ Z = \big(C_1(v),\ C_2(v),\ C_3(v),\ \ldots,\ C_{|K|}(v)\big) \quad \text{s.t. } FeC\_FD,\ SC \quad (2)$$

where the indices $1, 2, 3, \ldots, |K|$ refer to different objectives. More precisely, one has to find a point on the Pareto front of this program (see [8, 11]). In what follows we will consider the Pareto point given as the minimizer of the (special) MO program:

$$MO: \quad \min_v\ Z := \sum_{k\in K} C_k(v) \quad \text{s.t. } FeC\_FD,\ SC \quad (3)$$

Note that by choosing different weight factors for the objectives in the MO, we could model preferences for some externalities.

2.3.2 (Road) User Problem (UP)

Without loss of generality, we assume that the only determinant of user's route choice behaviour is the travel costs of a trip. Under Assumption 1, the well-known Beckmann's formulation [1] of Wardrop's user equilibrium (UE) describes the users' behaviour mathematically by the convex program:

$$UP: \quad \min_{v} \sum_{a \in A} \int_{0}^{v_a} \beta t_a(u) du \quad \text{s.t. } FeC\_FD \tag{4}$$

where β is the value of time (VOT). We consider homogeneous users only and assume a unity VOT β for simplicity.

2.4 First and Second-Best Pricing

To solve the toll pricing problem in the presence of a single leader, first and second best pricing techniques are mostly used. The theory behind road pricing is the theory of Stackelberg games where a leader (an actor) moves first, followed by sequential moves of other players (road users). The leader anticipates the followers move, and thus designs the tolls in such a way that the subsequent move by the followers will result in a flow pattern desired by this leader. For travelers, the generalized travel cost of making one trip on link a consists of the charged toll, θ_a, and the experienced travel time cost $\beta t_a(v_a) \geq 0$. The first-best pricing idea is based on a comparison between the KKT-conditions for MO and the KKT-conditions for UP. In general the first best prices are not unique. We summarize the result in the following corollary (see [15, 32] for a proof).

Corollary 1 *Suppose $\bar{v}$ is a solution for MO, then any social toll vector θ (with toll θ_a on link a) satisfying the following set of linear conditions is a toll such that $\bar{v}$ is also user equilibrium with respect to costs $\beta t(v) + \theta$:*

$$\begin{array}{l} \sum_{a \in A} (\beta t_a(\bar{v}_a) + \theta_a)\delta_{ar} \geq \lambda_w \quad \forall r \epsilon R_w, \forall w \epsilon W \\ \sum_{a \in A} (\beta t_a(\bar{v}_a) + \theta_a)\bar{v}_a = \sum_{w \in W} \bar{d}_w \lambda_w \end{array} \quad \text{or in short} \quad \begin{array}{l} \Lambda^T(\beta t(\bar{v}) + \theta) \geq \Gamma^T \lambda \\ (\beta t(\bar{v}) + \theta)^T \bar{v} = \bar{d}^T \lambda \end{array} \tag{5}$$

where λ is a free vector (of multipliers, see Eq. 1*) with components λ_w representing the minimum route travel cost for a given OD pair w. We will refer to* Eq. (5) *as equilibrium condition for fixed demand (EqC_FD). For elastic demand, the matrix form of* Eq. (5) *becomes*

$$\begin{aligned} \Lambda^T(\beta t(\bar{v}) + \theta) &\geq \Gamma^T B(\bar{d}) \\ (\beta t(\bar{v}) + \theta)^T \bar{v} &= B(\bar{d})^T \bar{d} \end{aligned} \tag{6}$$

where $B(d)$ is the vector of inverse demand functions with components $B_w(d_w)$ representing the inverse demand function for OD pair w. One of the possible tolls is given by the "first-best pricing" toll [15, 32]:

$$\bar{\theta} = \nabla \sum_k C_k(\bar{v}) - \beta t(\bar{v}) \tag{7}$$

where ∇ is the derivative with respect to v.

If there are extra conditions on the toll vector θ [e.g., some links $a \in Y$ are non-tollable $(\theta_a = 0)$] there might be no feasible first-best pricing toll. In this case one has to find a second-best pricing vector, and instead of a standard program MO, one has to solve the following program:

$$\min_{v,\theta} Z = \sum_k C_k(v) \quad \text{s.t} \quad \begin{array}{l} \Lambda^T(\beta t(v) + \theta) \geq \Gamma^T \lambda \\ (\beta t(v) + \theta)^T v = \bar{d}^T \lambda \\ \theta_a = 0 \quad \forall a \in Y \\ g(v) \leq 0 \\ FeC\_FD \end{array} \tag{8}$$

Note that the above "single level" program results from a bi-level program where the upper level solves the MO and the lower level solves the UE. In program (8), the objective is still the one from MO and the lower level UE problem is now replaced with an equilibrium condition (5) and the feasibility conditions. These conditions ensure that the solution of (8) is feasible and in user equilibrium.

3 Multi-leader Model in Road Pricing

In the foregoing models, we discussed a one-leader road pricing problem using the multi-objective (MO) program. Such models have their shortcomings; when one decision maker (*dm*), (e.g. the government or a private road owner), controls the traffic flow of a transportation system through road pricing, then it is likely that some other stakeholders affected by activities of transportation may not be happy with the decisions made by this *dm*. This is because when the *dm* models the MO road pricing problem, all traffic externalities are simultaneously considered with or without preference for any externality (see MO Eq. 3). When preference is given, say, to congestion, it may translate to huge costs for some other stakeholders. For example, lower travel time (say high speeds) may translate to more accidents (say costs for insurance companies). Even without preference for any externality, it is intuitive that stakeholders will still prefer to partake in toll setting to protect their interests.

The main problem of a classical approach from multi-objective optimization is the following: supposing that each stakeholder can influence the toll setting, why should an independent player accept a situation which he can improve by changing the tolls?

In such situation the classical concept of Nash Equilibrium in game theory gives an appropriate alternative model [18]. Such models are accepted in economics in situations where independent players may influence the market with their strategies in order to optimize their specific objectives.

The question we like to address from a game theoretical/economic point of view is: What happens when each stakeholder optimizes his objective by tolling the same network, given that other stakeholders are doing the same? Formally, we again introduce the mathematical and economic theory as given in [18].

3.1 Mathematical and Economic Theory

The Mathematical Program with Equilibrium Constraints (MPEC) [Eq. (8)] described in the previous section is a Stackelberg game where a leader (*dm*) moves first, followed by sequential moves of other players (road users). If we assume that various stakeholders are allowed to propose a toll (or at least influence the tolls) for a network, then users are influenced not only by just one leader as in Stackelberg game, but by more than one decision maker. In a multi-leader-multi-follower game/problem, the leaders take decisions (search for toll vectors $\theta^k,\ k \in K$, that optimize their respective objectives) at the upper level which influence the followers (users) at the lower level. The followers then react accordingly (user/Wardrop equilibrium), which in turn may cause the leaders to update their individual decisions leading to lower level players reactions again. These updates continue until a stable situation is reached. A stable state is reached if no stakeholder can improve his objective by unilaterally changing his proposed toll. Note however, that given the stable state decision tolls of leaders, the lower level stable situation is given by the (unique) Wardrop equilibrium. So the bi-level game can be seen as a single (upper) level game with additional equilibrium conditions (for the lower level).

In the above non-cooperative scenario, each actor continuously solves a *mathematical program with equilibrium conditions* which is influenced by other actors' *program with equilibrium conditions*, and this translates to an *equilibrium problem subject to equilibrium condition*. Since stable state upper level tolls will lead to a (unique) Wardrop's equilibrium at the lower level, our aim therefore is to find a Nash toll vector for the leaders (see Fig. 1).

After settling on a Nash toll vector, users represented in the upper level may search for an alternative but lower toll vector using Eq. (5).

Remark The theory described above does not necessarily mean that stakeholders have different toll collecting machines on the links. Our model describes the Nash toll vector that can be reached during policy making or debate when stakeholders choose not to form a grand coalition.

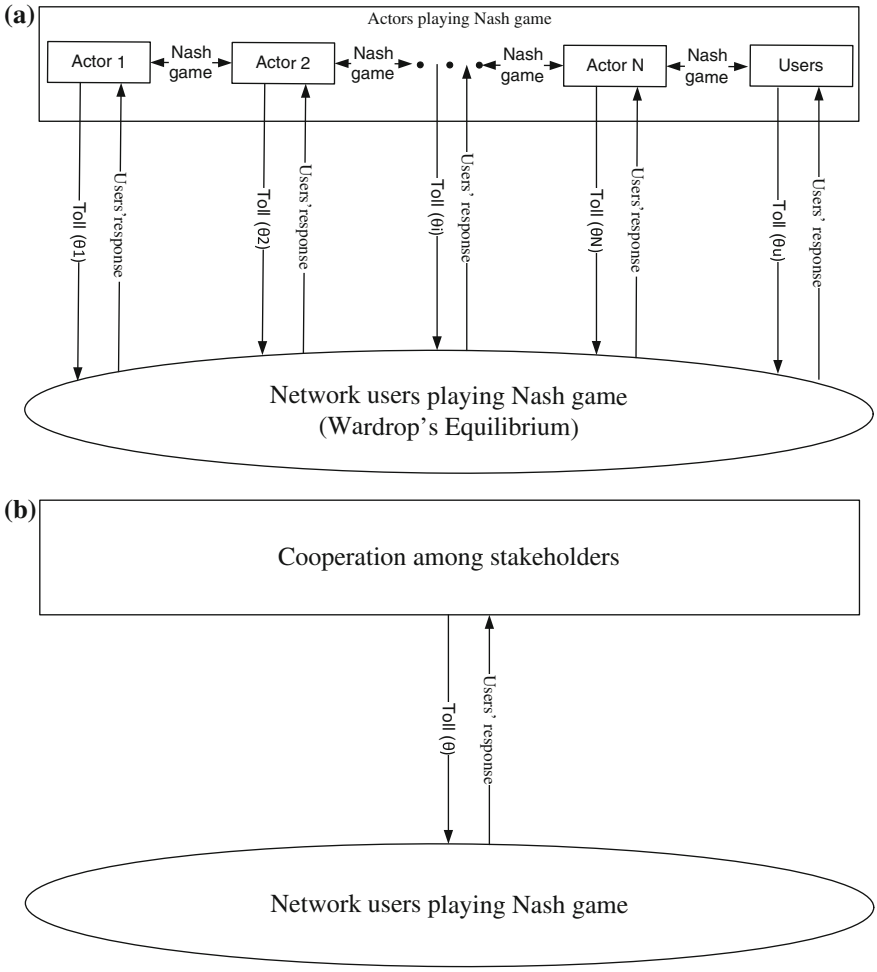

Fig. 1 **a** Non-cooperative and **b** cooperative road pricing game

3.2 Mathematical Models for the Bi-level Nash Equilibrium Game

Assume that Assumption 1 holds, so in particular the Wardrop equilibrium (WE) v is unique. Let θ^k be the link toll vector of player $k \in K$. We use θ^{-k} to denote all toll vectors in $K \backslash k$. In the Nash game, for given $\bar{\theta}^{-k}$, the kth stakeholder tries to find a solution toll $\bar{\theta}^k$ for the following problem:

$$\Psi_k\left(\bar{\theta}^k, \bar{\theta}^{-k}\right) = \min_{\theta^k} \ \Psi_k\left(\theta^k, \bar{\theta}^{-k}\right)$$

where for given θ^k (and $\bar{\theta}^{-k}$)

$$\begin{aligned} &\Psi_k(\theta^k, \bar{\theta}^{-k}) := \min_{v^k} \ Z_k = C_k(v^k) \quad \text{s.t} \\ &\Lambda^T\left(\beta t(v^k) + \theta^k + \sum_{j \in K \setminus k} \bar{\theta}^j\right) \geq \Gamma^T \lambda^k \qquad v^k = \Lambda f^k \\ &\left(\beta t(v^k) + \theta^k + \sum_{j \in K \setminus k} \bar{\theta}^j\right)^T v^k = \bar{d}^T \lambda^k \quad \text{and} \quad \begin{array}{l} \Gamma f^k = \bar{d} \\ f^k \geq 0 \\ (\theta^k \geq 0) \end{array} \end{aligned} \tag{9}$$

For an elastic demand model where actors and users take into account the consumer surplus, then system (9) is equivalent to:

$$\begin{aligned} &\Psi_k\left(\theta^k, \bar{\theta}^{-k}\right) := \max_{v^k} \ Z_k = \gamma_k \sum_{w \in W} \int_0^{d_w^k} B_w(\varsigma) d\varsigma - C_k(v^k) \quad \text{s.t} \\ &\Lambda^T\left(\beta t(v^k) + \theta^k + \sum_{j \in K \setminus k} \bar{\theta}^j\right) \geq \Gamma^T B(d^k) \qquad v^k = \Lambda f^k \\ &\left(\beta t(v^k) + \theta^k + \sum_{j \in K \setminus k} \bar{\theta}^j\right)^T v^k = B\left(d^k\right)^T d^k \quad \text{and} \quad \begin{array}{l} \Gamma f^k = d \\ f^k \geq 0 \\ \left(\theta^k \geq 0\right) \end{array} \end{aligned} \tag{10}$$

Note that in the optimization problem above, each leader k can only change his own link toll vector θ^k. The strategies $\bar{\theta}^j, j \neq k$ of the other leaders are fixed in $k's$ problem. The left hand constraints are the equilibrium conditions and the right ones are the feasibility conditions.

A pure Nash Equilibrium (NE) defines a situation where for fixed strategies $\bar{\theta}^{-k}$ of the opponent players, the best that player k can do is to stick to his own toll $\bar{\theta}^k$. A NE is thus a set of toll vectors $\bar{\theta} = \left(\bar{\theta}^k, k \in K\right)$ such that for each player k the following holds:

$$\Psi_k(\bar{\theta}^k, \bar{\theta}^{-k}) \leq \Psi_k(\theta^k, \bar{\theta}^{-k}) \quad \text{for all feasible tolls } \theta^k \text{ and all } k \in K \tag{11}$$

For numerical examples, an interested reader is referred to [16].

3.3 Existence of Nash Equilibrium

In game theory, it is often interesting to know if Nash Equilibrium (NE) exists for non-cooperative games, and how to find it if it exists. Further, it will also be appealing to know if coalitions leave the players better off. In our road pricing

game, NE translates to a tolling pattern that is stable among the stakeholders. Stability is used to mean a toll pattern where no stakeholder can improve his objective by changing his toll strategy given other players' toll pattern. If we can find a Nash toll pattern, then stakeholders can be presented with such a toll pattern since this will save them from time consuming debates and feelings of unfairness. Before we continue, we recall.

Assumption 1

- (*in* Sect. 2) We assume throughout that the link cost (or travel time) function vector $t(v)$ is continuous and satisfies $(t(v) - t(\bar{v}))^T(v - \bar{v}) > 0 \; \forall v \neq \bar{v}, \; v, \; \bar{v} \in V$ and all functions $C_k(v)$ are continuous, strictly convex, and strictly monotone (in the sense that $\partial C_k(v)/\partial v_a \geq 0 \, \forall k, a$), and the side constraints $g(v) \leq 0$ [see Eq. (1)], if used, are linear.

In this subsection, we investigate the existence of Nash Equilibrium (NE) in our tolling game. We show below that this simple standard Nash Equilibrium concept as described in the preceding section (see Eqs. 9 and 11) is not always applicable to the tolling problem. The main reason lies in the special structure of the problems $\Psi_k(\bar{\theta}^k, \bar{\theta}^{-k})$ in (9) leading to the following fact:

Fact: *Due to Assumption 1, for given vectors* $\bar{\theta}^k, k \in K$ *the corresponding solution* $(\bar{v}, \bar{\lambda})$ *of the system (9) (i.e., user equilibrium with respect to the costs* $[\beta t(v) + \sum_{j \epsilon K} \bar{\theta}^j]$*) is unique.* Therefore:

Assertion: *If* $\bar{\theta}$ *is a Nash Equilibrium toll vector, then all corresponding solution vectors* $\left(\bar{v}^k, \bar{\lambda}^k\right)$ *are identical for all actors, hence*

$$(\bar{v}^k, \bar{\lambda}^k) = (\bar{v}, \bar{\lambda}), \quad k \in K. \tag{12}$$

Proof Given that $\bar{\theta}^k$ solves problem (9) for all actors $k \in K$, then it means that at Nash Equilibrium, the link toll vector $\bar{\theta}$ is given by $\bar{\theta} = \sum_{k \in K} \bar{\theta}^k$, where $\bar{\theta}_a = \sum_{k \in K} \bar{\theta}_a^k, \; \forall a \in A$. Due to *Assumption* 1, this toll vector $\bar{\theta}$ yields a unique flow pattern $\bar{v}$ and unique minimum route cost $\bar{\lambda}$. Of course, the users do not differentiate the tolls (per actor k), what they experience is the total toll vector $\bar{\theta}$, and as such, the vector $\bar{\theta}$ (together with the travel time costs) determines the unique user/Wardrop's equilibrium flow $\bar{v}$ and unique cost $\bar{\lambda}$ for the system. □

3.4 Unrestricted Toll Values

From Eq. (12) we can directly deduce the following result.

Corollary 2 *Suppose the leaders can toll all links with no restrictions {no constraint* $\theta^k \geq 0$ *in [*Eq. (9)*)]}, then, for the tolling game, there does not exist a Nash*

Equilibrium in general for fixed and elastic demand cases. Moreover, for this game, there is no stable coalition among players.

Proof For fixed demand, recall that by Eq. (12) the vector $(\bar{v}, \bar{\lambda})$ are the same for all actors at Nash Equilibrium.

Assume that the actors' toll vector $\bar{\theta}$ is a Nash Equilibrium toll with $(\bar{v}, \bar{\lambda}, \bar{\theta}^k)$ the solution of player k. Under the fact that at least one of the players, say player ℓ, has a different ideal (or optimal) link flow $\tilde{v}^\ell$ in SP_k [see Eq. (1)] since players are assumed to have conflicting objectives, and by our discussion in Sect. 2.4 [see Eq. (7)], player ℓ can achieve this flow $(\tilde{v}^\ell)$ in $\Psi_\ell(\tilde{\theta}^\ell, \bar{\theta}^{-\ell})$ by choosing e.g., the first-best pricing toll

$$\tilde{\theta}^\ell = \nabla C_\ell(\tilde{v}^\ell) - \beta t(\tilde{v}^\ell) - \sum_{k \in K \setminus \ell} \bar{\theta}^k \tag{13}$$

Since at any turn of the game (assuming now it is player ℓ's turn to play), player ℓ can toll $\tilde{\theta}^\ell$ as in Eq. (13) leading to his ideal flow $\tilde{v}^\ell$ in SP_ℓ [Eq. (1)], clearly no Nash Equilibrium can be reached. Furthermore, since every actor ℓ can find a feasible $\tilde{\theta}^\ell$ as in (13), then there is no stable coalition among players since each actor $k \in K$ can always achieve SP_k on his own. □

A similar discussion clearly holds for the case of elastic demand. Note that a link component of the toll vector $\tilde{\theta}^\ell$ given in (13) may be negative. In the next subsection, we show that the result of Corollary 2 can be achieved even with restriction to non-negative tolls.

3.5 Restricted Toll Values

Corollary 3 *Even under the extra conditions* $\theta^k \geq 0$ *in* Eq. (9)*, there does not exist a Nash Equilibrium in general.*

Proof For a fixed demand model, we can always achieve a first-best pricing toll in Eq. (5) satisfying $\tilde{\theta}^\ell \geq 0$: To see this, note that any leader $\ell \in K$ has the following valid toll vectors as part of a whole polyhedron (see proof below) that achieve the ideal flow vector $\tilde{v}^\ell$ in system (1) for leader ℓ:

$$\tilde{\theta}^\ell = \left[\alpha(\nabla C_\ell(\tilde{v}^\ell)) - \beta t(\tilde{v}^\ell)\right] - \sum_{k \in K \setminus \ell} \bar{\theta}^k; \quad \text{where } \alpha > 0 \tag{14}$$

By making α large enough (in view that C_ℓ is strictly monotonically increasing—see *Assumption* 1) we can assure $\tilde{\theta}^\ell \geq 0$. Again as in Corollary 2, at any point in the

game, a player, say player ℓ, can toll $\tilde{\theta}^{\ell}$ as in (14) leading to his ideal flow $\tilde{v}^{\ell}$ in SP_{ℓ} [Eq. (1)], clearly no Nash Equilibrium can be reached even with $\tilde{\theta}^{\ell} \geq 0$. □

Proof of (14) Suppose $\tilde{v}^{\ell}$ is an ideal flow vector that solves (1) for player ℓ. Let θ^{ℓ} be the corresponding toll vector satisfying (5). By using the variational inequality transformation of the user equilibrium problem UE [30], it means that $\tilde{v}^{\ell}$ is a solution of the UP

$$\min_{v^{\ell}} \left(\beta t(\tilde{v}^{\ell}) + \theta^{\ell}\right)^{T} v^{\ell} \quad \text{s.t.} \quad v \in V \tag{15}$$

where $\beta t(v)$ is a vector of link travel time functions. Obviously $\tilde{v}^{\ell}$ also solves the following UP:

$$\min_{v^{\ell}} \alpha\left(\beta t(\tilde{v}^{\ell}) + \theta^{\ell}\right)^{T} v^{\ell} \quad \text{s.t.} \quad v \in V \quad \text{where } \alpha > 0 \tag{16}$$

but,

$$\begin{aligned} \alpha\left(\beta t(\tilde{v}^{\ell}) + \theta^{\ell}\right)^{T} v^{\ell} &= \left(\left(\beta t(\tilde{v}^{\ell}) + \theta^{\ell}\right) + (\alpha - 1)\left(\beta t(\tilde{v}^{\ell}) + \theta^{\ell}\right)\right)^{T} v^{\ell} \\ &= \left(\beta t(\tilde{v}^{\ell}) + \left[\theta^{\ell} + (\alpha - 1)\left(\beta t(\tilde{v}^{\ell}) + \theta^{\ell}\right)\right]\right)^{T} v^{\ell} \end{aligned}$$

this means that with θ^{ℓ}, any vector

$$\tilde{\theta}^{\ell} = \left[\theta^{\ell} + (\alpha - 1)\left(\beta t(\tilde{v}^{\ell}) + \theta^{\ell}\right)\right] = \alpha\left(\beta t(\tilde{v}^{\ell}) + \theta^{\ell}\right) - \beta t(\tilde{v})$$

is a valid toll vector as well. Recall that for one objective C^{ℓ}, the marginal social cost (MSC) toll given by [see also Eq. (7)]

$$\theta^{\ell} = \nabla C_{\ell}(\tilde{v}^{\ell}) - \beta t(\tilde{v}^{\ell})$$

is one toll vector that achieves the ideal flow vector $\tilde{v}^{\ell}$, therefore

$$\begin{aligned} \tilde{\theta}^{\ell} &= \alpha\left(\beta t(\tilde{v}^{\ell}) + \theta^{\ell}\right) - \beta t(\tilde{v}^{\ell}) = \alpha\left(\beta t(\tilde{v}^{\ell}) + \left(\nabla C_{\ell}(\tilde{v}^{\ell}) - \beta t(\tilde{v}^{\ell})\right)\right) - \beta t(\tilde{v}^{\ell}) \\ &= \alpha\left(\nabla C_{\ell}(\tilde{v}^{\ell})\right) - \beta t(\tilde{v}^{\ell}) \end{aligned}$$

In the presence of other actors' toll $\sum_{k \varepsilon K \setminus \ell} \bar{\theta}^{k}$, $\tilde{\theta}^{\ell}$ now becomes

$$\tilde{\theta}^{\ell} = \alpha(\nabla C_{\ell}(\tilde{v})) - \beta t(\tilde{v}) - \sum_{k \in K \setminus \ell} \bar{\theta}^{k}; \quad \text{where } \alpha > 0. \qquad \square$$

Equation (14) suggests that the tolls could grow infinitely large as a result of actors' move to achieve their ideal or optimal objective values (see the numerical example on the non-existence of NE in [16]). Such a high toll, though theoretically possible due to fixed demand, is, in fact, not realistic since high tolls may discourage some users from travelling or at least make them change their mode of transportation. This phenomenon is captured when demand is allowed to be elastic; when tolls are restricted to be non-negative, and demand assumed elastic, a very high toll pattern implies that OD demands will near zero, which in turn lowers the societal welfare or economic benefit of the actors as described in the actors' objectives. Further, from Eq. (6), we have that for any given flow pattern $(\hat{v}, \hat{d})$, the total network toll is given by

$$\theta^T \hat{v} = B(\hat{d})^T \hat{d} - \beta t(\hat{v}) \tag{17}$$

revealing that the link toll vector θ is bounded. Note that the boundedness of the tolls in elastic demand does not guarantee the existence of Nash Equilibrium (see Braess example below).

We emphasize that extra restrictions on the tolls θ^k may play in favour of the existence of a Nash Equilibrium as demonstrated in [16].

In general, what can we say about the existence of NE? A well-known theorem in game theory [25] states that a game has a Nash Equilibrium if the following conditions are met:

- the strategy sets for each player are compact and convex, and
- each player's cost function $\Psi_k(\theta^k, \bar{\theta}^{-k})$ is continuous and quasi-convex in his strategy θ^k.

However, in general, we cannot expect such a convexity property. Even the mostly used "system optimization" function, the travel time function, is in general not convex as we will show with an illustrative example (see Braess network example below).

Since we do not expect a Nash Equilibrium to exist in general for the road pricing game, it means that in practice, rational stakeholders or actors may never reach an agreement on a given toll pattern. This may be an indication why road pricing, even with its rich potentials in alleviating a lot of traffic externalities, is still unpopular among stakeholders and road users. In most countries, such as the United States (New York City in 2008) and The Netherlands (in 2011), the road pricing scheme was almost at implementation stages when the parliament withdrew the idea due to conflicts of interests.

3.6 Numerical Examples

3.6.1 The Braess Network Example

We use a well-known network to show that even for the total network travel time (objective), the function $\Psi_k(\bar{\theta}^k, \bar{\theta}^{-k})$ in general, may not be convex in the tolls (strategy set). Such a drawback is enough to imply non-existence of Nash Equilibrium (NE) in the road pricing game [25]. This shows that we do not expect NE in the road pricing game in general. The square labels numbered 1–5 (Fig. 2) are the unique link identities. The other labels are the costs a user encounters by using the links (for example, v_2 for *link* 2 and $v_4 - 0.5v_4^2$ for *link 4*, where v_i is the flow on link i). The fixed demand from node a to node d is 1. $\theta_i \in [0, 1]$ represents the toll on link i where $\theta_i = 0$, for $i \neq 1, 3$. For two classes of tolls, namely; $\theta_3 \leq \theta_1$ and $\theta_3 \geq \theta_1$ we derive the following user equilibrated flows v_i on the links:

for $\theta_3 \leq \theta_1$

if $\theta_3 \leq 0.5$, then $v_1 = v_5 = 0,\ v_2 = v_3 = v_4 = 1$
if $\theta_3 \geq 0.5$, then $v_1 = 0, v_2 = 1,\ v_3 = v_4 = 1 - (1 + 2(\theta_3 - 1))^{1/2},\ v_5 = (1 + 2(\theta_3 - 1))^{1/2}$.

for $\theta_3 \geq \theta_1$

if $\theta_3 \leq 0.5$, then $v_1 = (\theta_3 - \theta_1),\ v_2 = v_3 = 1 - (\theta_3 - \theta_1),\ v_4 = 1, v_5 = 0$
if $\theta_3 \geq 0.5$

$$v_1 = \begin{cases} (\theta_3 - \theta_1) & \text{if} \quad (\theta_3 - \theta_1) \leq 1 - (1 + 2(\theta_3 - 1))^{1/2} \\ 2 - 2(0.5 + 0.5\theta_1)^{1/2} & \text{otherwise} \end{cases}$$

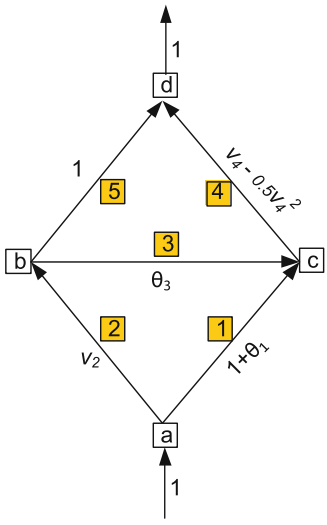

Fig. 2 Braess network

$$v_2 = \begin{cases} 1-(\theta_3-\theta_1) & \text{if } (\theta_3-\theta_1) \le 1-(1+2(\theta_3-1))^{1/2} \\ 2(0.5+0.5\theta_1)^{1/2}-1 & \text{otherwise} \end{cases}$$

$$v_3 = \begin{cases} 1-(1+2(\theta_3-1))^{1/2}-(\theta_3-\theta_1) & \text{if } (\theta_3-\theta_1) \le 1-(1+2(\theta_3-1))^{1/2} \\ 0 & \text{otherwise} \end{cases}$$

$$v_4 = \begin{cases} 1-(1+2(\theta_3-1))^{1/2} & \text{if } (\theta_3-\theta_1) \le 1-(1+2(\theta_3-1))^{1/2} \\ 2-2(0.5+0.5\theta_1)^{1/2} & \text{otherwise} \end{cases}$$

$$v_5 = \begin{cases} (1+2(\theta_3-1))^{1/2} & \text{if } (\theta_3-\theta_1) \le 1-(1+2(\theta_3-1))^{1/2} \\ 2(0.5+0.5\theta_1)^{1/2}-1 & \text{otherwise} \end{cases}$$

Let the tolls now satisfy $\theta_3 \ge \theta_1$ and $\theta_3 \ge 0.5$ and $(\theta_3-\theta_1) \le 1-(1+2(\theta_3-1))^{1/2}$, then the system travel time function $v^T t(v)$ is given by:

$$v^T t(\theta) = 1.5-(\theta_3-\theta_1)+(\theta_3-\theta_1)^2+0.5(1+2(\theta_3-1))^{1/2}-0.5(1+2(\theta_3-1)) + 0.5(1+2(\theta_3-1))^{3/2}$$

Note that we follow the traditional way of modelling travel time function in which the tolls are not optimized in $v^T t(v)$, so, for example, the travel time for the object $v^T t(v)$ on link 1 is $v_1(1+0) = v_1$, and that of link 3 is $v_3 \cdot 0 = 0$.

The Hessian of the travel time (TT) function $v^T t(\theta)$, H_{TT} given above is

$$H_{TT} = \begin{bmatrix} 2 & -2 \\ -2 & 2+\frac{3}{2}(1+2(\theta_3-1))^{-(1/2)}-\frac{1}{2}(1+2(\theta_3-1))^{-(3/2)} \end{bmatrix}$$

The major determinant of this matrix is negative if $\theta_3 \in \left(\frac{1}{2}, \frac{2}{3}\right)$, thus, we conclude that the travel time function $v^T t(v)$ is in general not convex in the strategy set $\{\theta_1, \theta_3\}$. So, a Nash Equilibrium may not exist for the road pricing game. This non-convexity property does not change even when other players' objectives are convex in their strategy sets [25].

3.7 *Solving General Multi-objective Problem Using the Game Model*

As a by-product of our game theoretic model for road pricing, it turns out that the proposed game model presents an alternative way to solve general multi-objective problems. The setup is as follows: (1) each objective is modelled as being controlled and optimized by one actor without changing other actors' chosen strategies, (2) as in road pricing game, actors optimize their objectives in turns, (3) each turn or move by the actors corresponds to an iteration, and each iteration results in a feasible solution, (4) solutions of all iterations are then plotted to display the

solution trend to Nash Equilibrium point. Note that Nash Equilibrium, in general, may not exist, or if it exists, may not be Pareto optimal.

Definition If for objective $k \in K$, $C_k(v)$ denotes the cost or objective function (to be minimized), then a solution vector $\bar{v} \in V$ dominates a solution vector $v \in V$ if and only if the following holds:

$$\begin{array}{ll} C_k(\bar{v}) \leq C_k(v) & \forall k \in K \quad \text{and} \\ C_j(\bar{v}) < C_j(v) & \text{for at least one } j \in K \end{array}$$

the solution $\bar{v} \in V$ is *Pareto optimal* if there does not exist any other solution vector $v \in V$ that dominates $\bar{v}$.

Definition A point is a Nash Equilibrium point if at this point, no player can improve his objective by unilaterally changing his strategy without deteriorating at least one of other players' objectives.

Since multi-objective problems usually have possibly many Pareto solutions, plotting the game iterations as described in step 4 above graphically displays the solution space of a multi-objective problem, aiding the policy makers to choose a solution point for implementation. The graphical display may show how far the NE point is from the Pareto optimal solutions.

In particular, the game approach can list Pareto optimal solutions of an MOP very fast in the game without depending on the prior definition of Pareto dominance. The fact that almost all known (genetic) algorithms for solving MOPs depend on *Pareto dominance* to generate non-dominated solutions makes it difficult to solve MOPs when the objective number exceeds four. The algorithms begin to deteriorate in efficiency as the objective number increases. The game mechanism we describe does not deteriorate with objective number, and has nothing to do with *Pareto dominance,* so it could be a promising tool for solving multi-objective problems. An interested reader is referred to [17] for comparison of the game approach with a genetic algorithm in solving MOPs.

3.8 Compromise Between Nash and Multi-objective (MO) Optimization

Assume that we have a concrete multi-leader tolling problem wherein the Nash Equilibrium exists. Can we find a "better" toll vector? Stakeholders can possibly improve the system welfare (by solving a modified MO) without deteriorating their individual utilities with reference to Nash outcome $\bar{v}$. On the other hand, if side payments are allowed, stakeholders will be better off cooperating or solving the MO (see Eq. 3). A possible model is given below: given the actors Nash Equilibrium flow pattern $\bar{v}$, the grand coalition game that guarantees every actor his Nash outcome is given by

$$\begin{aligned} &\min_{v} \; Z = \sum_{k \in K} C_k(v) \\ &\text{s.t} \\ &FeC\_FD \\ &C_k(v) \leq C_k(\bar{v}) \quad \forall k \epsilon K \end{aligned} \tag{18}$$

The objective minimizes the actors collective cost or the system cost. The first constraint contains the flow feasibility conditions [see Eq. (1)], and the second constraint ensures that no actor is worse off than in the Nash outcome $\bar{v}$. Since the Nash flow pattern $\bar{v}$ is a feasible solution for the above problem, it serves as an upper bound for the above problem. Given that $\breve{v}$ solves the MO above, then it is always profitable for the stakeholders to agree on the solution $\breve{v}$ of the above program (see [16]). Note that given this solution $\breve{v}$, a corresponding "first-best" pricing toll has to be chosen to induce $\breve{v}$ as a UE. If extra constraints on the tolls θ are present, then a second-best pricing approach can be used in the same way. Omitting the last constraint implies that some actors may be worse off than in the Nash game, making such a coalition unpopular, but then with side payments across the actors, the MO can guarantee each player his Nash outcome, and even more, additional benefits. This is always true since the total utility is optimal in the MO (Eq. 3). Similar and even more elaborate discussion on Pareto-improving congestion pricing can also be found in [5].

In the next section we propose a new way to combine the multi-objective model with NE concept and overcome the problem of non-existence studied in [18].

4 Optimal Nash Inducing Mechanism

We showed in our Sect. 3.3 that the existence of a NE cannot be guaranteed for the road pricing game. In practice such a phenomenon is not desirable since it makes the whole pricing game unstable. Further, even if Nash Equilibrium exists among the actors, the resulting flow may be far from (Pareto) optimal flow. Therefore the question we would like to answer is: Can we design a tolling game that yields a stable outcome for the actors? In this section we design a mechanism which induces a NE and even more returns the system optimal strategy as the optimal strategy for each actor. For this model we will assume that there exists a "grand leader (GL)" who has authority over all other leaders (by adding one more uppermost level in Fig. 1—see Fig. 3), and be seen as the central (or federal) government. His sole objective is to ensure (Pareto) optimal social welfare of the entire system. Since competition may lead to tolls that deteriorate the social welfare, and since it is not clear if there is a profit sharing rule that leaves grand coalition as the only stable coalition among the actors (the *core* of the game), we develop a mechanism that achieves efficient and desirable global outcome irrespective of what the actors do. This mechanism aligns the objective of each actor with that of the GL. Thus, actors

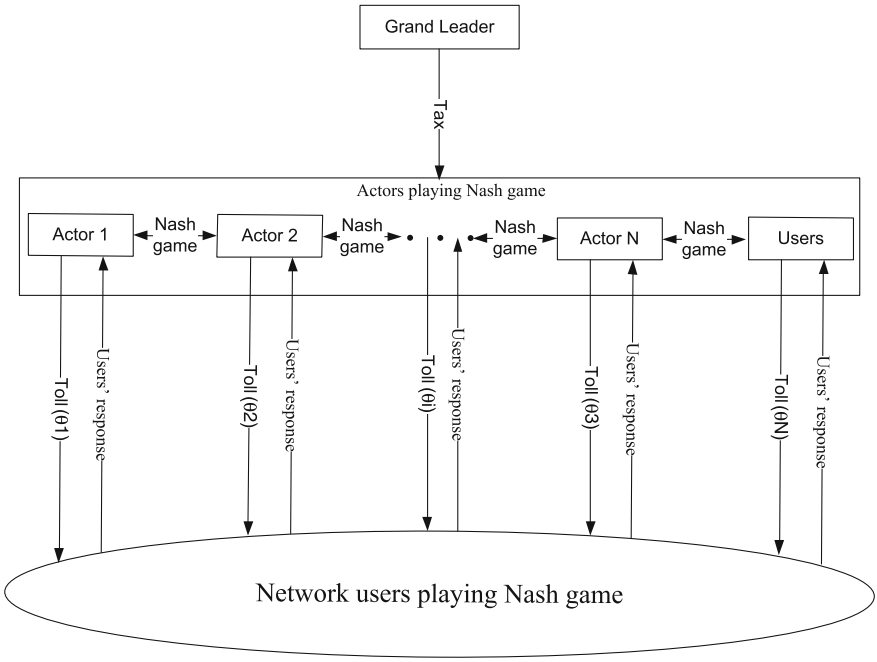

Fig. 3 Multi-level-multi-leader road pricing game

with once conflicting interests, now indirectly pursue common (GL's) interest. To achieve this goal, the mechanism uses taxing scheme to simultaneously induce a pure NE and cooperative behaviour among actors, thus, yielding tolls that are optimal for the system (Fig. 3).

We assume that the total revenue generated from the taxing scheme, just as the tolls (by the stakeholders), are invested back into the system. We also assume that the actors' utility functions are known to the GL. The tax can be seen as what an actor pays on the utility he enjoys for taking part in road pricing, which (the tax) depends on the flow pattern (and hence the toll pattern) proposed or chosen by this actor.

Recall that for any solution $\bar{v}$ of the models below, we can always choose a first-best pricing toll which ensures that $\bar{v}$ is UE.

4.1 Mathematical Formulation of the Mechanism

4.1.1 Grand Leader's Problem

Again for simplicity, we restrict ourselves to fixed origin-destination demands (extension to Elastic demand model is straightforward).

The GL problem is a multi-objective (grand coalition) optimization problem MO (see Eqs. 2 and 3) that searches for a flow pattern minimizing the stakeholders collective (or entire system) cost. Using the weighted sum method, we aggregate the objectives into one, converting it to a single objective optimization problem. Here we have used equal weights on the objectives. Note that the grand leader "*reserves the right"* to choose weights on the objectives as he deems socially equitable/profitable for the system. The formulation is as follows:

$$GL: \quad \min_{v} Z(v) = \sum_{k \in K} C_k(v) \quad s.t \quad \begin{matrix} v = \Lambda f & \psi \\ \Gamma f = \bar{d} & \lambda \\ f \geq 0 & \rho \end{matrix} \tag{19}$$

The constraints are the flow feasibility constraints and $\psi \in \mathbb{R}^{|A|}$, $\lambda \in \mathbb{R}^{|W|}$, $\rho \in \mathbb{R}^{|R|}$ are the *KKT* multipliers associated with the constraints.

Let L be the Lagrangian and $\bar{v}$ the solution to (19), then, there exists $(\bar{\psi}, \bar{\lambda}, \bar{\rho})$ such that the following *KKT optimality conditions* hold:

$$L = \sum_{k \in K} C_k(v) + (\Lambda f - v)^T \psi + (d - \Gamma f)^T \lambda - f^T \rho$$

$$\nabla_v L = \sum_{k \in K} \nabla C_k(\bar{v}) - \bar{\psi} = 0 \; or \; \frac{d}{d v_a} \sum_{k \in K} C_k^a(\bar{v}_a) - \bar{\psi}_a = 0 \quad \forall a \epsilon A \tag{20}$$

$$\nabla_f L = \Lambda^T \bar{\psi} - \Gamma^T \bar{\lambda} - \bar{\rho} = 0 \; or \; \sum_{a \in A} \bar{\psi}_a \delta_{ar} - \bar{\lambda}_w - \bar{\rho}_r = 0 \quad \forall r \epsilon R_w, \; \forall w \epsilon W \tag{21}$$

$$\begin{matrix} f^T \bar{\rho} = 0 \; or \; \bar{\rho}_r f_r = 0 \quad \forall r \epsilon R \\ \bar{\rho} \geq 0 \\ f \geq 0 \end{matrix} \tag{22}$$

Equation (22) is called complementarity equation.

4.1.2 Stakeholder's (or Actor's) Problem

Having shown that NE does not exist in general, we discuss a mechanism where the GL chooses appropriate taxes x^k, $k \in K$ that force the game into a NE. This taxing mechanism is as follows.

The GL penalizes (taxes) the kth actor by $v^T x^k$, where v^T is the transpose vector of link flows and $x^k \in \mathbb{R}^{|A|}$ is a leader specific constant tax vector. The tax term $\left(v^k\right)^T x^k$ should be seen as what actor k pays for proposing flow vector v^k (or toll pattern θ^k, since the flows v are toll dependent). We omit the superscript k on the flow vector of actor k since the actors' flows are identical at NE [18].

Now for fixed tax x^k each of the stakeholders $k \in K$ solves the following optimization problem:

$$\min_{v} Z_k(v) = C_k(v) + v^T x^k \quad s.t \quad \begin{array}{ll} v = \Lambda f & \psi \\ \Gamma f = \bar{d} & \lambda \\ f \geq 0 & \rho \end{array} \tag{23}$$

Let L be the Lagrangian and $\tilde{v} = v^k$ the solution to (23), then, with appropriate (ψ, λ, ρ), the following *KKT conditions* hold:

$$L = C_k(v) + v^T x^k + (\Lambda f - v)^T \psi + (d - \Gamma f)^T \lambda \pm f^T \rho$$

$$\nabla_v L = \nabla C_k(\tilde{v}) + x^k - \psi = 0 \; or \; \tfrac{d}{dv_a} C_k^a(\tilde{v}_a) + x_a^k - \psi_a = 0 \quad \forall a \epsilon A \tag{24}$$

$$\nabla_f L = \Lambda^T \psi - \Gamma^T \lambda - \rho = 0 \; or \; \sum_{a \varepsilon A} \psi_a \delta_{ar} - \lambda_w - \rho_r = 0 \quad \forall r \epsilon R_w, \; \forall w \epsilon W \tag{25}$$

$$\begin{array}{l} f^T \rho = 0 \; or \; \rho_r f_r \quad \forall r \epsilon R \\ \rho \geq 0 \\ f \geq 0 \end{array} \tag{26}$$

Observe that the only difference between the GL's and the stakeholder's *KKT* conditions is in Eqs. (20) and (24). Now, the GL can choose taxes $x^k \; \forall k \in K$ such that the optimal strategies coincide with the optimal strategy $\bar{v}$ of GL. To force Eq. (24) to be exactly the same as Eq. (20), i.e.

$$\nabla C_k(v)|_{v=\tilde{v}} + x^k - \psi = \sum_{k \in K} \nabla C_k(v) \Big|_{v=\bar{v}} - \bar{\psi}$$

$$\Rightarrow x^k = \sum_{k \in K} \nabla C_k(v) \Big|_{v=\bar{v}} - \nabla C_k(v)|_{v=\tilde{v}} + \psi - \bar{\psi}$$

To achieve this, for each k we can choose the same flow $v^k = \tilde{v} = \bar{v}$ and $\psi = \bar{\psi}$, and choose the taxes

$$x^k = \sum_{l \in K \setminus k} \nabla C_l(v) \Big|_{\bar{v}} \tag{27}$$

Note that by the convexity assumptions on $C_k(v)$, the solutions $\bar{v}$ and $\tilde{v}$ of programs (19) and (23) are unique.

To summarize:

- By our construction, we have shown that if the GL chooses taxes $x^k \; \forall k \in K$ as in (27) then the solution strategies $v^k = \tilde{v}$ of the all stakeholders in (23) coincide with GL's solution $\bar{v}$ in (19).
- So, any toll vector $\bar{\theta}$ which induces $\bar{v}$ to be a UE can be chosen [e.g. the first-best toll given in (7)] by the first actor (say actor k). Since the flow $v^k = \tilde{v} = \bar{v}$ is

optimal for all actors, it then means that together with the taxes x^k the toll $\bar{\theta}$ is also optimal for other actors, and therefore is a cumulative NE toll in the Nash game of Sect. 3.2.

Remark Observe from Eq. (24) that a taxing scheme defined by the tax function $v^T x^k$ with

$$x^k = \bar{\psi} - \nabla C_k(v)|_{v=\bar{v}} \tag{28}$$

is also an optimal Nash inducing scheme, where $\bar{\psi}$ is as defined in grand leader's problem (19).

This means that with the taxes in (27) or (28), the objectives of the players are now aligned, and they now pursue common interest. This mechanism is analogous to the first-best pricing where a stakeholder, knowing road users reaction (user equilibrium), chooses a toll such that the user equilibrium coincides with his desired flow pattern. So, Eq. (27) could be called *first-best taxes*.

Interpretation of the taxes: Now we interpret the tax function $v^T x^k$ for actor $k \in K$. The term $\nabla C_l(v)$ in Eq. (27) measures how sensitive actor l*'s* objective is to changes in the link flow vector v. A high value of $\nabla C_l(v)$ means that the objective $C_l(v)$ of actor l is very sensitive to changes in link volumes, and a low value suggests otherwise. The whole term $\sum_{l \in K \backslash k} \nabla C_l(v)$ in (27) measures the cumulative change in the objectives (of actors $l \in K \backslash k$) with respective to a unit increase in the link flow. Consequently, the tax function $v^T x^k = v^T \left(\sum_{l \in K \backslash k} \nabla C_l(v) \right)$ for actor k measures the total change in other actors' objectives ($l \in K \backslash k$) when the link flow vector is increased at v. A large tax $v^T x^k$ on k means that actor k*'s* "optimal" choice of v contradicts to a large extent the interests of actors in $K \backslash k$. In fact, the tax function $v^T x^k$ is the marginal cost which actor $k \in K$ imposes on the system by not considering other actors' objectives during his choice of v. Therefore, by taxing actor k the quantity $v^T x^k$ we internalize in his objective the cost he imposes on other actors, and indirectly make him aware of other actors' objective. In this way, his choice for the link flow vector v or more precisely, his choice of θ^k inducing v is optimal for the system.

4.2 Flexible Taxing Scheme

It will be interesting to see if there are other taxing schemes [other than those defined in Eqs. (27) and (28)] that induce NE and system optimal behaviour among the actors. It turns out that as in the first-best tolls in (6), there are (possibly) infinitely many values for x^k in the taxing schemes $v^T x^k$ (other than those defined in

Eqs. 27 and 28) that induce optimal Nash. Using the *KKT optimality conditions* above, we state the following corollary

Corollary 4 *If $\tilde{v}$ is the optimal flow vector in (23) for actor $k \in K$, then the following holds:*

$$\begin{aligned} &\sum_{a\in A}\left(\frac{d}{dv_a}C_k^a(v_a)\Big|_{v_a=\tilde{v}_a}+x_a^k\right)\delta_{ar} = \lambda_w + \rho_r \geq \lambda_w \quad \forall r \in R_w,\ \forall w \in W \\ &\sum_{a\in A}\left(\frac{d}{dv_a}C_k^a(v_a)\Big|_{v_a=\tilde{v}_a}+x_a^k\right)\tilde{v}_a = \sum_{w\in W}\lambda_w \bar{d}_w \end{aligned} \tag{29}$$

condensed to

$$\begin{aligned} &\Lambda^T\left(\nabla C_k(v)|_{v=\tilde{v}}+x^k\right) \geq \Gamma^T\lambda \\ &\left(\nabla C_k(v)|_{v=\tilde{v}}+x^k\right)^T\tilde{v} = \bar{d}^T\lambda \end{aligned} \quad \text{for some } \lambda \geq 0 \tag{30}$$

Proof The proof follows the idea from the first-best toll as well as the proof for the alternative first-best pricing tolls given in [32]. □

The first line of Eq. (29) states that each leader $k \in K$ would want each road user to follow the route that minimizes his (user's) travel cost with respect to his (leader's) objective function. The second line balances the network travel cost (*w.r.t. k's* objective function). The following result on the *first-best taxes* is analogous to Corollary 1.

Corollary 5 *Suppose $\bar{v}$ solves the GL's problem (19), then any taxing scheme $v^T\breve{x}^k$ such that $\breve{x}^k$ satisfies the following linear conditions is an optimal Nash inducing taxing scheme on actor $k \in K$:*

$$\begin{aligned} &\Lambda^T\left(\nabla C_k(v)|_{v=\bar{v}}+\breve{x}^k\right) \geq \Gamma^T\lambda \\ &\left(\nabla C_k(v)|_{v=\bar{v}}+\breve{x}^k\right)^T\bar{v} = \bar{d}^T\lambda \end{aligned} \quad \text{for some } \lambda \geq 0 \tag{31}$$

where $\breve{x}^k$ may be different from x^k given in Eq. (30).

Proof The proof follows from Eq. (30). □

In particular, for example, actor k might wish to minimize "his tolls" by minimizing v^Tx subject to (31).

Remarks

1. Equations (27) and (28) directly satisfy condition (31).

2. By just knowing the objective $C_k(v)$ of stakeholder k, the flexible taxing scheme enables the grand leader (with a desired flow pattern $\bar{v}$) to determine x^k for stakeholder k (see Eq. 31); Eq. (27) requires that he knows other stakeholders objective, and Eq. (28) yields only one possible value for x^k. Also, any of the stakeholders can pull out of the road pricing scheme/game without altering the taxing model. The taxing mechanism can be compared with the usual social taxing scheme where taxes depend on income, and you only need to know one's income to compute the tax.

4.3 Coalition Among Leaders Under the Mechanism

In game theory and mechanism design, stability of solutions has always been of great interest. In this section, we would want to investigate how stable the optimal Nash inducing mechanism is. In particular, if side payments are allowed for the actors, we would like to know whether the actors will be better off forming coalitions than staying as a single player in the road pricing game under the taxing scheme described above.

It turns out that the Nash inducing scheme is stable (see Corollary 6). In particular, we prove that there is no coalition formed by actors that will lead to a better payoff than in the induced Nash scenario. We therefore state the following corollary:

Corollary 6 *With the taxing scheme described, there does not exist a coalition in which any of the actors is better off than in the induced Nash scenario.*

Proof Suppose such a coalition exists, say with a feasible flow vector $\hat{v}$ in which actor $k \in K$ is better off than in the Nash scenario, then, it simply contradicts the already established fact that the induced Nash flow vector $\bar{v} \neq \hat{v}$ is the optimal (idle) flow vector for all leaders under the taxing scheme. Hence, such a coalition does not exist. In fact, for an arbitrary coalition say of two leaders k and m:

Let

$$\tilde{C}_k(v) = C_k(v) + v^T x^k$$
$$\tilde{C}_m(v) = C_m(v) + v^T x^m$$

where

$$x^k = \sum_{l \in K \setminus k} \nabla C_l(v)\Big|_{v=\bar{v}}, \quad x^m = \sum_{l \in K \setminus m} \nabla C_l(v)\Big|_{v=\bar{v}}$$

as given in Eq. (27) and $\bar{v}$ is the GL solution (see Eq. (19)). After coalition, their objective function is

$$\tilde{C}_k(v) + \tilde{C}_m(v) = C_k(v) + C_m(v) + v^T(x^k + x^m) \tag{32}$$

□

Proof Given that $\tilde{v} \in V$ minimizes objective (32), then *KKT conditions* for the minimization problem differ from those of stakeholder's problem (Eq. 23) only in $\nabla_v L$ which is given by:

$$\nabla_v L = \nabla C_k(v)|_{v=\tilde{v}} + \nabla C_m(v)|_{v=\tilde{v}} + \sum_{l \in K \setminus k} \nabla C_l(v)\Big|_{v=\bar{v}} + \sum_{l \in K \setminus m} \nabla C_l(v)\Big|_{v=\bar{v}} - \psi = 0 \tag{33}$$

where $\bar{v}$ is the GL's optimal flow pattern. Since $\bar{\psi}$ exists for the GL's problem, then with $\psi = 2\bar{\psi}$, it means that $\tilde{v} = \bar{v}$ is a feasible solution for Eq. (33), and hence optimal (see Eq. 20). Therefore, for $\tilde{v} = \bar{v}$, Eq. (33) becomes

$$2\left(\sum_{l \in K} \nabla C_l(v)\Big|_{v=\bar{v}}\right) - 2\bar{\psi} = 0 \tag{34}$$

due to Eq. (20). □

In the taxing scheme described above, we assumed that we can toll all links without bounds. This is the so called first-best pricing scheme. In the next section, we discuss the taxing mechanism with toll constraints/bounds. It is worthwhile stating that when tolls are not allowed on some links (the so called second-best pricing scheme), we face even a harder problem.

4.4 Optimal Nash Inducing Scheme for Second-Best Pricing

Due to the practical flavour of the second-best road pricing scheme, where only a subset of the network links is allowed to be tolled, we establish in this subsection, results on the second-best scheme for the Nash Equilibrium inducing mechanism. In particular, we would want to know how robust our Nash inducing mechanism is when the tolls are constrained.

4.4.1 Unbounded Tolls

Here, we will see that the taxing scheme is also applicable when extra conditions on tolls are present and the first-best tolls are no longer feasible.

Grand leader's problem
Suppose we have the toll constraints $\theta_a \geq 0\ \forall a \in A$, $\theta_a = 0\ \forall a \in Y$, where $Y \subseteq A$. As a single-level non-linear program, the bi-level optimization problem (mathematical problem with equilibrium conditions—MPEC) can be reformulated as follows (see Eq. 8):

$$\min_{v,\theta,\lambda} \sum_{k \in K} C_k(v) \quad s.t \quad \begin{array}{l} \Lambda^T(\beta t(v) + \theta) \geq \Gamma^T \lambda \\ (\beta t(v) + \theta)^T v = \bar{d}^T \lambda \\ \lambda \geq 0 \\ \theta_a \geq 0\ \forall a \in A \\ \theta_a = 0\ \forall a \in Y \\ v \in V \end{array} \tag{35}$$

Stakeholder's problem
Each actor $k \in K$, instead of Eq. 23, now solves the following non-linear program (see system 10):

$$\min_{v,\theta^k,\lambda} Z_k(v) = C_k(v) + v^T x^k \quad s.t \quad \begin{array}{l} \Lambda^T \left[\beta t(v) + \left(\theta^k + \sum_{l \varepsilon K \backslash k} \bar{\theta}^l \right) \right] \geq \Gamma^T \lambda \\ \left[\beta t(v) + \left(\theta^k + \sum_{l \varepsilon K \backslash k} \bar{\theta}^l \right) \right]^T v = \bar{d}^T \lambda \\ \lambda \geq 0 \\ \theta_a^k \geq 0\ \forall a \in A \\ \theta_a^k = 0\ \forall a \in Y \\ v \in V \end{array} \tag{36}$$

If we compare the KKT conditions of systems (35) and (36) (under the assumption that solutions of (35) and (36) satisfy the KKT conditions), then as in subsection 4.1, we have the following:

- let $\bar{v}$ be the solution of program (35). If the GL chooses taxes x^k as in (27), then the $\bar{v}$ is also optimal for problem (36) for all stakeholders.

In fact, there is no problem arising from the extra conditions on tolls since system (36) holds for all $k \in K$, so the resulting toll vector $\theta = \sum_{k \epsilon K} \theta^k$ will satisfy $\theta_a = 0,\ \forall a \in Y$ (since $\theta_a^k = 0\ \forall a \in Y, \forall k \in K$).

Remarks The *GL's* optimal link toll vector $\bar{\theta}$ is a valid (cumulative) Nash toll vector for the actors (recall the optimal Nash inducing scheme), i.e., $\theta^k = \bar{\theta}$ and $\theta^l = 0$ for $l \neq k$ yield a NE (inducing flow $\bar{v}$).

One possible optimal toll vector for the actors is $\tilde{\theta}^k = \bar{\theta}$ and $\tilde{\theta}^l = 0\ \forall l \in K \backslash k$ assuming that actor k makes the first move (i.e. actor k is *player* 1). Though these optimal link tolls are not unique in general, *a toll vector* $\tilde{\theta}^k\ \forall k \in K$ *is Nash optimal*

for the actors if the cumulative Nash toll $\sum_{k\in K}\tilde{\theta}_a^k = \theta_a\ \forall a \in A$ *yields the unique flow vector* $\bar{v}$ *that solves the GL's problem* (35).

4.4.2 Bounded Tolls

We consider further constraints on the tolls, for example, upper bound constraints requiring that $\theta_a \leq \phi_a\ \forall a \in A$; with $\phi_a \in \mathbb{R}_+$. In this case, and for equity reasons, one may assume that each stakeholder has a link toll bound given by: $\phi_a^k = \frac{\phi_a}{|K|}$.

In fact, we make the following observation:

1. Any link toll vector $\bar{\theta}_a \leq \phi_a\ \forall a \in A$ that yields the unique flow vector $\bar{v}$ which solves the *GL's* problem (35) is also a valid Nash link toll vector for the actors, with

$$\sum_{k\in K}\tilde{\theta}_a^k = \bar{\theta}_a \quad \forall a \in A \tag{37}$$

   irrespective of how $\bar{\theta}_a$ is distributed among the actors.
2. The toll vectors $\tilde{\theta}$ in 1 are in general not unique. This means that a link toll outcome of the actors' Nash game may be optimal and at the same time not sum up to the pre-calculated *GL's* toll as in Eq. (37).
3. Again, though these link tolls are not unique in general, *a toll vector* $\tilde{\theta}^k\ \forall k \in K$ *is Nash optimal for the actors if the cumulative Nash toll* $\sum_{k\in K}\tilde{\theta}_a^k = \theta_a\ \forall a \in A$ *yields the unique flow vector* $\bar{v}$ *that solves the GL's problem* (35).

4.5 General Application of the Optimal Nash Equilibrium Inducing Mechanism

The optimal inducing mechanism can also be used to induce system optimal performance in the following scenarios:

1. Malicious nodes in car to car communication where cars exchange data/information within a limited time frame
   In telecommunication networks where cars equipped with sensors exchange (say) traffic and environmental information (such as weather, road closure, accidents and so on), it is assumed that "rational" cars will send a piece of information depending on what they get in return. This decision is made within a limited time since the cars are in motion and have limited radius of broadcast. This means that car "A" will "only" send valuable data to car "B" if car "A" gets some worthwhile data in return, and this of course may not be socially optimal, so using our mechanism, we can induce a system optimal data exchange among the cars by making the system optimal data exchange the optimal strategies for the cars [19–22].

2. Local authorities tolling separate regions of the network.
   As we explained in our taxing scheme, the GL now will be the federal government asking each local authorities to pay tax to the federal government based on the tolls they collect on these roads. But then, these taxes will be chosen in a way to induce optimal road tolls among these local authorities. The induced optimal tolls are such that the entire nation's network flow is optimized or at least enables the optimization of the GL's objective.
3. Energy producers in the energy market liberalization problem.
   Governments can force energy marketers to set prices that are socially desirable using the taxing scheme model. The government will tax marketers' profit in a way that if they try to maximize their profit, they will end up setting the socially desired price.
4. Agents in the principal-agents model. The principal will set tax on agents' salaries such that agents' optimal salary quotations will be the desired amount that the principal is willing to pay.
5. Internet providers in the providers-subscribers Internet price setting problem. As in 3.
6. Competition of firms over the same market shares. As in 3.
7. Employees that have flexibility on the number of workdays.
   The employer will set taxes based on the number of working hours such that when the employees try to maximize their net income, they will end up working exactly the number of working hours desired by the employer.

5 Concluding Remarks and Future Research

5.1 Contributions and Conclusion

We presented a game theoretical approach to solve the multi-objective road pricing including externalities other than congestion. Due to political and equity reasons, various stakeholders and/or regions may partake in toll setting on the same network infrastructure. We studied the existence of Nash Equilibrium (NE) for the road pricing game. Even when tolls may be bounded, we show that in many practical settings, NE need not exist. We also represent the road users' interest at the upper level and argue that such an idea can lead to better acceptance of road pricing schemes. Since actors cannot be forced to form the grand coalition, and since competition may deteriorate the social welfare, we develop a mechanism that simultaneously induces a pure NE and cooperative behaviour among actors, thus, yielding optimal tolls for the system. The road pricing game can be remodelled and be used as a fast tool for generating Pareto points for multi-objective problems. The chapter also sheds some light on how the models developed can be applied in other real life instances.

5.2 Research Extensions and Recommendations

Since the models used in this chapter centred on classical optimization formulations, the number of variables can grow large with large networks. This calls for efficient optimization heuristic algorithms for large networks. Since flat link charge alone as described in this chapter may not fully attribute an externality to a car, for example, emission costs, we will extend our models to a kilometre charge, which will then take care of the (current) taxes on gasoline, diesel and petrol. Furthermore, a working paper is extending the models of this chapter to multimodal settings and time dependent models.

References

1. Beckmann M, McGuire C, Winsten C (1955) Studies in the economics of transportation. Yale University Press, New Haven
2. De Borger B, Proost S, Van Dender K (2004) Congestion and tax competition in a parallel network. Eur Econ Rev 49(8):2013–2040
3. de Palma A, Lindsey R (2000) Private toll roads: competition under various ownership regimes. Ann Reg Sci 34(1):13–35
4. Guo X, Yang H (2009) User heterogeneity and bi-criteria system optimum. Transp Res Part B 43(4):379–390
5. Guo X, Yang H (2010) Pareto-improving congestion pricing and revenue refunding with multiple user classes. Transp Res Part B 44(8–9):972–982
6. Heaney Q, O'Mahony M, Gibbons E (1999) External costs associated with interregional transport. Transp Res Rec 1659(1):79–86
7. Johansson O (1997) Optimal road-pricing: simultaneous treatment of time losses, increased fuel consumption, and emissions. Transp Res Part D 2(2):77–87
8. Liu GP, Yang JB, Whidborne JF (2003) Multiobjective optimization and control. Research Studies Press Ltd, Hertfordshire
9. Liu TL, Chen J, Huang HJ (2011) Existence and efficiency of oligopoly equilibrium under toll and capacity competition. Transp Res Part E 47(6):908–919
10. Lu CC, Zhou X, Mahmassani H (2006) Variable toll pricing and heterogeneous users: model and solution algorithm for bicriterion dynamic traffic assignment problem. Transp Res Rec 1964(1):19–26
11. Mardle S, Miettinen KM (2000) Nonlinear multiobjective optimization, vol 51. Kluwer Academic Publishers, Massachusetts
12. Mun SI, Ahn KJ (2008) Road pricing in a serial network. J Transp Econ Policy (JTEP) 42 (3):367–395
13. Mun SI, Nakagawa S (2010) Pricing and investment of cross-border transport infrastructure. Reg Sci Urban Econ 40(4):228–240
14. Newbery DM (1988) Road damage externalities and road user charges. Econometrica 56 (2):295–316
15. Ohazulike AE (2009) Multi-objective road pricing problem: a cooperative and competitive bilevel optimization approach. Master thesis, University of Twente
16. Ohazulike AE (2014) Road pricing mechanisms. A game theoretic and multi-level approach. PhD thesis, University of Twente, Enschede

17. Ohazulike AE, Brands T (2013) Multi-objective optimization of traffic externalities using tolls: a comparison of genetic algorithm and game theoretical approach. In: 2013 IEEE congress on evolutionary computation. IEEE, New York, pp 2465–2472
18. Ohazulike AE, Still G, Kern W, Van Berkum EC (2012) Multi-stakeholder road pricing game: solution concepts. Int J Comput Math Sci World Acad Sci Eng Technol 6:1–12
19. Schwartz RS, Ohazulike AE, van Dijk HW, Scholten H (2011) Analysis of utility-based data dissemination approaches in VANETs. In: 4th international symposium on wireless vehicular communications (WIVEC 2011)—VTC 2011 fall. IEEE Vehicular Technology Society, San Francisco, pp 1–5. ISSN 1090-3038 ISBN 978-1-4244-8328-0
20. Schwartz R, Ohazulike A, Sommer C, Scholten H, Dressler F, Havinga P (2012) Fair and adaptive data dissemination for traffic information systems. In: Fourth IEEE vehicular networking conference 2012 (IEEE VNC 2012). IEEE Intelligent Transportation Systems Society, Seoul, pp 1–8. ISBN 978-1-4673-4996-3
21. Schwartz RS, Ohazulike AE, Scholten H (2012) Achieving data utility fairness in periodic dissemination for VANETs. In: IEEE 75th vehicular technology conference (VTC2012-Spring). IEEE Vehicular Technology Society, Yokohama, pp 1–5. ISSN 1550-2252, ISBN 978-1-4673-0989-9
22. Schwartz RS, Ohazulike AE, Sommer C, Scholten H, Dressler F, Havinga P (2014) On the applicability of fair and adaptive data dissemination in traffic information systems. Ad Hoc Netw 13:428–443
23. Small K, Verhoef E (2007) The economics of urban transportation, 2nd edn. Harwood Fundamentals of Pure and Applied Economics Series, Routledge
24. Sumalee A, Shepherd S, May A (2009) Road user charging design: dealing with multi-objectives and constraints. Transportation 36(2):167–186
25. Tan KK, Yu J, Yuan XZ (1995) Existence theorems of nash equilibria for non-cooperative n-person games. Int J Game Theory 24(3):217–222
26. Verhoef E (2007) Second-best road pricing through highway franchising. J Urban Econ 62:337–361
27. Wang JYT, Yang HAI, Verhoef ET (2004) Strategic interactions of bilateral monopoly on a private highway. Netw Spat Econ 4:203–235
28. Wu D, Yin Y, Yang H (2011) The independence of volume-capacity ratio of private toll roads in general networks. Transp Res Part B 45(1):96–101
29. Xiao F, Yang H, Han D (2007) Competition and efficiency of private toll roads. Transp Res Part B 41(3):292–308
30. Yang H, Huang HJ (2005) Mathematical and economic theory of road pricing. Elsevier, UK
31. Yang H, Xiao F, Huang H (2006) Competition and equilibria of private toll roads with elastic demand. In: Transportation Research Board 85th Annual Meeting
32. Yildirim MB, Hearn DW (2005) A first best toll pricing framework for variable demand traffic assignment problems. Transp Res Part B 39(8):659–678
33. Yin Y, Lawphongpanich S (2006) Internalizing emission externality on road networks. Transp Res Part D 11(4):292–301
34. Yin Y, Yang H (2004) Optimal tolls with a multiclass, bicriterion traffic network equilibrium. Transp Res Rec 1882(1):45–52
35. Zhang L, Levinson D (2005) Road pricing with autonomous links. Transp Res Record: J Transp Res Board 1932:147–155
36. Zhang X, Zhang HM, Huang HJ, Sun L, Tang TQ (2011) Competitive, cooperative and Stackelberg congestion pricing for multiple regions in transportation networks. Transportmetrica 7(4):297–320

Stackelberg and Inverse Stackelberg Road Pricing Games: State of the Art and Future Research

Kateřina Staňková and Alexander Boudewijn

Abstract Optimal toll design deals with the problem of determining toll which improves performance of a road traffic system. Noncooperative game theory is an excellent tool to investigate possible strategies to analyze such a problem, in which one has to take drivers' reaction to toll and consequent changes in the traffic flow into account. Depending on the toll structure, the problem may be formulated as a Stackelberg game (when toll is uniform or time-varying) or as an inverse Stackelberg game (when toll is traffic-flow dependent), with the road authority as the leader and drivers as followers. While the inverse Stackelberg approach is more complex to adopt, it has been shown in our previous work that in most situations it brings better outcome for the road authority. This chapter reviews existing results on this topic, discusses our recent case studies within this framework, develops new properties, and brings forward the open issues within this area.

Keywords Game theory · Second-best road pricing · Stackelberg games · Inverse Stackelberg games · Dynamic optimal toll design

1 Introduction

The subject of this chapter is the game of the dynamic optimal toll design problem played on a given road network, with the road authority as the leader and drivers in the road network as the followers. The aim of the road authority is to reach her (a priori defined) objective by setting tolls on a proper subset of the links, the so-called tollable links. The drivers make their travel decisions, taking the tolls into account.

There exists an extensive amount of literature dealing with the optimal toll design problem and impacts of toll on various performance criteria in the network [1–8]. The literature can be subdivided in research addressing the first-best and the

K. Staňková (✉) · A. Boudewijn
Department of Knowledge Engineering, Maastricht University, Maastricht, The Netherlands
e-mail: k.stankova@maastrichtuniversity.nl

K. Hausken and J. Zhuang (eds.), *Game Theoretic Analysis of Congestion, Safety and Security*, Springer Series in Reliability Engineering,
DOI 10.1007/978-3-319-11674-7_8

second-best optimal toll design problems. In the former problem, toll can be imposed on all the links of a given network, whereas only a proper subset of the links is tollable in the latter. While research addressing the first-best optimal toll design problem is focused on the structure of the optimal toll the research dealing with the second-best (dynamic) toll is mainly restricted to simulation examples. Exception is the research on static optimal toll design problem [8]. The optimal first-best toll was proven to be a function of the traffic flows in the network (although with rather strong restrictions). For the second-best optimal toll design problem, the first heuristics appeared rather recently, in [4, 9, 10]. These heuristics suggest that finding the optimal toll as a function of the traffic flows in the road network may improve the system performance remarkably (and will never lead to the worse performance than one would get with uniform toll).

The problem of finding the toll as a function of traffic flow fits within the framework of the so-called inverse Stackelberg games [9–11]. In the inverse Stackelberg game, the road authority calculates tolls as mappings of the traffic flows in the network, and therefore, the possible responses of the drivers are taken into account at the first place, while in the classical Stackelberg game the traffic-flow invariant toll is imposed first and the drivers react second [9, 12].

The inverse Stackelberg games are extensions of Stackelberg games [12, 13]. While the term "inverse Stackelberg games" is widely used in the existing literature [9, 11, 14–17] and captures the basis of these games very well, in some references different terms are used to refer to these games. In [12] these games can be found under term "incentives", while in [18] the term "reverse Stackelberg games:" is used. Since the notion of "incentives" was already used in the economical theory in a slightly different context[1] [19, 20], in this chapter we will confine ourselves to the standardly used term "inverse Stackelberg games".

The problem to find the optimal second-best toll is not a trivial one, as the optimal outcome for the road authority often cannot be reached and even if it can be reached, it might be impossible to compute it. Computation of the first-best outcome (i.e., the optimal toll value for the situation with all links tollable), if applicable, is often used to estimate what result one can reach with the second-best tolling. However, even if it was realistic to assume that the road authority knows the optimal first-best tolls, having this information does not necessarily help to estimate how close to this outcome one can get if only a limited number of links is tollable.

This chapter reviews existing results on this topic, discusses our recent case studies within this framework, develops new properties, and brings forward the open issues within this area. The optimal toll design problem is formulated in a general manner and on a general network, with only a few restrictions on the network properties and on the drivers' behavior. However, in the case studies we will confine ourselves to simple traffic models for which solution of the Stackelberg and inverse Stackelberg road pricing games can be found analytically and can therefore be easily verified. The same observations can be made using more

[1] In fact, for a subset of inverse Stackelberg problems.

complex models and therefore our conclusions are not restricted to simple models only. Similarly, while the results presented in this chapter are stated with route-based equilibria in mind [21, 22], they can be transformed to the problems with link-based equilibria as well [23, 24].

We will also explain surprising results and point out unresolved issues. For example, it is obvious that with more sophisticated toll choices one can get much better outcomes than with the standard toll, however using the complicated toll mechanisms might lead to exactly the same outcomes as using standard toll in some situations. Moreover, the idea that toll should increase with congestion to motivate drivers to use alternative links intuitively seems to hold, but we show that this needs not be the case.

This chapter is organized as follows. In Sect. 2 we formulate the standard game-theoretical model of the optimal toll design problem with the road authority as a leader and drivers as followers. In Sect. 3 we present our findings related to the problem properties and illustrate the problem solution procedure and its properties via examples. In Sect. 4 we will discuss what problems still remain to be solved within this area. Conclusions will be given in Sect. 5. Appendix 1 gives simple introduction to the Stackelberg and inverse Stackelberg games and Appendix 2 gives introduction to standard traffic models used to capture drivers' behavior.

2 Road Pricing Games

2.1 Motivation: Game Theory and Optimal Toll Design Problem

Given a traffic network defined as a collection of nodes, directed links, and set of origin-destination pairs, imposing tolls on a subset of the links in this network may improve its traffic performance remarkably. The traffic performance is evaluated via the objective function of the road authority who imposes the tolls. Such a function is commonly defined as the total travel time (time that all drivers spend when traveling from their origin to their destination), as a total toll revenue (money that all drivers spend), a linear combination of both, or for example reliability of the traffic system [5, 18].

Any update of the toll on any of the routes in the network might cause change of the drivers' behavior, while a change in drivers' behavior might call for toll update, as this should reflect the current traffic conditions. This is schematically depicted in Fig. 1. How would we look for the optimal toll on a given traffic network without mathematical modeling? Most probably we would try out different toll values on different links and observe how these tolls influence traffic behavior in our network. With each choice of tolls, we would have to wait until the situation becomes more less stable, i.e., until we get a behavioral pattern which does not change from day to day very much, as no traveler can improve her situation by unilateral change of her route. Instead of long-term observations, we use mathematical models to analyze

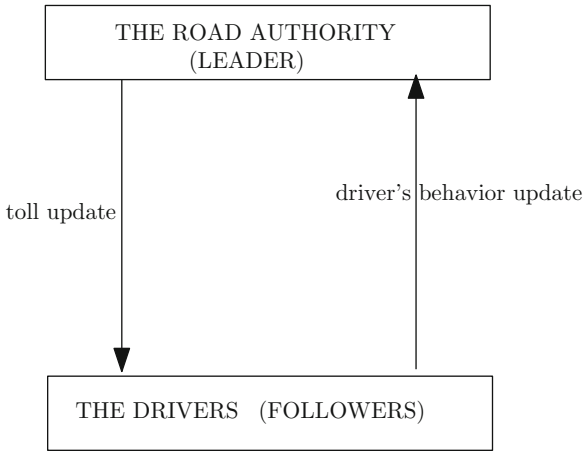

Fig. 1 The scheme of the game between the road authority and the drivers

different toll schemes. In these models, it is assumed that the drivers' behavior is in certain equilibrium [21, 25, 26] and we can analyze how the road authority should act in order to improve the system performance. With use of the equilibrium models of the drivers' behavior one can compute the optimal drivers' response to any toll choice and subsequently, we can compute an equilibrium situation between the road authority and the drivers. Game theory turns out to be an excellent tool to model and solve situations in which multiple parties interact with different, often conflicting, objectives [9, 12, 27–29].

If one assumes that all links in the network can be tolled (the so-called first-best tolling), while the optimal tolls can achieve negative values, the problem is rather easy to solve even for very complex traffic models, with both fixed and elastic (variable) traffic demand [30, 31]. Therefore, this chapter focuses on the situation in which only proper subset of links can be tolled (the so-called second-best pricing). While there exists a large body of literature focusing on finding solution to this problem via heuristic algorithms [4, 6, 32, 33], we would like to express how game theory can help to solve this problem and what general properties and phenomena one can observe when finding the optimal tolls using game-theoretic models. As we will express in detail below, we can formulate the optimal toll design problem as an inverse Stackelberg game (if tolls are defined explicitly as functions of past and current traffic flows) or as a Stackelberg games (if tolls are assumed to be constants for each time period). For basic introduction to these two types of games, see Appendix 1.

2.2 Preliminaries and Notation

Let $G = (\mathcal{N}, \mathcal{A})$ be a strongly connected road network, where $\mathcal{N}$ and $\mathcal{A}$ are finite nonempty sets of nodes and directed arcs (also called *directed links*), respectively. The set of tollable arcs will be denoted by $\mathcal{T} \subseteq \mathcal{A}$. There is a finite, nonempty set

of origin-destination pairs $\mathscr{RS} \subset \mathscr{N} \times \mathscr{N}$. Let the set $\mathscr{K} = \{1, 2, \ldots, |\mathscr{K}|\}$ be a time index set. Each$k \in \mathscr{K}$ refers to the interval $[(k-1)\Delta, k\,\Delta)$, where Δ [h] is the length of each time interval in hours. In this chapter we will confine ourselves to the fixed demand case, however the theory presented here also applies to the elastic (variable) demand case. Therefore, for an ordered pair of nodes (r, s), where r is an origin and s is a destination, there is a positive travel demand $d^{(r,s)}$ [veh] on the number of drivers traveling from r to s during the observed time period.

Let $\mathscr{P}$ be the set of all simple paths (i.e., paths without cycles) in the network and let $\mathscr{P}^{(r,s)} \subset \mathscr{P}$ be the set of all paths between an origin-destination pair (r, s). Each path is formed by one or more directed arcs.

The route flow rate[2] on path $p \in \mathscr{P}$ during the k-th time interval will be denoted by $f_p^{(k)}$ ([veh/h]), the arc flow rate on arc a during the k-th time interval will be denoted by $q_a^{(k)}$ ([veh/h]).

The route travel cost on the route $p \in \mathscr{P}$ for the travelers entering p during the k-th time interval will be denoted by $c_p^{(k)}$, the arc travel cost for the drivers entering a during the k-th time interval will be denoted by $\varsigma_a^{(k)}$ ([euro]).

The route and arc tolls, times, costs, and flows are related through a dynamic route-arc incidence indicator $\delta_{p,a}^{(k),(k')} \in \{0, 1\}$, which equals 1, if the travelers entering the route $p \in \mathscr{P}$ during the k-th time interval enter the arc a during the k'-th time interval, and 0 otherwise. We will assume that the route times, costs, and tolls are additive,[3] and that the flow conservation constraints hold, i.e.,

$$\theta_p^{(k)} = \sum_{k' \in \mathscr{K}} \sum_{a \in \mathscr{A}} \delta_{p,a}^{(k),(k')} \theta_a^{(k')}, \tag{1}$$

$$\tau_p^{(k)} = \sum_{k' \in \mathscr{K}} \sum_{a \in \mathscr{A}} \delta_{p,a}^{(k),(k')} t_a^{(k')}, \tag{2}$$

$$c_p^{(k)} = \sum_{k' \in \mathscr{K}} \sum_{a \in \mathscr{A}} \delta_{p,a}^{(k),(k')} \varsigma_a^{(k')}, \tag{3}$$

$$q_a^{(k')} = \sum_{k \in \mathscr{K}} \sum_{a \in \mathscr{A}} \delta_{p,a}^{(k),(k')} f_p^{(k)}, \tag{4}$$

where $\theta_p^{(k)}$ and $\tau_p^{(k)}$ are the total toll to be paid by travelers who are using the route p, entering this route during the k-th time interval, and the travel time of such travelers, respectively, and $t_a^{(k')}$ is the arc travel time of the drivers entering link a during the k'-th time interval. The link travel time is a function of the link flow on the same arc $q_a^{(k')}$.

---

[2] In the remainder of this paper we will use the term "route flow" instead of the "route flow rate".

[3] In reality, this does not need to be the case. For research dealing with non-additive costs, tolls, or flows we refer the reader to [34].

For each arc $a \in \mathscr{A}$, the arc travel cost $\varsigma_a^{(k)}$ for the k-th time interval is a linear combination of the actual arc travel time t_a and the actual arc toll θ_a with coefficients α [veh/h] and 1, i.e.,

$$\varsigma_a^{(k)} \stackrel{\text{def}}{=} \alpha\, t_a + \theta_a, \tag{5}$$

where α [euro/time unit] is called the value of time, which is supposed to be independent of $\mathbf{q}$.[4]

Let $\mathbf{q}$ denote the vector of all link flows in the network for all times, i.e., $\mathbf{q} \stackrel{\text{def}}{=} (q_1^{(1)}, \ldots, q_{|\mathscr{A}|}^{(1)}, q_1^{(2)}, \ldots q_{|\mathscr{A}|}^{(|\mathscr{K}|)})^T$. Similarly, let $\mathbf{c}$ be the vector of all route costs in the network for all times. For each link from $\mathscr{T}$ a traffic-flow dependent toll can be imposed. The traffic-flow dependent toll on link $a \in \mathscr{T}$ will be given by function $F_{\theta_a} : \mathbf{q} \to \mathbb{R}_+^0$. The traffic-flow dependent toll on all tollable links is then given by a vector function $F_{\theta_a} : \mathbf{q} \to \left(\mathbb{R}_+^0\right)^{|\mathscr{T}|}$. For each k-th time this toll is a function which maps past and current traffic flows in the network to a nonnegative number. Such a function can be very simple, such as a polynomial function of actual link flow on the same link, i.e.,

$$\theta_a = F_{\theta_a}\left(q_a^{(k)}\right) \stackrel{\text{def}}{=} \sum_{m=0}^{M} w_a^{(m),(k)} \left(q_a^{(k)}\right)^m, \tag{6}$$

where

$$w_a^{(m),(k)} \stackrel{\text{def}}{=} \begin{cases} 0 & \text{for} \quad a \in \mathscr{A} \setminus \mathscr{T}, \\ \in \mathbb{R} & \text{for} \quad a \in \mathscr{T}, \end{cases}, \qquad M \in \mathbb{N}_0. \tag{7}$$

There are of course other options for such a toll function. Moreover, a time-varying but traffic-flow independent toll is obviously a special case of (6) with $M = 0$.

2.3 Drivers' Behavior–Dynamic Traffic Assignment

A standard way to model the drivers' behavior is the so-called *dynamic traffic assignment (DTA) model*, which determines driver-optimal traffic flows over a network. The DTA model also has to take into account the dynamic rules according to which the traffic spreads. Therefore, the DTA model describes the drivers' optimal response to the current traffic conditions under the assumption that the

[4] There are various ways in which the route cost functions can be defined, another common way is based on a so-called generalized cost function, as described in [5]. In fact, any function which includes toll can be taken as a cost measure.

traffic dynamics follows certain rules (which are also included into the DTA model).

The DTA model consists of the *dynamic network loading* (DNL) model, which describes the dynamics of the traffic system, and the *dynamic travel choice* (DTC) model, which describes how the drivers make their travel decisions [21, 35]. Typical DNL and DTC models are described in Appendix 2. Without the loss of generality, in the beginning of the game the network is assumed to be empty.

2.4 Formulation of Road Pricing Games

Let Z denote the objective function of the road authority (to be minimized). Then the **inverse Stackelberg pricing game** is defined as follows:

$$(\mathrm{ISG})\begin{cases} \text{Find optimal toll function } F_\theta^* : \mathbf{q} \to (\mathbb{R}_0^+)^{|\mathscr{T}|} \text{ so that} \\ Z^{\mathrm{ISG}} = Z\big(\mathbf{q}^*, F_\theta^*(\mathbf{q}^*)\big) = \min\limits_{(\mathbf{q}, F_\theta(\mathbf{q}))} Z(\mathbf{q}, F_\theta(\mathbf{q})), \\ \text{where } \mathbf{q}^* \text{ is the vector of dynamic user equilibrium flows} \\ \text{with the tolls given by } F_\theta^*(\mathbf{q}) \end{cases} \tag{8}$$

Note that final toll values are then given by $F_\theta(\mathbf{q})$.

The "standard" **Stackelberg pricing game** is then defined as a subproblem of (ISG):

$$(SG)\begin{cases} \text{Find optimal toll vector } \theta^* \in (\mathbb{R}_0^+)^{|\mathscr{T}|} \text{ so that} \\ Z^{\mathrm{SG}} = Z(\mathbf{q}^*, \boldsymbol{\theta}^*) = \min\limits_{(\mathbf{q}, \boldsymbol{\theta})} Z(\mathbf{q}, \theta)), \\ \text{where } q^* \text{ is the vector of dynamic user equilibrium flows} \\ \text{with the tolls } \boldsymbol{\theta}^* \end{cases} \tag{9}$$

3 Main Properties of the Road Pricing Games

Note that Problems SG and ISG are nonlinear programming problems. Moreover, SG is a special case of ISG, thus most theory summarized in this section refers to ISG.

Definition 3.1 (*Admissible toll functions*) Function $F_\theta : \mathbf{q} \to (\mathbb{R}_0^+)^{|\mathscr{T}|}$ is an admissible toll function if it is continuous on $(\mathbb{R}_+^0)^{|\mathbf{q}|}$.

Proposition 3.1 (Existence of Z^{ISG}) *Suppose that for any given admissible F_θ there exists a unique vector* $\mathbf{q^o}$ *which is in dynamic user equilibrium. Let $D^{\max}$ denote the*

maximal travel demand for all origin-destination pairs, i.e., $D^{\max} \stackrel{\text{def}}{=} \max \{d^{(r,s)}\}_{\forall (r,s) \in \mathscr{R}\mathscr{S}}$, *and let* Z *be continuous on* $([0, D^{\max}])^{|\mathbf{q}|}$. *Then there exists an optimal* Z^{ISG} *value.*

Proof Any continuous function defined on a compact set S has a global minimum in S. The rest readily follows from the definition of ISG. □

The optimal value Z^{ISG} is referred to as the *team optimum* of the road authority. This value would be achieved if the drivers disregarded their own aims and helped the road authority minimize its objective function Z. As such, the existence of the optimal value Z^{ISG} does not assure the existence of toll mechanisms that achieve this outcome.

Proposition 3.2 (Uniqueness of Z^{ISG}) *Let there exist a problem DP dual to the dynamic user equilibrium (DUE) problem so that (DP) is a minimization of a real-valued convex function with respect to* $\mathbf{q}$ *(i.e., the DUE traffic flow vector solves DP). Let for any given admissible* F_θ *there exist a unique vector* $\mathbf{q^o}$ *which satisfies the dynamic user equilibrium. Let* Z *be continuous and convex on* $([0, D^{\max}])^{|\mathbf{q}|}$. *Then there exists a unique optimal value* $Z^{\text{ISG}} \stackrel{\text{def}}{=} Z(\mathbf{q}^*, \theta^*)$, *but optimal toll mapping* $F_{\boldsymbol{\theta}}$ *might be non-unique or might not exist at all.*

Proof If DUE can be written as a minimization of a convex function with respect to $\mathbf{q}$, then ISG can be formulated as a two-player static inverse Stackelberg game with convex costs. Moreover, if certain leader's toll function F_θ is a solution of the 2-player inverse Stackelberg game with follower's cost function defined on a $|\mathbf{q}|$–dimensional domain, then this leader's toll function is any surface tangent to the $|\mathbf{q}|$–dimensional level set of the follower's cost function at the $\mathbf{q}$-coordinates of the leader's team minimum. There are infinitely many such tangent surfaces, differing in their complexity (similarly as in Fig. 4 a linear tangent could be replaced by for example a quadratic surface tangent to the level curve of $\mathscr{J}_F$ at the team minimum coordinates). It might still happen that the optimal function F_θ does not exist, for example if the number of tollable links is too low compared to the total number of links. In such a case we cannot construct the tangent hyperplane of the level set of the follower's cost function at the $\mathbf{q}$-coordinates of the leader's team minimum. □

Note that it was proven in [34] that the static (Wardrop) user equilibrium satisfies the assumption of Proposition 3.2 regarding the existence of DP. Note also that any open-loop dynamic game can be converted into a static game and therefore Proposition 3.2 holds for a wide class of road pricing games with open-loop dynamic user equilibria, such as the logit-based stochastic user equilibrium or the deterministic dynamic user equilibrium [21].

Theorem 3.1 *Both problems (SG) and (ISG) are strongly NP-hard.*

Proof The proof follows from the fact that problem (SG) is a quadratic bilevel programming problem [36]. Even a static linear-linear variant (with linear cost

functions for the travelers and a linear objective function) of the SG problem was proven to be strongly NP-hard (see [5, 9, 37, 38]). Therefore, the problem ISG is strongly NP-hard, too. □

This theorem shows us that it is extremely hard to find the toll schemes that would be optimal. Often restricting ourselves for certain (low) number of parameters in toll scheme (which indicates number of tollable links for SG and number of parameters in toll function in ISG) might simplify the problem.

Proposition 3.3 (Tolls decreasing with traffic flow) *There exist ISG problems in which optimal tolls are decreasing with traffic flows.*

Proof Let us consider a simple example of a static optimal toll design problem on a network with three parallel links between one origin-destination pair, travelers driven by the Deterministic User Equilibrium (DUE), and the road authority minimizing the total travel time of the system. For the sake of simplicity both traffic demand for the origin-destination pair and value of time are normalized to one and the link cost and time functions are linear i.e.,

$$d = q_1 + q_2 + q_3, \tag{10}$$

$$\varsigma_1 = \alpha t_1(q_1) + \theta_1(q_1),\ \varsigma_2 = \alpha t_2(q_2) + \theta_2(q_2),\ \varsigma_3 = \alpha t_3(q_3), \tag{11}$$

$$t_1(q_1) = \beta_1 q_1 + \delta_1, t_2(q_2) = \beta_2 q_2 + \delta_2, t_3(q_3) = \beta_3 q_3 + \delta_3. \tag{12}$$

with $d = 1$, $\alpha = 1$, $\beta_1 = 1$, $\beta_2 = 2$, $\beta_3 = 0.05$, $\delta_1 = 1.008$, $\delta_2 = 0.672$, $\delta_3 = 2$. Then the total travel time function can be computed as

$$\begin{aligned} Z(q_1, q_2, q_3) &= \sum_{j=1}^{3} q_j t_j(q_j) \\ &= 1.05q_1^2 + 2.05\,q_2^2 - 1.092\,q_1 - 1.428q_2 + 2.05 + 0.1q_1\,q_2. \end{aligned} \tag{13}$$

The global minimum of $Z(q_1, q_2, q_3)$ is in $q_1^* = 0.504$, $q_2^* = 0.336$, $q_3^* = 0.16$ and $F(q_1^*, q_2^*, q_3^*) = 1.53$. This is what the road authority hopes to obtain.

Let us assume that the road authority calculates the tolls on links 1 and 2 as linear functions of the link flows on the same links, i.e., $\theta_1(q_1) = aq_1 + b$, $\theta_2(q_2) = a\,q_2 + b$, with $\theta_1(\cdot), \theta_2(\cdot) > 0$ on (0, 1). With DUE, $\varsigma_1 = \varsigma_2 = \varsigma_3$ holds if all three links are used. The following linear system has to be solved:

$$\beta_1 q_1^* + \delta_1 + aq_1^* + b = \beta_2 q_2^* + \delta_2 + aq_2^* + b \tag{14}$$

$$\beta_2 q_2^* + \delta_2 + aq_2^* + b = \beta_3 q_3^* + \delta_3, \tag{15}$$

The solution is $a = -1$, $b = 1$ Thus, if the road authority sets tolls on links 1 and 2 as

$$\theta_1(q_1) = 1 - q_1, \quad \theta_2(q_2) = 1 - q_2, \tag{16}$$

(q_1^*, q_2^*, q_3^*) is an optimal response of the travelers and the optimal value of the total travel time (team minimum) for the road authority will be reached. Obviously, we could construct similar example in a dynamic setting. □

Proposition 3.4 (Comparison of outcomes of ISG and SG) *Let* Z^{ISG} *denote the minimal value of the objective function with a toll function solving ISG and let* Z^{SG} *denote the corresponding minimal value of the objective function with toll solving SG. Then* $Z^{\mathrm{ISG}} \leq Z^{\mathrm{SG}}$

Proof This follows from definition of SG and ISG, where SG is a special case of ISG, and general properties of the inverse Stackelberg games. □

Note that for most problems $Z^{\mathrm{ISG}} < Z^{\mathrm{SG}}$ even with toll function being polynomial (6). Moreover, when having $|\mathscr{T}|$ tollable links, even when we restrict the number of parameters of toll function in ISG to $|\mathscr{T}|$, the inequality $Z^{\mathrm{ISG}} \leq Z^{\mathrm{SG}}$ will still hold.

Proposition 3.5 (Comparison of outcomes of ISG and SG 2) *For one origin-destination problems with linear link travel time function* $Z^{\mathrm{ISG}} = Z^{\mathrm{SG}}$.

Proof Follows from [9]. □

To summarize the theory presented in this section, we can show that ISG brings at least as good results as SG, even when we restrict toll functions to relatively simple schemes (and therefore we are looking for suboptimal solution of ISG).

Example 3.1 Let us consider the Beltway network in Fig. 2, with stochastic (logit-based) dynamic user equilibrium for the drivers. The set of origins $\mathscr{R}$ contains nodes from North, East, and West, while the set of destinations $\mathscr{S}$ comprises nodes from the south, $\mathscr{RS} = \mathscr{R} \times \mathscr{S}$. Therefore, there are 27 origin-destination pairs and 1357 routes in the network. The link speed $\vartheta_a^{(k)}$ [km/h] is given by the Smulders speed-density function [33]. All parameters of this case study coincide with those in [33].

The total travel time obtained with the first-best tolling is $1.3286 \cdot 10^4$[h]. The total travel time with no tolls is $1.6025 \cdot 10^4$[h]. In Table 1 you can see Z^{ISG} and Z^{SG} with different number of tolled links. For ISG we used polynomial tolls with degree equal to the number of tolled links. The total travel time will for sure change if we choose different links to toll, but it is obvious that the tolling improves the system performance and that the inverse Stackelberg based tolling outperforms the Stackelberg based tolling.

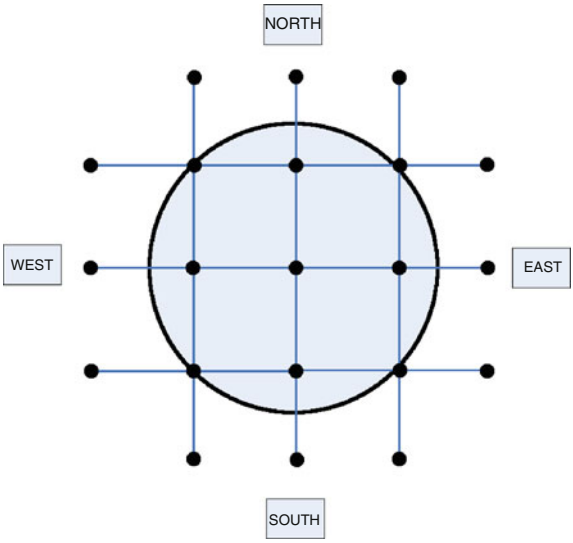

Fig. 2 Beltway network

Table 1 Comparison of SG and ISG results for case study on the Beltway network

Number of tolled links	Z^{SG} (h)	Z^{ISG} (h)
1	1.5999×10^4	1.5128×10^4
2	1.5379×10^4	1.4998×10^4
4	1.4877×10^4	1.4315×10^4
8	1.4435×10^4	1.3698×10^4

4 Solved and Open Problems

As shown in [5], even the optimal toll design problem with traffic-flow invariant tolls may lead to an objective function (of the road authority) which is very irregular, even non-smooth, and with multiple local extremes. Such a function may be very difficult to minimize by standard optimization techniques (e.g., gradient-based methods), as the risk of reaching a local minimum with such methods is rather high. Although for very specific objective functions (e.g., the convex functions) classical methods can find the solution of the SG and ISG problems (see [9, 10] for analytical solution of the ISG problem for networks with one original-destination pair, polynomial link travel times and tolls, and deterministic dynamic user equilibrium).

When solving a general inverse Stackelberg game, one first needs to determine the best possible outcome for the leader, the team optimum. This is impossible to obtain with very complicated DUE models and objective functions. In such a situation, it is better to look for sub-optimal solutions of ISG, assuming for example the toll function being defined by (6). In [18, 33, 39] such a toll was imposed on

various networks, including Beltway network. It has been shown that ISG toll outperformed SG toll remarkably. It remains to be seen how to resolve the ISG problem with F_θ not being given a priori, for nontrivial scenarios. It might, however, be sufficient to adopt a sub-optimal ISG toll instead, as this already gives excellent results. Moreover, with the toll defined by (6), the problem simplifies to finding optimal coefficients of a given function.

Regarding the simpler SG problems, it is still not clear how to determine the optimal toll values in general. Nevertheless, many heuristic methods have successfully been adopted to determine solutions.

Another issue which remains to be solved is how to select a set of m links to toll so that the performance of the system will be as good as possible, if m is a fixed number.

5 Conclusions and Future Research

In this chapter we dealt with optimal toll design problem with traffic flow-dependent second-best tolling from a game theoretic viewpoint. We discussed the properties of these problems in a general setting, illustrated our results by means of examples, and included solved and open issues in this area.

If the set of tollable links is restricted and the first-best system optimum cannot be reached, one can try to get as close as possible to this optimal value. It is clear that the inverse Stackelberg toll strategy can improve the system performance remarkably.

We showed some phenomena of inverse Stackelberg games when applied to the optimal toll design problem, e.g., that in some cases the toll on the tolled link might be decreasing with the link flow on the same link. If the flow-dependent toll is decreasing with the link flow, some very congested links remain untolled. This conclusion cannot be drawn with use of a traffic flow-invariant tolls.

Other question to be discussed is practical relevance of the proposed concept of the traffic-flow dependent tolls. Currently tested car devices using global positioning systems (GPS) which can "punish" the driver for certain route choices more, while giving the complete information about the costs of available routes, make our approach practically applicable.

Appendix 1: Basics of Stackelberg and Inverse Stackelberg Games

For the sake of simplicity we will outline here only static 2-player Stackelberg and inverse Stackelberg games. For more advanced introduction, see [9].

Players in these games are called *leader* and *follower*. The leader has the decision variable $u_L \in \mathscr{D}_L$, while the follower has the decision variable $u_F \in \mathscr{D}_F$, $\mathscr{D}_L$ and $\mathscr{D}_F$ are called the decision spaces of the leader and the follower, respectively. For the sake of clarity, let us assume that both $\mathscr{D}_L$ and $\mathscr{D}_F$ are real. Let us assumed that the leader and the follower have the real-valued cost functions $\mathscr{J}_L : \mathscr{D}_L \times \mathscr{D}_F \to \mathbb{R}$, $\mathscr{J}_F : \mathscr{D}_L \times \mathscr{D}_F \to \mathbb{R}$, respectively, which are known to both players. Each player wants to choose her decision variable in such a way as to minimize her own cost function. In a Stackelberg game, the leader announces her decision u_L, which is subsequently made known to the follower. Subsequently, the follower chooses u_F. Hence, u_F becomes a function of u_L, written as

$$u_F = \rho_F(u_L), \tag{17}$$

which is determined through the relation

$$\min_{u_F} \mathscr{J}_F(u_L, u_F) = \mathscr{J}_F(u_L, \rho_F(u_L)). \tag{18}$$

In (18) it is assumed that this minimum exists and that it is unique for each possible choice u_L of the leader. The function $\rho_F(\cdot)$ is sometimes called a *reaction function* of the follower. Before the leader announces her decision u_L, she will realize how the follower will react; hence, the leader will choose, and subsequently announce, u_L so as to minimize $\mathscr{J}_L(u_L, \rho_F(u_L))$.

Example 5.1 Let

$$\mathscr{J}_L(u_L, u_F) = u_L^2 + (u_F - 5)^2, \tag{19}$$

$$\mathscr{J}_F(u_L, u_F) = {u_L}^2 + {u_F}^2 - u_L\, u_F. \tag{20}$$

The reaction curve is given by $u_F = \rho_F(u_L) = \frac{1}{2} u_L$. Hence, the leader will choose u_L by minimizing

$$\mathscr{J}_L\left(u_L, \frac{1}{2}\, u_L\right), \tag{21}$$

which immediately results in $u_L = 2$. With this decision of the leader, the follower will choose $u_F = 1$. The costs for the leader and the follower are given by 20 and 3, respectively. In Fig. 3 the important contours of the leader's and the follower's cost functions and the reaction curve of the follower are depicted. Point $u_L = 1$, $u_F = 2$ is the closest point to the point $u_L = 5$, $u_F = 0$ lying on the reaction curve of the follower. □

Another concept, to be dealt with now, is the concept of *inverse Stackelberg game*, introduced in, e.g., [9, 11, 14]. Unlike in the Stackelberg game, the leader

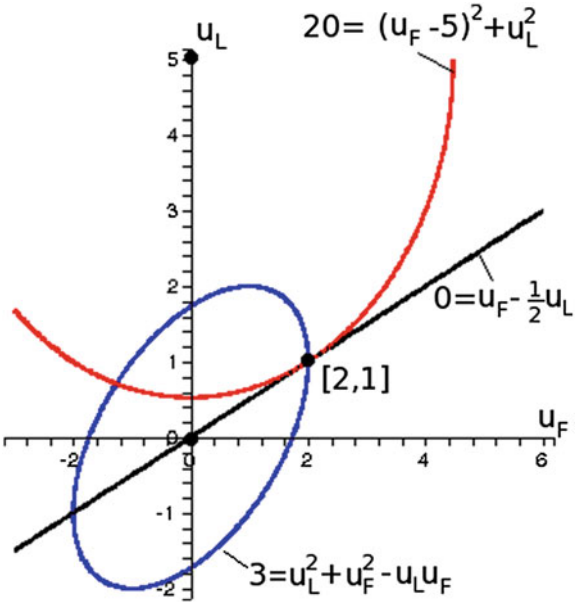

Fig. 3 Graphical illustration of the Stackelberg solution

does not announce the scalar u_L, as above, but a "decision rule" given by the function $\rho_L(\cdot) : \mathscr{D}_F \to \mathscr{D}_L$, instead.

Given the function $\rho_L(\cdot)$ (in [18] called leader's function), the follower will make his optimal choice u_F^* according to

$$u_F^* = \arg\min_{u_F} \mathscr{J}_F(\rho_L(u_F), u_F). \tag{22}$$

The leader, before announcing her $\rho_L(\cdot)$, will realize how the follower will play and he can exploit this knowledge in order to choose the best possible ρ_L-function, such that ultimately her own cost is minimized. Symbolically, we could write

$$\rho_L^*(\cdot) = \arg\min_{\rho_L(\cdot)} \mathscr{J}_L(\rho_L(u_F^*(\rho_L(\cdot))), u_F^*(\rho_L(\cdot))). \tag{23}$$

In this way one enters the realm of composed functions [40], which is known to be a notoriously complex area. It turns out to be difficult to find the optimal ρ_L function analytically. However, in the following example we will show a situation in which such a ρ_L can be found.

Example 5.2 Suppose the cost functions are those of the previous example and $\mathscr{D}_L = \mathscr{D}_F = \mathbb{R}$. If both the follower and the leader would be so kind as to minimize $\mathscr{J}_L(u_L, u_F)$, the follower totally disregarding his own cost function, the leader would obtain

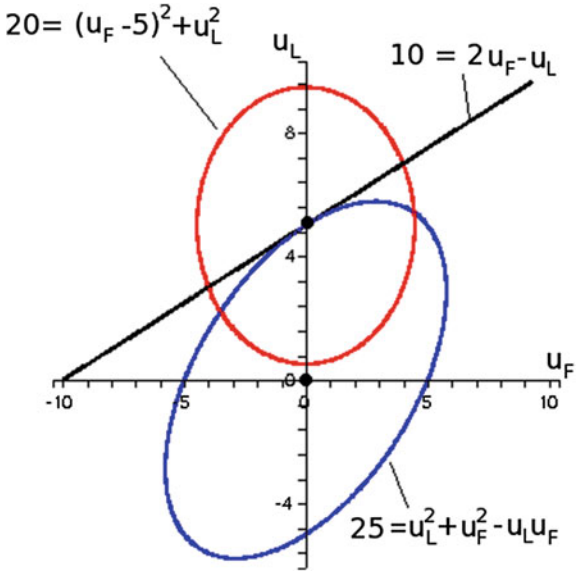

Fig. 4 Graphical illustration of the inverse Stackelberg solution

$$\min_{u_L, u_F} \mathscr{J}_L(u_L, u_F) = J_L(0, 5) = 0. \tag{24}$$

This value is called the team minimum. Now the lealignder should choose the curve $u_L = \rho_L(u_F)$ in such a way that the point $(u_L, u_F) = (0, 5)$ lies on this curve and, moreover, that this curve does not have other points in common with the set

$$\{(u_L, u_F) : \mathscr{J}_F(u_L, u_F) \leq \mathscr{J}_F(0, 5)\}. \tag{25}$$

To keep the problem simple a linear curve is chosen. Clearly, there exists only one line satisfying the required conditions and it is line

$$u_L = \rho_L(u_F) = 2u_F - 10. \tag{26}$$

With this choice of the leader, the best for the follower to do is to minimize

$$\mathscr{J}_F(2u_F - 10, u_F), \tag{27}$$

which leads to $u_F = 5$. The situation is depicted in Fig. 4. Hence $u_L = 0$ and, interestingly, the leader obtained his team minimum in spite of the fact that the follower minimized his own cost function (though with the constraint $u_L = 2u_F - 10$. The costs for the leader and the follower will be 0 and 25, respectively. Compared with the previous example, the leader is much better off ($0 < 20$) while the follower is worse off ($25 > 3$).

Notice that a "classical" Stackelberg game is a special case of an inverse Stackelberg game with $\rho_{\mathrm{L}}(\cdot)$ being constant.

In the dynamic setting, optimal leader's behavior is much more difficult to find than in the static setting and depends on the information that is available to both players. For more information about this, see [9, 12].

Appendix 2

Dynamic Network Loading (DNL) Model

The DNL model is formulated as a system of equations expressing link dynamics, flow conservation, flow propagation, and boundary constraints. The DNL model simulates the route flows in the network, yielding link flows, link volumes, and link travel times. Typically, the DNL model is defined by the following set of equations used in this paper is adapted from [35][5]:

$$v_{a,p}^{(r,s),\left(k+\tilde{t}_a^{(k)}\right)} = u_{a,p}^{(r,s),(k)} \tag{28}$$

$$u_{a,p}^{(r,s),(k)} = \begin{cases} q_p^{(r,s),(k)}, & \text{if } \quad a \text{ is the first link} \\ & \text{on path } p, \\ v_{a-,p}^{(r,s),(k)}, & \text{if } a- \text{ is the preceding link of} \\ & a. \end{cases} \tag{29}$$

$$u_a^{(k)} = \sum_{p \in \mathscr{P}} u_{a,p}^{(r,s),(k)} \tag{30}$$

$$v_a^{(k)} = \sum_{p \in \mathscr{P}} v_{a,p}^{(r,s),(k)} \tag{31}$$

$$x_a^{(k)} = \sum_{k' \leq k} \left(u_a^{(k')} - v_a^{(k')} \right) \Delta, \tag{32}$$

where $\tilde{t}_a^{(k)}$ is integer-valued. In addition, the link travel time function for the k-th time interval is a nondecreasing and link-specific function of the link volume on the link. Δ [h] is the time interval length.

Equation (28) is a *flow propagation* equation. It describes the propagation of the inflows $u_{a,p}^{(r,s),(k)}$ through the link and therefore it determines the outflows $v_{a,p}^{(r,s),(k)}$. Additionally, it relates the inflows and the outflows of link a at the k-th time interval

[5] Please note that inflows and outflows are expressed in terms of flows; the DNL model is implicit.

of vehicles traveling on route p from origin r to destination s. Variable $\tilde{t}_a^{(k)}$ is defined as follows:

$$\tilde{t}_a^{(k)} \stackrel{\text{def}}{=} \chi, \quad \text{if} \quad t_a^{(k)} \in [(\chi - 0.5, \chi + 0.5)\Delta). \tag{33}$$

Equation (29) describes the *flow conservation* conditions. If link a is the first link on route p, the inflow rate is equal to the corresponding route flows determined by the route choice model. If link a is not the first link on the route, then the inflow rate $u_{a,p}^{(r,s),(k)}$ is equal to the link outflow rate $v_{a-,p}^{(r,s),(k)}$ of the preceding link $a-$.

Equation (30) states that the total link inflows are determined by summing all link inflows for all routes that flow into link a at that time interval.

Equation (31) states that the total link outflows are determined by summing all link outflows for all routes that flow out of link a at that time interval.

Equation (32) defines the link volume $x_a^{(k)}$, i.e., the number of travelers present at the beginning of the k-th time interval on link a.

The interested reader is referred to [35] and [5], where the standard DNL model is introduced with a high level of detail.

Dynamic Travel Choice (DTC) Model

Each driver chooses her route from her origin to her destination in order to minimize her perceived travel costs.

The DTC determines how for all observed time intervals the drivers are distributed on all available routes in the network so that some specific dynamic user equilibrium (DUE) is achieved.

There are many different DUE models; for an explanation of the most important DUE models see, e.g., [21] or [5].

References

1. Arnott R, de Palma A, Lindsey R (1990) Economics of a bottleneck. J Urban Econ 27:11–30
2. Huang H, Yang H (1996) Optimal variable road-use pricing on a congested network of parallel routes with elastic demands. In: Proceedings of the 13th international symposium on the theory of flow and transportation, pp 479–500
3. Wie B, Tobin R (1998) Dynamic congestion pricing models for general traffic networks. Transp Res Part 32:313–327
4. Joksimovič D, Bliemer MCJ, Bovy PHL (2004) Optimal toll design problem in dynamic trafic networks-with joint route and departure time choice. Transp Res Rec 1923:61–72
5. Joksimovič D (2007) Dynamic bi-level optimal toll design approach for dynamic traffic networks. Ph.D. thesis, Delft University of Technology, Delft, The Netherlands
6. Verhoef ET (2002) Second-best congestion pricing in general networks. Heuristic algorithms for finding second-best optimal toll levels and toll points. Transp Res Part B 36:707–729

7. Verhoef ET (2002) Second best congestion pricing in general static transportation networks with elastic demands. Reg Sci Urban Econ 32:281–310
8. Patriksson M, Rockefellar RT (2002) A mathematical model and descent algorithm for bilevel traffic management. Transp Sci 36(3):271–291
9. Staňková, K. (2009) On Stackelberg and inverse Stackelberg games & their applications in the optimal yoll design problem, the energy market liberalization problem, and in the theory of incentives. Ph.D. thesis, Delft University of Technology, Delft, The Netherlands
10. Staňková K, Olsder GJ, Bliemer MCJ (2009) Comparison of different toll policies in the dynamic second-best optimal toll design problem: case study on a three-link network. Eur J Transp Infrastruct Res 9(4):1–17
11. Olsder GJ (2009) Phenomena in inverse Stackelberg games, part 1: static problems. J Optim Theory Appl 143(3):589–600
12. Basar T, Olsder GJ (1999) Dynamic noncooperative game theory. SIAM, Philadelphia
13. Shen H, Basar T (2006) Incentive-based pricing for network games with complete and incomplete information, vol 8., Annals of dynamic gamesBirkhäuser, Boston
14. Olsder GJ (2009) Phenomena in inverse Stackelberg games, part 2: dynamic problems. J Optim Theory Appl 143(3):601–618
15. Engwerda J, Reddy, P (2011) A positioning of cooperative differential games. In: Proceedings of the 5th international ICST conference on performance evaluation methodologies and tools, ICST (Institute for Computer Sciences, Social-Informatics and Telecommunications Engineering), pp 1–8
16. Mu Y (2013) Inverse Stackelberg public goods game with multiple hierarchies under global and local information structures. J Optim Theory Appl 163:1–19
17. Averboukh Y, Baklanov A (2013) Stackelberg solutions of differential games in the class of nonanticipative strategies. Dyn Games Appl 4:1–9
18. Groot, N (2013) Reverse Stackelberg games: theory and applications in traffic control. Ph.D. thesis, Delft University of Technology, Delft
19. Laffont JJ, Martiomort D (2002) The theory of incentives: the principal-agent model. Princeton University Press, Princeton
20. Macho-Stadler I, Pérez-Castrillo JD (1997) An introduction to the economics of information. Oxford University Press, Oxford
21. Bliemer, MCJ (2001) Analytical dynamic traffic assignment with interacting user-classes. Ph. D. thesis, Delft University of Technology, Delft
22. Han S (2007) A route-based solution algorithm for dynamic user equilibrium assignments. Transp Res Part B: Methodol 41(10):1094–1113
23. Ran B, Hall RW, Boyce DE (1996) A link-based variational inequality model for dynamic departure time/route choice. Transp Res Part B: Methodol 30(1):31–46
24. Chen M, Chien SI (2001) Dynamic freeway travel-time prediction with probe vehicle data: link based versus path based. Transp Res Rec: J Transp Res Board 1768(1):157–161
25. Wardrop JG (1952) Some theoretical aspects of road traffic research. In: Proceedings of the Institute of Civil Engineers, Part II, pp 325–378
26. Patriksson M (1999) Nonlinear programming and variational inequality problems: a unified approach. Kluwer, The Netherlands
27. Staňková K, Olsder G, De Schutter B (2010) On European electricity market liberalization: a game-theoretic approach. INFOR: Inf Syst Oper Res 48(4):267–280
28. Koepsell D, Staňková K (2012) Non-proliferation regimes: immoral and risky—a game-theoretic approach. Int J World Peace 29(2):63–83
29. Staňková K, Abate A, Sabelis M (2013) Irreversible prey diapause as an optimal strategy of a physiologically extended Lotka-Volterra model. J Math Biol 66(4):767–794
30. Yildirim MB, Hearn DW (2005) A first best toll pricing framework for variable demand traffic assignment problems. Transp Res Part B: Methodol 39(8):659–678
31. Hearn DW, Yildirim MB (2002) A toll pricing framework for traffic assignment problems with elastic demand. Springer, Berlin

32. Verhoef ET (2002) Second-best congestion pricing in general networks. Heuristic algorithms for finding second-best optimal toll levels and toll points. Transp Res Part B: Methodol 36 (8):707–729
33. Staňková K, Von Mettenheim HJ, Olsder GJ (2008), Dynamic optimal toll design problem with second-best-flow-dependent tolling solved using neural networks. In: Proceedings of the 10th international conference on applications of advanced technologies in transportation, Athens
34. Patriksson M (1994) The traffic assignment problem: models and methods. VSP, The Netherlands
35. Yiyi H (1997) A flow-based approach to the dynamic traffic assignment problem: formulations, algorithms, and computer implementations
36. Colson B, Marcotte P, Savard G (2007) An overview of bilevel optimization. Ann Oper Res 153:235–256
37. Hansen P, Jaumard B, Savard G (1992) New branch and bound rules for linear bilevel programming. SIAM J Sci Stat Comput 13:1194–1217
38. Vicente L, Calamai P (1995) Geometry and local optimality conditions for bilevel programs with quadratic strictly convex lower levels. In: Du D-Z, Pardalos M (eds) Minimax and applications, vol 4. Pub-kluwer, pp 141–151.http://dial.uwaterloo.ca/∼phcalama/cpp.html
39. Staňková K, Bliemer MCJ, Olsder GJ (2006) Inverse Stackelberg games and their application to dynamic bilevel optimal toll design problem. In: Proceedings of the 12th International symposium on dynamic games and applications, INRIA, France
40. Kuczma M (1968) Functional equations in a single variable. Polish Scientific Publishers, Warsaw

Author Index

K. Hausken and J. Zhuang (eds.), *Game Theoretic Analysis of Congestion, Safety and Security*, Springer Series in Reliability Engineering,
DOI 10.1007/978-3-319-11674-7

Subject Index

K. Hausken and J. Zhuang (eds.), *Game Theoretic Analysis of Congestion, Safety and Security*, Springer Series in Reliability Engineering,
DOI 10.1007/978-3-319-11674-7